

Evolution of the Platoro Caldera Complex and Related Volcanic Rocks, Southeastern San Juan Mountains, Colorado

G E O L O G I C A L S U R V E Y P R O F E S S I O N A L P A P E R 8 5 2



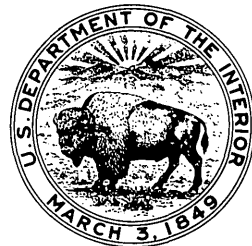
WEB

Evolution of the Platoro Caldera Complex and Related Volcanic Rocks, Southeastern San Juan Mountains, Colorado

By PETER W. LIPMAN

GEOLOGICAL SURVEY PROFESSIONAL PAPER 852

*A study of relations between ash-flow eruptions,
lava-flow activity, and caldera structure at a
mineralized volcanic center*



vent fac. p 9

UNITED STATES GOVERNMENT PRINTING OFFICE, WASHINGTON : 1975

UNITED STATES DEPARTMENT OF THE INTERIOR

ROGERS C. B. MORTON, *Secretary*

GEOLOGICAL SURVEY

V. E. McKelvey, *Director*

Library of Congress Cataloging in Publication Data
Lipman, Peter W.
Evolution of the Platoro caldera complex and related volcanic rocks, southeastern San Juan Mountains, Colorado.
(Geological Survey Professional Paper 852)
Includes bibliographical references and index.
Supt. of Docs. No.: I 19.16:852
1. Volcanism—San Juan Mountains. 2. Volcanic ash, tuff, etc.—San Juan Mountains.
I. Title. II. Series: United States Geological Survey Professional Paper 852.
QE461.L626 552'.2'0978838 74-20902

For sale by the Superintendent of Documents, U.S. Government Printing Office
Washington, D.C. 20402 — Price \$3.25 (paper cover)
Stock Number 2401-02586

CONTENTS

| | Page |
|--|------|
| ✓Abstract | 1 |
| ✓Introduction | 2 |
| Present investigation | 2 |
| ✓Geologic setting | 6 |
| ✓Prevolcanic rocks | 8 |
| ✓Early intermediate-composition rocks (Conejos Formation) | 8 |
| Vent facies | 12 |
| Volcaniclastic facies | 13 |
| Upper lava unit | 13 |
| Ash-flow sheets | 14 |
| Tuff of Rock Creek | 14 |
| Treasure Mountain Tuff | 16 |
| Lower tuff | 19 |
| La Jara Canyon Member | 25 |
| Middle tuff | 30 |
| Ojito Creek Member | 33 |
| Ra Jadero Member | 36 |
| Upper tuff | 40 |
| Younger ash-flow sheets and interlayered lavas | 41 |
| Masonic Park Tuff | 41 |
| Fish Canyon Tuff | 47 |
| Carpenter Ridge Tuff | 49 |
| Wason Park Tuff | 53 |
| Snowshoe Mountain Tuff | 54 |
| Interlayered lava flows | 54 |
| Sheep Mountain Andesite | 55 |
| Huerto Andesite | 55 |
| Volcanics of Table Mountain | 55 |
| Lavas and related rocks of the Platoro caldera complex | 55 |
| Rhyodacite of Fisher Gulch | 56 |
| Summitville Andesite | 58 |
| Andesite of Summit Peak | 67 |
| Volcanics of Green Ridge | 67 |
| Rhyolite unit | 67 |
| Andesite-rhyodacite unit | 68 |
| Porphyritic rhyodacite unit | 70 |
| Rhyodacite of Park Creek | 70 |
| Quartz latite of South Mountain | 73 |
| Rhyolite of Cropsy Mountain | 74 |
| Volcaniclastic rocks (Los Pinos Formation) | 76 |
| Intrusive rocks | 78 |
| Granitic intrusions | 78 |
| Alamosa River stock | 78 |
| Cat Creek stock | 82 |
| Lavas and related rocks of the Platoro caldera complex—Continued | 84 |
| Intrusive rocks—Continued | 86 |
| Granitic intrusions—Continued | 86 |
| Jasper stock | 86 |
| Bear Creek stock cluster | 86 |
| Other stocks | 86 |
| Porphyro-aphanitic intrusions | 86 |
| Andesitic rocks | 87 |
| Rhyodacitic rocks | 87 |
| Quartz latitic and rhyolitic rocks | 88 |
| Late basalt and rhyolite (Hinsdale Formation) | 90 |
| Basaltic lavas | 90 |
| Rhyolitic lavas and tuffs | 93 |
| Mixed lavas | 97 |
| Surficial deposits | 101 |
| Structural evolution | 101 |
| Pre-Tertiary structures | 101 |
| Tertiary volcanic structures | 101 |
| San Juan caldera cluster | 101 |
| Platoro caldera | 103 |
| Premonitory volcanism | 103 |
| Ash-flow eruptions and caldera collapse | 104 |
| Resurgent uplift | 107 |
| Postresurgence volcanism | 107 |
| Summitville caldera | 108 |
| Arcuate faulting | 108 |
| Topographic wall | 109 |
| Postcollapse volcanism | 109 |
| Caldera-related regional faulting | 110 |
| Rio Grande fault zone | 110 |
| Pass Creek-Elwood Creek-Platoro fault system | 110 |
| Late Cenozoic extensional faulting | 112 |
| Alteration and mineralization | 113 |
| Summitville district | 113 |
| Stunner and Gilmore districts | 114 |
| Platoro district | 114 |
| Jasper area | 114 |
| Crater Creek area | 114 |
| Cat Creek area | 114 |
| Economic significance | 115 |
| Petrologic evolution | 115 |
| References cited | 120 |
| Index | 125 |

ILLUSTRATIONS

| FIGURE | | Page |
|--------|--|------|
| 1. | Index map showing location of San Juan volcanic field | 3 |
| 2. | Index map of the southeastern San Juan Mountains, showing areas covered by published topographic maps | 4 |
| 3. | Diagram showing approximate relations between SiO_2 content and phenocryst constituents of volcanic rocks | 5 |
| 4. | Histograms of SiO_2 contents for major divisions of Tertiary volcanic rocks in the San Juan Mountains | 7 |
| 5. | Map showing outcrop areas of the vent facies and volcaniclastic facies of the Conejos Formation | 10 |
| 6. | Photograph and photomicrograph showing porphyritic andesite of the Conejos Formation | 13 |

| FIGURE | | Page |
|--------|--|------|
| 7. | Photographs of cone and explosion breccia from the Adams Fork volcano | 14 |
| 8. | Photograph showing a thick section of the clastic facies of the Conejos Formation | 15 |
| 9. | Map showing outcrop area, approximate thickness of selected sections, and inferred original depositional extent of the tuff of Rock Creek and the lower tuff of the Treasure Mountain Tuff | 17 |
| 10. | Photograph showing densely welded tuff of Rock Creek | 18 |
| 11. | Photograph showing weakly welded tuff of Rock Creek | 19 |
| 12. | Graphs showing petrologic features of the major ash-flow members of the Treasure Mountain Tuff | 22 |
| 13. | Geologic map of the Banded Peak area | 24 |
| 14. | Map showing outcrop area, approximate thickness of selected sections, and inferred original depositional extent of the La Jara Canyon Member, Treasure Mountain Tuff | 26 |
| 15. | Photograph of ash-flow boundary within densely welded devitrified tuff of the La Jara Canyon Member | 28 |
| 16. | Photomicrographs of ash-flow boundary within densely welded devitrified tuff of the La Jara Canyon Member | 29 |
| 17. | Photographs showing field appearance of intracaldera La Jara Canyon Member | 30 |
| 18. | Photomicrographs of intracaldera La Jara Canyon Member | 31 |
| 19. | Photograph showing moderately welded La Jara Canyon Member | 32 |
| 20. | Diagram showing geometric model for volume calculations of the three major ash-flow sheets of the Treasure Mountain Tuff | 33 |
| 21. | Generalized geologic map of the Black Mountain area | 34 |
| 22. | Photograph showing well-bedded ash-fall tuffs of the middle tuff of the Treasure Mountain Tuff | 36 |
| 23. | Map showing outcrop area, approximate thickness of selected sections, and inferred original depositional extent of the Ojito Creek Member, Treasure Mountain Tuff | 37 |
| 24. | Photomicrographs of the Ojito Creek and Ra Jadero Members | 38 |
| 25. | Map showing outcrop area, approximate thickness of selected sections, and inferred original depositional extent of the Ra Jadero Member, Treasure Mountain Tuff | 39 |
| 26. | Map showing outcrop area and inferred original depositional extent of the Masonic Park Tuff | 44 |
| 27. | Photograph showing ash-flow sheets along the Rio Grande valley near Masonic Park | 45 |
| 28. | Graphs showing phenocryst variations in a section of the Masonic Park Tuff | 46 |
| 29. | Photograph showing crudely bedded welded tuff near the base of the upper member of the Masonic Park Tuff | 46 |
| 30. | Map showing outcrop area and inferred original depositional extent of the Fish Canyon Tuff | 48 |
| 31. | Map showing outcrop area and inferred original depositional extent of the Carpenter Ridge Tuff | 50 |
| 32. | Graphs showing petrographic variations in a section of the Carpenter Ridge Tuff | 51 |
| 33. | Photomicrographs of Carpenter Ridge Tuff | 52 |
| 34. | Graph showing inverse correlation between SiO_2 and total phenocryst contents | 53 |
| 35. | Photograph showing Snowshoe Mountain Tuff interlayered with late volcanic products from the Platoro caldera complex | 54 |
| 36. | Map showing distribution of postcollapse lavas and related monzonitic intrusives of the Platoro caldera complex | 57 |
| 37. | Photograph and photomicrograph of rhyodacite of Fisher Gulch | 59 |
| 38. | Photomicrographs of the lower member of the Summitville Andesite | 63 |
| 39. | Photographs showing features of the lower member of the Summitville Andesite | 64 |
| 40. | Photographs showing intracaldera volcanioclastic sedimentary rocks of the Summitville Andesite | 65 |
| 41. | Photomicrographs of characteristic rock types of volcanics of Green Ridge | 68 |
| 42. | Photograph showing volcanioclastic sedimentary rocks of the Los Pinos Formation overlain and fused by thick lava flow | 70 |
| 43. | Photomicrographs of typical lavas of the late viscous domes around the margins of the Summitville caldera | 72 |
| 44. | Photograph showing rhyolite of Cropsy Mountain | 74 |
| 45. | Photomicrographs of mixed-lava complex at North Mountain | 76 |
| 46. | Diagrammatic cross section through the Cat Creek volcano | 77 |
| 47. | Map showing distribution of major groups of intrusive rocks in the southeastern San Juan Mountains | 79 |
| 48. | Photomicrographs of rocks of the Alamosa River stock | 83 |
| 49. | Photomicrographs of rocks of the Bear Creek stock cluster | 85 |
| 50. | Photograph and photomicrographs showing phenocryst variations at the margin of a rhyodacite porphyry sill | 88 |
| 51. | Photograph showing typical exposure of quartz latite porphyry dike | 89 |
| 52. | Photograph showing low-angle flow grooves in quartz latite porphyry dike | 89 |
| 53. | Map showing distribution of basaltic and rhyolitic lavas of the Hinsdale Formation | 91 |
| 54. | Photomicrographs of common basalt and rhyolite types of the Hinsdale Formation | 93 |
| 55. | Graph showing total alkalis and SiO_2 for basalts of the southeastern San Juan Mountains and the northern end of the Rio Grande depression | 93 |
| 56-58. | Photographs showing the Beaver Creek vent-dome complex: | |
| 56. | Feeder dike | 96 |
| 57. | Depositional units | 97 |
| 58. | Upper part of the vitrophyric zone | 98 |
| 59. | Photomicrographs showing petrographic variations within the mixed lava on the southwest side of Handkerchief Mesa | 99 |
| 60. | Photographs and photomicrographs of the Handkerchief Mesa mixed-lava complex | 100 |
| 61. | Map showing distribution of faults, stocks, and areas of hydrothermal alteration in the southeastern San Juan Mountains | 102 |
| 62-65. | Photographs: | |
| 62. | Creede caldera from the north | 103 |
| 63. | Depositional contact against south caldera wall below Conejos Peak | 105 |

CONTENTS

V

FIGURES 62-65. Photographs—Continued

| | Page |
|---|------|
| 64. Depositional relations at west wall of Platoro caldera, south slope of Prospect Mountain | 106 |
| 65. Displacement in faulted ridge east of Crater Creek | 111 |
| 66. SiO ₂ variation diagram for major igneous units of the Platoro caldera complex | 118 |
| 67. Outlines of Platoro caldera complex in Colorado and Aso caldera in Japan | 120 |

TABLES

| TABLE | | Page |
|-------|---|------|
| 1. | Generalized Tertiary volcanic stratigraphy of the San Juan Mountains | 6 |
| 2. | Analyses of lava flows of the Conejos Formation | 11 |
| 3. | Summary of petrologic features of ash-flow tuffs of the southeastern San Juan Mountains | 15 |
| 4. | Analyses of the Treasure Mountain Tuff and the tuff of Rock Creek | 20 |
| 5. | Estimated volumes of ash-flow sheets related to the Platoro caldera complex | 32 |
| 6. | Analyses of the younger ash-flow sheets | 42 |
| 7. | Analyses of lava flows interlayered with the younger ash-flow sheets | 56 |
| 8. | Summary of general features of lavas and related rocks of the Platoro caldera complex | 58 |
| 9. | Analyses of lava flows and related rocks of the Platoro caldera complex | 60 |
| 10. | Analyses of intrusive rocks of the Platoro caldera area | 80 |
| 11. | Analyses of basaltic and rhyolitic lavas of the Hinsdale Formation | 94 |
| 12. | Measurements of slopes of Platoro caldera walls | 106 |

EVOLUTION OF THE PLATORO CALDERA COMPLEX AND RELATED VOLCANIC ROCKS, SOUTHEASTERN SAN JUAN MOUNTAINS, COLORADO

By PETER W. LIPMAN

ABSTRACT

Volcanic rocks in the San Juan Mountains constitute the largest erosional remnant of a once nearly continuous volcanic field that extended over much of the southern Rocky Mountains and adjacent areas in Oligocene and later time. Recent regional studies have shown that the gross petrologic evolution of the San Juan remnant of this field was relatively simple, beginning with intermediate-composition lavas and breccias, followed closely in time by more silicic ash-flow tuff, and ending with a bimodal association of basalt and alkali rhyolite.

In the southeastern San Juan Mountains, voluminous early lavas and breccias of the Conejos Formation—mainly alkali andesite, rhyodacite, and mafic quartz latite—were erupted from numerous scattered central volcanoes onto an eroded tectonically stable terrane. These rocks were erupted mostly during the interval 35-30 m.y. (million years) ago, and they volumetrically represent about two-thirds of the volcanism.

About 30 m.y. ago, major volcanic activity changed to explosive ash-flow eruptions of quartz latite and low-silica rhyolite that persisted until about 26 m.y. ago. Source areas for the ash flows are marked by large calderas in the central San Juan Mountains. Among the earliest and most southeastern of these is the Platoro caldera complex, a composite collapse structure about 20 kilometers in diameter that formed as a result of ash-flow eruption of the 29- to 30-m.y.-old Treasure Mountain Tuff. Three major ash-flow sheets of the Treasure Mountain Tuff—the La Jara Canyon, Ojito Creek, and Ra Jadero Members in ascending order—are approximately coextensive and cover about 5,000 square kilometers in the southeastern San Juan Mountains. Major collapse of the Platoro caldera occurred during eruption of phenocryst-rich quartz latitic ash flows that form the La Jara Canyon Member, and late ash flows of this member accumulated within the collapsing caldera to a thickness of more than 800 meters. The core of the collapsed block was resurgently uplifted to form an unbroken homoclinally tilted block, in contrast to the fractured domical uplifts that characterize other known resurgent calderas; and the marginal moat was filled by as much as 1 kilometer of lavas and interbedded volcaniclastic sedimentary rocks of the lower member of the Summitville Andesite (name reinstated in this report).

Renewed ash-flow eruption of the quartz latitic Ojito Creek and Ra Jadero Members resulted in further collapse to form the Summitville caldera within the northwest part of the Platoro caldera. No resurgence is associated with this late caldera, but it was also filled to overflowing by a thick accumulation of upper member lavas of the Summitville Andesite.

Porphyritic rhyodacitic to rhyolitic lavas, and genetically related dikes and granitic stocks, were emplaced repeatedly around margins of the Platoro caldera complex during the interval 29-20 m.y., with dated events at 29.1, 26.7-27.8, 25.8, 22.8, and 20.2 m.y. Volcaniclastic sedimentary rocks, interbedded with these late lavas, record erosion of the primary volcanic topography, and young ash-flow sheets erupted from other calderas northwest of Platoro show variations in distribu-

tion and thickness near the Platoro caldera complex that correlate with the growing constructional topography of the caldera-margin volcanoes. One of these sheets is the Masonic Park Tuff, a new name in this report.

In the early Miocene the character of volcanism changed notably. Whereas the Oligocene volcanic rocks are predominantly intermediate lavas and genetically related more silicic ash-flow tuffs, the younger rocks are a bimodal association of basalt and highly silicic alkali rhyolite of the Hinsdale Formation. Locally interbedded intermediate-composition rocks are, at least in places, mixed-lava complexes with basaltic and rhyolitic end members. Basalt and minor rhyolite were erupted intermittently through the Miocene and Pliocene, and at one time they formed a widespread veneer over most of the older volcanic terrane.

The general petrologic progression of the postcollapse igneous activity at the Platoro caldera complex is toward more silicic rocks as age decreases, from voluminous dark andesites (56-59 percent SiO₂) to minor scattered lava domes of porphyritic rhyolite (73-76 percent SiO₂) that are contemporaneous with nearby widespread flows of alkali olivine basalt. This postcollapse igneous activity at the Platoro caldera therefore spans the regional transition from predominantly andesitic volcanism to the bimodal basalt-rhyolite suites.

The major Tertiary structural features of the southeastern San Juan Mountains, in addition to the calderas, are two major northwest-trending fault systems that run between several of the major calderas: (1) the Rio Grande fault zone that extends from the northeast side of the Creede caldera toward the north rim of the Summitville caldera and (2) the Pass Creek-Elwood Creek-Platoro fault system that connects the Mount Hope caldera with the Platoro caldera complex. These major zones had lengthy histories of recurrent movement, but their initiation and much of their total displacement occurred during the period of ash-flow eruption and major caldera collapse. In the southeastern area, however, these faults were reactivated during later Cenozoic antithetic block faulting that is related to regional eastward tilting of the volcanic rocks toward the San Luis Valley in response to development of the Rio Grande rift depression to the east.

Hydrothermal alteration and ore deposition of late Oligocene and early Miocene age is locally associated with the postcollapse volcanics and intrusives around the margins of the Platoro caldera complex. Economic deposits occur where the northwest-trending Pass Creek-Elwood Creek-Platoro fault system intersects the ring fractures of the caldera complex at the Summitville, Stunner, and Platoro mining districts. Other mineralized areas, at Crater Creek, Jasper, and Cat Creek, are also localized by caldera-margin faulting and igneous activity. The mineralization of these areas, which had previously appeared anomalous, is therefore comparable to other caldera-associated mineralization in the central and western San Juan Mountains.

The Oligocene andesite to quartz latite associations of the Platoro

caldera complex, as well as similar ash-flow assemblages elsewhere in the San Juan field, contrast with other continental-interior ash-flow associations which are predominantly rhyolitic in composition. Close spatial and temporal association of the quartz latitic ash-flow tuffs and the voluminous andesitic lava flows in the Platoro area, both within and outside the calderas, indicates that the ash-flow tuffs represent differentiated upper parts of a magma body of predominantly intermediate composition that was similar to the composition of the andesitic lavas and monzonitic stocks. The Oligocene San Juan volcanic associations in general resemble andesitic associations that are found along most of the Pacific margin, where continental plates override oceanic crust along active trench-Benioff zone systems. A related mechanism probably operated in the Western United States until late Cenozoic time.

The contrast between the Oligocene intermediate to low-silica rhyolitic magmas and the later basaltic and rhyolitic bimodal magmas implies either different conditions of magma generation or different processes of fractionation for the two magmatic assemblages. This petrologic change coincides approximately in time with nearby development of the Rio Grande depression, a major rift that is the local expression of widespread late Cenozoic crustal extension. The change from predominantly intermediate to bimodal basalt-rhyolite volcanism, approximately concurrent with initiation of late Tertiary crustal extension, seems to be characteristic of Cenozoic volcanism for much of the Western United States. These changes also coincided in time with changes in the geometry of sea-floor spreading recorded in magnetic anomaly patterns in the northeast Pacific, apparently reflecting initial intersection of North America with the East Pacific Rise and destruction of the trench-Benioff zone system.

INTRODUCTION

This report describes the evolution of the Platoro caldera complex and related middle Tertiary volcanic rocks that cover about 5,000 km² (square kilometers) in the southeastern San Juan Mountains, Colo. (fig. 1). The caldera complex is a composite collapse structure about 20 km (kilometers) in diameter that formed as a result of ash-flow eruptions of the upper Oligocene Treasure Mountain Tuff. Close spatial and temporal association of the quartz latitic ash-flow tuffs with voluminous andesitic lava flows, both within and outside the caldera, indicates that the ash-flow tuffs represent differentiated upper parts of a magma body of predominantly intermediate composition that was similar to the composition of the andesitic lavas. Significant hydrothermal alteration and copper-molybdenum-gold mineralization are associated with prolonged post-collapse igneous activity that was localized around margins of the caldera complex.

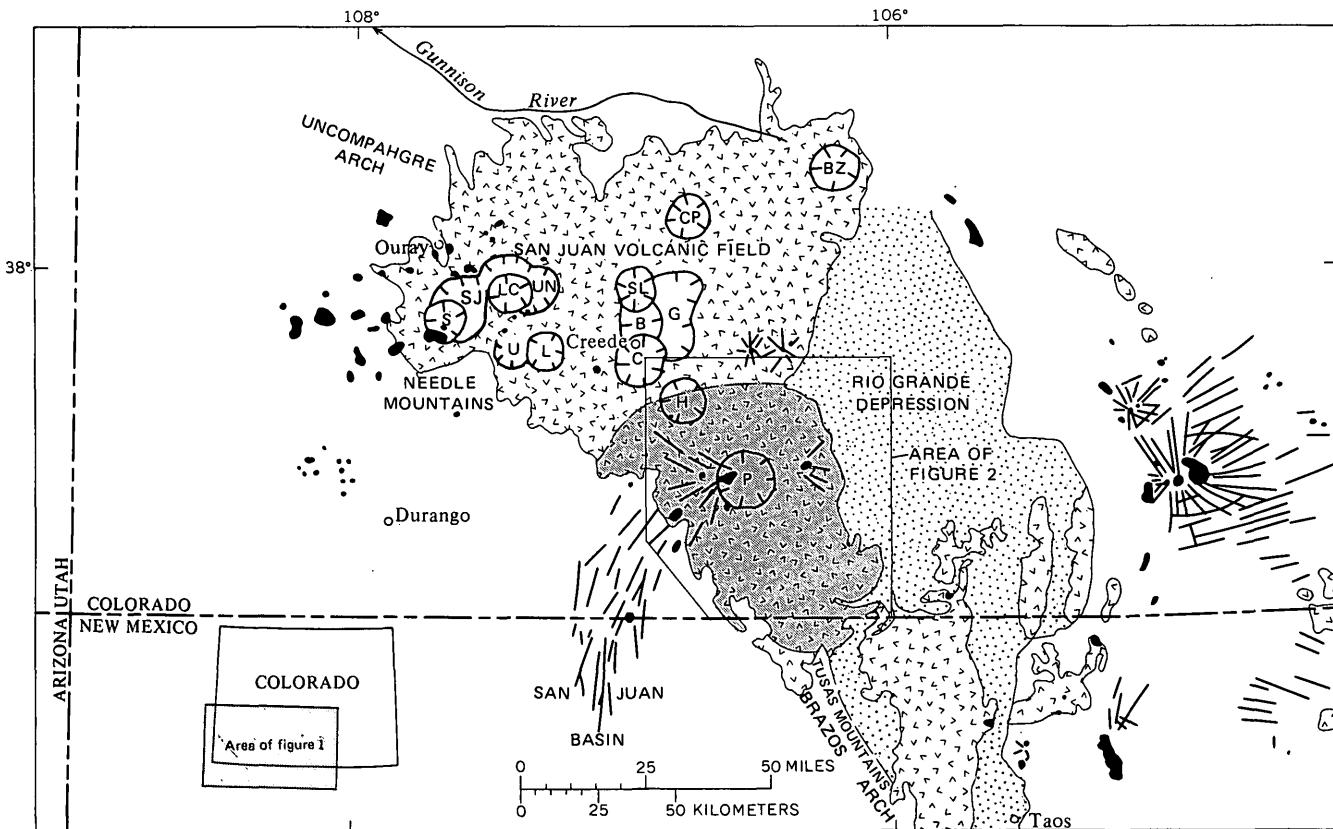
The Platoro caldera complex was first recognized during reconnaissance mapping of the southeastern San Juan Mountains during 1965-67, as part of a project directed by T. A. Steven to prepare a geologic map of the Durango 2-degree sheet on a scale of 1:250,000 (Steven, Lipman, Hail, Barker, and Luedke, 1974). Features of the Platoro caldera complex have been described in preliminary form (Lipman and Steven, 1970), but because the reconnaissance mapping for the Durango project was deemed inadequate to establish firmly the complex geology of the caldera area, two 15-minute

quadangles that cover this area (fig. 2) were mapped in greater detail during 1970-71. This report is mainly concerned with the detailed geology of the Platoro caldera area (Lipman, 1974), but also included is considerable discussion—especially in the stratigraphic descriptions—of adjacent parts of the southeastern San Juan Mountains that are illustrated only by the 2-degree Durango map. Frequent reference will be made to topographic and geologic features illustrated by these two maps, hereafter referred to as the Durango map and the Platoro map, and the serious reader will find it convenient to have both maps at hand.

The only significant previous regional study of the volcanic rocks of the southeastern San Juan Mountains was summarized by Larsen and Cross (1956) in their description of the geology and petrology of the entire San Juan region. Study of the southeastern part of this large region was mainly detailed reconnaissance; fieldwork was mostly by Larsen, assisted by J. F. Hunter from 1911 to 1917 and by C. S. Ross in 1920-21 (Larsen and Cross, 1956, preface). This work, although done without benefit of modern concepts of ash-flow tuffs and their relation to caldera structures, succeeded in delimiting the regional stratigraphy fairly well, except within the Platoro caldera area. Previously, Patton (1917) had presented an excellent early description of the geology and ore deposits of the Platoro-Summitville area. The rock units distinguished by Patton differed significantly from those used by subsequent workers in the area, but Patton's stratigraphic interpretations generally seem to have been valid. Steven and Ratté (1960) made a detailed study of the geology and ore deposits of the Summitville mining district; although their study was hampered by a lack of information on regional stratigraphy or on relations of the Summitville rocks to the then-unrecognized Platoro caldera structure, the local geologic sequence they determined for the Summitville district remains valid. Fragmentary 19th and early 20th century studies in the Summitville-Platoro area, concerned primarily with the mineralization, were summarized by Patton (1917) and Steven and Ratté (1960).

PRESENT INVESTIGATION

The present report is based on a total of about 15 months' fieldwork during the summers of 1965-67 and 1970-71. Reconnaissance mapping of the entire southeastern San Juan Mountains in 1965-67 for the 1:250,000 Durango map (Steven, Lipman, Hail, Barker, and Luedke, 1974) was done on 1:40,000 black-and-white aerial photographs, with an intermediate stage of compilation on 1:24,000 and 1:62,500 topographic quadrangle maps wherever available. The area of the Platoro caldera complex was remapped in greater detail in 1970-71 by use of 1:16,000 color aerial photographs for most of the area; this work was compiled at 1:24,000 and



EXPLANATION

| | |
|--------------------|---|
| | Alluvial deposits |
| | Volcanic rocks |
| | Shaded area underlain by Treasure Mountain Tuff |
| | Intrusive rocks |
| | Calderas of the San Juan volcanic field |
| B, Bachelor | LC, Lake City |
| BZ, Bonanza | P, Platoro |
| C, Creede | S, Silverton |
| CP, Cochetopa Park | SJ, San Juan |
| G, La Garita | SL, San Luis |
| H, Mount Hope | U, Ute Creek |
| L, Lost Lake | UN, Uncompahgre |

FIGURE 1.—Index map showing location of the San Juan volcanic field, calderas of the San Juan Mountains, and ash-flow tuffs erupted from the Platoro caldera complex. In part modified from Cohee (1961).

reduced for publication as a single 1:48,000-scale map (Lipman, 1974). Assistance in fieldwork was ably given by Russel F. Burmester in 1966, Harry R. Covington in 1970, and David A. Johnston in 1971. This report was written during the winter of 1971-72.

For this report a series of 12 summary maps, showing distribution, thickness, and other features of major volcanic units in the southeastern San Juan Mountains, was prepared from the Durango map, the Platoro map, and data from unpublished compilations. On the summary maps the outcrop distribution is slightly generalized, and small patches of overlying units are in places omitted for clarity. The thickness values were determined from 1:24,000 quadrangles with 40-foot contours, except for the southwestern part of the area, where 1:62,500 quadrangles with 80-foot contours (fig. 2) were

used. Most thicknesses were estimated to the nearest 30 m (30 meters, or 100 feet), but thicknesses for very thin parts of units were estimated to the nearest 15 m.

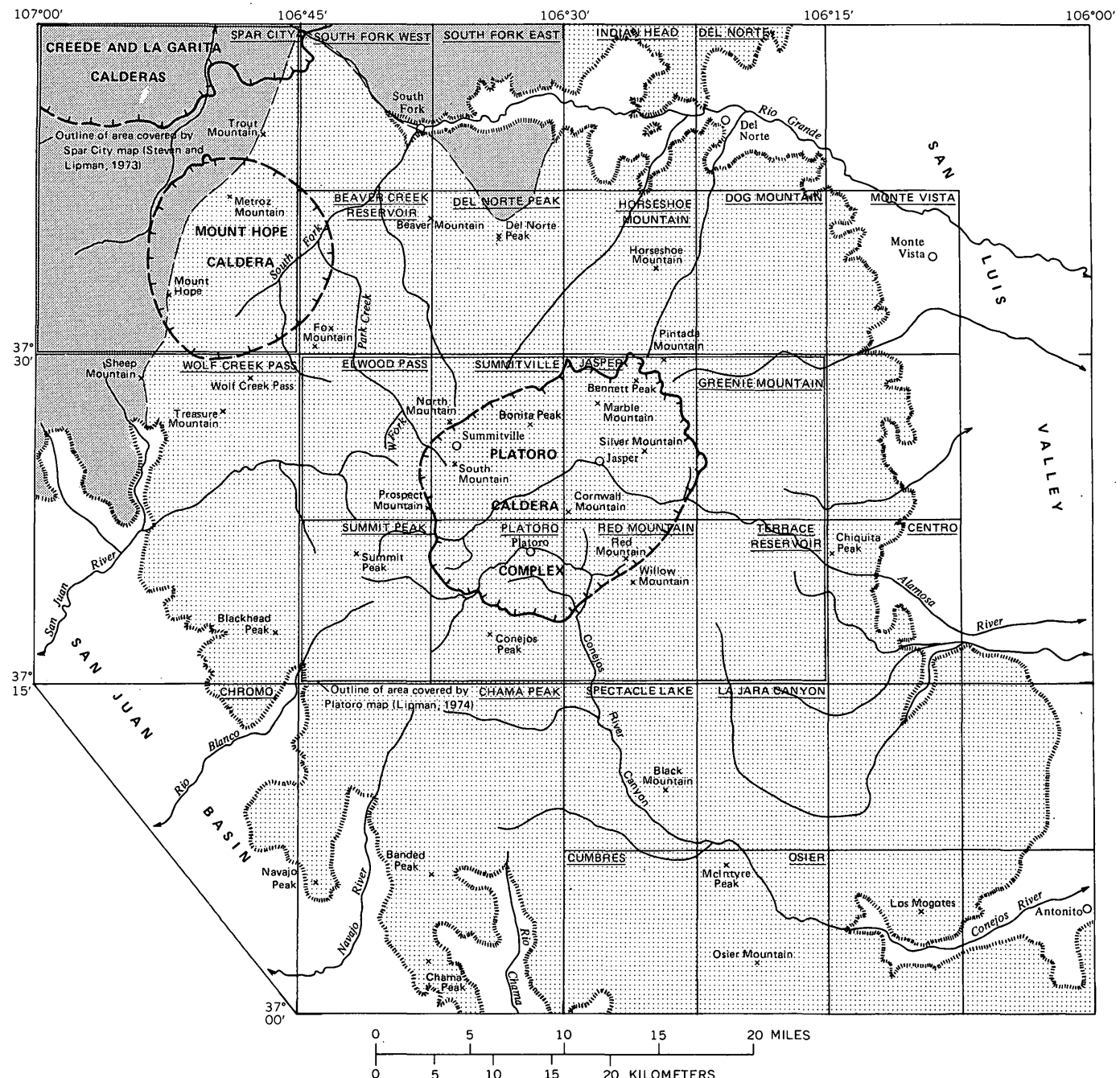
Terminology of ash-flow tuffs generally is that of R. L. Smith (Smith, 1960a, b; Ross and Smith, 1961).

Petrographic interpretations are based on study of approximately 800 thin sections from the southeastern San Juan Mountains, supplemented by several hundred more from adjacent parts of the volcanic field being studied by T. A. Steven. Modal compositions were determined for about 200 specimens; most were determined by point-counting methods on a single 25x40 mm thin section. Spacing of point-count traverses was adjusted to yield 400-800 phenocryst points over the area of the entire section, wherever possible. For a few phenocryst-poor rocks this number of points could not be attained, even

PLATORO CALDERA COMPLEX, SAN JUAN MOUNTAINS, COLORADO

with the closest possible (0.3 mm) traverses. Modal compositions are tabulated in this report only for analyzed specimens, but discussion of compositions of the

various units is also based on other unpublished modal data. In addition to the author's determinations, some modes were counted by James Kirkpatrick, Harry



EXPLANATION

- Mapped by P. W. Lipman, 1965-67, 1970-71
- Mapped by T. A. Steven, 1965-66
- Limit of exposed volcanic rocks
- Caldera wall (topographic)—Dashed where covered by younger rocks

FIGURE 2.—Index map of the southeastern San Juan Mountains, showing areas covered by published 15- and 7½-minute topographic and geologic maps and indicating sources of unpublished geologic data utilized in following figures. Names of topographic maps are underscored.

Covington, Thomas Steven, Leonard Schmidt, and James Ratté. Modes listed only to the nearest percent concentration were estimated rather than counted.

Most stated compositions of phenocryst minerals are based on routine thin-section examination, but feldspar compositions of several samples from each major unit were determined more precisely. Discussions of compositions and structural states of alkali feldspars are based on X-ray measurements of phenocryst separates, by use of the "three-peak" method of Wright (1968) or the unit-cell refinement technique of Wright and Stewart (1968). Plagioclase compositions were determined routinely by maximum extinction angles normal to 010, using the high-temperature curves of Deer, Howie, and Zussman (1963); more precise determinations for some plagioclases were made by universal-stage methods. Partial chemical analyses of some feldspars, as well as a few biotites and clinopyroxenes, were determined by microprobe techniques.

All available seemingly satisfactory chemical analyses of volcanic rocks from the southeastern San Juan field are given in tables 2, 4, 6, 7, and 9-11. Of the 129 analyses, 94 are new; the others are from Patton (1917), Larsen and Cross (1956), and Steven and Ratté (1960). A few analyses of rocks that apparently have been altered significantly have been excluded from the tables.

The major-oxide analyses have been recalculated to 100 percent free of volatiles in order to facilitate comparisons among specimens having different amounts of secondary water and carbonates. Secondary hydration is especially evident in the glassy rocks. Silicic glasses contain at most a few tenths of a percent water upon initial cooling (Ross and Smith, 1955), whereas some analyzed glasses reported here contain as much as 2.5 percent H₂O+. In general, glassy rocks have not been newly analyzed for this study because of the possibility of alkali exchange with ground water (Lipman, 1965; Truesdell, 1966), but some previously published analyses (Larsen and Cross, 1956; Steven and Ratté, 1960) are of glassy samples. All CO₂ in the analyses has been calculated out as CaCO₃ if the carbonate mainly fills cavities such as vesicles but as CO₂ if the carbonate mainly replaces phenocrysts or groundmass. The analytically determined contents of H₂O and CO₂ are listed in the tables following the recalculated analyses.

Most of the new major-oxide analyses were made by the rapid methods of Shapiro and Brannock (1962) and Shapiro (1967); a few samples were analyzed by the standard wet-chemical methods of Peck (1964). Most of the minor-element analyses were made by the quantitative spectrographic methods of Bastron, Barnett, and Murata (1960); results are reported to two significant figures and have an overall accuracy of ± 15 percent; they are less accurate near limits of detection, where only one digit is significant. Elements that are reported

as zero were not detected. A few minor-element analyses were made by the semiquantitative spectrographic methods of Myers, Havens, and Dunton (1961) and are reported as midpoint values of logarithmic third divisions; the precision of a reported value is approximately plus or minus one division at 68-percent confidence or two divisions at 95-percent confidence. All analyses were made in the laboratories of the U.S. Geological Survey between 1966 and 1972.

Names chosen for the volcanic rocks require discussion, because no single classification system has yet been accepted widely enough to be used without comment. Because most of the rocks in the area studied are at least partly aphanitic or glassy, names based upon chemical composition are necessary for consistency. Because the middle Tertiary volcanic rocks of the San Juan field tend to form a single variation series ranging from mafic to silicic (Lipman and others, 1969, fig. 3), it has seemed expedient to divide this series somewhat arbitrarily by percent SiO₂:

| Rock name | Percent SiO ₂ | see p 49 Nockolds, Wox, Chinner |
|---------------------|--------------------------|------------------------------------|
| Basalt | <52 | |
| Andesite | 52-60 | |
| Rhyodacite | 60-65 | |
| Quartz latite | 65-70 | rhyd. |
| Rhyolite | >70 | |

These simple divisions have the advantage for the San Juan rocks of coinciding approximately with phenocryst variations recognizable in the field (fig. 3). Where chemical analyses are not available, rocks are classified by petrographic similarity to analyzed samples; in uncertain cases, terms such as "basaltic," "intermediate-composition," and "rhyolitic" are used in a loose sense. Such usage should be apparent in context. Mineral-name modifiers are used only for rocks containing the minerals as phenocrysts, but the term "quartz latite" is used for a specific compositional type whether or not phenocrystic quartz is present.

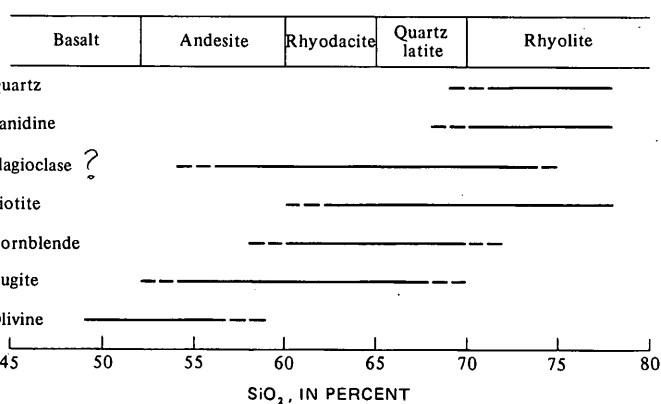


FIGURE 3.—Approximate relations between SiO₂ content and phenocryst constituents of volcanic rocks of the southeastern San Juan Mountains, as related to volcanic rock names used in this report.

Natural remanent magnetic polarities of many of the volcanic units, including all the major ash-flow sheets, were determined in the field during 1966-67 by use of a portable transistorized fluxgate magnetometer (Doell and Cox, 1962). At each locality, determinations were made on three to five oriented samples, collected at 10- to 20-m intervals along the outcrop; determinations were made at as many as 30 localities for a single volcanic unit. The measurements, though neither exceptionally sensitive nor precise, were clearly consistent—especially for the ash-flow tuffs—except for a few outcrops that probably were lightning struck. Numerous polarity changes were found within the ash-flow sequence (table 3), and the polarity determinations have provided a valuable confirmatory correlation technique. The field polarity determinations of many of the units have been confirmed by more precise laboratory determinations (M. E. Beck, Jr., and James Diehl, written commun., 1971).

All isotopic ages reported here for rocks of the southeastern San Juan Mountains were determined by H. H. Mehnert of the U.S. Geological Survey, unless indicated otherwise; most of the radiometric results have already been reported elsewhere (Steven and others, 1967; Lipman and others, 1970; Mehnert and others, 1973). In relating the radiometric ages to Cenozoic time units, the Geological Society of London Phanerozoic time scale (Harland and others, 1964, p. 26) has been used.

I especially thank my colleague Thomas A. Steven, with whom many of the regional interpretations were jointly developed; without his recurrent encouragement and friendly criticism this study might never have been undertaken and certainly would have been less adequately completed.

GEOLOGIC SETTING

The San Juan volcanic field, which covers about 25,000 km² in southwestern Colorado and adjacent parts of New Mexico (fig. 1), is the largest erosional remnant of a once nearly continuous volcanic field that extended over much of the southern Rocky Mountains in Oligocene and later time (Steven and Epis, 1968). Throughout the San Juan remnant of this volcanic field, the general volcanic sequence was relatively simple (table 1): initial intermediate-composition lavas and breccias, followed closely in time by more silicic ash-flow tuffs, and ending with a compositionally bimodal association of basalt and rhyolite (Lipman and others, 1970). The general petrology of the main volcanic groupings of the San Juan field can be seen from a histogram of SiO₂ contents (fig. 4).

In the western part of the San Juan region, a Late Cretaceous and Paleocene episode of volcanic activity (Burbank and Lovering, 1933, p. 297-298; Shoemaker, 1956, p. 162; Dickinson and others, 1968), which occurred contemporaneously with Laramide uplift,

TABLE 1.—Generalized Tertiary volcanic stratigraphy of the San Juan Mountains

[Modified from Lipman, Steven, and Mehnert (1970)]

| | |
|---|--|
| LATE BASALTS AND RHYOLITES: | |
| Basalt of the Servilleta Formation (3.6-4.5 m.y.) | |
| Hinsdale Formation | |
| Basalt (4.7-23.4 m.y.) | |
| Rhyolite (4.8-22.4 m.y.) | |
| Sunshine Peak Tuff (ash-flow tuff of Lake City caldera, 22.5 m.y.) | |
| MAIN ASH-FLOW TUFFS: | |
| Snowshoe Mountain Tuff (>26.4 m.y.) | |
| Nelson Mountain Tuff | |
| Rat Creek Tuff | |
| Waso Park Tuff | |
| Mammoth Mountain Tuff (26.7 m.y.) | |
| Carpenter Ridge Tuff | |
| Fish Canyon Tuff (27.8 m.y.) | |
| Masonic Park Tuff (28.2 m.y.) | |
| Sapinero Mesa Tuff | |
| Dillon Mesa Tuff | |
| Blue Mesa Tuff | |
| Tuff of Ute Ridge (28.4 m.y.) | |
| Treasure Mountain Tuff | |
| Ra Jadero Member | LAVAS AND RELATED ROCKS ERUPTED CONCURRENTLY WITH THE ASH-FLOW TUFFS: |
| Ojito Creek Member | Local andesitic to quartz latitic flows and breccias that intertongue with the ash-flow sequence in and near their source calderas; Fisher Quartz Latite (26.4 m.y.) overlies the entire ash-flow sequence |
| La Jara Canyon Member (29.8 m.y.) | |
| Tuff of Rock Creek | |
| EARLY INTERMEDIATE LAVAS AND BRECCIAS: | |
| Andesitic to quartz latitic rocks of the Conejos Formation and related units (31.1-34.7 m.y.) | |

preceded the middle Tertiary volcanism. Because both igneous suites are dominated by intermediate compositional types, they are not easily separated in some places.

Following Laramide upwarping of the Uncompahgre arch, Needle Mountain uplift, San Luis highlands, and related structures in early Tertiary time, the sedimentary cover was eroded from the upwarped areas; and aprons of fluvial gravel, sand, and clay of the Telluride Conglomerate and Blanco Basin Formation were deposited around the margins. The age and interrelations of these formations have never been determined with certainty, but in recent years both the Telluride and the Blanco Basin have been correlated, on lithology and stratigraphic position, with the San Jose Formation of early Eocene age in the central part of the San Juan Basin (Kelley, 1952; Van Houten, 1957; Dunn, 1964).

After deposition of the Telluride and Blanco Basin sediments, volcanism broke out over an area larger than the now-preserved San Juan volcanic field. Initially, intermediate-composition lavas and breccias were erupted from numerous local volcanoes. Most centers erupted monotonously uniform sequences of alkali andesite, rhyodacite, or mafic quartz latite, but a few produced rocks ranging from basaltic andesite to rhyolite (Lipman, 1968). Basalt is absent or extremely rare. These early intermediate-composition rocks constitute about two-thirds of the volume of the San Juan field, were deposited over more than 25,000 km², and probably had an original volume of at least 40,000 km³ (cubic

kilometers). They were formed mostly during the interval 35-30 m.y. (million years) ago (Lipman and others, 1970). In the southeastern San Juan Mountains such rocks have been collectively designated the Conejos Formation (Cross and Larsen, 1935, p. 69).

About 30 m.y. ago, major volcanic activity changed to explosive ash-flow eruptions of quartz latite and low-silica rhyolite that persisted until about 26 m.y. ago. More than 16 separate ash-flow sheets have been recognized (table 1); the source areas for these sheets are marked by at least 14 large calderas (fig. 1) in the western and central San Juan Mountains (Steven and Ratté, 1965; Luedke and Burbank, 1968; Steven and Lipman, 1968). The original extent of the ash-flow tuffs (about 25,000 km²) was similar to that of the early intermediate lavas, but their volume (about 20,000 km³) was only about half as great. Some individual ash-flow

sheets were very large, spreading over as much as 15,000 km² and having a volume as great as 3,000 km³.

Intermediate to silicic lava flows and breccias are interlayered with and overlie the ash-flow sequence (table 1). Although difficult to estimate because of irregular distribution and extensive erosion, the initial volume of these lavas probably aggregated between 5,000 and 10,000 km³. Some of the lavas adjacent to caldera-collapse structures are petrographically and chemically similar to the ash-flow tuffs and are clearly related genetically to the pyroclastic rocks. Other more mafic lavas that are indistinguishable lithologically from the early intermediate-composition lavas and breccias are also interlayered with the ash-flow sequence, and they represent a continuation and waning of the early type of eruptions. Some of these are spatially unrelated to the caldera sources of the ash-flow eruptions, but several of the calderas—Platoro, Uncompahgre, San Juan, and probably Bonanza—were filled to overflowing by such rocks after collapse.

A few small epizonal stocks and laccoliths cut the volcanic pile, especially near the margins of calderas in the northern, western, and southeastern parts of the volcanic field; numerous dikes and less regular satellite intrusions radiate outward from some of these bodies. Although Larsen and Cross (1956, pl. 1) thought most of these intrusives to be comparable in age with the early intermediate lavas and breccias, some of the stocks intrude the ash-flow sequence in both the western (Bromfield, 1967, p. 57) and the southeastern San Juan Mountains and are demonstrably younger. The intrusive rocks are mainly monzonites and granodiorites; they are chemically similar to the early intermediate flows and breccias, and distinctly less silicic than most rocks of the ash-flow sequence.

Locally associated with these caldera-margin intrusives and similarly situated postcollapse lavas are striking areas of hydrothermal alteration and important Pb-Zn-Ag-Au-Cu-Mo mineralization, especially in the Silverton-Ouray area, at Creede, and near Summitville. Mineralization in the San Juan region appears to correlate with the margins of calderas that are characterized by complex postcollapse structural features and igneous activity (Steven, Luedke, and Lipman, 1974).

Near the end of the period of major ash-flow eruptions, both tectonic environment and nature of volcanic activity changed notably. The eastern part of the volcanic field was broadly warped, regionally faulted, and tilted to the east in response to initial development of the Rio Grande rift depression (Lipman and Mehnert, 1969). Near the Platoro caldera complex this deformation also produced a broad anticline, which plunges gently to the northeast from near Summitville to the vicinity of Del Norte. Southeast of the anticlinal axis the volcanic se-

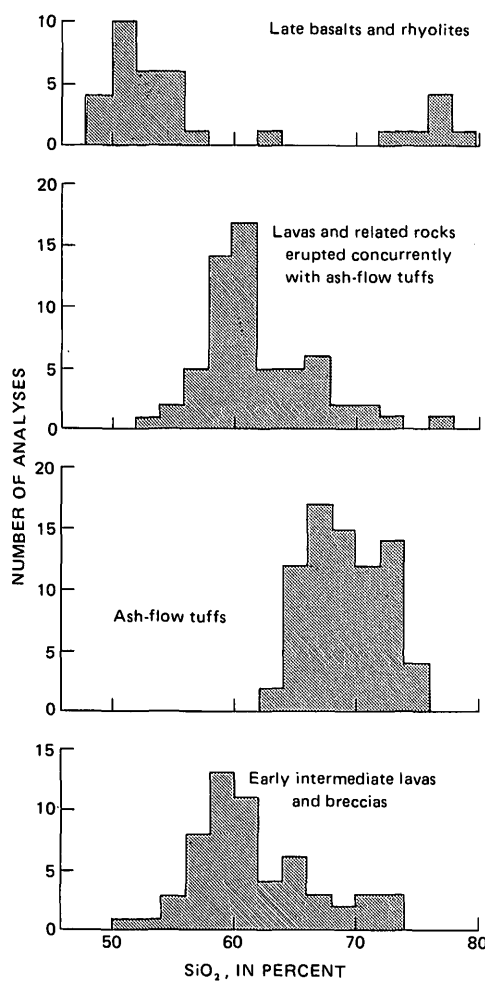


FIGURE 4.—Histograms of SiO₂ contents for major divisions of Tertiary volcanic rocks in the San Juan Mountains. Histogram interval is 2 percent SiO₂. Analyses are from Larsen and Cross (1956), Varnes (1963), Bromfield (1967), Ratté and Steven (1967), Olson, Hedlund, and Hansen (1968), Doe, Lipman, Hedge, and Kurasawa (1969), and Lipman (1968, 1969, this report).

quence dips 5°-10° to the east, toward the San Luis Valley; northwest of the axis the sequence dips about 10° to the north, toward the valley of the Rio Grande. This broad deformation has important effects on the levels of exposure within the Platoro caldera complex: in general, higher structural levels are exposed on the east and north sides, lower levels on the west and south sides.

Concurrently with this deformation, widespread basalt and local silicic alkali rhyolite flows were emplaced (fig. 4). Most of these rocks constitute the Hinsdale Formation, which is mainly alkali olivine basalt and basaltic andesite, with associated small scattered rhyolite plug domes, ranging in age from about 24 to 5 m.y. The youngest major ash-flow sheet in the San Juan field, erupted from the Lake City caldera about 22.5 m.y. ago (H. H. Mehnert, written commun., 1971; see also Lipman and others, 1970, p. 2344), is petrographically similar to rhyolites of the Hinsdale Formation and can be considered as part of the same volcanotectonic assemblage. Basaltic lavas of the Hinsdale Formation range from scattered highly eroded remnants in central parts of the field to widespread sheets surrounded by relatively less eroded cinder cones near the Rio Grande along the southeast margin of the field. These upper Cenozoic basalt flows, now much eroded, probably originally covered 15,000-20,000 km², but total volume may have been no more than 1,000 km³. The rhyolites of the Hinsdale Formation, except for the ash-flow sheet from Lake City caldera, were relatively minor, with an initial area of a few hundred square kilometers and volume of a few tens of cubic kilometers.

A younger sequence of largely tholeiitic basalts, the Servilleta Formation, accumulated within the Rio Grande depression adjacent to the southeastern part of the San Juan Mountains from about 4.5 to 3.5 m.y. ago (Ozima and others, 1967; Aoki, 1967; Lipman, 1968).

The marked change between the Oligocene intermediate to low-silica rhyolitic magmas and the later bimodal basaltic and rhyolitic magmatic association in the San Juan field and adjacent parts of the southern Rocky Mountains implies different conditions of magma generation for the two suites. This petrologic change coincides approximately with initial nearby development of the Rio Grande depression, a major rift that is the local expression of widespread late Cenozoic crustal extension. Progression from predominantly intermediate eruptions to bimodal basalt-rhyolite volcanism, approximately concurrent with initiation of late Tertiary crustal extension, is characteristic of much of western Cordilleran North America. This intracontinental volcanotectonic transition seems to correlate with times at which tectonic boundaries between North American and Pacific plates underwent drastic changes (Christiansen and Lipman, 1972).

PREVOLCANIC ROCKS

Two small outcrops of Precambrian granite gneiss, exposed along the lower Conejos River valley (Durango map), are the tops of hills buried by the middle Tertiary volcanic rocks; a more extensive terrane of Precambrian crystalline rocks is exposed beneath the volcanics 30 km to the south, in the Tusas Mountains of New Mexico (Barker, 1958; Bingler, 1968; Butler, 1971).

Cretaceous sedimentary rocks, including the Dakota Sandstone, Mancos Shale, Mesaverde Formation, Lewis Shale, Pictured Cliffs Sandstone, Fruitland Formation, and Kirtland Shale (Dunn, 1964; Durango map), are widely distributed around the southwest margin of the San Juan Mountains, where the mountains merge with the San Juan Basin. The Cretaceous and Tertiary Animas Formation, consisting of interbedded shale, arkosic sandstone, and conglomerate, locally contains abundant volcanic detritus of andesitic to rhyolitic composition that records a Late Cretaceous episode of volcanism (Larsen and Cross, 1956, p. 56).

After Laramide deformation in Late Cretaceous and early Tertiary time that produced dips of the Animas Formation locally as high as 50° (Platoro map), the uplifted sedimentary cover was eroded, and non-volcanic sediments of the Blanco Basin Formation were deposited around the margins of the highlands. The Blanco Basin Formation apparently formed as discontinuous valley-fill deposits, with the Tertiary volcanic rocks in places resting directly on older deformed sedimentary rocks.

EARLY INTERMEDIATE-COMPOSITION ROCKS (CONEJOS FORMATION)

All the early intermediate-composition lavas and breccias in the southeastern San Juan Mountains were assigned by Cross and Larsen (1935, p. 69) to the Conejos Formation, named for the great cliff exposures in the Conejos River Canyon. As thus defined, the Conejos Formation is similar in age and petrology to other named formations elsewhere in the San Juan volcanic field—including the San Juan and the Lake Fork Formations in the western part of the volcanic field and the West Elk Breccia at the north edge of the field (Lipman and others, 1970). Equivalent early intermediate rocks in the northeastern part of the field include the Beidell and Tracy Creek Quartz Latites (Larsen and Cross, 1956, p. 83-86) and the Rawley Andesite and other unnamed rocks of the Bonanza area (Burbank, 1932).

The early intermediate-composition rocks of the Conejos Formation were erupted from numerous volcanoes in the southeastern San Juan Mountains. Individual centers mostly erupted monotonously uniform sequences of alkali andesite, rhyodacite, or mafic quartz latite, although at a few volcanoes the rocks range from

basaltic andesite to rhyolite (Lipman, 1968). Flanking the central volcanoes are volcaniclastic sedimentary rocks of the Conejos Formation that reflect penecontemporaneous erosion of the constructional volcanic topography; these clastic rocks represent approximately half the volume of the Conejos Formation. Accordingly, the Conejos Formation has been divided into a vent facies, consisting principally of lava flows, flow breccias, and explosion breccias that represent the primary products of the early-intermediate volcanic activity, and a volcaniclastic facies, consisting of the mudflow breccias, conglomerates, and other volcanic sedimentary deposits that resulted from erosion of the central volcanoes (fig. 5). Two additional local units of stratigraphic and structural significance, which are in essence subdivisions of the vent facies, are separated on the Platoro map: a thick local accumulation of cone breccias that mark a major vent on the southwest side of the Platoro caldera and an upper lava unit that interfingers with or overlies the Tuff of Rock Creek and the lower tuff of the Treasure Mountain Tuff.

Rocks of the volcaniclastic facies tend to fill in the basins and other topographically low regions between the central volcanoes, but the two facies of the Conejos Formation are penecontemporaneous and tend to interfinger complexly in map pattern. Such interfingering was only locally worked out in detail for the Platoro and Durango maps. In general, areas that contain more than about 50 percent primary volcanic products have been mapped as vent facies, because minor sedimentary interbeds between thick lava flows are typically poorly exposed. In contrast, areas mapped as volcaniclastic facies consist overwhelmingly of reworked sedimentary material, as local lavas and flow breccias tend to be conspicuous in such sequences and therefore are easily mapped separately. Although the division of the Conejos Formation into vent and volcaniclastic facies is relatively crude in comparison with the delineation of other mapped units, this distinction serves well to identify the approximate locations of Conejos volcanoes and provides insight into the volcanic topography before eruption of the ash-flow sheets.

The Conejos Formation was deposited on a surface of substantial local relief, and the underlying rocks range in age from Tertiary to Precambrian. In places the Conejos Formation rests on the Eocene Blanco Basin Formation, the Tertiary and Cretaceous Animas Formation, the Cretaceous Lewis Shale, or Precambrian crystalline rocks. The Animas and the Lewis were deformed—they dip as much as 50° (Platoro map)—and were eroded before deposition of the subhorizontal Blanco Basin and Conejos Formations. Along the East Fork of the San Juan River, just above the junction with Quartz Creek, mudflow deposits of basal Conejos Formation appear to

have covered a middle Tertiary hill of Lewis Shale and Animas Formation. Others have interpreted this contact as a fault (Dunn, 1964; Sinclair, 1963); but excellent exposures along the stream channel indicate that the contact is extremely irregular, having variations in strike of as much as 60°. Along the lower Conejos River, rocks of the Conejos Formation were deposited around and over hills of Precambrian granite gneiss having more than 150 m of exposed relief; and 20 km to the south, along the canyon of Rio de los Pinos in New Mexico, the Conejos Formation buried a rugged Precambrian terrane which had at least 300 m of relief (Butler, 1971, p. 294). The lower contact of the Conejos Formation along the southwest front of the San Juan Mountains is commonly obscured by landslides.

Andesite and rhyodacite lava flows 10-50 m thick are the predominant compositional types of the Conejos Formation, which has less voluminous amounts of more silicic rocks. Most of the lava flows are entirely devitrified, and the predominant colors of rocks are various shades of dark gray, brown, and red. Basal vitrophyres occur only in silicic rhyodacite and more leucocratic rocks. Basal flow breccias are common, and in places much of the flow appears pervasively autobrecciated. These lava types also make up the fragmental constituents of the volcaniclastic facies.

Ash-flow tuff is very rare in the Conejos Formation, constituting much less than 1 percent of the unit by volume. The few tuffs recognized are typically weakly welded, less than 10 m thick, and traceable laterally for only a few hundred meters. They are phenocryst poor and probably are rhyodacitic in composition. One such tuff is well exposed in a roadcut along the Conejos River road immediately south of the southern Platoro quadrangle boundary.

The eight analyzed rocks of the Conejos Formation range from 53.8 to 67.0 percent SiO₂ (table 2). A more volumetrically representative sampling would probably show that the bulk of the early intermediate rocks are within a more restricted compositional range, between about 57 and 62 percent SiO₂, with a mean near 60 percent SiO₂ (fig. 4).

The Conejos Formation and equivalent formations are largely or entirely Oligocene in age, as indicated by K-Ar results for nine samples from seven different centers in the San Juan field, which range in age from 31.1 to 35.0 m.y. (Lipman and others, 1970, table 2). Three of these ages are from the Conejos Formation within the area of this report (fig. 5): 32.4 m.y. for biotite and hornblende from a rhyodacite flow breccia at Navajo Peak, 32.4 m.y. for biotite from a rhyolite dike at Summer Coon volcano, and 31.1 m.y. for plagioclase from an andesite flow at Snowball Park. Although none of these samples necessarily represents the actual beginning of volcanic

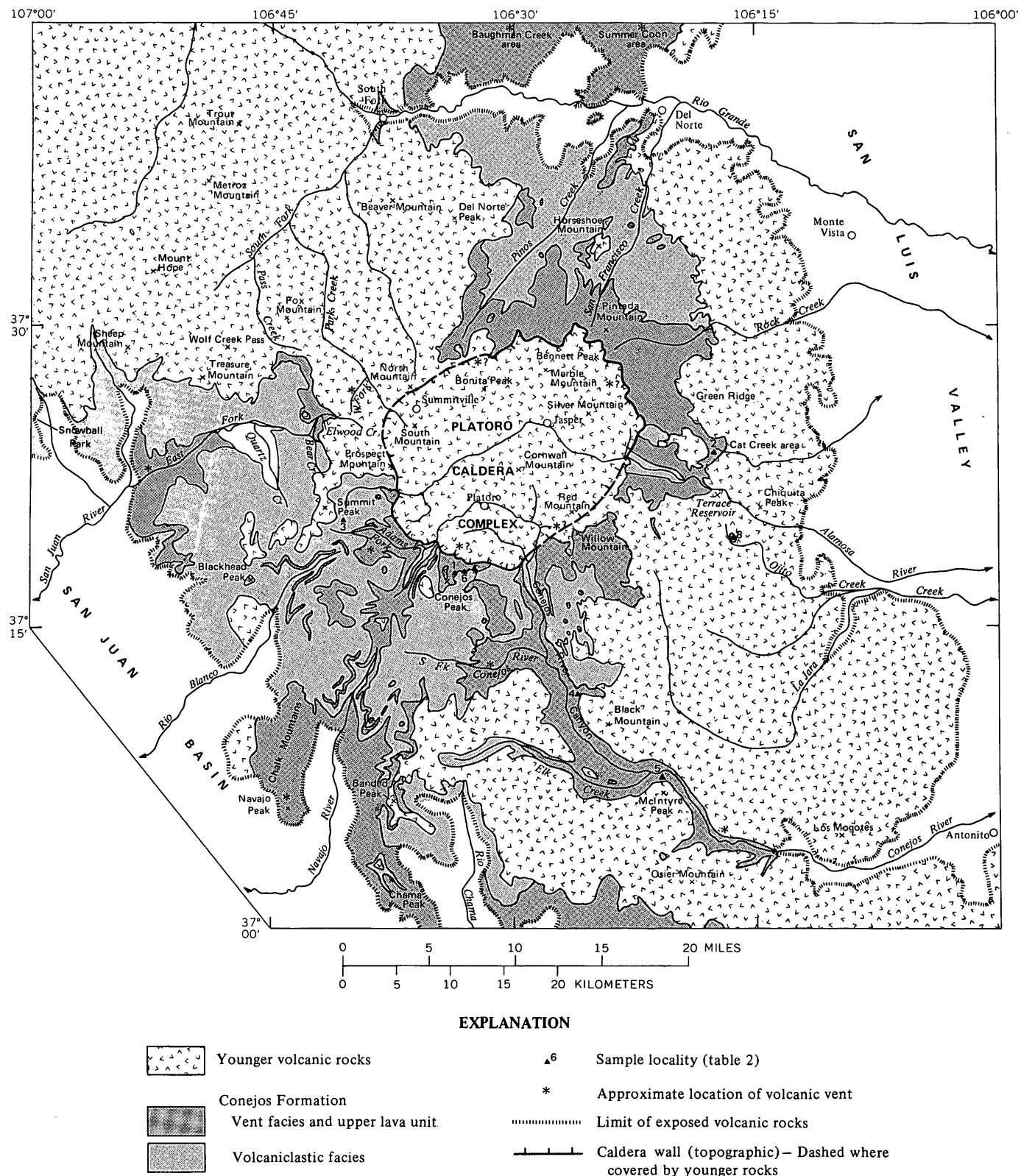


FIGURE 5.—Outcrop areas of the vent facies and volcaniclastic facies of the Conejos Formation, southeastern San Juan Mountains. Based on mapping by P. W. Lipman, 1965-67, 1970-71.

TABLE 2.—Analyses of lava flows of the Conejos Formation

[Sample localities shown in fig. 5. Analyses 3-5 are from Larsen and Cross (1956, table 21). Other major-oxide analyses are by rapid methods by P. L. D. Elmore, Samuel Botts, Gillison Chloe, Lowell Artis, H. Smith, John Glenn, and James Kelsey. Minor-element analyses 2 and 8 are by quantitative methods by Norma Rait; remaining analyses are by J. D. Fletcher. <, less than; leaders (. .), looked for but not found]

| Sample----- Field No.----- Lab. No.----- | Vent facies | | | | | | | Upper lava unit 8 66L-16 W168530 |
|--|--|------------------------|---------------------|----------------------|----------------------|-----------------------|-----------------------|---|
| | 1 71J-6 W176172 | 2 70L-32 W174434 | 3 SV113 ----- | 4 Con262 ----- | 5 Con591 ----- | 6 71J-7 W176173 | 7 71J-8 W176174 | |
| | Major oxides (weight percent), recalculated without H ₂ O and CO ₂ (original values listed separately below) | | | | | | | |
| SiO ₂ ----- | 53.8 | 55.7 | 58.95 | 60.62 | 61.23 | 63.3 | 67.0 | 59.8 |
| Al ₂ O ₃ ----- | 16.7 | 17.0 | 16.57 | 16.26 | 17.71 | 17.3 | 16.7 | 18.3 |
| Fe ₂ O ₃ ----- | 4.1 | 4.9 | 3.95 | 4.82 | 5.48 | 3.4 | 2.9 | 5.6 |
| FeO----- | 5.8 | 4.2 | 3.61 | 2.25 | .56 | 1.4 | .61 | 1.1 |
| MgO----- | 4.4 | 3.1 | 2.82 | 2.22 | 2.01 | 1.7 | .86 | 1.4 |
| CaO----- | 8.3 | 6.2 | 6.58 | 6.39 | 5.73 | 3.7 | 1.7 | 5.8 |
| Na ₂ O----- | 3.1 | 3.4 | 3.38 | 3.70 | 3.23 | 4.3 | 4.3 | 3.4 |
| K ₂ O----- | 2.0 | 3.1 | 2.64 | 2.65 | 2.97 | 4.0 | 5.2 | 3.1 |
| TiO ₂ ----- | 1.2 | 1.4 | 1.02 | 1.00 | .64 | .69 | .56 | 1.1 |
| P ₂ O ₅ ----- | .43 | .81 | .36 | ----- | .32 | .14 | .10 | .27 |
| MnO----- | .20 | .21 | .11 | .10 | .11 | .13 | .08 | .06 |
| TOTAL----- | 100.03 | 100.02 | 99.99 | 100.01 | 99.99 | 100.06 | 100.01 | 99.93 |
| H ₂ O+----- | .60 | 1.8 | .72 | .12 | 1.64 | .50 | .50 | .70 |
| H ₂ O----- | 1.3 | .65 | .80 | .44 | .46 | 1.1 | 1.6 | .80 |
| CO ₂ ----- | <.05 | 1.1 | .00 | .00 | ----- | .12 | <.05 | <.05 |
| Norms (weight percent) | | | | | | | | |
| Quartz----- | 5.37 | 8.20 | 12.79 | 14.51 | 17.00 | 13.43 | 17.33 | 14.80 |
| Orthoclase----- | 11.55 | 18.39 | 15.62 | 15.65 | 17.53 | 23.46 | 30.82 | 18.14 |
| Albite----- | 26.11 | 28.97 | 28.57 | 31.31 | 27.34 | 36.17 | 36.35 | 28.58 |
| Anorthite----- | 25.85 | 21.87 | 22.26 | 19.92 | 25.06 | 16.30 | 7.96 | 25.76 |
| Wollastonite----- | 5.29 | 1.56 | 3.36 | 4.92 | .54 | .40 | ----- | .60 |
| Eustatite----- | 11.01 | 7.75 | 7.01 | 5.59 | 4.99 | 4.31 | 2.14 | 3.57 |
| Ferrasilite----- | 5.50 | 1.75 | 1.89 | ----- | ----- | ----- | ----- | ----- |
| Magnetite----- | 5.97 | 7.07 | 5.72 | 4.66 | .31 | 3.02 | .61 | .56 |
| Hematite----- | ----- | ----- | ----- | 1.60 | 5.27 | 1.28 | 2.44 | 5.24 |
| Ilmenite----- | 2.34 | 2.56 | 1.94 | 1.91 | 1.22 | 1.31 | 1.07 | 2.14 |
| Apatite----- | 1.02 | 1.92 | .85 | ----- | .75 | .34 | .24 | .63 |
| Minor elements (parts per million) | | | | | | | | |
| B----- | ----- | ----- | ----- | ----- | ----- | ----- | ----- | ----- |
| Ba----- | 560 | 2400 | ----- | ----- | 1500 | 1100 | 1400 | ----- |
| Be----- | ----- | <2 | ----- | ----- | ----- | ----- | ----- | ----- |
| Ca----- | ----- | ----- | ----- | ----- | ----- | ----- | ----- | ----- |
| Co----- | 24 | 16 | ----- | ----- | ----- | ----- | ----- | <4 |
| Cr----- | 58 | 59 | ----- | ----- | 3 | 2 | 2 | ----- |
| Cu----- | 66 | 490 | ----- | ----- | 21 | 5 | 17 | ----- |
| Ga----- | 20 | 20 | ----- | ----- | 20 | 20 | 30 | ----- |
| La----- | 100 | ----- | ----- | ----- | 80 | 100 | ----- | ----- |
| Mo----- | ----- | ----- | ----- | ----- | ----- | ----- | ----- | ----- |
| Nb----- | 30 | ----- | ----- | ----- | 20 | 20 | ----- | ----- |
| Ni----- | 16 | 17 | ----- | ----- | ----- | ----- | <4 | ----- |
| Pb----- | 20 | ----- | ----- | ----- | 10 | 10 | 34 | ----- |
| Sc----- | 40 | 22 | ----- | ----- | 14 | 10 | 5 | ----- |
| Sn----- | ----- | ----- | ----- | ----- | ----- | ----- | 40 | ----- |
| Sr----- | 2000 | 480 | ----- | ----- | 680 | 390 | 360 | ----- |
| V----- | 300 | 180 | ----- | ----- | 80 | 20 | 60 | ----- |
| Y----- | 40 | <40 | ----- | ----- | 30 | 30 | 30 | ----- |
| Yb----- | 2 | 4 | ----- | ----- | 3 | 3 | ----- | ----- |
| Zr----- | 100 | 370 | ----- | ----- | 280 | 200 | 320 | ----- |
| Phenocrysts (volume percent) | | | | | | | | |
| Plagioclase----- | 3 | 17 | 18 | 33 | 25 | 13.1 | 11.6 | 9.8 |
| Biotite----- | ----- | ----- | ----- | ----- | ----- | 2.9 | 3.2 | ----- |
| Hornblende----- | ----- | ----- | 1.5 | ----- | 10 | .2 | ----- | ----- |
| Augite----- | ----- | 2 | 3 | 2.5 | .5 | 1.2 | ----- | 1.6 |
| Hypersthene----- | ----- | ----- | 2 | 3.5 | .5 | ----- | ----- | ----- |
| Opalites----- | ----- | 1 | 1.5 | 2 | 4 | .9 | 1.1 | .9 |
| Groundmass----- | 97 | 80 | 74 | 59 | 60 | 81.7 | 84.1 | 87.7 |

SAMPLE DESCRIPTIONS

- Dense dark-gray basaltic andesite, containing sparse small (1-2 mm) tabular phenocrysts of plagioclase (An₄₀₋₅₀), set in a coarsely microcrystalline intergranular groundmass of plagioclase, augite, opaques, and iddingsite pseudomorphs after olivine. Saddle Creek road, at 11,400 ft.
- Gray platy plagioclase andesite, containing about 20 percent phenocrysts. (See fig. 6B.) Tabular euhedral plagioclase phenocrysts (An₄₀₋₅₀) are as much as 1 cm long and are charged with small inclusions of glass and other phenocrysts. Some carbonate is present, replacing both phenocrysts and groundmass, as is typical for this rock type. Cat Creek road, north side of Cat Creek, at about 8,800 ft.
- Gray pyroxene andesite, in which all phenocrysts are less than 1 mm across. "Near the head of the Alamosa River, and about 1 mile southeast of Summit Peak" (Larsen and Cross, 1956, table 21, No. 11). Vent-facies assignment of this sample is uncertain.
- Dark-red-brown pyroxene-hornblende rhyodacite, containing "abundant white plagioclase in stout tablets about 1 mm long,
- and some pyroxene * * * along sheep trail near crest of Nigger [Black] Mountain, at altitude of 10,000 feet" (Larsen and Cross, 1956, table 21, No. 12).
- Dark-red-brown hornblende rhyodacite. "The north base of McIntyre Point [Peak]" (Larsen and Cross, 1956, table 21, No. 15).
- Gray porphyritic rhyodacite, containing phenocrysts of plagioclase (An₄₀₋₅₀) as much as 4 mm in diameter, set in a microcrystalline intergranular groundmass. Biotite is oxidized, and hornblende is brown and resorbed. Saddle Creek road, at just above 11,000 ft.
- Red-brown porphyritic quartz latite, containing phenocrysts of plagioclase (An₃₅₋₅₀) as much as 3 mm in diameter, set in a fine-grained pilotaxitic groundmass. Chemically anomalous: high K₂O and low CaO. This flow immediately underlies flow of No. 6. Saddle Creek road, at just below 11,000 ft.
- Dark-brownish-gray andesite, containing small phenocrysts less than 1 mm in diameter, set in a fine-grained pilotaxitic ground mass. 1.3 km south of Jacobs Hill on 8,912-ft knob

activity in middle Tertiary time, the samples do suggest that most of the early intermediate-composition activity was during a very restricted span of time. A limit on the termination of Conejos volcanism is provided by a date of 29.8 m.y. for the overlying La Jara Canyon Member of the Treasure Mountain Tuff (Lipman and others, 1970, table 3, No. 1).

VENT FACIES

As mapped, the vent facies of the Conejos Formation consists mainly of intermediate-composition lava flows, flow breccias, and explosion breccias from widely scattered central volcanoes. Interbedded with these rocks are volcaniclastic sedimentary rocks that are too thin or poorly exposed to map separately. These Oligocene central volcanoes were extensively eroded and largely mantled in their own debris shortly after formation.

Perhaps the most conspicuous volcanoes of the Conejos Formation are the Summer Coon and Baughman Creek centers at the north edge of the area of this report (fig. 5; Durango map; Lipman, 1968), where erosion has exposed spectacular dikes radiating outward from central stocks, which are flanked by outward dipping lavas. These two Conejos volcanoes are also distinctive in that they contain a variety of lava types ranging from basaltic andesite to rhyolite (52-73 percent SiO_2 ; Lipman, 1968; Mertzman, 1971). At each volcano, however, most of the exposed rock is monotonous olivine andesite (56-58 percent SiO_2), forming a crudely stratified cone of explosion breccia that intertongues with minor lavas on the lower flanks. After a period of quiescence marked by erosion of the andesitic cone, volumetrically minor rhyolite was erupted first, then varied quartz latitic and rhyodacitic lava types (Lipman, 1968). This late sequence is thought to reflect progressive eruption of the fractionated upper part of a magma chamber of predominantly andesitic composition.

The Platoro caldera appears to have formed within a cluster of five or more Conejos volcanoes, parts of which have been caved away by caldera collapse. These Conejos volcanoes tend to be petrologically uniform, having few clearly comagmatic intrusives at present levels of exposure. In general, intrusives of Conejos age are difficult to distinguish from the numerous younger intrusives that are clearly related to the postcaldera activity. These Conejos volcanoes have not been studied in detail, and only general aspects of their compositional variations and primary constructional geometry are known.

In the thick pile of Conejos lavas east of the caldera, from the Alamosa River to the head of Rock Creek (fig. 5), the predominant lava type is a distinctive dark-gray andesite that contains large tabular phenocrysts of labradorite (fig. 6B). Interlayered with these lavas are sparsely porphyritic gray andesites and, high in the sequence, red-brown lavas that contain small phenocrysts

of plagioclase and augite, that are of more silicic appearance, and that may be rhyodacites. The vent for this near-source accumulation has not been determined with confidence, but it probably lay within the collapsed eastern side of Platoro caldera (fig. 5).

The thick accumulation of lava flows north of the caldera, in the Pinos Creek and San Francisco Creek areas, also appears to represent the flanks of a large stratovolcano centered farther south, within the caldera area (fig. 5). These lavas are petrographically different from those to the east and consist of light-brown to gray hornblende-bearing rhyodacitic lavas associated with brown or red-brown augite-plagioclase rhyodacites or andesites.

West of the caldera the vent-facies lavas and breccias near the top of the formation consist largely of platy-plagioclase andesite (fig. 6A) like that east of the caldera. These lavas represent the thin margin of a late volcano that must have had its center farther to the northeast.

On the southwest side of Platoro caldera, in the Adams Fork area; a cone of andesitic explosion breccia about 5 km in diameter is largely mantled by mudflow breccias of the volcaniclastic facies (Platoro map; fig. 5). The dominant rock type of the Adams Fork cone is gray to brown andesite that either is nonporphyritic or contains sparse small phenocrysts of plagioclase and augite. The cone breccias of explosive origin are monolithologic, angular to subrounded, crudely bedded and sorted, and largely lacking in fine-grained matrix. They dip outward 10°-35° from a central area (fig. 7A, 7B). In places the explosion breccias, especially the vesicular varieties, are indurated and agglutinated—apparently as a result of deposition while still hot (fig. 7C). Interlayered with the explosion breccias of the cone complex are local bedded fine-grained tuff and, in places, mudflow breccias that differ from the explosion breccia in having poorer sorting and more abundant matrix; in contrast with the regional mudflow deposits of the volcaniclastic facies, these have steep primary dips down the slope of the volcanic cone.

Just south of Platoro caldera on the upper slopes of Conejos Peak, several thick flows of distinctive hornblende-plagioclase rhyodacite dip gently to the south and may represent the south flank of a relatively young Conejos volcano centered to the north within the caldera (fig. 5). In contrast, older, sparsely porphyritic andesitic or rhyodacitic lava flows, which interfinger complexly with mudflow deposits of the volcaniclastic facies on the lower west slope of Conejos Peak, seem to be the northwest flank of a thick pile of sparsely porphyritic andesite or rhyodacite that accumulated to maximum thickness in the South Fork of the Conejos (fig. 5), where individual viscous flows are as much as 150 m thick.

The thick accumulation of vent-facies rocks, near

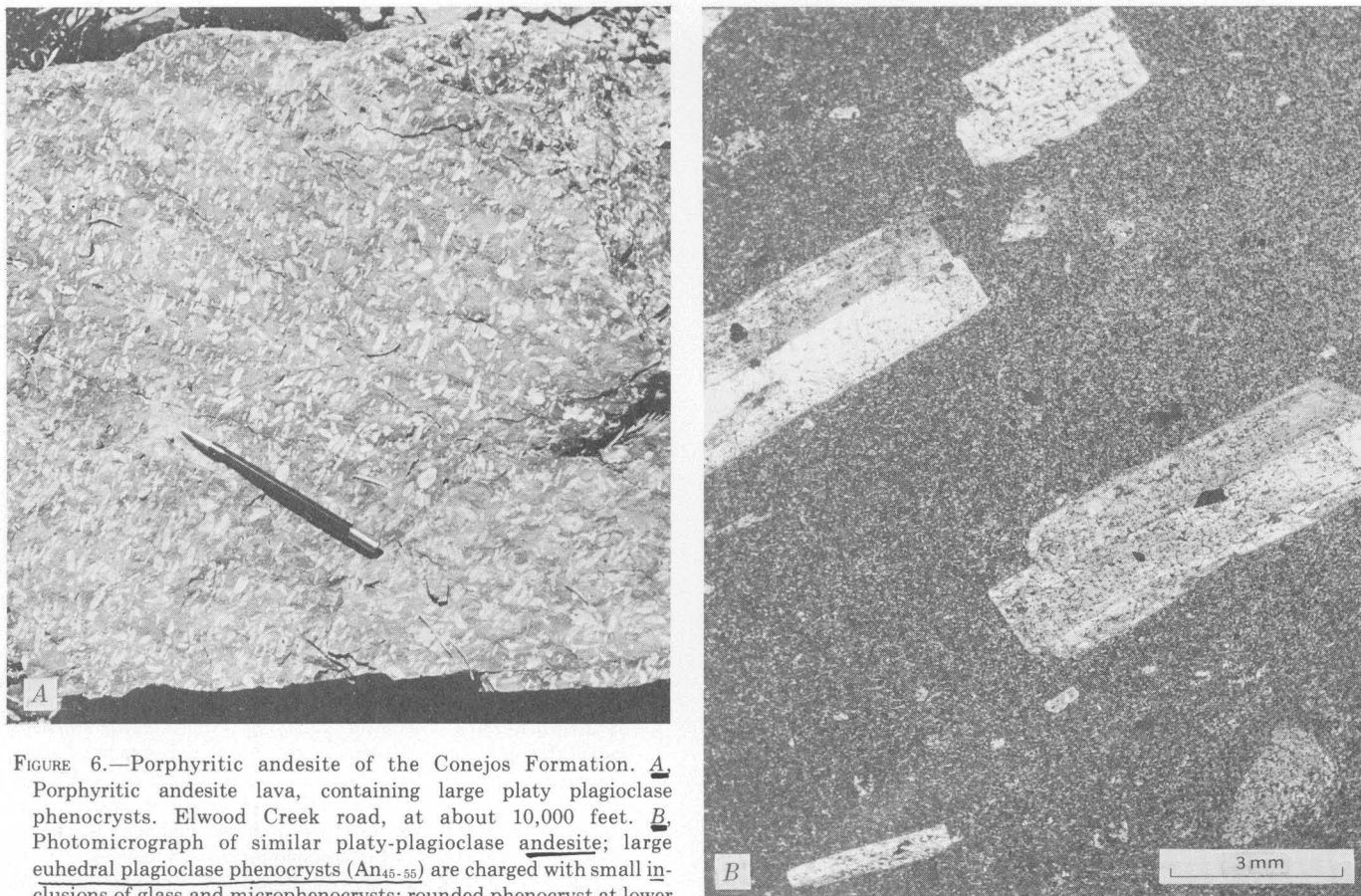


FIGURE 6.—Porphyritic andesite of the Conejos Formation. *A*, Porphyritic andesite lava, containing large platy plagioclase phenocrysts. Elwood Creek road, at about 10,000 feet. *B*, Photomicrograph of similar platy-plagioclase andesite; large euhedral plagioclase phenocrysts (An_{45-55}) are charged with small inclusions of glass and microphenocrysts; rounded phenocryst at lower right is augite. Cat Creek road, north side of Cat Creek at about 8,800 feet. Analyzed sample 2, table 2.

Willow Mountain on the southeast side of the Platoro caldera (fig. 5), apparently represents the southeast flank of another stratovolcano, the center of which lay just within the area of subsequent caldera collapse. These lavas are mainly gray or brown andesite or rhyodacite containing fairly abundant small phenocrysts of augite and plagioclase; hornblende-bearing rhyodacite is present locally.

Other major accumulations of vent facies of the Conejos Formation (fig. 5) include a pile of platy-plagioclase andesite at least 500 m thick centered near the mouth of the East Fork of the San Juan River, a pile of dark andesitic lavas and breccias at least 25 km across in the Chalk Mountains-Navajo Peak-Chama Peak area that was examined only cursorily, and an accumulation of distinctive olivine-augite andesite exposed along the lower Conejos River in Colorado and also near the mouth of Rio de los Pinos just across the State line in New Mexico (Butler, 1971).

VOLCANICLASTIC FACIES

The volcaniclastic facies of the Conejos Formation (fig. 8) consists of mudflow breccias and conglomerates, accompanied by minor amounts of better sorted tuf-

faceous sandstone; all were formed by erosion of the vent-facies rocks just described.

The mudflow deposits are volumetrically by far the most important. They typically are crudely bedded and poorly sorted, having abundant sandy or tuffaceous matrix between heterogeneous angular to rounded blocks. The mudflow breccias differ from explosion breccia of the vent facies in having more abundant matrix, poorer sorting, lithologically heterogeneous fragmental material, and subhorizontal dips. Lithologic variations in the fragmental material from place to place clearly are related to petrology of source rocks, and sufficiently detailed mapping would enable the volcaniclastic facies to be subdivided by provenance.

The mudflow breccias and other volcaniclastic rocks filled topographic depressions between the central volcanoes of the Conejos Formation. In places, monotonous sequences of such sedimentary deposits accumulated to thicknesses in excess of 700 m (fig. 8). Elsewhere, interfingering between vent and volcaniclastic facies is very complex, such as on the west slope of Conejos Peak and in Rio Blanco (Platoro map).

UPPER LAVA UNIT

Lava flows that intertongue with or overlie the tuff of Rock Creek or the lower tuff of the Treasure Mountain

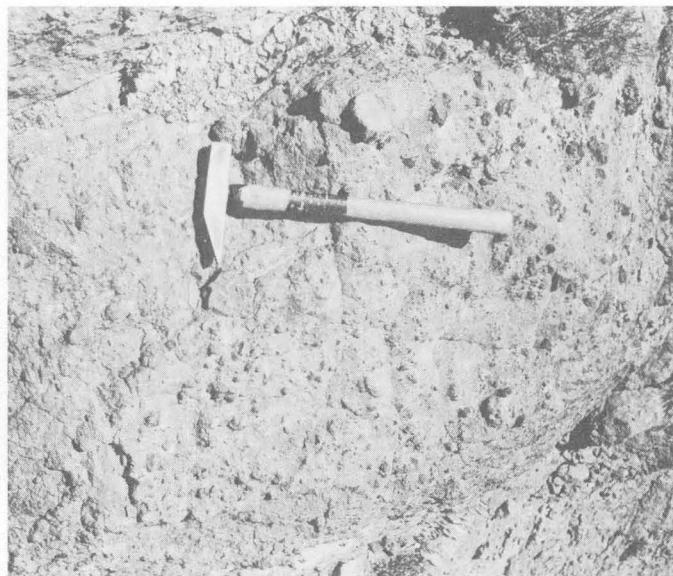


A



B

Tuff locally have been mapped as the upper lava unit of the Conejos Formation to determine important structural and stratigraphic relations near the Platoro caldera complex (Platoro map). Flows of the upper lava unit overlie all rocks of the volcaniclastic facies; in essence, the upper lava unit is part of the vent facies, and its separation into a distinct unit is arbitrary in the sense that it cannot be distinguished petrographically from older rocks of the vent facies and can only be separated from them where ash-flow tuff intervenes. As thus defined, the Conejos Formation includes all intermediate-composition volcanic rocks in the southeastern San Juan Mountains that predate the major collapse of Platoro caldera during eruption of the La Jara Canyon Member of the Treasure Mountain Tuff. The upper lava unit of the Conejos Formation has been recognized at Chama Peak, in the Elk Creek area, north



C

FIGURE 7.—Adams Fork volcano. A, Eroded cone breccia of Conejos Formation, showing steep primary dips. Along Continental Divide, at head of North Fork of Conejos River. B, Typical explosion breccia of Adams Fork volcano, Conejos Formation, showing monolithologic composition, angularity, and crude sorting. Fragments are dense dark-gray andesite. Southeast side of Haskell Rincón, at 11,300 feet. C, Agglutinated explosion breccia, consisting of monolithologic blocks of rounded vesicular red-brown andesite or rhyodacite in fine-grained matrix of same material. At 11,800 feet at end of ridge northeast of triangulation point "Velvet."

of Elwood Creek, south of Pass Creek, west of Bear Creek, south of Del Norte, in the Rock Creek area, north of the Terrace Reservoir, and along Ojito Creek (fig. 5). Typically it consists of only one or two flows of dark-gray or brown sparsely porphyritic andesite or rhyodacite.

ASH-FLOW SHEETS

In contrast to the few small ash-flow tuffs locally interlayered with the early intermediate lavas and breccias of the Conejos Formation the ash-flow tuffs overlying the early intermediate rocks in the southern San Juan Mountains are widespread and numerous. These quartz latitic and rhyolitic ash-flow sheets were derived from the Platoro caldera complex and from younger calderas in the central part of the San Juan volcanic field. Nine of these ash-flow sheets are of sufficient size and importance to be mapped and described separately. Some general petrologic features of these sheets are summarized in table 3.

TUFF OF ROCK CREEK

The tuff of Rock Creek, the oldest sizable ash-flow sheet in the southeastern San Juan Mountains, apparently represents the first significant pyroclastic eruptions from the Platoro area. It is here described as an informal unit, distinguished from the Treasure Mountain



FIGURE 8.—Thick section of the volcaniclastic facies of the Conejos Formation, on the great cliffs east of Summit Creek. Thin rim at top of cliffs is La Jara Canyon Member of Treasure Mountain Tuff; below it is exposed approximately 700 m of crudely sorted and bedded subhorizontal volcaniclastic rocks, mostly mudflow breccias of andesitic and rhyodacitic composition. Photograph taken from Rio Blanco trail at 10,700 feet (Platoro quadrangle).

TABLE 3.—Summary of petrologic features of ash-flow sheets of the southeastern San Juan Mountains

[Magnetic polarity: N, normal; R, reversed]

| Unit | Number of analyses | SiO ₂ content (percent) | Phenocryst content (percent) | Sanidine-plagioclase ratio | Magnetic polarity | Source caldera | K-Ar age (m.y.) |
|-------------------------------------|--------------------|------------------------------------|------------------------------|----------------------------|-------------------|-----------------------------------|-----------------|
| Young ash-flow sheets: | | | | | | | |
| Snowshoe Mountain Tuff ¹ | 3 | 63-67 | 34-58 | 0.01-0.1 | N | Creede | >26.4 |
| Wason Park Tuff ¹ | 6 | 68-72 | 25-38 | .3 - .5 | R | (Near Creede) | <26.7 |
| Carpenter Ridge Tuff | 6 | 61-74 | 5-26 | .2 - 5.0 | R | Bachelor | >26.7 |
| Fish Canyon Tuff | 11 | 66-69 | 34-52 | .1 - .3 | N | La Garita | 27.8 |
| Masonic Park Tuff | 1 | 68 | 38-52 | 0 - .01 | R | Mount Hope | 28.2 |
| Treasure Mountain Tuff: | | | | | | | |
| Upper tuff ² | .. | ³ ≈ 70 | 5-15 | .1 - .3 | R | Platoro caldera complex | |
| Ra Jadero Member | 4 | 64-66 | 10-17 | .2 - .6 | R | Summitville caldera | |
| Ojito Creek Member | 9 | 68-71 | 6-12 | 0 - .02 | N | ... do | |
| Middle tuff ² | .. | ³ ≈ 70 | 5-10 | 0 - .02 | N, R | Platoro caldera complex | |
| La Jara Canyon Member | 6 | 65-70 | 20-45 | 0 - .03 | R | Platoro caldera | 29.8 |
| Lower tuff ² | 1 | 69 | 3-11 | 0 - .03 | R | Platoro caldera complex | |
| Tuff of Rock Creek | 2 | 64-65 | 2- 3 | (⁴) | N | ... do | |

¹ Data, other than magnetic polarities and K-Ar ages, are from Ratté and Steven (1967).

² Assemblage of several small ash-flow sheets.

³ Estimated.

⁴ No sanidine.

Tuff by absence of biotite phenocrysts and by its relatively mafic composition. The tuff of Rock Creek rests on lavas and breccias of the main body of the Conejos Formation; it is overlain by andesitic or rhyodacitic lava flows that have also been assigned to the Conejos Formation (upper lava unit) because a contact cannot readily be located between the two groups of intermediate-composition rocks where the tuff of Rock Creek is absent.

The tuff of Rock Creek is confined to the northeast sector of the area (fig. 9) and is everywhere less than 100 m thick. Its best exposures and maximum thickness are in the Rock Creek drainage (fig. 10), where it filled broad valleys on the northeast flank of the large stratovolcano of Conejos age centered somewhere near Bennett Peak. The tuff of Rock Creek thins upslope and is overlapped by the upper lava unit of the Conejos Formation (Platoro map). The tuff of Rock Creek appears to have flowed down the flank of the stratovolcano from a source somewhere in the volcanic highlands to the southwest, within the area of the subsequently formed Platoro caldera.

The tuff of Rock Creek forms a single, apparently simple cooling unit. Whether weakly or densely welded, it commonly contains large black scoria blocks as much as 75 cm long in a red-brown or orange-brown fragmental matrix (fig. 11). The scoria blocks tend to be elongate and to define a crude foliation even in weakly welded rock, indicating primary shape orientation during flowage and emplacement as well as any later welding compaction. At the south margin of the tuff, in the Cat Creek area, the scoria blocks decrease in size as the tuff sheet thins, and the resulting brown lithic-rich pyroclastic breccia becomes poorly exposed and difficult to separate from other volcanic breccias of the Conejos Formation. In contrast, at the most northern outcrops near Del Norte, the tuff of Rock Creek is a partly welded glass, in which the black scoria lenses are surrounded by gray glassy fragmental matrix.

Phenocrysts in the tuff of Rock Creek are sparse (3-8 percent) and are plagioclase and minor amounts of augite and Fe-Ti oxides; biotite is absent. One sample contains hypersthene, but it may be xenocrystic. Small andesitic lithic fragments are very common.

The tuff of Rock Creek is relatively mafic—a rhyodacite or mafic quartz latite, as might be predicted from its phenocryst mineralogy. A bulk sample and an individual scoria block both contain 64-65 percent SiO₂ (table 4); this is the least silicic ash-flow tuff in the southeastern San Juan Mountains. Because the tuff of Rock Creek contains only sparse phenocrysts, its bulk composition and groundmass composition differ only slightly. The mafic composition of the groundmass contrasts with that of the other ash-flow sheets whose relatively mafic bulk-rock compositions (table 3) are due

to abundant phenocrysts in a significantly more silicic groundmass.

The volume of the tuff of Rock Creek is estimated as about 10 km³ (table 5), but this figure is very approximate because exposures are fragmentary (fig. 9). No caldera collapse feature has been preserved that can be related to eruption of the tuff of Rock Creek, but subsidence need not necessarily have accompanied this small-volume eruption. (See Smith, 1960a, fig. 3.)

Field measurements, not checked in the laboratory, suggest that the tuff of Rock Creek (like the overlying upper lava unit of the Conejos Formation) has normal magnetic polarity.

The tuff of Rock Creek has not been dated directly, but it is bracketed by K-Ar determinations of other units (Lipman and others, 1970). At Del Norte the tuff of Rock Creek is underlain by hornblende rhyodacite lavas related to the Summer Coon volcano of Conejos age, which has yielded radiometric dates as young as 32.4 m.y. The tuff of Rock Creek is overlain by the La Jara Canyon Member of the Treasure Mountain Tuff, dated as 29.8 m.y., and its source from within the Platoro caldera area suggests that it may only slightly predate the beginning of Treasure Mountain eruptions.

TREASURE MOUNTAIN TUFF

The Treasure Mountain Tuff has been redefined (Lipman and Steven, 1970) from the Treasure Mountain Rhyolite of Larsen and Cross (1956) to include the units present at the type locality at Treasure Mountain, about 20 km west of Summitville, Colo. (fig. 9), plus additional intertonguing units farther south.

As redefined, the Treasure Mountain Tuff is a coextensive assemblage of ash-flow tuffs, largely or entirely related to the Platoro caldera complex. Three large ash-flow sheets in the Treasure Mountain Tuff that have been mapped over nearly 5,000 km² have been formally designated as members: the La Jara Canyon, Ojito Creek, and Ra Jadero Members, in ascending order (Lipman and Steven, 1970). Less widespread ash-fall and ash-flow tuffs below the La Jara Canyon Member, between the La Jara Canyon and Ojito Creek Members, and above the Ra Jadero Member have been informally designated the lower, middle, and upper tuffs, respectively.

Excluded from the Treasure Mountain Tuff as here defined are thick sections of welded ash-flow tuffs, erupted from other volcanic centers, that were mapped as Treasure Mountain Rhyolite by Larsen and Cross (1956, pl. 1) in the western, central, and northeastern San Juan Mountains. The largest of these, a sequence of four major ash-flow sheets in the western San Juan Mountains, was designated the Gilpin Peak Tuff by Luedke and Burbank (1963), but the Gilpin Peak Tuff is

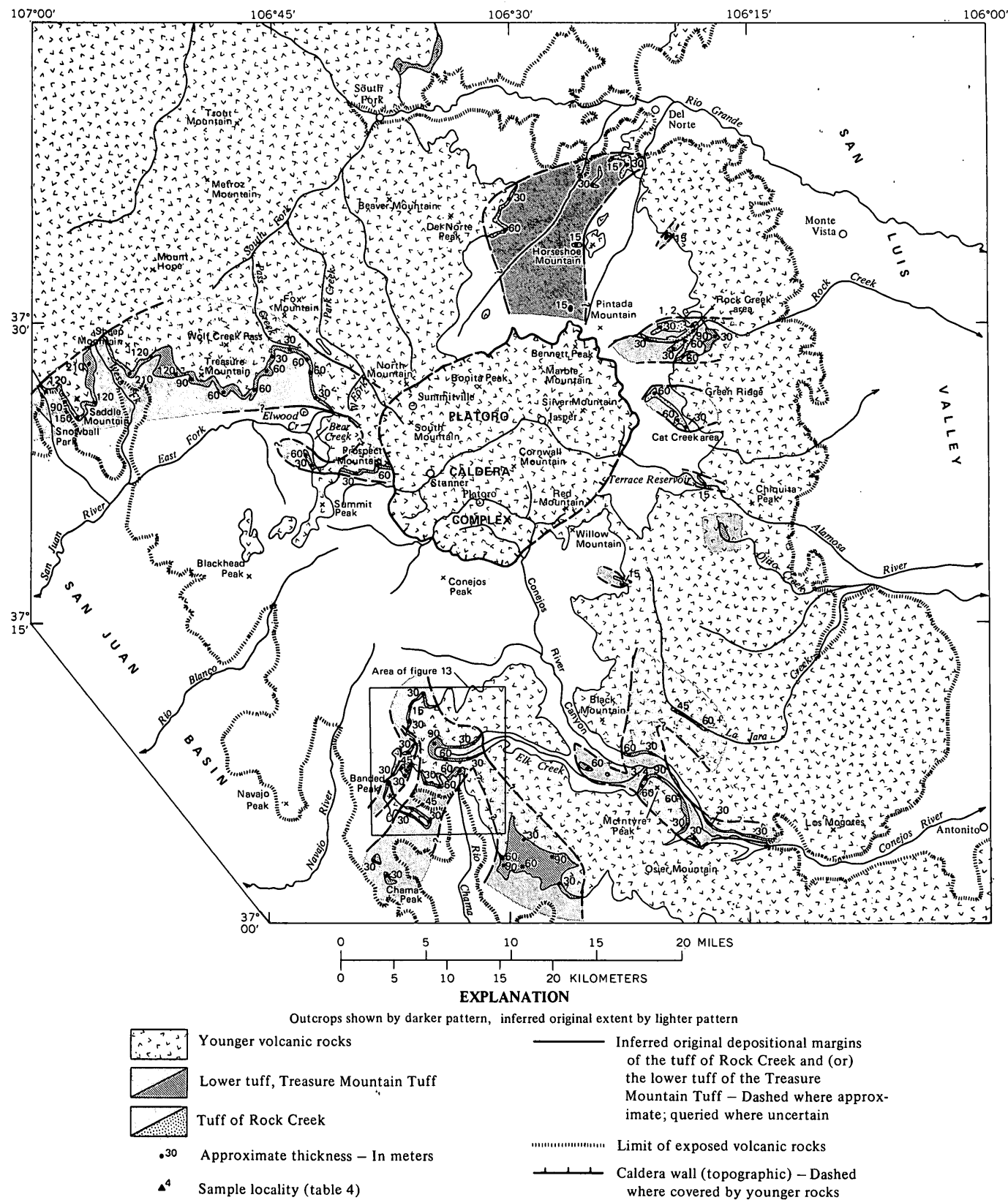


FIGURE 9.—Outcrop area, approximate thickness of selected sections, and inferred original depositional extent of the tuff of Rock Creek and the lower tuff of the Treasure Mountain Tuff. Based on mapping by P.W. Lipman, 1965-67, 1970-71.

now known to be equivalent to older parts of the ash-flow sequence (Sapinero Mesa Tuff, Dillon Mesa Tuff, Blue Mesa Tuff, and underlying tuffs) described by Olson, Hedlund, and Hansen (1968) in the Gunnison River area (Lipman and others, 1970, p. 2340-2341; Lipman and others, 1973). These tuffs were all erupted from centers in the western San Juan Mountains, including San Juan, Uncompahgre, Lost Lake, and Ute Creek calderas (fig. 1). A second body of ash-flow tuff, mapped as Treasure Mountain Rhyolite by Larsen and Cross (1956, pl. 1) in the northeastern San Juan Mountains, has been reassigned to Patton's (1916) Bonanza Tuff by Mayhew (1969) (Knepper and Marrs, 1971) and is inferred to have been erupted from a caldera near Bonanza (fig. 1). One major ash-flow sheet in the southeastern San Juan Mountains, generally mapped by Larsen and Cross (1956) in their Treasure Mountain Rhyolite, is thought to have been erupted from a caldera centered near

Mount Hope (fig. 1) and is described as the Masonic Park Tuff, a new name in this report. (See also Lipman and others, 1970; Steven and Lipman, 1973.)

Units of the Treasure Mountain Tuff are petrographically fairly uniform quartz latites and less abundant low-silica rhyolites. All contain phenocrysts of plagioclase and biotite, and most contain augite; sanidine is characteristically sparse (table 3), and quartz is absent. Phenocryst contents and welding characteristics vary widely, but phenocrysts are typically more abundant and welding more dense in the three major ash-flow sheets that constitute the formal members than in the more local informal tuff members. Similar chemistry, phenocryst mineralogy, and areal distribution of the units of the Treasure Mountain Tuff indicate that the units are closely interrelated. Despite the similarities, the units can be distinguished in part by differences in proportion of phenocrysts (fig. 12) and by



FIGURE 10.—Densely welded tuff of Rock Creek forms gently dipping palisades in middle distance (arrow). The tuff of Rock Creek is underlain here by mudflow breccias of the Conejos Formation and is overlain by andesitic and rhyodacitic lavas of the upper lava unit, Conejos Formation. Pintada Mountain, in left distance, consists of Conejos lava on the northeast wall of Platoro caldera. Photographed from Rock Creek road at divide above Lost Cabin Ranch.



FIGURE 11.—Weakly welded tuff of Rock Creek, showing characteristic large black scoria blocks in red-brown fragmental matrix. West side of Horseshoe Mountain, at about 10,300 feet (Horseshoe Mountain quadrangle).

differences in their natural remanent magnetic polarities (table 3). The Ojito Creek Member and part of the middle tuff have normal polarities; all the other units of the Treasure Mountain have reverse polarities. Of the three widespread formally named ash-flow sheets, the La Jara Canyon Member is significantly higher in total phenocrysts than the other two, and the Ra Jadero has significantly more sanidine (fig. 12).

SiO_2 contents in 22 analyses of Treasure Mountain Tuff (table 4) range from 64.2 to 71.2 percent. Most of the bulk-rock compositions thus are quartz latite; a few phenocryst-poor tuffs and pumice blocks are low-silica rhyolite. In general, SiO_2 increases as total phenocrysts decrease (fig. 12B), a relation especially evident if variations within individual ash-flow sheets are examined. Such examination indicates that much of the total compositional variation of the Treasure Mountain is due to differing amounts of phenocrysts. The ground-mass composition for all the tuffs appears to be low-silica rhyolite. Although all Tertiary volcanic rocks of

the San Juan field of any given SiO_2 content tend to be similar in other oxide contents within the scatter of the chemical data, the Treasure Mountain Tuff is slightly higher in both alkalis and is lower in CaO than most of the younger volcanic rocks of the area, including both the younger ash-flow sheets and the lavas and intrusives of the caldera complex (fig. 66).

LOWER TUFF

The lower tuff of the Treasure Mountain consists of a varied assemblage of biotite-bearing ash-flow tuffs and a minor amount of interlayered ash-fall tuff; these ash-flow and ash-fall tuffs are thought to mark the beginning of silicic volcanic activity at the area that was subsequently to develop into the Platoro caldera complex. The lower tuff rests on lavas, breccias, or mudflow conglomerates of the Conejos Formation everywhere except for a small area south of Rock Creek, where it directly overlies the tuff of Rock Creek. The lower tuff is overlain by the La Jara Canyon Member, except in a few places

PLATORO CALDERA COMPLEX, SAN JUAN MOUNTAINS, COLORADO

TABLE 4.—Analyses of Treasure

[Sample localities shown in figs. 9, 14, 23, and 25. Analyses 3-5, 8, 9, and 11 are from Larsen and Cross (1956, table 21). Other major-oxide analyses are by rapid methods methods by J. C. Hamilton; remaining analyses are by quantitative methods by

| Sample----- | Tuff of Rock Creek | | Lower tuff | | La Jara Canyon Member | | | | | Ojito Creek Member | | | | |
|---|--------------------|----------------|-------------|-------------|-----------------------|--------------|---------------|-------------|-----------|--------------------|--------------|----------------|---------------|---------------|
| | | | | | Intracaldera tuff | | Outflow sheet | | | Intracaldera | Lower unit | | | |
| | 1 65L-170-m | 2 65L-170-s | 3 Con595 | 4 Con596 | 5 Con563 | 6 66L-208 | 7 66L-13-A | 8 Con597 | 9 SV20 | 10 66L-22 | 11 Con532 | 12 66L-19-B | 13 W168463 | 14 W168462 |
| Major oxides (weight percent) calculated without H ₂ O and CO ₂ (original values listed separately below) | | | | | | | | | | | | | | |
| SiO ₂ ----- | 64.3 | 64.6 | 65.15 | 69.09 | 65.03 | 65.1 | 66.1 | 66.88 | 68.11 | 69.9 | 65.18 | 67.7 | 69.6 | 70.4 |
| Al ₂ O ₃ ----- | 17.0 | 17.3 | 16.27 | 15.05 | 16.82 | 17.6 | 17.3 | 16.17 | 15.96 | 17.0 | 17.40 | 16.0 | 16.3 | 15.4 |
| Fe ₂ O ₃ ----- | 5.17 | 3.7 | 4.48 | 2.77 | 3.69 | 2.7 | 3.9 | 2.99 | 2.78 | 2.5 | 3.89 | 2.1 | 2.2 | 1.2 |
| FeO----- | .32 | .9 | .54 | .36 | .30 | .81 | .14 | .49 | .70 | .12 | .53 | .06 | .24 | .85 |
| MgO----- | .55 | .7 | 2.06 | .12 | 1.06 | 1.4 | .69 | .16 | .61 | .66 | .56 | .65 | .36 | .33 |
| CaO----- | 3.24 | 2.8 | 3.69 | 2.23 | 3.47 | 3.6 | 2.7 | 2.86 | 2.18 | 2.1 | 1.88 | 3.0 | 1.4 | 1.2 |
| Na ₂ O----- | 3.85 | 4.1 | 2.81 | 4.28 | 4.38 | 3.9 | 4.3 | 4.64 | 4.00 | 3.5 | 4.00 | 4.6 | 4.1 | 4.6 |
| K ₂ O----- | 4.05 | 4.6 | 4.05 | 5.26 | 4.44 | 3.7 | 4.0 | 4.87 | 4.80 | 3.4 | 5.46 | 5.1 | 5.2 | 5.4 |
| TiO ₂ ----- | .94 | 1.0 | .66 | .69 | .60 | .87 | .63 | .63 | .65 | .41 | .91 | .47 | .42 | .39 |
| P ₂ O ₅ ----- | .41 | .37 | .28 | .14 | .20 | .21 | .18 | .17 | .20 | .14 | .20 | .08 | .00 | .00 |
| MnO----- | .12 | .09 | ---- | ---- | ---- | .07 | .16 | .14 | ---- | .12 | ---- | .14 | .08 | .08 |
| TOTAL----- | 99.95 | 100.16 | 99.99 | 99.99 | 99.99 | 99.96 | 100.10 | 100.00 | 99.99 | 99.85 | 100.00 | 99.90 | 99.90 | 99.87 |
| H ₂ O+----- | .52 | .69 | 2.90 | .47 | 1.06 | .60 | .84 | .10 | .75 | .50 | 1.05 | .51 | .43 | .49 |
| H ₂ O----- | .48 | .71 | 2.08 | .43 | .20 | .90 | .56 | .26 | .47 | .40 | 1.03 | .10 | .57 | .37 |
| CO ₂ ----- | <.05 | <.05 | ---- | ---- | ---- | .20 | <.05 | ---- | ---- | .21 | ---- | <.05 | <.05 | <.05 |
| Norms (weight percent) | | | | | | | | | | | | | | |
| Quartz----- | 19.81 | 17.58 | 23.17 | 20.33 | 14.74 | 19.47 | 19.67 | 16.27 | 21.47 | 30.88 | 16.81 | 15.3 | 21.83 | 19.63 |
| Orthoclase----- | 23.95 | 27.06 | 23.93 | 31.09 | 26.23 | 21.66 | 23.43 | 28.78 | 28.33 | 20.37 | 32.23 | 30.32 | 31.04 | 31.19 |
| Albite----- | 32.57 | 34.44 | 23.73 | 36.22 | 37.03 | 32.73 | 36.12 | 39.26 | 33.86 | 30.03 | 33.79 | 39.16 | 35.04 | 39.26 |
| Anorthite----- | 13.43 | 11.24 | 16.45 | 6.31 | 13.14 | 16.28 | 12.42 | 8.91 | 9.51 | 9.63 | 7.98 | 7.72 | 7.02 | 5.20 |
| Corundum----- | 1.38 | 1.53 | 1.24 | ---- | ---- | 1.31 | 1.41 | ---- | .70 | 3.93 | 2.00 | ---- | 1.19 | ---- |
| Wollastonite----- | ---- | ---- | ---- | 1.19 | .77 | ---- | ---- | 1.74 | ---- | ---- | ---- | 2.45 | ---- | .34 |
| Enstatite----- | 1.36 | 1.65 | 5.12 | .30 | 2.63 | 3.55 | 1.72 | .40 | 1.52 | 1.64 | 1.39 | 1.63 | .91 | .83 |
| Ferrosilite----- | ---- | ---- | ---- | ---- | ---- | ---- | ---- | ---- | ---- | ---- | ---- | ---- | ---- | .06 |
| Magnetite----- | ---- | .24 | ---- | ---- | ---- | .35 | ---- | .21 | .37 | ---- | ---- | ---- | ---- | 1.75 |
| Hematite----- | 5.17 | 3.5 | 4.48 | 2.77 | 3.69 | 2.51 | 3.86 | 2.84 | 2.52 | 2.53 | 3.89 | 2.11 | 2.22 | ---- |
| Ilmenite----- | .94 | 1.93 | 1.14 | .77 | .64 | 1.64 | .45 | 1.20 | 1.23 | .52 | 1.11 | .43 | .68 | .75 |
| Titanite----- | ---- | ---- | ---- | .69 | .66 | ---- | ---- | ---- | ---- | ---- | ---- | .61 | ---- | ---- |
| Rutile----- | .44 | ---- | .07 | ---- | ---- | ---- | ---- | .29 | ---- | .13 | .33 | ---- | .06 | ---- |
| Apatite----- | .96 | .87 | .67 | .33 | .48 | .51 | .43 | .40 | .48 | .34 | .48 | .19 | ---- | ---- |
| Minor elements (parts per million) | | | | | | | | | | | | | | |
| B----- | 20 | 20 | ---- | ---- | ---- | ---- | <20 | ---- | ---- | <20 | ---- | ---- | ---- | ---- |
| Ba----- | 140 | 140 | ---- | ---- | ---- | 1000 | 1000 | ---- | ---- | 1000 | ---- | 1100 | 1300 | 1200 |
| Ce----- | ---- | ---- | ---- | ---- | 100 | ---- | ---- | ---- | ---- | ---- | ---- | ---- | ---- | ---- |
| Co----- | 5 | <4 | ---- | ---- | ---- | 10 | 5 | ---- | <4 | ---- | ---- | <4 | 5 | ---- |
| Cr----- | 7 | 3 | ---- | ---- | ---- | ---- | 3 | 2 | ---- | ---- | 2 | ---- | ---- | ---- |
| Cu----- | 58 | 100 | ---- | ---- | ---- | 10 | 14 | ---- | 36 | ---- | ---- | 12 | 7 | 8 |
| Ga----- | 10 | 20 | ---- | ---- | ---- | 150 | 20 | 20 | 20 | ---- | ---- | 20 | 20 | 20 |
| La----- | ---- | ---- | ---- | ---- | 70 | 70 | ---- | ---- | ---- | ---- | ---- | 90 | 80 | 80 |
| Ni----- | 45 | 240 | ---- | ---- | ---- | 7 | 7 | 9 | 9 | ---- | 6 | 4 | ---- | ---- |
| Pb----- | 30 | 50 | ---- | ---- | 200 | 40 | 40 | 30 | 30 | ---- | 40 | 20 | 20 | 20 |
| Sc----- | 16 | 16 | ---- | ---- | 10 | 12 | 12 | 8 | 8 | ---- | 7 | 6 | 7 | 7 |
| Sn----- | ---- | ---- | ---- | ---- | 30 | ---- | ---- | ---- | ---- | ---- | ---- | ---- | ---- | ---- |
| Sr----- | 250 | 250 | ---- | ---- | 1000 | 240 | 240 | 240 | 240 | ---- | 160 | 240 | 200 | 200 |
| V----- | ---- | ---- | ---- | ---- | 70 | ---- | ---- | ---- | ---- | ---- | ---- | 20 | 20 | 20 |
| Y----- | 50 | 50 | ---- | ---- | 30 | 40 | 40 | 40 | 40 | ---- | 40 | 30 | 30 | 30 |
| Yb----- | ---- | ---- | ---- | ---- | 3 | ---- | ---- | ---- | ---- | ---- | ---- | 3 | 3 | 3 |
| Zr----- | 390 | 450 | ---- | ---- | 150 | 250 | 250 | 250 | 250 | ---- | 310 | 300 | 320 | 320 |
| Phenocrysts (volume percent) | | | | | | | | | | | | | | |
| Plagioclase----- | 2.7 | 4 | ---- | 7 | 28 | 34.2 | 24.6 | 25 | 21 | 13.9 | 6 | 6.0 | 5.2 | 5.9 |
| Sandine----- | ---- | ---- | ---- | 5 | .8 | .4 | 4 | ---- | 1.1 | ---- | ---- | Tr. | ---- | ---- |
| Quartz----- | ---- | ---- | ---- | 2 | 8 | 4.3 | 3.8 | 3 | 5 | 2.4 | 1 | 8 | .8 | .9 |
| Biotite----- | Tr. | Tr. | ---- | ---- | ---- | ---- | ---- | ---- | ---- | ---- | ---- | ---- | ---- | ---- |
| Augite----- | .1 | Tr. | ---- | 1 | 1.5 | ---- | .3 | 1 | ---- | .4 | ---- | .1 | ---- | ---- |
| Hornblende----- | ---- | ---- | 2 | 1 | 2.4 | ---- | 1.4 | 2 | 2 | .9 | Tr. | ---- | ---- | ---- |
| Opalines----- | .4 | 1 | ---- | 88 | 56 | 56.5 | 69.5 | 69 | 72 | 81.3 | 92 | .4 | .2 | .2 |
| Groundmass----- | 96.8 | 95 | ---- | ---- | ---- | ---- | ---- | ---- | ---- | ---- | 92.7 | 93.8 | 93.0 | 93.0 |

SAMPLE DESCRIPTIONS

- Densely welded devitrified purple-brown matrix of ash-flow sheet from near top of unit. Ojito Creek, at sheet is about 100 m thick. North side of North Fork Rock Creek near mouth, at about 8,850 ft. (See fig. 9.)
- Dark-gray devitrified scoraceous pumice block. Same locality as No. 1.
- Pale-purple porous tuff, containing hydrated glass. Anomalously low in Na₂O. "West slope of McIntyre Point [Peak] at altitude of 10,000 feet" (Larsen and Cross, 1956, table 21, No. 55). (See fig. 9.)
- Dark-red-brown devitrified tuff, containing porous lighter colored streaky pumice lenses. "West slope of McIntyre Point [Peak], at an altitude of 9,840 feet" (Larsen and Cross, 1956, table 21, No. 50). (See fig. 9.)
- Dense purple-gray devitrified welded tuff, probably propylitically altered. "East slope of Cornwall Mountain, at altitude of 10,500 feet" (Larsen and Cross, 1956, table 21, No. 22). (See fig. 14.)
- Relatively fresh densely welded devitrified tuff, showing well-preserved shard and pumice foliation (fig. 17B). Platoro Reservoir road, 1.2 km southwest of Rito Gato. (See fig. 14.)
- Pale red-brown densely welded devitrified tuff from near top of unit. Ojito Creek, at 8,516-ft bench mark. (See fig. 14.)
- Dark-red-brown devitrified welded tuff. "West slope of McIntyre Mountain [Peak] at altitude of 10,000 feet" (Larsen and Cross, 1956, table 21, No. 33). (See fig. 14.)
- Densely welded devitrified tuff, "West slope of Treasure Mountain at altitude of 11,200 feet" (Larsen and Cross, 1956, table 21, No. 35). (See fig. 14.)
- Brick-red densely welded finely devitrified tuff from near top of ash-flow sheet. Phenocrysts are small and fairly sparse probably because of winnowing. Along jeep trail, at 8,750 ft, 1.4 km southwest of junction between Hot Creek and Piedrosa Creek. (See fig. 14.)
- Densely welded devitrified reddish-brown tuff. "Along trail from Alamosa River to the head of Cat Creek and 2 miles north of Alamosa ranger station" (Larsen and Cross, 1956, table 21, No. 24). (See fig. 23.)
- Densely welded devitrified light-brown tuff. Seems anomalously low in SiO₂ and high in CaO. Cliffs east of Ojito Creek, 2 km north of junction with Hot Creek. (See fig. 23.)

Mountain Tuff and tuff of Rock Creek

by P. L. D. Elmore, Samuel Botts, Gillison Chloe, Lowell Artis, H. Smith, John Glenn, and James Kelsey. Minor-element analysis 6 is by semiquantitative J. D. Fletcher. <, less than. All samples except 1 and 2 are Treasure Mountain Tuff]

| Ojito Creek Member--Continued | | | | | | Ra Jadero Member | | | | | | Sample No. Field No. Lab. No. | |
|--|---------------------------|---------------------------|-----------------------------|----------------------------|--|---------------------------|---------------------------|---------------------------|--------------------------|--------------------------|--|-------------------------------------|--|
| Upper unit | | | Pumice blocks, upper unit | | | Bulk rock | | | | Pumice block | | | |
| 15 70L-40-F W176181 | 16 66L-13-C W168464 | 17 66L-13-B W168458 | 18 70L-40-Fp W1761812 | 19 66L-13-Bp W168457 | | 20 70L-40-B W176177 | 21 70L-40-C W176178 | 22 70L-40-A W176176 | 23 66L-118 W168460 | 24 66L-4-A W168459 | | | |
| Major oxides (weight percent) calculated without H ₂ O and CO ₂ (original values listed separately below)--Continued | | | | | | | | | | | | | |
| 68.0 | 68.6 | 68.8 | 70.4 | 71.2 | | 64.2 | 66.8 | 65.3 | 65.6 | 70.4 | | SiO ₂ | |
| 16.4 | 16.4 | 16.5 | 15.7 | 15.8 | | 17.3 | 17.3 | 17.0 | 16.6 | 15.9 | | Al ₂ O ₃ | |
| 2.3 | 2.4 | 2.8 | 1.0 | 1.3 | | 3.4 | 3.5 | 3.5 | 3.6 | 1.8 | | Fe ₂ O ₃ | |
| .61 | .12 | .27 | .89 | .63 | | 1.1 | .77 | .57 | .32 | .16 | | FeO | |
| .46 | .60 | .57 | .33 | .29 | | .91 | .81 | .79 | .96 | .38 | | MgO | |
| 2.0 | 1.8 | 1.9 | 1.2 | 1.1 | | 3.0 | 2.4 | 2.3 | 2.7 | 1.1 | | CaO | |
| 4.6 | 4.7 | 4.3 | 3.9 | 4.2 | | 4.2 | 4.2 | 4.2 | 4.2 | 4.0 | | Na ₂ O | |
| 5.0 | 4.6 | 4.0 | 6.0 | 5.0 | | 4.8 | 5.2 | 5.3 | 4.9 | 5.4 | | K ₂ O | |
| .50 | .47 | .60 | .39 | .39 | | .77 | .73 | .72 | .73 | .57 | | TiO ₂ | |
| .02 | .10 | .15 | .00 | .07 | | .18 | .09 | .11 | .18 | .11 | | P ₂ O ₅ | |
| .09 | .15 | .12 | .11 | .09 | | .10 | .11 | .18 | .06 | .06 | | MnO | |
| 99.98 | 99.94 | 100.01 | 99.92 | 100.07 | | 99.90 | 99.91 | 99.97 | 99.85 | 99.88 | | TOTAL | |
| .46 | .28 | .64 | .45 | .49 | | .45 | .41 | .51 | .53 | .56 | | H ₂ O+ | |
| .64 | .22 | .56 | .22 | .19 | | .50 | .79 | .49 | .16 | .64 | | H ₂ O- | |
| <.05 | <.05 | .12 | <.05 | <.05 | | <.05 | <.05 | <.05 | <.05 | <.05 | | CO ₂ | |
| Norms (weight percent)--Continued | | | | | | | | | | | | | |
| 17.57 | 18.81 | 24.13 | 21.51 | 25.35 | | 13.51 | 14.14 | 14.56 | 15.37 | 23.84 | | Quartz | |
| 29.35 | 27.36 | 23.50 | 35.18 | 29.35 | | 28.66 | 30.51 | 31.09 | 29.21 | 32.00 | | Orthoclase | |
| 38.60 | 40.03 | 36.24 | 33.30 | 35.17 | | 35.90 | 35.98 | 35.96 | 35.85 | 33.72 | | Albite | |
| 9.66 | 8.33 | 8.61 | 6.01 | 5.07 | | 13.77 | 11.46 | 10.82 | 11.80 | 4.84 | | Anorthite | |
| ----- | .56 | 2.01 | .62 | 1.74 | | ----- | .53 | .35 | ----- | 1.75 | | Corundum | |
| .11 | ----- | ----- | ----- | ----- | | .20 | ----- | ----- | ----- | ----- | | Wollastonite | |
| 1.14 | 1.50 | 1.42 | .83 | .73 | | 2.26 | 2.02 | 1.96 | 2.39 | .94 | | Enstatite | |
| ----- | ----- | ----- | .35 | ----- | | ----- | ----- | ----- | ----- | ----- | | Ferrrosilite | |
| .82 | ----- | ----- | 1.46 | 1.21 | | 1.69 | .73 | .34 | ----- | ----- | | Magnetite | |
| 1.77 | 2.42 | 2.75 | ----- | .48 | | 2.27 | 3.04 | 3.31 | 3.63 | 1.84 | | Hematite | |
| .94 | .58 | .82 | .75 | .73 | | 1.46 | 1.38 | 1.36 | .81 | .48 | | Ilmenite | |
| ----- | ----- | ----- | ----- | ----- | | ----- | ----- | ----- | .37 | ----- | | Titanite | |
| ----- | .17 | .17 | ----- | ----- | | ----- | ----- | ----- | .15 | .32 | | Rutile | |
| .05 | .24 | .36 | ----- | .17 | | .29 | .22 | .26 | .43 | .27 | | Apatite | |
| Minor elements (parts per million)--Continued | | | | | | | | | | | | | |
| ----- | <20 | <20 | ----- | <20 | | 20 | 20 | 20 | <20 | <20 | | B | |
| 1500 | 1400 | 2000 | 1300 | 2100 | | 1400 | 1800 | 2000 | 880 | 1600 | | Ba | |
| ----- | ----- | ----- | ----- | ----- | | ----- | ----- | ----- | ----- | ----- | | Ce | |
| ----- | <4 | <4 | ----- | <4 | | 6 | 7 | 6 | 5 | <4 | | Co | |
| ----- | 2 | <2 | ----- | <2 | | 7 | 5 | 4 | 7 | <2 | | Cr | |
| 10 | 14 | 16 | 7 | 15 | | 20 | 24 | 20 | 32 | 14 | | Cu | |
| 20 | 20 | 20 | 20 | 20 | | 20 | 20 | 20 | 20 | 20 | | Ga | |
| 100 | ----- | ----- | 70 | ----- | | 90 | 100 | 100 | ----- | ----- | | La | |
| ----- | 6 | 18 | ----- | 12 | | 3 | 5 | 6 | 10 | 30 | | Ni | |
| 20 | 30 | 40 | 20 | 40 | | 20 | 20 | 20 | 40 | 30 | | Pb | |
| 8 | 7 | 8 | 6 | 8 | | 13 | 14 | 13 | 17 | 9 | | Sc | |
| ----- | ----- | ----- | ----- | ----- | | ----- | ----- | ----- | ----- | ----- | | Sr | |
| 340 | 240 | 240 | 240 | 150 | | 440 | 490 | 440 | 180 | 180 | | | |
| 30 | ----- | ----- | 20 | ----- | | 60 | 50 | 40 | ----- | ----- | | V | |
| 30 | 40 | 40 | 30 | 40 | | 30 | 30 | 30 | 50 | 40 | | Y | |
| 3 | ----- | ----- | ----- | ----- | | 3 | 3 | 4 | ----- | ----- | | Yb | |
| 280 | 180 | 250 | 280 | 300 | | 300 | 320 | 290 | 400 | 380 | | Zr | |
| Phenocrysts (volume percent)--Continued | | | | | | | | | | | | | |
| 12.8 | 10.3 | 11.9 | 7.1 | 2.7 | | 13.5 | 11.3 | 11.7 | 11.5 | 7.3 | | Plagioclase | |
| .1 | ----- | ----- | ----- | ----- | | 1.3 | 1.7 | .9 | 2.1 | .7 | | Sandidine | |
| ----- | ----- | ----- | ----- | ----- | | ----- | ----- | ----- | ----- | ----- | | Quartz | |
| 1.3 | 1.7 | 1.3 | 1.3 | .9 | | 2.0 | 1.8 | 1.4 | 2.1 | 1.3 | | Biotite | |
| Tr. | .3 | ----- | ----- | .2 | | .6 | .4 | .5 | .5 | ----- | | Augite | |
| ----- | Tr. | ----- | ----- | ----- | | ----- | ----- | ----- | ----- | ----- | | Hornblende | |
| .4 | .5 | .8 | .2 | .3 | | .9 | .6 | 1.0 | .6 | .6 | | Opaques | |
| 85.3 | 87.2 | 86.0 | 93.4 | 95.9 | | 81.7 | 84.3 | 84.5 | 83.2 | 90.1 | | Groundmass | |

SAMPLE DESCRIPTIONS—Continued

13. Densely welded devitrified light-brown tuff from near base of ash-flow sheet (fig. 24A). At about 8,450 ft, along southwest base of Chiquita Peak, 2.4 km southeast of Terrace Reservoir spillway. (See fig. 23.)
14. Densely welded dark-gray nearly vitrophyric weakly devitrified tuff from just above basal vitrophyre. About 2 m below No. 13. (See fig. 23.)
15. Densely welded devitrified gray tuff, containing large feathery black pumice lenses (fig. 24B), from middle of upper unit. At about 8,500 ft, same locality as No. 13. (See fig. 23.)
16. Very densely welded devitrified red-brown tuff from near base of upper unit, near margin of ash-flow sheet, where lower unit is absent. Large pumice lenses are oxidized and leached. Cliff north or Ojito Creek road near 9,169-ft bench mark. (See fig. 23.)
17. Densely welded devitrified tuff from near top of upper unit, where pumice lenses are black. Same locality as No. 16. (See fig. 23.)
18. Black pumice lens from upper part of upper unit. Same locality as No. 15. (See fig. 23.)
19. Black pumice lens from upper part of upper unit. Same locality as No. 17. (See fig. 23.)
20. Dark-gray weakly devitrified tuff from just below upper vitrophyre (fig. 24C). At about 8,600 ft, same locality as No. 13. (See fig. 25.)
21. Red-brown densely welded devitrified tuff from lower part of sheet, just above basal vitrophyre. At about 8,500 ft, same locality as No. 13. (See fig. 25.)
22. Red-brown densely welded devitrified tuff from upper part of ash-flow sheet, just below upper vitrophyre. At about 8,600 ft, same locality as No. 13. (See fig. 25.)
23. Red-brown densely welded devitrified tuff from interior of ash-flow sheet. Northeast of Terrace Reservoir, 0.2 km north of 8,685-ft bench mark along Cat Creek road (See fig. 25.)
24. Large red-brown devitrified scoraceous pumice lens from upper part of ash-flow sheet. Same locality as No. 23 (fig. 25).

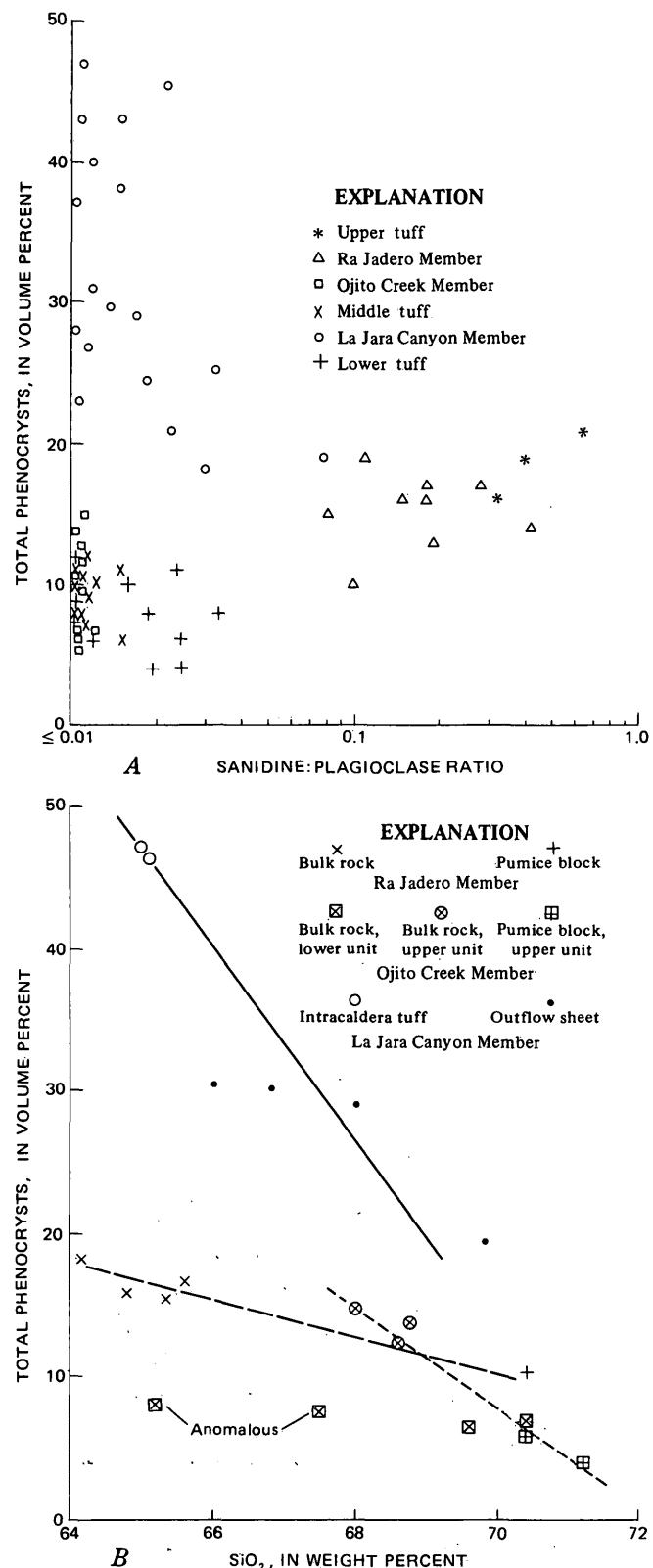


FIGURE 12.—Petrologic features of the major ash-flow members of the Treasure Mountain Tuff. A, Relations between feldspar proportions and total phenocryst contents. B, Relations between SiO_2 and total phenocryst contents.

where andesitic lavas intervene. Intermediate-composition lava flows that occur locally between the lower tuff and the La Jara Canyon or that are interlayered within the lower tuff are included in the Conejos Formation (upper lava unit), because these lavas could not be separated readily from other Conejos lavas in places where the lower tuff has wedged out. Such andesitic flows occur within the lower tuff near Elwood Creek (fig. 9) and in the Banded Peak area (figs. 9, 13). Andesitic lavas occur between the lower tuff and the La Jara Canyon Member at Chama Peak, in an area of at least 50 km^2 from the head of Elk Creek to Banded Peak, north of Elwood Creek, south of Pass Creek, west of Bear Creek, north of the Terrace Reservoir, and along Ojito Creek.

DISTRIBUTION AND THICKNESS

Cover by younger volcanic units and extensive erosion have left only a fragmentary record of the distribution of the lower tuff of the Treasure Mountain, but existing outcrops clearly indicate that the lower tuff covered sizable areas but did not form a continuous sheet (fig. 9). Most plausibly, several irregularly elongate lobes extended in a crude radial pattern outward from the area of the subsequent Platoro caldera. These lobes extended as much as 35 km to the west and south, farther than later members of the Treasure Mountain Tuff.

Maximum thicknesses—as much as 200 m—are generally at intermediate distances from the caldera area (fig. 9), but some local thickness variations are substantial. Deposition of the lower tuff in local valleys that were cut into the Conejos Formation can be seen on outcrop scale at many places in the southeastern San Juan Mountains; easily accessible examples occur on the canyon walls above the Conejos River north of Elk Creek. This distribution suggests deposition controlled by several broad valleys that extended irregularly outward from a central highland of eroded stratovolcanoes of Conejos age in the Platoro area. Such a paleogeographic reconstruction is consistent with the distribution of vent and volcaniclastic facies of the Conejos Formation, as discussed previously, and also with features of the distribution and thickness of later ash-flow sheets of the Treasure Mountain.

The volume of the lower tuff of the Treasure Mountain is estimated to be about 30 km^3 , but this figure is very uncertain. (See table 5.) No single ash-flow sheet within the lower tuff is likely to have had an original volume exceeding 5 km^3 .

LITHOLOGIC DESCRIPTION

The lower tuff of the Treasure Mountain is an assemblage of numerous seemingly local, small ash-flow sheets and minor beds of ash-fall tuff. Except where densely welded units predominate, the lower tuff is relatively poorly exposed. Ash-flow units of the lower tuff

are relatively phenocryst poor (fig. 12), commonly are only slightly welded, and are distinguished from the tuff of Rock Creek and the minor ash-flow tuffs within the underlying Conejos Formation by the presence of phenocrystic biotite. Total phenocryst content is generally in the range 5-10 percent, and phenocrysts consist of plagioclase, sparse biotite and opaques, and rare augite. Much of the lower tuff, including all fairly thick accumulations, is outside the Platoro map area and accordingly has not been studied in detail.

Where the lobe of lower tuff extending west from the Platoro area is thickest and best exposed—in the area from Treasure Mountain to Wolf Creek Pass—it consists of at least three separate cooling units of phenocryst-poor (5-10 percent) ash-flow tuff, each 20-30 m thick, that grade from gray or tan nonwelded margins into light-purplish-brown densely welded devitrified interiors. Eastward from Treasure Mountain, these units thin, and welding decreases. At the east end of this lobe, however, the lower tuff, which is well exposed on the southwest slope of Prospect Mountain and along the Stunner-Summitville road, is again brown phenocryst-poor (5-10 percent) densely welded devitrified tuff and has faint bedding on a scale of 10-50 cm (centimeters) defined by subtle variations in number and size of pumice fragments and phenocrysts. This welded bedded tuff is believed to represent agglutinated ash fall that was deposited so close to its source that it was still sufficiently hot to weld (Lipman and others, 1966, p. F18).

A few meters of similar bedded welded tuff, mapped as lower tuff of the Treasure Mountain because of the presence of biotite phenocrysts, is also present east of the Platoro caldera area along the Terrace Reservoir road. These tuff beds are separated from the overlying La Jara Canyon Member by two dark-gray nonporphyritic andesitic lava flows, assigned to the upper lava unit of the Conejos Formation.

In the Rock Creek area the lower tuff consists of at least two thin ash-flow sheets. The upper sheet contains more phenocrysts than normal (about 10 percent) and, where thin, is densely welded to a black vitrophyre. Where the sheet is thickest, as much as 50 m, its center has been devitrified to dark-red-brown tuff that contains dark-gray scoriaceous pumice lenses as much as 30 cm long and abundant andesitic lithic fragments a few centimeters across. The lower sheet is as much as 30 m thick and consists of phenocryst-poor (5 percent) lighter colored tuff of more silicic appearance; this tuff is also densely welded and devitrified in thick sections.

In the southern area, from the Conejos River to Banded Peak, two main ash-flow sheets are present in the lower tuff. The lower sheet is as much as 40 m thick, but it varies abruptly in thickness owing to irregular preeruption topography. It consists of white to pink nonwelded to partly welded tuff containing only about 5 per-

cent phenocrysts. Small light-colored pumice lapilli and dark volcanic rock fragments are abundant. Overlying this unit is a sheet consisting mostly of densely welded dark-brown devitrified tuff, characterized by lithophysal gas cavities a few centimeters in diameter and by collapsed pumice lenses as much as 60 cm long; this sheet grades upward into less welded pink tuff at its top. It contains 6-8 percent phenocrysts and sparse lithic fragments. In the Banded Peak area (fig. 13) a thick dark-gray andesite or rhyodacite lava flow (Conejos Formation, upper lava unit), containing small plagioclase and augite phenocrysts, is locally present between these two ash-flow sheets. In other places the upper sheet is absent and the La Jara Canyon Member of the Treasure Mountain directly overlies the lava flow. On the ridge crest east of Rio Chama, two or three separate non-welded to partly welded phenocryst-poor tuff units that resemble the lower ash-flow sheet described above are overlain directly by the La Jara Canyon Member.

AGE AND MAGNETIC POLARITY

No samples of the lower tuff have been dated radiometrically, but two dated lava flows from the Conejos Formation provide a maximum limit on its age (Lipman and others, 1970, table 2). At Snowball Park an andesitic lava, more than 700 m below the lower tuff, yielded a K-Ar age of 31.1 m.y., and at Navajo Peak a rhyodacite, deep in a volcanic pile overlain around its margins by lower tuff, was dated at 32.4 m.y. The lower tuff is overlain by the La Jara Canyon Member, well dated at 29.8 m.y. (Lipman and others, 1970, table 3, no. 1), and petrologic affinities with the La Jara Canyon Member suggest that the lower tuff of the Treasure Mountain is only slightly older.

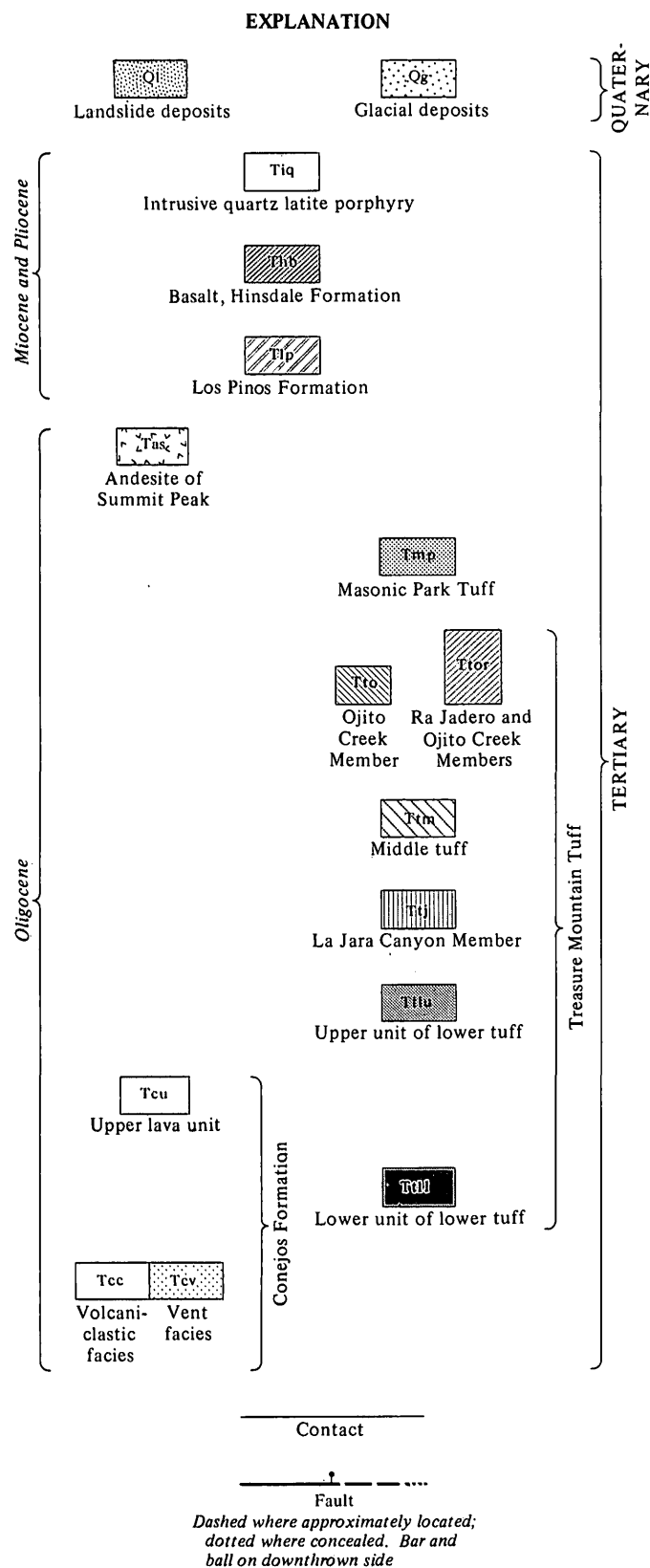
Densely welded units of the lower tuff have yielded seemingly reliable field determinations indicating reverse magnetic polarity at these sites: the Wolf Creek Pass road, the south slope of Treasure Mountain, the Rock Creek area, the lower Conejos River area, and Banded Peak. Laboratory demagnetization studies have not yet been made.

SOURCE

The nature of the lower tuff—a diverse assemblage of local ash-flow units that have not been successfully correlated over sizable areas—and the fragmentary outcrop pattern make any discussion of source somewhat hazardous. Nevertheless, it seems fairly certain that at least most of the ash-flow units included in the lower tuff represent premonitory eruptions of the volcanic events that led to formation of the Platoro caldera complex. The major features of the lower tuff in support of such an interpretation are (1) the radial distribution of lobes, converging toward the caldera area (fig. 9), (2) the presence, near the caldera margins, of agglutinated ash



FIGURE 13 (above and right).—Geologic map of the Banded Peak area, showing complex intertonguing relations between andesitic lava flows and units of the Treasure Mountain Tuff. Location of area shown in figure 9.



falls that are necessarily near-source deposits, and (3) the general petrologic affinity with subsequent units of the Treasure Mountain Tuff.

LA JARA CANYON MEMBER

The La Jara Canyon Member is a multiple-flow compound cooling unit of phenocryst-rich quartz latite that makes up the first widespread ash-flow sheet in the eastern and central San Juan Mountains; eruption of these ash flows resulted in collapse of the main Platoro caldera. The La Jara Canyon Member was named (Lipman and Steven, 1970) for cliff exposures along the rims of La Jara Canyon, about 27 km southeast of Platoro (fig. 14). It rests conformably on the lower tuff of the Treasure Mountain over much of its extent, but where the lower tuff was not deposited, the La Jara rests directly on eroded Conejos lavas and breccias. The La Jara Canyon Member is in general overlain by the middle tuff of the Treasure Mountain, although in the northeastern part of the mapped area where the middle tuff is thin or absent, the La Jara Canyon is directly overlain by the Ra Jadero Member of the Treasure Mountain.

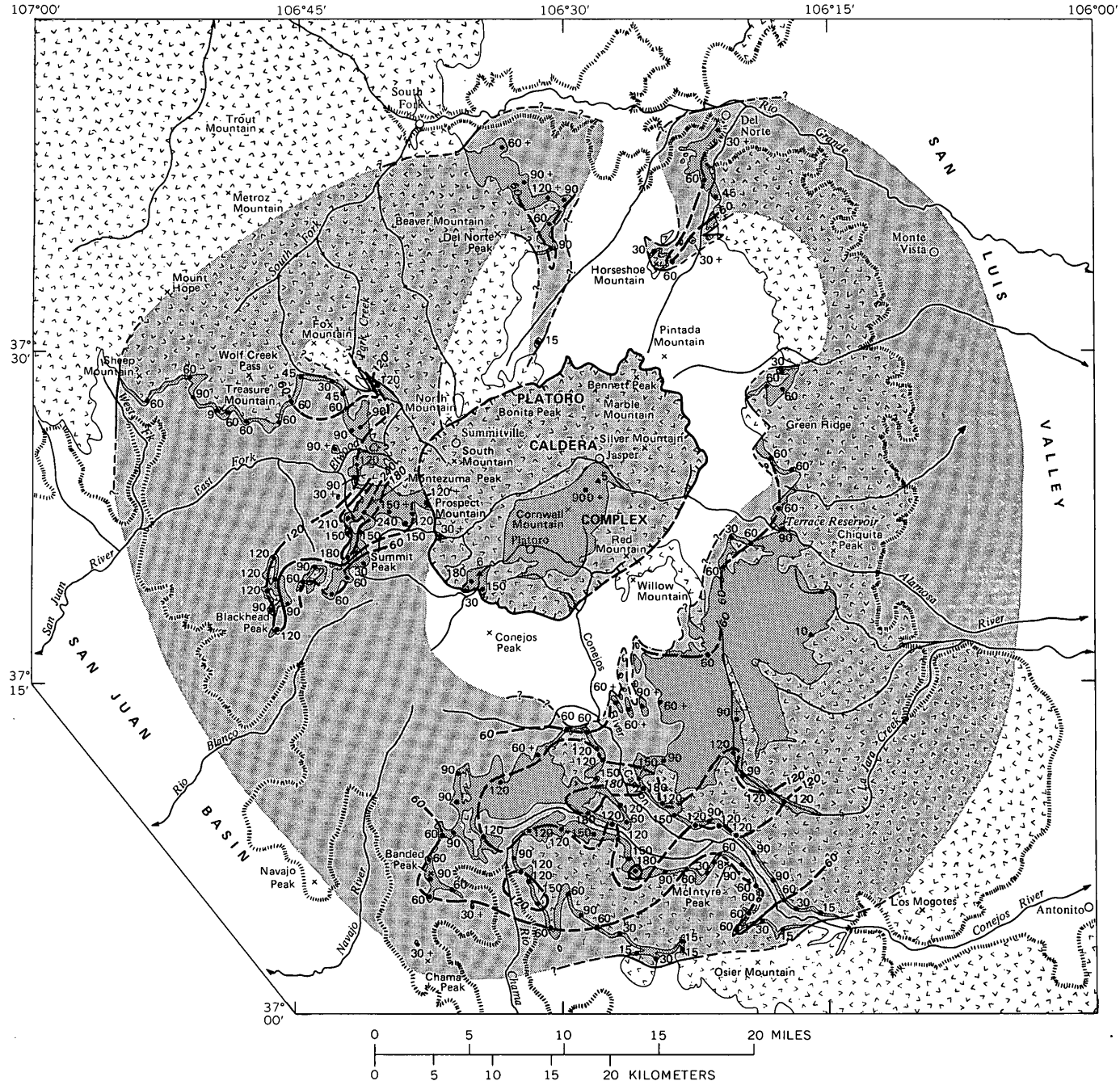
DISTRIBUTION AND THICKNESS

The distribution, thickness, and other features of the La Jara Canyon Member are most readily described in terms of two assemblages: (1) an outflow sheet that spread widely over an erosional surface of low relief cut in the Conejos Formation and previously partly mantled by the lower tuff of the Treasure Mountain, and (2) a thick local accumulation of tuff that ponded within the caldera concurrently with subsidence.

Preserved remnants of the outflow sheet (fig. 14) indicate that it extended outward 20-30 km in nearly every direction from Platoro caldera. The record is fragmentary, however, especially on the southwest side. In the three areas where the original depositional margin of the La Jara Canyon Member can be established with confidence—near the West Fork of the San Juan River, along the Rio Grande between South Fork and Del Norte, and in the lower Conejos River drainage—the ash-flow tuffs wedge out against the subdued erosional remnants of volcanoes of Conejos age. Elsewhere, the location of the depositional edge of the sheet is conjectural. If the original margins of the body were better known, they would probably appear irregularly lobate, owing to topographic irregularities in the preeruption surface, rather than smoothly subcircular as schematically shown in figure 14.

Variations in thickness and welding features of the La Jara Canyon also indicate significant topographic irregularity near the rims of the Platoro caldera. In

PLATERO CALDERA COMPLEX, SAN JUAN MOUNTAINS, COLORADO



EXPLANATION

Outcrops shown by darker pattern, inferred original extent by lighter pattern

- | | | | |
|--------|---|--|--|
| | Younger volcanic rocks | | Inferred original depositional margins of La Jara Canyon Member – |
| | La Jara Canyon Member | Dashed where approximate; queried where uncertain | |
| •60 | Approximate thickness – In meters | | Limit of exposed volcanic rocks |
| ▲5 | Sample locality (table 4) | — — — | Caldera wall (topographic) – Dashed where covered by younger rocks |
| — 60 — | Isopach – Dashed where approximate. Interval 60 meters | | |

FIGURE 14.—Outcrop area, approximate thickness of selected sections, and inferred original depositional extent of the La Jara Canyon Member, Treasure Mountain Tuff. Based on mapping by P. W. Lipman, 1965-67, 1970-71.

general, the caldera area apparently was topographically high before the eruption. This is especially clear on the south side of the caldera, south of Willow Mountain, where the La Jara Canyon Member fills south-trending valleys between ridges of Conejos lava. Although the less welded upper parts of the La Jara Canyon have been erosionally removed from this area, the welding-crystallization zonations indicate that the ash-flow deposits were thin and discontinuous. Farther south, the ash-flow deposits are several times thicker and form a continuous sheet. Depositional wedging of the La Jara Canyon against erosional topography is also well displayed north of Platoro caldera, especially at Horseshoe Mountain, near Del Norte Peak, and a few kilometers northwest of North Mountain. In each of these areas, younger units of the Treasure Mountain Tuff lap higher onto Conejos lavas than does the La Jara Canyon Member. In the one area where the La Jara Canyon is preserved on the caldera rim, at Prospect Mountain on the west side of the caldera, it thins toward the caldera from a much thicker accumulation farther west. These relations clearly indicate that the cluster of volcanoes of Conejos age in the Platoro caldera area remained, during eruption of the Treasure Mountain, as topographic highs having at least several hundred meters of relief above the surrounding aprons of volcaniclastic sedimentary rocks of the Conejos Formation.

The preserved thickness of the outflow sheet of the La Jara Canyon Member varies greatly but is commonly about 50-100 m. Its maximum preserved thickness, about 250 m, is north of Summit Peak, but the thickness decreases within a few kilometers to the southeast to less than 20 m (fig. 14). This ash-flow sheet is about 100 m thick at the La Jara Canyon area and about 60 m thick at Treasure Mountain. Crude isopachs have been plotted for the La Jara Canyon Member wherever the data are adequate (fig. 14). Near the volcanoes of Conejos age clustered in the Platoro caldera area, the isopachs define the radial valleys described above. Farther from the caldera area thickness variations in the La Jara Canyon Member are more subdued, and the average thickness is greater. The zone of maximum accumulation of the La Jara Canyon is concentric to the caldera, especially on its south side, and roughly coincides with alluviated basins between volcanoes of Conejos age in the caldera area and volcanoes along the north and south margins of the mapped area.

Despite the wedging out of the La Jara Canyon outflow sheet toward the Platoro caldera, the ash-flow tuff accumulated to great thickness within the caldera, a relation which indicates beginning of caldera collapse during the eruption and which characterizes many San Juan ash-flow eruptions (Steven and Lipman, 1968). Exposures of the intracaldera tuff are mainly on the Cornwall Mountain resurgent block. Near Jasper, where

its top is eroded and its base is not exposed, the intracaldera tuff is continuously exposed at elevations from 9,100 feet to over 12,000 feet on the northeast side of Cornwall Mountain (Platoro map). Even after correction for the gentle southwest dip of the resurgent block, the exposed thickness is greater than 800 m. Thinner sections of the La Jara Canyon within the caldera are exposed where the tuff wedges against the topographic walls of the caldera, especially on the southwest side (figs. 14, 63).

LITHOLOGIC DESCRIPTION

Densely welded devitrified tuff, which constitutes most of the La Jara Canyon Member, is typically light red brown and forms rounded blocky outcrops that weather to a sandy grus. A black basal vitrophyre is commonly present where the ash-flow sheet is 50-100 m thick; where the sheet is very thick or very thin, the zone of devitrification generally extends down into the zone of partial welding. (See Smith, 1960b.) Nonwelded to partly welded buff or gray glassy tuff at the base of the sheet is typically only a few meters thick and is rarely exposed. Where not removed by erosion, several tens of meters of gray partly welded tuff showing evidence of vapor-phase crystallization overlies the densely welded central part of the sheet. This upper vapor-phase zone is characterized by closely spaced, somewhat irregular subhorizontal joints 10-30 cm apart that are parallel to the compaction foliation.

The ash-flow sheet only locally displays clear evidence of compound cooling, as at the Terrace Reservoir dam, where a partly welded zone of gray tuff about 10 m thick separates two zones of red-brown more densely welded tuff. Contacts between individual ash-flow units are also generally obscure, as is typical of thick densely welded ash-flow sheets (Smith, 1960a, p. 811; Ratté and Steven, 1967, p. H29-H33); but in a few places, 5- to 10-cm-thick winnowed horizons containing fewer and smaller phenocrysts than typical appear to mark the tops of flow units (figs. 15, 16).

Most of the La Jara Canyon Member inside Platoro caldera appears very different from the outflow sheet, so different, in fact, that during initial stages of field study the equivalence was not recognized.¹ In the interior of the resurgent block, near Platoro, the intracaldera La Jara Canyon is dark-gray very dense propylitized rock with closely spaced nearly vertical joints 10-40 cm apart (fig. 17A). With rare exceptions (figs. 17B, 18B), the compaction foliation is obscure, both in the field and under the microscope (figs. 17A, 18A). Fine-grained secondary epidote, calcite, and chlorite have partly replaced

¹Patton (1917, p. 33-35) described the intracaldera tuff precisely enough that to a modern reader it is clearly a welded tuff. With impressive insight, he designated these rocks the "biotite latite of the Treasure Mountain Rhylolite." He did, however, separate an underlying unit near Platoro, "the Palisade andesite," which he considered to be part of the Conejos Formation; actually, these rocks constitute the more propylitically altered lower part of the intracaldera La Jara Canyon Member.

the devitrified groundmass and plagioclase and augite phenocrysts. Biotite phenocrysts are extremely oxidized and contain abundant exsolved fine-grained Fe-Ti oxides.

The size and abundance of phenocrysts in the La Jara Canyon Member vary appreciably but were not studied in detail. In general, phenocrysts are more abundant (40-

of the unit elsewhere; this variation may also possibly be due to sorting during emplacement of the ash flows.

Andesitic lithic fragments are common in the La Jara Canyon Member, especially near and within the caldera (fig. 19). The most common fragments are dark gray, aphanitic, and angular to slightly rounded; they are 2-10 cm in diameter and rarely constitute more than a few

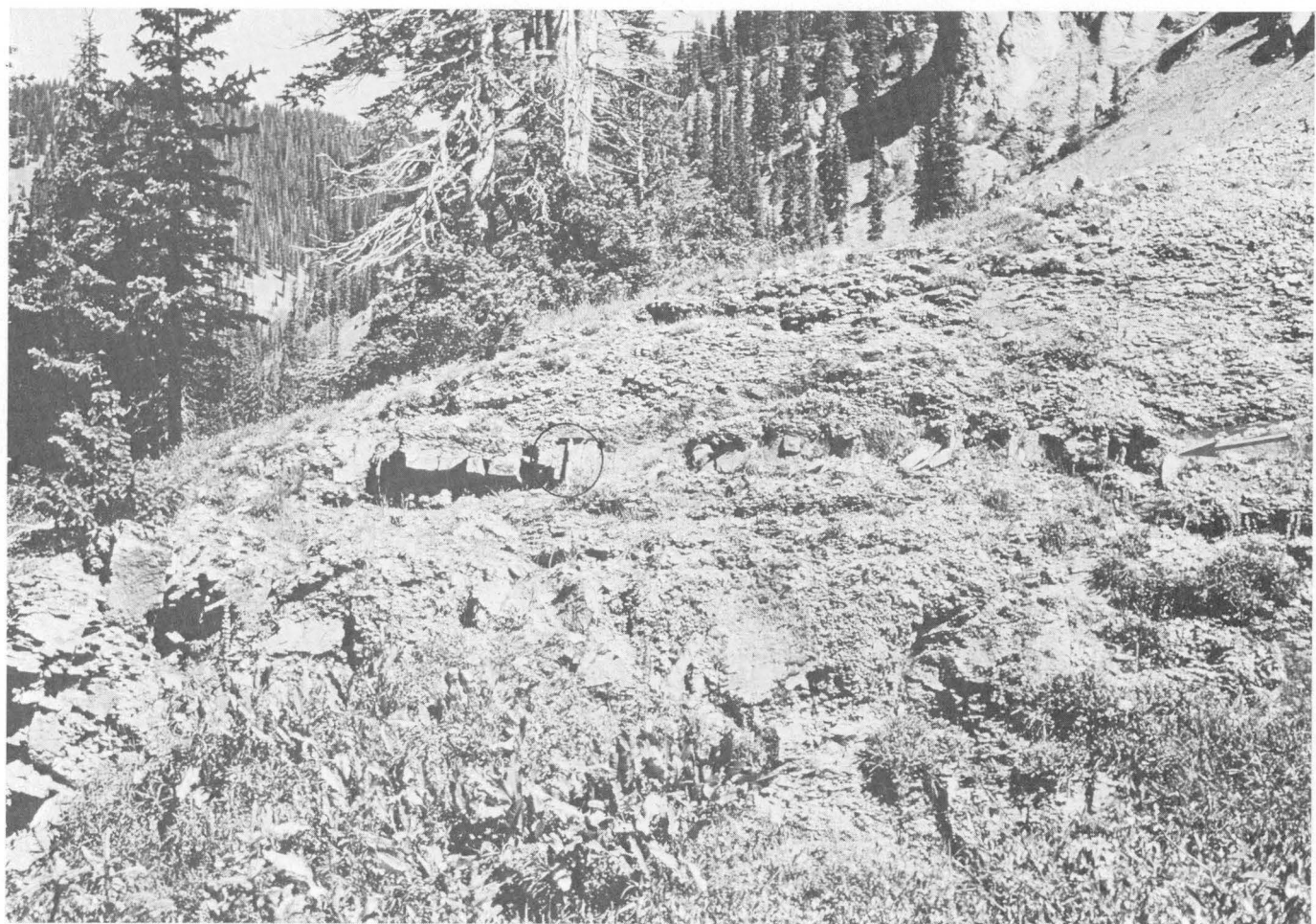


FIGURE 15.—Ash-flow boundary within densely welded devitrified tuff of the La Jara Canyon Member. North side of Elwood Pass road, along tributary of Elwood Creek, at 10,800 feet. Boundary is defined by thin resistant ledge (arrow), about 10 cm thick, that consists of shard-rich tuff at the top of the lower unit, from which phenocrysts have been winnowed. Note hammer (circled) for scale.

50 percent of the rock) and smaller (0.5-1.0 mm (millimeters) in diameter) in the intracaldera tuff than in the outflow sheet (20-35 percent phenocrysts; 1-2 mm in diameter). The abundance of phenocrysts within the caldera is probably due to near-source density concentration of phenocrysts relative to ash shards during emplacement (Fisher, 1966; Lipman, 1967), and the smaller average size may reflect a larger percentage of broken grains. Around the northern margin of the outflow sheet, from Del Norte to Treasure Mountain, the plagioclase phenocrysts are conspicuously more tabular in outline than are the large blocky feldspar phenocrysts

percent of the tuff. In one atypical small area within the caldera (southeast of the Lily Pond, on the Cornwall Mountain resurgent block), andesitic blocks as much as 25 cm across constitute about a third of the tuff. However, large tongues of landslide breccia, such as those interlayered with the intracaldera tuff of Creede, San Juan, Uncompahgre, and Lake City calderas (Steven and Ratté, 1965, p. 42-43; Lipman and others, 1973, p. 639-640), have not been recognized in the La Jara Canyon Member within Platoro caldera.

All rocks of the La Jara Canyon Member are quartz latite, but SiO_2 content ranges from 65 to almost 70 per-

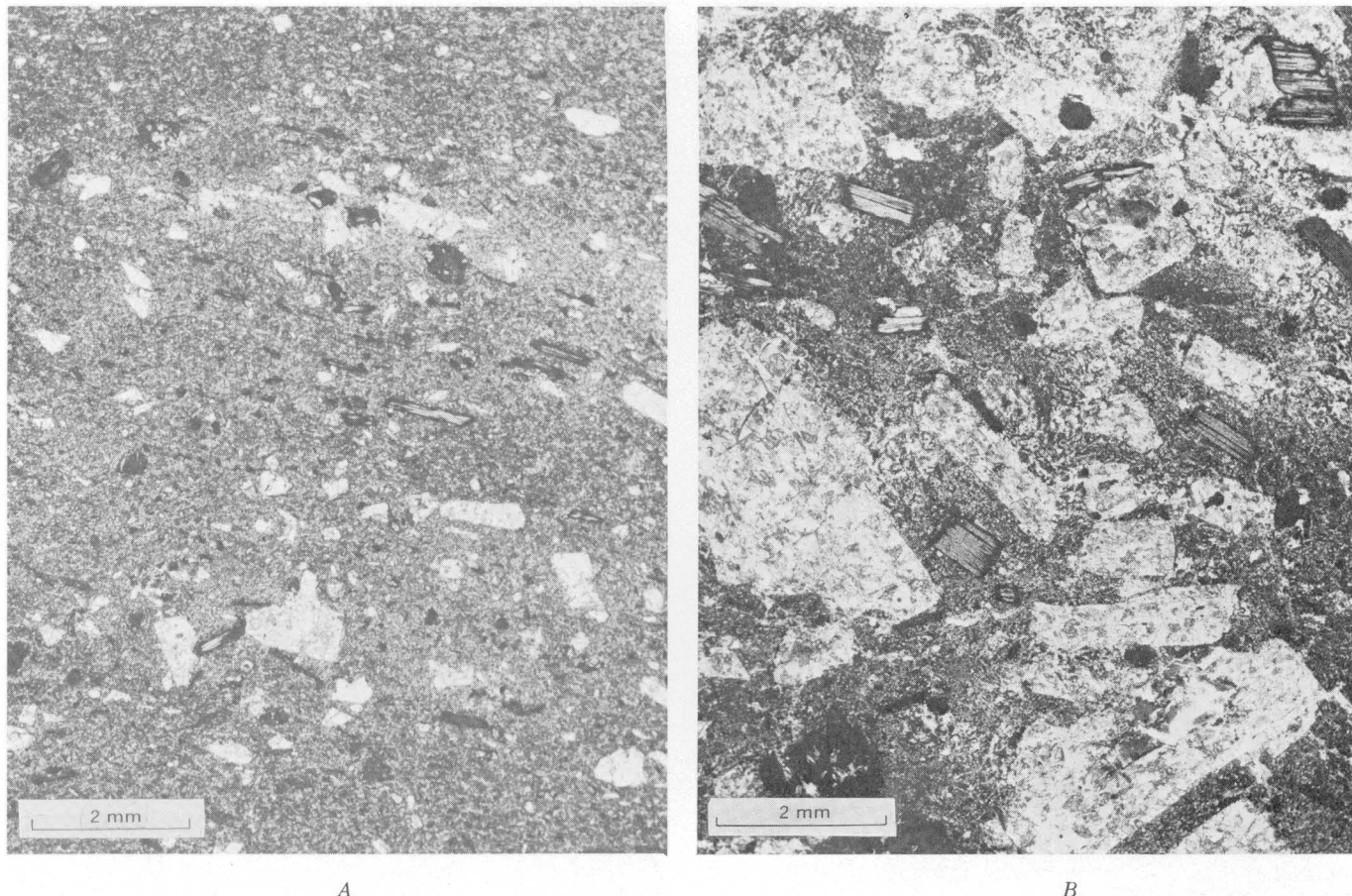


FIGURE 16.—Photomicrographs of rock from ash-flow boundary within densely welded devitrified tuff of the La Jara Canyon Member. North side of Elwood Pass road, along tributary of Elwood Creek, at 10,800 feet. A, Shard-rich tuff containing sparse small broken phenocrysts from base of resistant ledge shown in figure 15; compare

with B. B, Normally textured tuff containing more abundant and larger phenocrysts than A. Plagioclase phenocrysts are largely replaced by carbonate, which obscures the outlines of individual phenocrysts. Sample from just above the resistant ledge shown in figure 15.

cent (table 4). The most mafic rocks are the intracaldera tuffs, a fact suggesting that the later tuff, which erupted concurrently with caldera subsidence, represents the lower more mafic part of a differentiated magma chamber. Similar well-documented examples of this process occur elsewhere in the San Juan volcanic field (Steven and Ratté, 1964; Steven and Lipman, 1968) and in the Western United States (Lipman and others, 1966). However, the most mafic tuffs are also the most phenocryst rich (fig. 12B), and there seems to be a fairly good inverse correlation between phenocryst content and SiO_2 content. Calculated groundmass compositions of all analyzed samples are in the range 71-73 percent SiO_2 , and some of the differences in rock composition seem to be due to variable sorting of phenocrysts during eruption and emplacement rather than to primary magmatic differences.

AGE AND MAGNETIC POLARITY

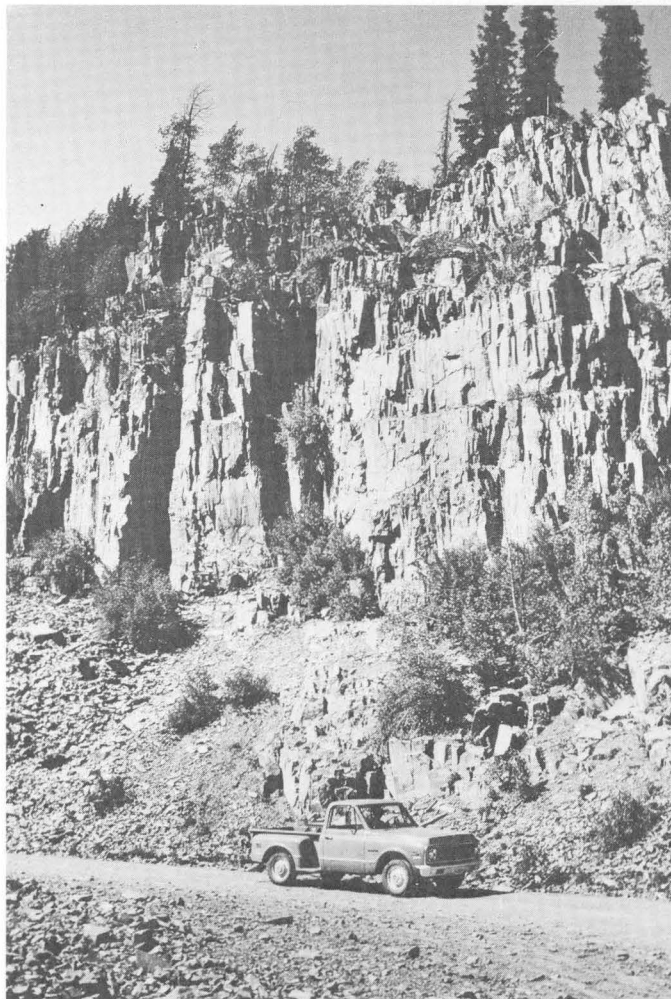
The preferred K-Ar radiometric age of the La Jara Canyon Member at Treasure Mountain is 29.8 m.y. (mean

of biotite and plagioclase from the basal vitrophyre; Lipman and others, 1970, table 3, No. 1). Phenocrysts from two samples of intracaldera tuff (Lipman and others, 1970, table 3, Nos. 2, 3) gave somewhat discordant K-Ar ages that range from 27.0 to 28.5 m.y. These slightly younger ages probably reflect argon loss due to heating by later caldera-related igneous activity at such volcanic centers as the Summitville-Green Ridge zone (29-20 m.y.).

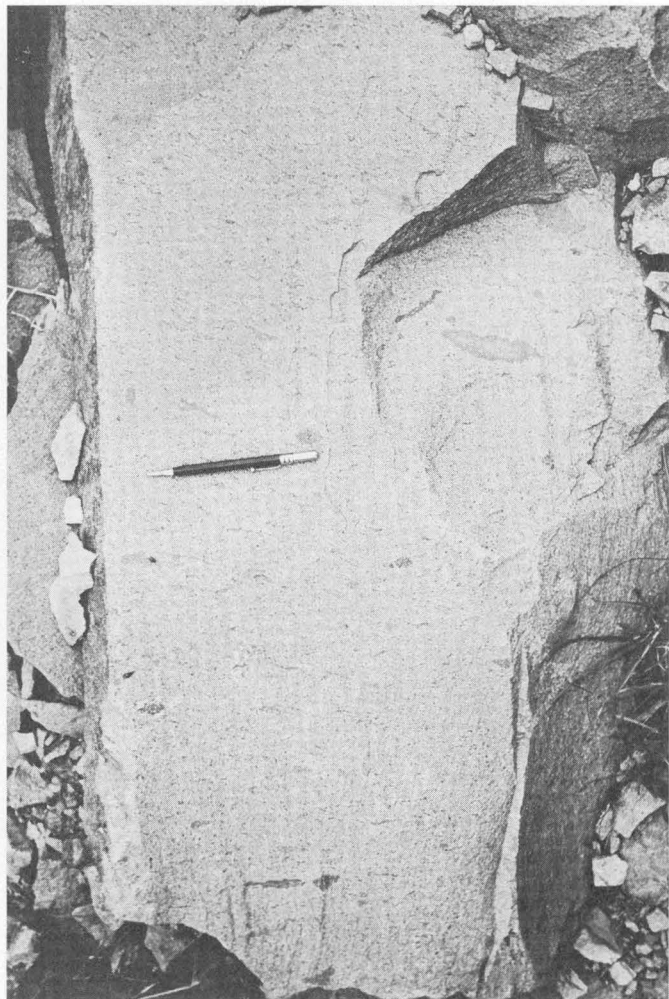
The La Jara Canyon Member is everywhere characterized by reversed magnetic polarity, as indicated by about 25 widely spaced field determinations by the author and by laboratory demagnetization studies of 12 oriented cores from four localities by M. E. Beck, Jr., and James Diehl (written commun., 1971).

VOLUME

Inferences about the original extent of the three main members of the Treasure Mountain Tuff (figs. 14, 23, 25) suggest a simple geometric model for estimation of original volume of these tuffs (fig. 20). This model



A



B

FIGURE 17.—Field appearance of intracaldera La Jara Canyon Member. A, Typical exposure of densely welded propylitized intracaldera La Jara Canyon Member. Closely spaced vertical jointing is most conspicuous feature; welding and compaction textures are

characteristically obscure in this rock type. Above Platoro on Stunner Pass road, at 10,100 feet. B, Densely welded intracaldera La Jara Canyon Member, showing exceptionally conspicuous foliation. Platoro Reservoir road. Analyzed sample 6, table 4.

assumes that the outflow deposits have the cross-sectional geometry of a double wedge that thins both toward the distal edge of the sheet and toward a topographically high caldera area as discussed previously. The intracaldera La Jara Canyon Member is inferred to be thick in the center of the caldera and thin toward the walls. (See cross sections, Platoro map.) This model is obviously much too simple, but the fragmentary record of the original extent of the sheets indicates that more detailed analysis would be unprofitable. The volume estimates are probably conservative, and the upper limit of the inferred possible range may well be more valid for some of the units. The original volume of the La Jara Canyon Member is estimated as 585 km^3 , but it could have been as great as 1000 km^3 (table 5).

MIDDLE TUFF

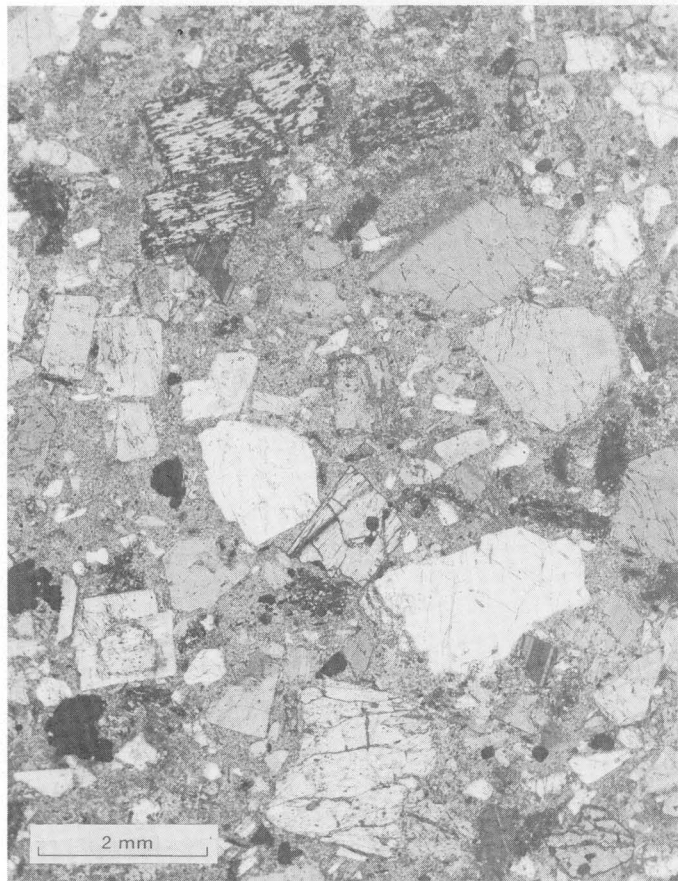
The middle tuff, the most widespread informally named unit of the Treasure Mountain, consists of several thin weakly welded ash-flow deposits and locally thick interbedded ash-fall tuff. The middle tuff rests on the La Jara Canyon Member, except where lava flows of Summitville Andesite occur along the contact, as at the mouth of the West Fork of Park Creek (Platoro map) and near Black Mountain in the Spectacle Lake quadrangle (figs. 2, 21). The middle tuff is overlain by the Ojito Creek Member, or by the Ra Jadero Member where the Ojito Creek is absent. Flows of Summitville Andesite also locally intertongue with the middle tuff, as at McIntyre Peak in the Osier quadrangle (fig. 2).

The distribution and thickness variations of the middle tuff are more like those of the lower tuff (fig. 9) than any of the major Treasure Mountain ash-flow sheets; a separate distribution map has not been prepared. The middle tuff is present on all sides of the caldera, except the southwest. Like other units of the Treasure Mountain, the middle tuff wedges out toward the caldera rim. It is especially thick and widely distributed west of the caldera, in the Treasure Mountain-Wolf Creek Pass area, and along the east front of the San Juan Mountains from the Alamosa River to the south. Maximum thicknesses, about 100 m, are at intermediate distances from the caldera rim, as at Treasure Mountain and along the lower Conejos River. No middle tuff is present between the La Jara Canyon and Ojito Creek Members of the Treasure Mountain in the Summit Peak-Blackhead Peak area or around Banded Peak, suggesting that little of this unit spread to the southwest. The middle tuff is also relatively thin, typically no more than 20

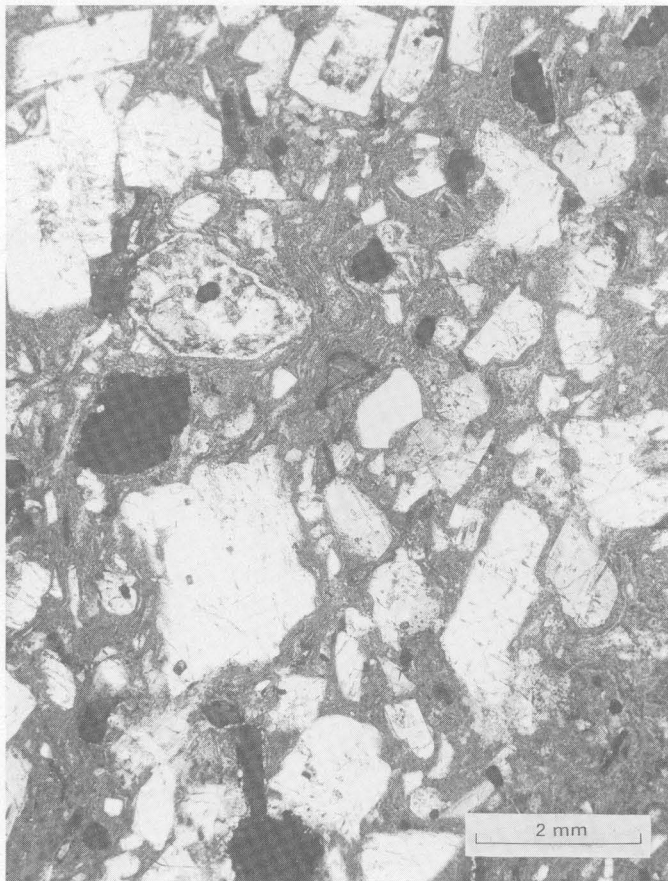
m, north of the caldera in the Del Norte Peak-Horseshoe Mountain area.

The middle tuff consists of local relatively thin and weakly welded ash-flow tuffs, interlayered with ash-fall tuffs. In general, both tuff types are only weakly indurated, and accordingly, exposures tend to be poor.

The middle tuff is the only unit of the Treasure Mountain that contains appreciable thicknesses of ash-fall tuff. Where best exposed, as along the lower Alamosa River (fig. 22), as much as 10 m of white to buff bedded tuff is exposed within single outcrops, and adjacent slopes undoubtedly conceal more. Individual beds, typically 2-50 cm thick, differ mainly in size and abundance of phenocrysts, pumice fragments, and andesitic lithic debris. Local crossbedding and channeling indicate minor reworking of the ash-fall deposits concurrently with deposition. Although dips are everywhere gentle, broad undulations appear to reflect local irregularities in the depositional topography which are



A



B

FIGURE 18.—Microscopic appearance of intracaldera La Jara Canyon Member. A, Photomicrograph of rock shown in figure 17A. Phenocrysts are mostly plagioclase and biotite, with plagioclase partly altered to carbonate and epidote and biotite to chlorite, a

typical propylitic alteration assemblage. Original shard texture of groundmass is completely obscured by devitrification and alteration. B, Photomicrograph of rock shown in figure 17B. Densely welded shard texture still discernible; compare with A.

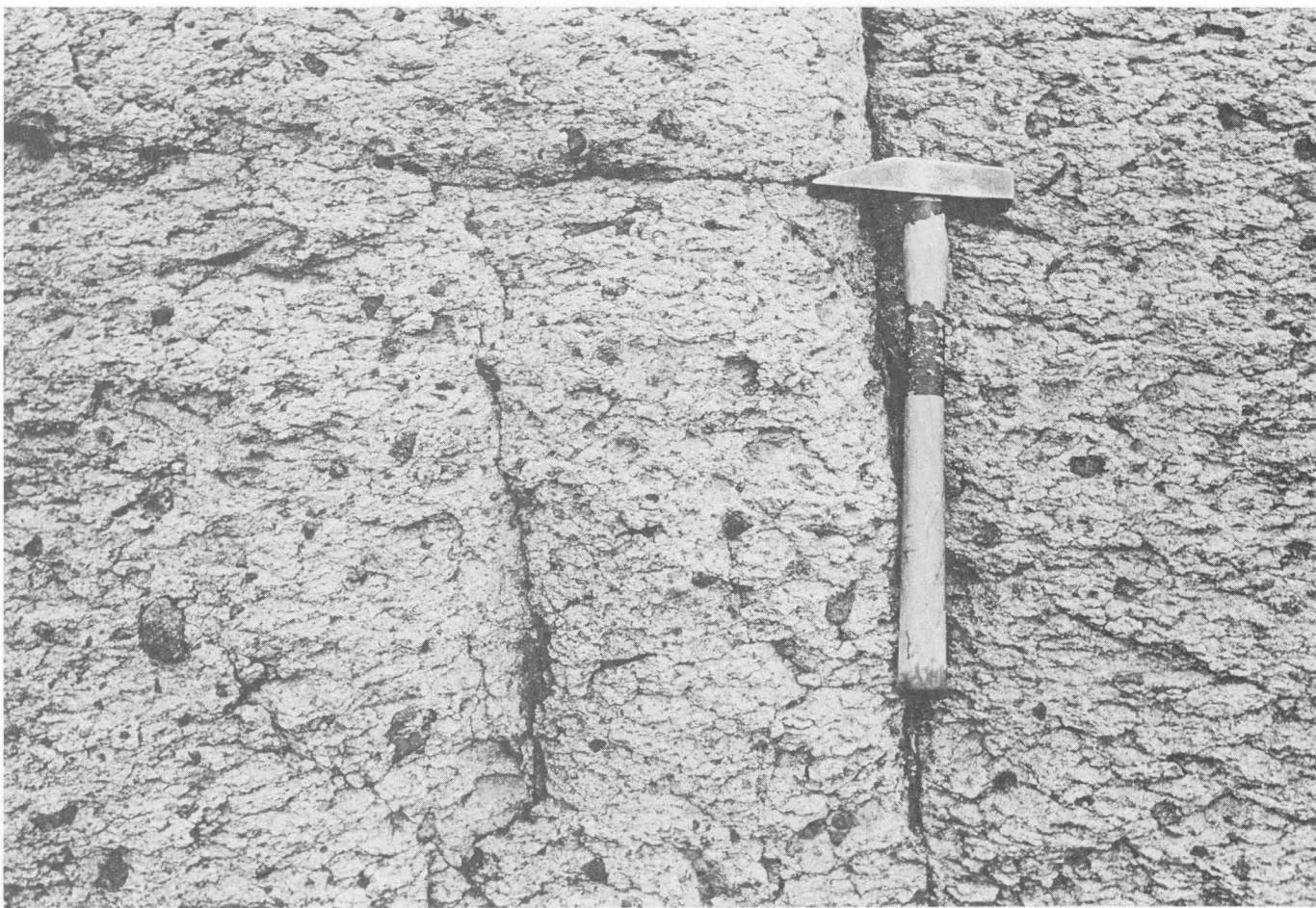


FIGURE 19.—Moderately welded La Jara Canyon Member, containing abundant small andesitic lithic fragments. East slope of Montezuma Peak at about 12,000 feet, just southwest of Cataract Creek stock.

presumably due to slight erosion of the weakly welded top of the La Jara Canyon Member. Near the roadcut shown in figure 22, a broad valley is well exposed in cross section, showing a "synclinal" draping of ash-fall tuff overlain by a lens of local glassy partly welded ash-flow tuff that was deposited in the channel and that contains a concentration of lithic rubble near its base along the channel axis.

The ash-flow deposits of the middle tuff are thin local nonwelded to partly welded sheets, mostly too thin to have devitrified during cooling. At Treasure Mountain, where the middle tuff is about 70 m thick, it contains four separate 10 to 20-m thick ash-flow sheets of non-welded to partly welded glassy tuffs. All are relatively phenocryst poor, containing 5-10 percent total phenocrysts—mainly plagioclase, accompanied by biotite and sparse augite. Petrologically similar ash-flow deposits, although not necessarily exactly correlative, also characterize the middle tuff to the east and south of Platoro caldera. However, at the one place where middle tuff underlies the Ojito Creek within the eastern moat of Platoro caldera (Platoro map), this unit consists of a

rather different densely welded devitrified ash-flow deposit that is exposed over a thickness of at least 60 m where it wedges against the caldera wall; it contains abundant andesitic fragments and about 20 percent phenocrysts of plagioclase, biotite, and augite (completely altered to carbonate).

Ash-flow deposits of the middle tuff appear to be largely or entirely characterized by reverse remanent magnetic polarities west of the caldera, as indicated by

TABLE 5.—*Estimated volumes of ash-flow sheets related to the Platoro caldera complex*

| Unit | Best estimate (km ³) (fig. 20) | Range of alternative estimates (km ³) |
|---|--|--|
| Tuff of Rock Creek | 10 | 5-20 |
| Treasure Mountain Tuff: | | |
| Lower tuff (many separate ash-flow sheets) ... | 30 | 20-40 |
| La Jara Canyon Member | 580 | 500-1,000 |
| Middle tuff (many separate ash-flow sheets) ... | 30 | 20-40 |
| Ojito Creek Member | 50 | 40-70 |
| Ra Jadero Member | 120 | 100-150 |
| Upper tuff (several separate ash-flow sheets) ... | 10 | 5-20 |
| Total | 830 | 690-1,340 |

field determinations near Wolf Creek Pass, but at least one of the ash-flow sheets southeast of the caldera (the one exposed in the channel along the lower Alamosa River canyon) has normal polarity, as measured both in the field and in the laboratory.

OJITO CREEK MEMBER

The Ojito Creek Member of the Treasure Mountain Tuff is a relatively widespread thin single cooling unit of quartz latitic ash-flow tuff which is inferred to have been erupted from the Summitville caldera, nestled within the northern part of the main Platoro caldera. The Ojito Creek Member was named for mesa rim exposures at the head of Ojito Creek (fig. 23), about 22 km east of Platoro (Lipman and Steven, 1970). Even better exposures along the lower Alamosa River canyon on the southwest slope of Chiquita Peak in secs. 24 and 25, T. 36 N., R. 6 E., are designated here as the principal reference section.

The Ojito Creek Member commonly rests on the middle tuff. Where the middle tuff is absent, as inside the Platoro caldera and along the continental divide from

Summit Peak south, the Ojito Creek Member rests directly on the La Jara Canyon. The Ojito Creek is generally overlain by the Ra Jadero Member, but the two densely welded cliff-forming zones are so close together that in most exposures it is not clear that two separate ash-flow sheets are present. In the southwestern part of the area, where the Ojito Creek Member was deposited slightly beyond the Ra Jadero, the Ojito Creek is overlain by various younger units—mainly Masonic Park Tuff, Los Pinos Formation, or basalt of the Hinsdale Formation.

DISTRIBUTION AND THICKNESS

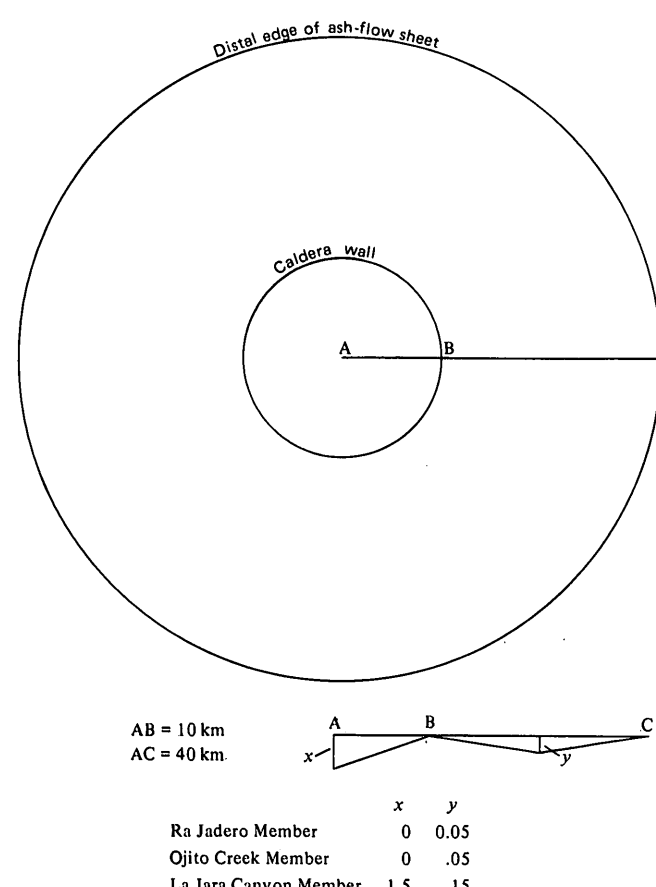
The Ojito Creek Member is most extensive south and southeast of the Platoro caldera (fig. 23), where it forms an apparently originally continuous sheet that is uniformly 15-30 m thick. This main sheet of the Ojito Creek extends south beyond the Conejos River, at least as far as the La Jara Canyon Member. Individual units of the Treasure Mountain have not been recognized farther south in New Mexico (Butler, 1971); if the Ojito Creek is present there, it is only weakly welded. Wedging out of the Ojito Creek Member on the southeast flank of the Platoro caldera highland is well exposed in the Alamosa River canyon and at the head of Ojito Creek (fig. 23); a similar wedging out of the La Jara Canyon Member (fig. 14) occurs somewhat higher on the outer caldera slope.

The western extent of the Ojito Creek Member is uncertain, but most likely only a few small thin lobes extended west from the Platoro caldera. Wedging out against older units is shown in small exposures at the mouth of the West Fork of Park Creek, at Summit Peak, and probably on Conejos Peak. The magnetic polarity of the outcrops on Conejos Peak could not be measured, owing to the effects of lightning strikes; thus, this identification of the Ojito Creek is less certain here than in the other exposures.

The Ojito Creek also was deposited within the main Platoro caldera, in the eastern part of the moat between the resurgent block and the topographic wall. It is exceptionally densely welded there and is as much as 180 m thick—four times as thick as anywhere outside the caldera. The Platoro caldera moat appears to have been lowest in its eastern part during deposition of the Ojito Creek, because this tuff is not exposed elsewhere within the caldera.

LITHOLOGIC DESCRIPTION

Exposures of the Ojito Creek Member are mostly densely welded devitrified red-brown tuff, in places having a distinctive waxy luster imparted by the devitrified groundmass. A black vitrophyre commonly present near the base of the sheet is rarely exposed. The upper 5-10 m of the sheet generally consists of partly welded pinkish-brown or gray tuff characterized by vapor-phase crystallization. This zone was variably eroded shortly



Volume of Ojito Creek Member calculated on basis of deposition over 120° arc (see fig. 23); volumes of other members, on basis of 360° arc

FIGURE 20.—Geometric model for volume calculations of the three major ash-flow sheets of the Treasure Mountain Tuff. See text for details. x and y are approximate thicknesses, in kilometers.

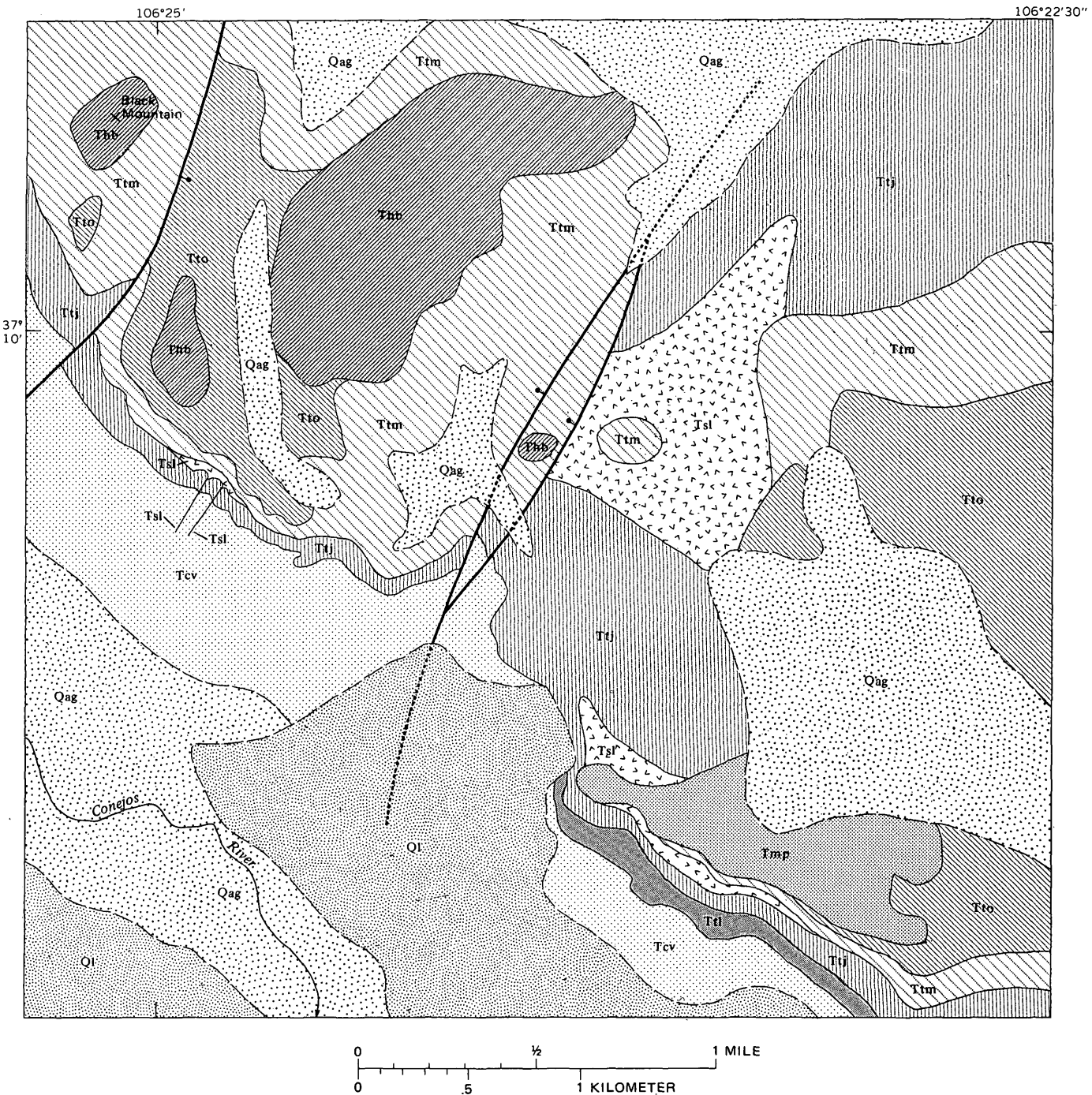
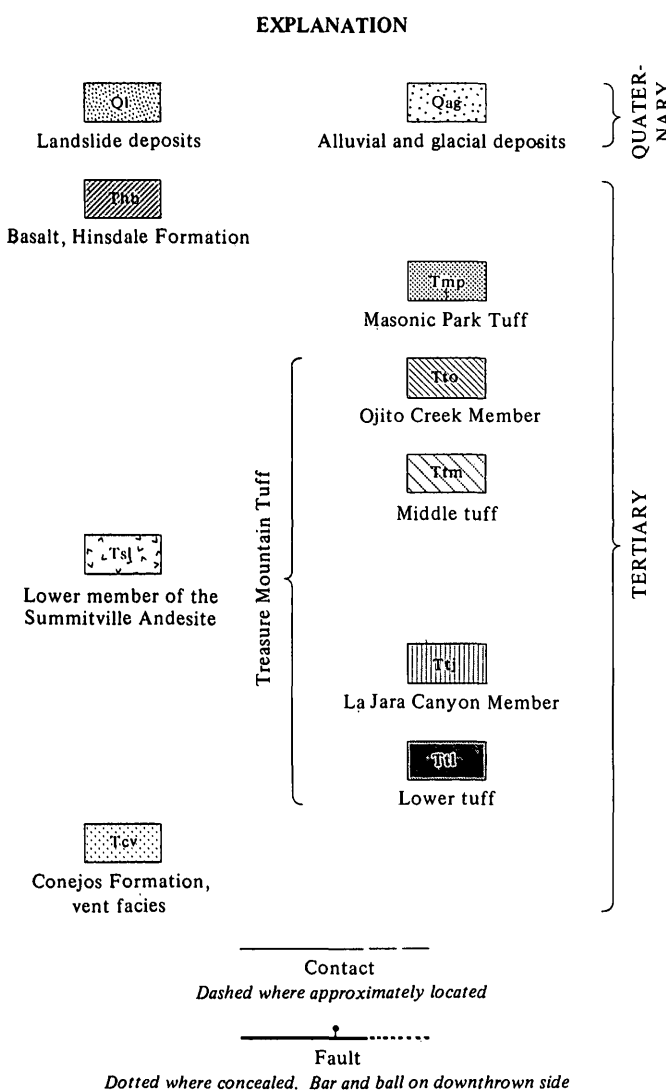


FIGURE 21 (above and right).—Generalized geologic map of the Black Mountain area, showing local flows of Summitville Andesite along contact between La Jara Canyon Member and middle tuff. In places, both the middle tuff and the Ojito Creek Member wedge out against the andesite flows. Two feeder dikes for the andesite are exposed in the cliffs above the Conejos River.

after deposition, and in places the Ra Jadero Member rests directly on the densely welded interior of the Ojito Creek; this relation is strikingly exposed along the lower Alamosa River canyon on the lower southwest slope of Chiquita Peak.

In most outcrops the Ojito Creek Member appears as a

simple cooling unit, although probably it is the result of numerous separate ash flows erupted rapidly and welded together. However, on the southeast side of the caldera, from Chiquita Peak to Ojito Creek, the ash-flow sheet clearly displays compound cooling, with a well-developed partial welding break a few meters thick



within the devitrified zone. The two cooling units in this area also have contrasting fragmental constituents. The lower unit is densely welded, red brown, and relatively phenocryst poor (6-9 percent phenocrysts); it contains sparse lithic fragments and obscure small pumices (fig. 24A). This is the characteristic lithology of the Ojito Creek Member elsewhere. The upper unit, in contrast, contains larger and more abundant phenocrysts (12-17 percent) and conspicuous large dark wispy pumice fragments as much as 30 cm long (fig. 24B); rock fragments are fairly abundant, and the devitrified shard matrix is light gray to pale brown, distinctly lighter colored than in the lower unit. The upper unit appears to be quite local and has only been found southeast of the caldera; it appears to be absent from the relatively thick Ojito Creek within the caldera.

The Ojito Creek Member within the southeastern part of Platoro caldera is petrographically similar to the phenocryst-poor lower unit just described, except that

the basal vitrophyre is lacking, and pumices near the base of the ash-flow sheet are larger and are exceptionally compacted to lineate lenses about 1 cm thick and as much as 40 cm long in the direction of lineation. The unit within the caldera has a chalky appearance, owing to intense devitrification; and in the upper third or half of the unit, where degree of welding decreases, vapor-phase crystallization predominates.

The Ojito Creek contains phenocrysts of plagioclase, biotite, Fe-Ti oxides and sparse augite. The sparse hornblende in a few samples may be xenocrystic. In general, the Ojito Creek Member contains fewer phenocrysts than the other two major ash-flow sheets of the Treasure Mountain; in addition, it can generally be distinguished from the La Jara Canyon Member by its lower augite content and from the Ra Jadero Member by its lower sanidine content (fig. 12).

The Ojito Creek tuffs are quartz latitic; SiO₂ content of six bulk-rock samples of the outflow sheet ranges only from 67.7 to 70.4 percent (table 4). Within this limited range, the phenocryst-rich tuffs of the upper unit appear to be distinctly more mafic (68.0-68.8 percent SiO₂) than two of the three samples of the phenocryst-poor lower unit (69.6-70.4 percent SiO₂). The one sample of the lower unit that has only 67.7 percent SiO₂ (table 4, No. 12) is thought to be abnormal, because it is also anomalous in other oxides, such as CaO and total iron. Pumice lenses from the upper unit contain fewer phenocrysts than the enclosing tuff, and two analyses (table 4, Nos. 18, 19) are compositionally very similar to bulk-rock analyses of the lower unit. This similarity suggests that petrologic differences between the two units are largely due to sorting and winnowing of fine shards and ash from the fragmental matrix of the upper unit during eruption and emplacement; such sorting has also been described in other ash-flow deposits (Fisher, 1966; Lipman, 1967). One old analysis of the Ojito Creek Member from within the Platoro caldera (table 4, No. 11) indicates that the intracaldera tuff is more mafic than the outflow sheet; but because the intracaldera tuff petrographically resembles silicic parts of the outflow sheet, probably this sample is anomalous, or the analysis is erroneous.

AGE AND MAGNETIC POLARITY

The Ojito Creek Member has not been radiometrically dated, but its age is bracketed by dates (Lipman and others, 1970) for the La Jara Canyon Member (29.8 m.y.) and for the overlying Masonic Park Tuff (28.2 m.y.). In addition, ring faults of the Summitville caldera, from which the Ojito Creek is thought to have erupted, localized the emplacement of the Alamosa River stock, dated at 29.1 m.y. This suggests eruption of the Ojito Creek and Ra Jadero Members between 29.8 and 29.1 m.y. This age bracket is sufficiently tight that little would be gained by radiometric determinations on the

Ojito Creek, because the precision of individual determinations by current techniques is approximately ± 3 percent—an uncertainty as great as the limits imposed by the dated rocks.

The Ojito Creek everywhere has normal magnetic polarity, as indicated by at least 30 field determinations, supplemented by laboratory study of oriented cores from one locality by M. E. Beck, Jr., and James Diehl (written commun., 1971). The normal polarity of the Ojito Creek, in contrast to the reverse polarities of the Ra Jadero and La Jara Canyon Members, was of particular assistance in initial unravelling of stratigraphic complexities in the field, especially in correlation of units within the southeastern part of Platoro caldera with the outflow Treasure Mountain sequence.

RA JADERO MEMBER

The Ra Jadero Member, a widespread thin densely welded quartz latitic tuff, is the last major ash-flow sheet of the Treasure Mountain Tuff. Like the Ojito Creek, it is thought to have been erupted from the Summitville caldera. The Ra Jadero Member was named (Lipman and Steven, 1970) for exposures in Ra Jadero Canyon,

about 26 km southeast of Platoro (fig. 25). The principal reference section is the same as that selected for the Ojito Creek—the area of excellent cliff exposures along the lower Alamosa River canyon, southwest of Chiquita Peak, in secs. 24 and 25, T. 36 N., R. 6 E.

The Ra Jadero Member rests on lower members of the Treasure Mountain Tuff over most of its extent: commonly on the Ojito Creek Member or on the middle tuff; directly on the La Jara Canyon Member in the northeastern area where the Ojito Creek was not deposited. In the Park Creek area the Ra Jadero is separated from the Ojito Creek by lava flows of Summitville Andesite (Platoro map), and in a few places the Ra Jadero laps up onto rocks of the Conejos Formation that stood high during the ash-flow eruptions. The Ra Jadero Member is generally overlain by the Masonic Park Tuff; in areas where the Masonic Park was eroded or was never deposited, the Ra Jadero is overlain by Los Pinos Formation or by basalt of the Hinsdale Formation.

DISTRIBUTION AND THICKNESS

The Ra Jadero Member is a widespread thin unit (fig. 25); among the units of Treasure Mountain Tuff, its ex-

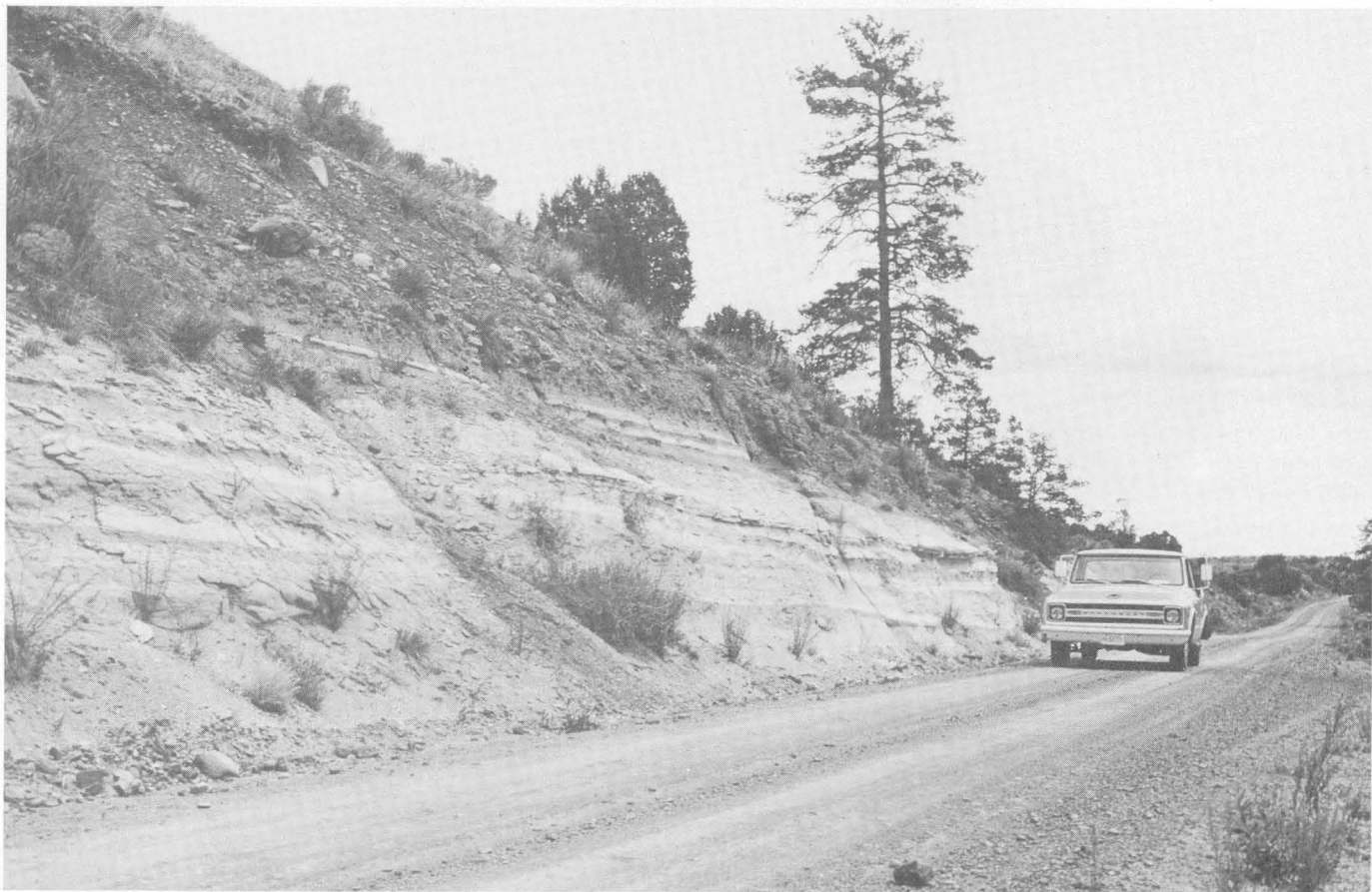


FIGURE 22.—Well-bedded ash-fall tuffs of the middle tuff of the Treasure Mountain Tuff, overlain by glacial outwash gravel. Alamosa River canyon, west of Chiquita Peak.

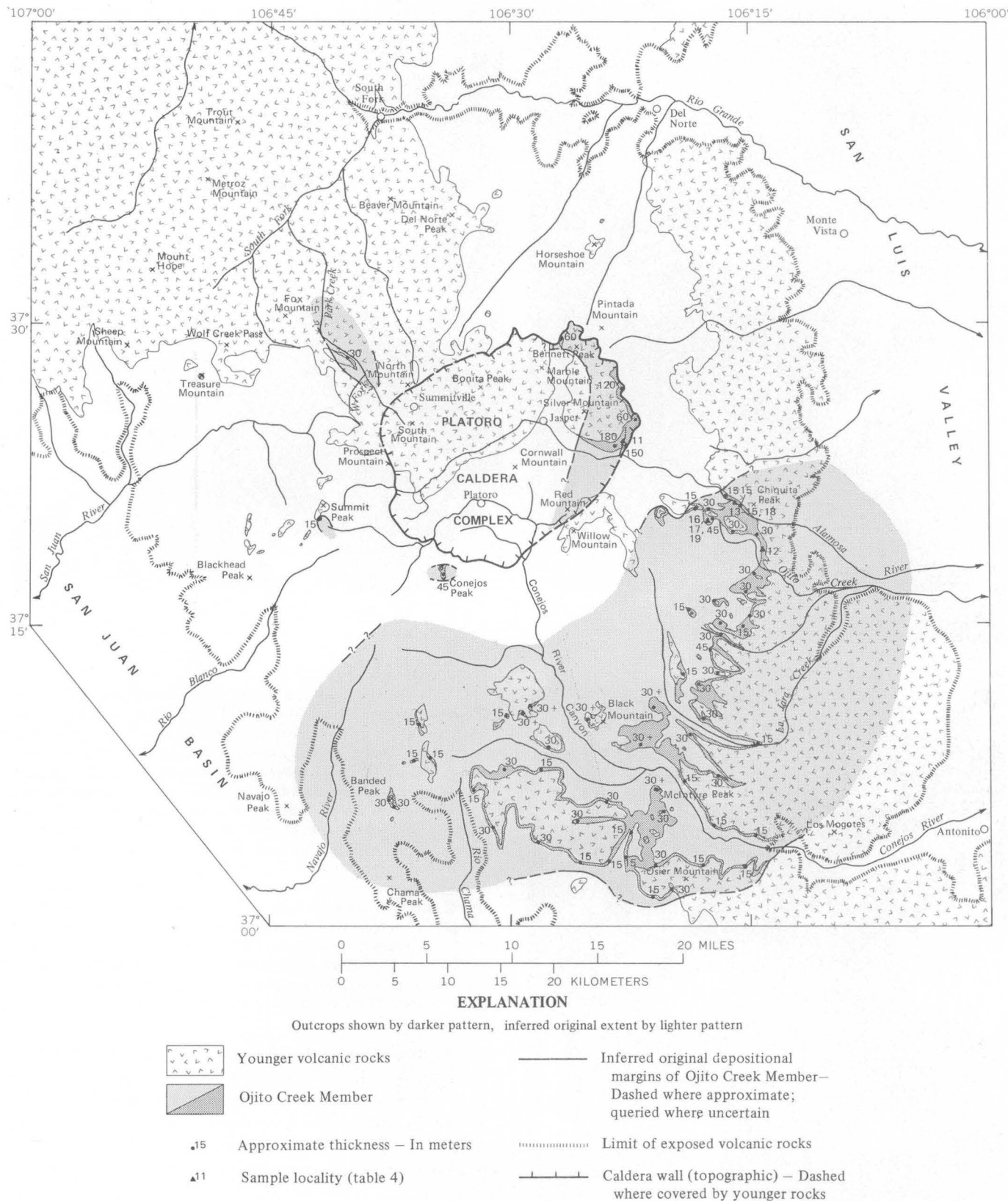


FIGURE 23.—Outcrop area, approximate thickness of selected sections, and inferred original depositional extent of the Ojito Creek Member, Treasure Mountain Tuff. Based on mapping by P. W. Lipman, 1965-67, 1970-71.

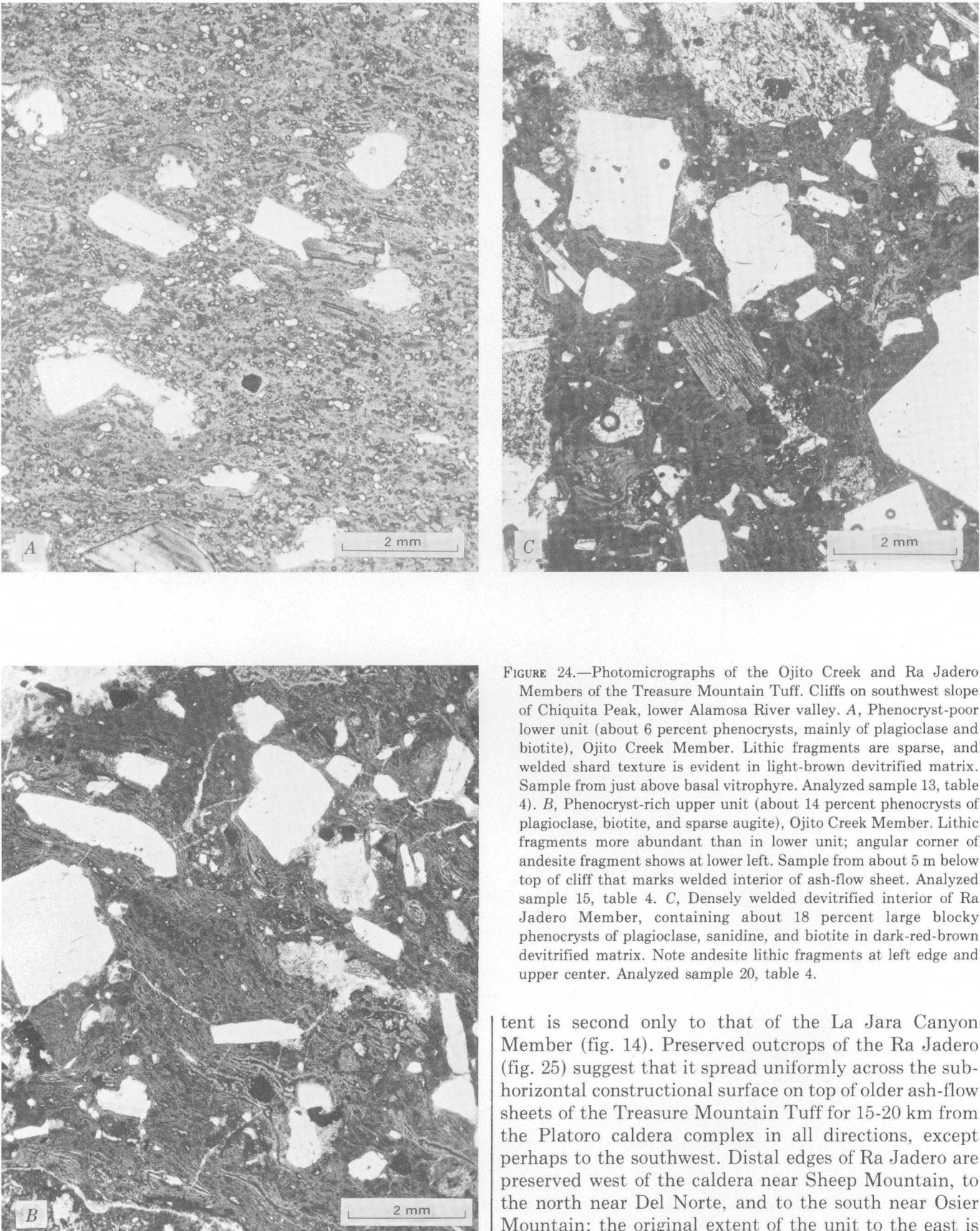
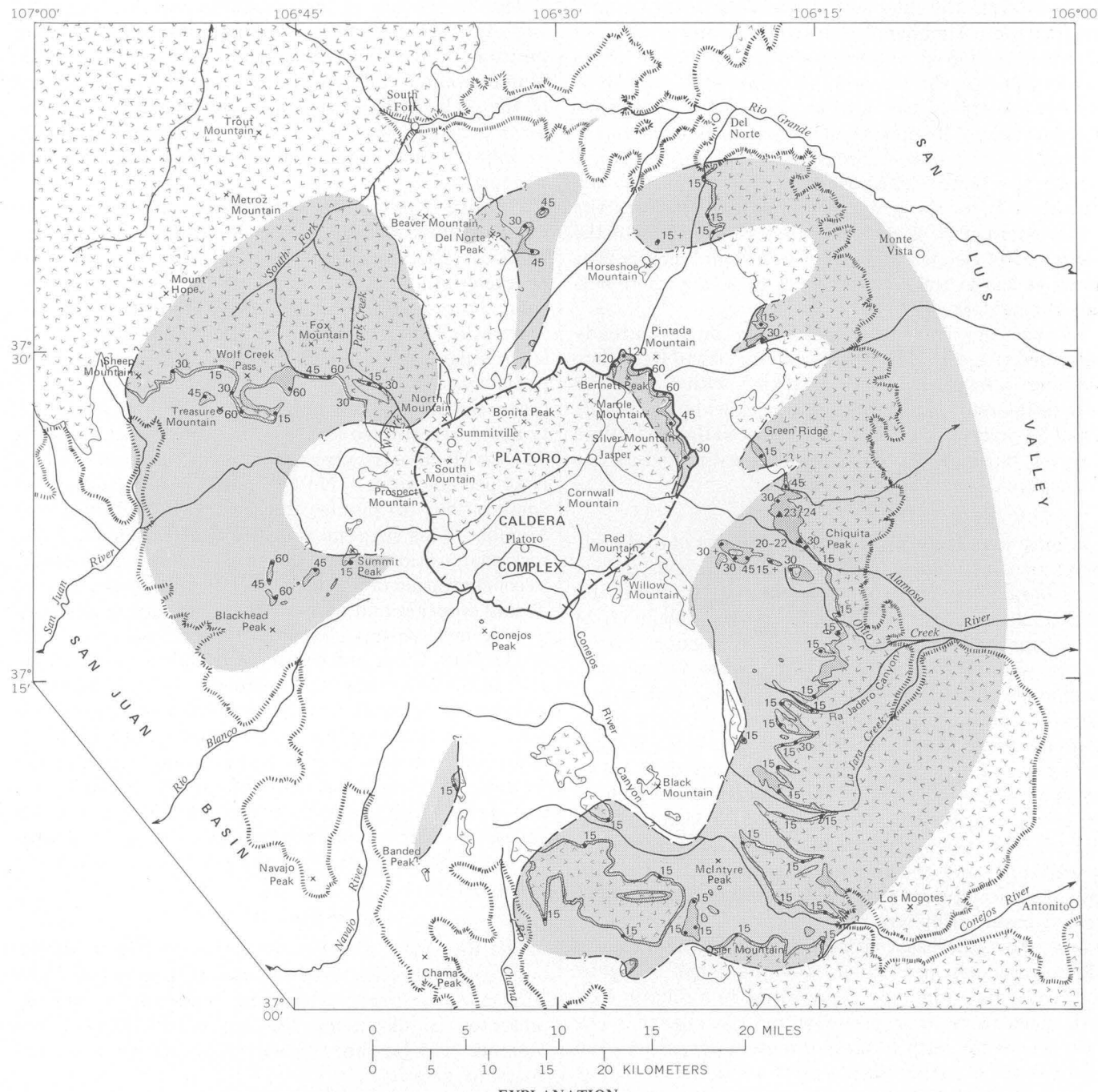


FIGURE 24.—Photomicrographs of the Ojito Creek and Ra Jadero Members of the Treasure Mountain Tuff. Cliffs on southwest slope of Chiquita Peak, lower Alamosa River valley. A, Phenocryst-poor lower unit (about 6 percent phenocrysts, mainly of plagioclase and biotite), Ojito Creek Member. Lithic fragments are sparse, and welded shard texture is evident in light-brown devitrified matrix. Sample from just above basal vitrophyre. Analyzed sample 13, table 4). B, Phenocryst-rich upper unit (about 14 percent phenocrysts of plagioclase, biotite, and sparse augite), Ojito Creek Member. Lithic fragments more abundant than in lower unit; angular corner of andesite fragment shows at lower left. Sample from about 5 m below top of cliff that marks welded interior of ash-flow sheet. Analyzed sample 15, table 4. C, Densely welded devitrified interior of Ra Jadero Member, containing about 18 percent large blocky phenocrysts of plagioclase, sanidine, and biotite in dark-red-brown devitrified matrix. Note andesite lithic fragments at left edge and upper center. Analyzed sample 20, table 4.

tent is second only to that of the La Jara Canyon Member (fig. 14). Preserved outcrops of the Ra Jadero (fig. 25) suggest that it spread uniformly across the subhorizontal constructional surface on top of older ash-flow sheets of the Treasure Mountain Tuff for 15-20 km from the Platoro caldera complex in all directions, except perhaps to the southwest. Distal edges of Ra Jadero are preserved west of the caldera near Sheep Mountain, to the north near Del Norte, and to the south near Osier Mountain; the original extent of the unit to the east is



EXPLANATION

Outcrops shown by darker pattern, inferred original extent by lighter pattern



Younger volcanic rocks



Ra Jadero Member

— Inferred original depositional margins
of Ra Jadero Member — Dashed
where approximate; queried where
uncertain

•¹⁵

Approximate thickness — In meters

..... Limit of exposed volcanic rocks

•³⁰

Sample locality (table 4)

— Caldera wall (topographic) — Dashed
where covered by younger rocks

FIGURE 25.—Outcrop area, approximate thickness of selected sections, and inferred original depositional extent of the Ra Jadero Member, Treasure Mountain Tuff. Based on mapping by P. W. Lipman, 1965-67, 1970-71.

unknown. Like the older units of the Treasure Mountain, the Ra Jadero Member also clearly thins and wedges out toward the Platoro caldera complex (fig. 25). The Ra Jadero ash-flow sheet is relatively thin—typically 10-40 m—everywhere on the outflow plateau that surrounds Platoro caldera. Its maximum thickness, about 60 m, occurs in the area east of Treasure Mountain (fig. 25).

Like the Ojito Creek Member, the Ra Jadero accumulated to its greatest thickness within the northeastern part of the main Platoro caldera. On the north side of Bennett Peak, the Ra Jadero Member is as much as 125 m thick—twice as thick as anywhere outside the caldera.

By use of the simple geometric model already described (fig. 20), the original volume of the Ra Jadero Member is estimated at 100-150 km³, with a preferred best estimate of 120 km³ (table 5). This volume is only about 20 percent of the volume estimated for the La Jara Canyon, but it is double the volume estimated for the Ojito Creek.

LITHOLOGIC DESCRIPTION

In most exposures the Ra Jadero consists of dark-red-brown densely welded tuff underlain by a conspicuous black basal vitrophyre zone about 5 m thick. Where the total thickness of the Ra Jadero is less than about 15-20 m, an upper thinner vitrophyre zone is commonly present as well. The base of the Ra Jadero is generally covered by debris and has only been observed at one place—on an inaccessible cliff exposure along the lower Alamosa River canyon on the southwest slope of Chiquita Peak. There, the Ra Jadero was deposited on an irregular surface of low relief eroded in the partly welded upper vapor-phase zone of the Ojito Creek Member. The two ash-flow sheets are separated by only about 0.5 m of bedded tuff, and the nonwelded basal tuff of the Ra Jadero grades upward within about 1 m into the densely welded basal vitrophyre zone.

Just above the basal vitrophyre the matrix of the Ra Jadero becomes devitrified, but the large collapsed pumice lenses remain glassy, resulting in a colorful rock with black lenses in a red-brown matrix. Higher in the unit, where the rock is most intensely devitrified, the pumices are a chalky purple brown with a fine porous texture, resulting from fine secondary vesiculation within the pumices during devitrification. In places the size of the pumice blocks increases upward, and northeast of the Terrace Reservoir (Platoro map), single lenses are as long as 0.5 m.

The Ra Jadero is fairly phenocryst rich, typically containing 12-18 percent phenocrysts of plagioclase, sanidine, biotite, and augite. In contrast to other major units of the Treasure Mountain, the Ra Jadero contains more abundant sanidine (fig. 12A), and the plagioclase phenocrysts are exceptionally large and blocky in outline (fig. 24C).

The Ra Jadero is also characterized by abundant volcanic rock fragments of varied intermediate compositional types. These fragments tend to be 1-5 cm in diameter and locally amount to as much as 5-10 percent of the rock. In hand specimen the Ra Jadero appears heterogeneous, as a result of the large pumice blocks, the abundant rock fragments, and the large size of phenocrysts.

Despite their heterogeneous appearance, four analyzed bulk-rock samples of Ra Jadero tuffs are uniform in chemical composition (table 4) and are characterized by SiO₂ contents (64.2-65.6 percent) lower than those of any other outflow units of the Treasure Mountain Tuff. These relatively mafic compositions are surprising, in light of the greater abundance of phenocrystic sanidine in the Ra Jadero tuffs than in other major Treasure Mountain ash-flow sheets. A typical large pumice lens from the upper part of the Ra Jadero Member is phenocryst poor and rather silicic (70.4 percent; table 4, No. 24), however, and is similar in composition to pumice blocks of the Ojito Creek Member. This suggests that the relatively mafic bulk-rock compositions of the Ra Jadero Member may be due to concentration of phenocrysts in the tuffaceous matrix, during eruption and emplacement, by sorting and winnowing mechanisms similar to those already discussed for the Ojito Creek and for the intracaldera La Jara Canyon tuffs. The andesitic fragments in the bulk-rock samples probably also contribute to the relatively mafic bulk compositions of the Ra Jadero Member, although abundant xenoliths were avoided in selecting material for analysis. In any case, the relations between bulk-rock and pumice compositions of the Ojito Creek and Ra Jadero Members show that bulk samples of these units do not closely approximate the preeruption magmatic compositions.

AGE AND MAGNETIC POLARITY

The Ra Jadero Member has not been directly dated, but its age is bracketed by radiometric dates of 29.8 and 29.1 m.y., by use of the same reasoning as already presented in discussing the age of the Ojito Creek Member. The Ra Jadero Member has reverse remanent magnetic polarity.

UPPER TUFF

The upper tuff is the most restricted and least studied unit of the Treasure Mountain. It is present mainly north of the Platoro caldera, where it includes a distinctive densely welded phenocryst-rich ash-flow sheet and minor less welded local tuffs. Relatively thin partly welded tuffs at the top of the Treasure Mountain Tuff near Wolf Creek Pass and south of Del Norte are also probably parts of the upper tuff, although poor exposures permit interpretation of these rocks as weakly welded upper parts of the Ra Jadero Member. The upper

tuff everywhere rests on the Ra Jadero Member and is overlain by Masonic Park Tuff. Correlatives of the upper tuff have not been recognized south of the caldera complex.

The distinctive phenocryst-rich ash-flow sheet of the upper tuff is 20-40 m thick where best exposed—at Bennett Peak just within the Platoro caldera, and on the slopes of Del Norte Peak outside the caldera to the north. At these localities, it is mainly densely welded red-brown devitrified tuff, with a conspicuous black vitrophyre zone near its base. It contains about 25 percent phenocrysts of plagioclase, sanidine, biotite, and augite. In places, it resembles the La Jara Canyon Member in hand specimen, but the higher ratio of sanidine to plagioclase—as great as 1:2 (fig. 124)—is diagnostic.

A densely welded tuff sheet that is about 20 m thick on the ridge between Burro and Pinos Creeks (Platoro map), apparently sandwiched between lavas of Summitville Andesite just within the Platoro caldera, is distinguished by abundant tabular plagioclase phenocrysts, accompanied by biotite and augite, but is entirely lacking in sanidine. Numerous separate ash flows are present within the unit, as indicated by conspicuous partings well defined by concentrations of pumices and andesitic lithic fragments. This unit has not been identified elsewhere, and its inclusion in the upper tuff is tentative.

YOUNGER ASH-FLOW SHEETS AND INTERLAYERED LAVAS

Overlying the Treasure Mountain Tuff over much of its extent is a sequence of younger ash-flow sheets that were erupted in late Oligocene time from calderas in the central part of the San Juan field. Although not directly related to the evolution of the Platoro caldera complex, these ash-flow sheets are described briefly because (1) variations in their distribution and thickness provide much information on the changing topography resulting from intermittent late volcanic activity in the Platoro caldera area, and (2) petrologic features of the younger sheets permit illuminating contrasts and comparisons with the Treasure Mountain Tuff. General petrologic features of these ash-flow sheets—the Masonic Park, Fish Canyon, Carpenter Ridge, Wason Park, and Snowshoe Mountain Tuffs—are summarized in table 3, and available chemical analyses are listed in table 6. Lava flows interlayered with these ash-flow sheets are also discussed briefly.

MASONIC PARK TUFF

The Masonic Park Tuff is named here for the great palisade exposures at the type area along the Rio Grande valley near Masonic Park, 5 km northwest of South Fork (fig. 26). It consists of two large ash-flow sheets of phenocryst-rich quartz latite that originally spread over much of the southeastern San Juan Mountains. The Masonic Park Tuff, generally mapped by Larsen and

Cross (1956) at the top of their Treasure Mountain Rhyolite, is separated from the Treasure Mountain Tuff and renamed here, because it is believed to have been erupted from a different source, the Mount Hope caldera (fig. 26). Recently, this unit has been informally called the tuff of Masonic Park (Lipman and others, 1970; Steven and Lipman, 1973).

The two ash-flow sheets of the Masonic Park Tuff, designated as the lower and upper members, seem petrographically indistinguishable. Near the Mount Hope caldera they interfinger complexly with penecontemporaneous lavas and breccias of the Sheep Mountain Andesite and other lava units (Steven and Lipman, 1973). Away from this caldera, the Masonic Park Tuff generally overlies upper units of the Treasure Mountain Tuff and is overlain by the Fish Canyon Tuff. South of an east-west zone running approximately from Summitville to Green Ridge where the Fish Canyon seems never to have been deposited, the Masonic Park is overlain by volcaniclastic sedimentary rocks of the Los Pinos Formation or by basalt of the Hinsdale Formation.

DISTRIBUTION AND THICKNESS

The lower member of the Masonic Park Tuff has been identified only west and southwest of the Mount Hope caldera; it crops out in the West Fork of the San Juan River and in Goose Creek (fig. 26) and has also been traced 25 km west of the mapped area, as far as Huerto Creek (Durango map). In these places the lower member is typically 30-50 m thick; its maximum thickness, in Goose Creek, is about 150 m.

The upper member of the Masonic Park overlies the lower member in the West Fork of the San Juan River, where it is generally about 50-75 m thick, but in places it wedges out against the Sheep Mountain Andesite. Where the upper member occurs above the lower member in Goose Creek, it is as much as 300 m thick, and at Masonic Park the upper member reaches its maximum known thickness—400 m, with no base exposed (fig. 26). East and southeast of the Mount Hope caldera only the upper member is present; it extends east as far as the San Luis Valley and south about 25 km into New Mexico (Butler, 1971). Although these exposures are discontinuous (fig. 26), only one ash-flow sheet of Masonic Park lithology is present, and there seems little doubt of its identity as the upper member. Over this vast area the upper member forms a relatively uniform thin sheet of partly welded tuff 15-50 m thick.

The Masonic Park Tuff is not present within the Platoro caldera or high on its outer slopes. Although the distribution of the Masonic Park shown in figure 26, is in part conjectural, depositional wedging of the Masonic Park on the flanks of the Platoro caldera complex is clearly evident from mapped relations northwest of Summitville, in the Del Norte Peak area, near Summit

PLATORO CALDERA COMPLEX, SAN JUAN MOUNTAINS, COLORADO

TABLE 6.—Analyses of the

[Sample localities shown in figs. 26, 30, and 31 and (or) described below. Analyses 8, 11, and 20 are from Larsen and Cross (1956, table 21); analyses from unpublished data provided by T. A. Steven and J. C. Ratté. Major-oxide analyses 1, 5, 9, 10, 12, 13, 15-17, and 19 are by rapid methods methods are No. 2 by F. H. Neurburg, No. 3 by V. C. Smith, and Nos. 4, 6, and 7 by C. L. Parker. Minor-element analyses 4, 6, by Norma Rait,>, more than; <, less than]

| Sample----- | Masonic Park Tuff | Fish Canyon Tuff | | | | | | | | |
|--|-------------------|----------------------------------|----------------------|-------------------------|-------------------------|---------------------|-------------------------|-------------------------|----------------|--------------------------|
| | | Intra-caldera (La Garita Member) | | | | | | Outflow | | |
| | | 1 65L-127 | 2 C-987 C-1165 | 3 S-352-A D100281 | 4 S-292-C D100011 | 5 C-95 151485 | 6 C-162-B D100009 | 7 S-292-B D100010 | 8 L+G 21-37 | 9 DS-34-A W-168465 |
| Major oxides (weight percent), recalculated without H ₂ O and CO ₂ | | | | | | | | | | |
| SiO ₂ ----- | 68.2 | 66.00 | 66.38 | 66.56 | 66.6 | 67.04 | 67.42 | 65.86 | 66.6 | 66.8 |
| Al ₂ O ₃ ----- | 16.4 | 16.20 | 15.87 | 15.93 | 16.1 | 15.77 | 15.41 | 15.81 | 16.3 | 17.0 |
| Fe ₂ O ₃ ----- | 2.6 | 4.00 | 3.07 | 3.92 | 4.0 | 2.39 | 3.75 | 3.51 | 3.4 | 3.9 |
| FeO----- | .70 | .28 | 1.28 | .29 | .20 | 1.61 | .27 | .95 | .61 | .08 |
| MgO----- | .76 | 1.14 | 1.48 | 1.27 | .94 | 1.10 | 1.20 | 1.43 | 1.2 | .55 |
| CaO----- | 2.8 | 3.10 | 3.39 | 3.35 | 3.4 | 3.05 | 3.41 | 3.73 | 3.4 | 3.4 |
| Na ₂ O----- | 3.4 | 3.27 | 3.75 | 3.89 | 3.9 | 3.52 | 3.77 | 3.65 | 3.6 | 3.6 |
| K ₂ O----- | 4.7 | 5.17 | 3.92 | 3.97 | 4.0 | 4.66 | 3.97 | 4.11 | 3.8 | 3.7 |
| TiO ₂ ----- | .49 | .54 | .56 | .52 | .53 | .56 | .51 | .71 | .57 | .53 |
| P ₂ O ₅ ----- | .00 | .21 | .21 | .20 | .21 | .20 | .20 | .23 | .18 | .21 |
| MnO----- | .10 | .09 | .08 | .10 | .06 | .09 | .09 | ---- | .22 | .10 |
| Total----- | 100.14 | 100.00 | 99.99 | 100.00 | ---- | 99.99 | 100.00 | 99.99 | 99.88 | 99.86 |
| H ₂ O----- | .69 | .88 | .34 | .30 | .48 | .33 | .22 | .57 | .48 | .18 |
| H ₂ O----- | .71 | .98 | .84 | .36 | .23 | .15 | .31 | .81 | .41 | .31 |
| CO ₂ ----- | <.05 | 1.10 | .04 | .02 | .10 | .01 | .23 | ---- | .15 | <.05 |
| Norms (weight percent) | | | | | | | | | | |
| Quartz----- | 23.45 | 19.4 | 20.8 | 20.51 | 26.65 | 21.13 | 22.25 | 19.96 | 22.0 | 23.78 |
| Orthoclase----- | 27.8 | 30.6 | 23.16 | 23.43 | 23.67 | 27.52 | 23.47 | 24.27 | 22.71 | 22.05 |
| Albite----- | 28.6 | 27.7 | 31.7 | 32.86 | 33.03 | 29.76 | 31.89 | 30.88 | 30.81 | 30.72 |
| Anorthite----- | 13.7 | 14.05 | 14.89 | 14.3 | 14.6 | 13.48 | 13.39 | 14.63 | 15.87 | 15.62 |
| Corundum----- | .7 | .07 | ---- | ---- | ---- | ---- | ---- | ---- | .32 | 1.30 |
| Wollastonite----- | ---- | ---- | .22 | .29 | .01 | .15 | .77 | .98 | ---- | ---- |
| Enstatite----- | 1.9 | 2.8 | 3.7 | 3.16 | 2.34 | 2.74 | 2.99 | 3.56 | 3.02 | 1.38 |
| Ferrosilite----- | ---- | ---- | ---- | ---- | ---- | .22 | ---- | ---- | ---- | ---- |
| Magnetite----- | 1.15 | ---- | 2.8 | ---- | ---- | 3.46 | ---- | 1.01 | 1.04 | ---- |
| Hematite----- | 1.8 | 3.99 | 1.15 | 3.9 | 4.0 | ---- | 3.75 | 2.81 | 2.72 | 3.93 |
| Ilmenite----- | .93 | .8 | 1.06 | .8 | .55 | 1.07 | .77 | 1.35 | 1.08 | .39 |
| Titanite----- | ---- | ---- | ---- | .21 | .59 | ---- | .24 | ---- | ---- | ---- |
| Rutile----- | ---- | .12 | ---- | ---- | ---- | ---- | ---- | ---- | ---- | .33 |
| Apatite----- | ---- | .49 | .50 | .5 | .49 | .48 | .48 | .55 | .43 | .50 |
| Minor elements (parts per million) | | | | | | | | | | |
| B----- | ---- | ---- | ---- | ---- | ---- | ---- | ---- | ---- | <20 | <20 |
| Ba----- | 1400 | 1000 | ---- | 2000 | 930 | 1500 | 1500 | ---- | 1200 | 1300 |
| Co----- | <4 | 8 | ---- | 7 | 5 | 7 | 7 | ---- | 7 | 6 |
| Cr----- | 2 | 3 | ---- | 5 | 5 | 7 | 5 | ---- | 5 | 5 |
| Cu----- | 17 | 4 | ---- | 20 | 12 | 15 | 15 | ---- | 24 | 18 |
| Ga----- | 30 | 10 | ---- | 30 | 20 | 30 | 30 | ---- | 20 | 20 |
| Ni----- | <4 | 7 | ---- | 5 | ---- | <3 | <3 | ---- | 7 | 8 |
| Pb----- | 340 | 30 | ---- | 20 | 97 | 20 | 20 | ---- | 40 | 30 |
| Sc----- | 5 | 10 | ---- | 10 | 10 | 10 | 10 | ---- | 12 | 10 |
| Sn----- | 40 | ---- | ---- | <10 | ---- | <10 | <10 | ---- | ---- | ---- |
| Sr----- | 360 | 400 | ---- | 150 | 660 | 150 | 150 | ---- | 320 | 280 |
| V----- | 60 | 80 | ---- | 100 | 70 | 100 | 100 | ---- | ---- | ---- |
| Y----- | 30 | 40 | ---- | 30 | 28 | 30 | 30 | ---- | 40 | 40 |
| Yb----- | 3 | ---- | ---- | 3 | 3 | 3 | 3 | ---- | ---- | ---- |
| Zr----- | 320 | 200 | ---- | 150 | 220 | 150 | 100 | ---- | 140 | 220 |
| Phenocrysts (volume percent) | | | | | | | | | | |
| Plagioclase----- | 32.6 | 30.0 | 33.8 | ---- | 28.0 | 29.0 | 30 | 27.0 | ---- | 20 |
| Sanidine----- | 6.5 | 4.7 | ---- | ---- | 4.2 | 5.5 | 4 | 6.0 | ---- | 5 |
| Quartz----- | 3.9 | 4.2 | ---- | ---- | 3.1 | 4.7 | 2 | 3.0 | ---- | 2 |
| Biotite----- | 4.3 | 4.0 | 4.1 | ---- | 6.5 | 3.9 | 4 | 5.0 | ---- | 4 |
| Augite----- | 1.7 | ---- | ---- | ---- | ---- | ---- | ---- | ---- | ---- | ---- |
| Hornblende----- | ---- | 3.4 | 2.5 | ---- | 2.4 | 2.9 | 3 | 3.0 | ---- | 2 |
| Sphene----- | ---- | .1 | .4 | ---- | .2 | .1 | Tr. | ---- | ---- | .5 |
| Opalines----- | 1.0 | 2.4 | .9 | ---- | 2.9 | 1.9 | 2 | 2.0 | ---- | 2 |
| Groundmass----- | 60.4 | 49.7 | 48.8 | ---- | 52.7 | 52.0 | 55 | 54.0 | ---- | 64.5 |

SAMPLE DESCRIPTIONS

1. Devitrified brown densely welded tuff. At about 10,600 ft, on slope east of Lake Creek (tributary of Wolf Creek). (See fig. 30.)
2. Densely welded devitrified La Garita Member. Dump of Outlet Tunnel, East Willow Creek, Creede district (beyond area of fig. 30).
3. Densely welded devitrified La Garita Member. North side of Cochetopa Creek, at about 10,800 ft, 0.7 km northeast of junction with Canyon Diablo (beyond area of fig. 30).
4. Bulk sample of densely welded La Garita Member. (For analysis of pumice fragment, see No. 7.) At about 12,900 ft, on cirque headwall, 0.5 km southeast of 13,718-ft bench mark "La Garita" along Continental Divide (beyond area of fig. 30).
5. Densely welded devitrified La Garita Member. At about 10,100 ft, along East Willow Creek (beyond area of fig. 30).
6. Densely welded devitrified Phoenix Park Member. At about 10,000 ft, on ridge east of Phoenix Park (beyond area of fig. 30).
7. Devitrified pumice fragment from La Garita Member. Same sample and locality as No. 4.
8. Pale-red-brown devitrified Fish Canyon Tuff, "Alder Creek" (Larsen and Cross, 1956, table 21, No. 37). (See fig. 30.)
9. Light-brown densely welded devitrified Fish Canyon Tuff from near base of unit. On 8,023-ft hill, 2.6 km southeast of East Butte. (See fig. 30.)
10. Light-gray densely welded devitrified Fish Canyon Tuff, from thick accumulation within the Mount Hope caldera. At about 10,850 ft, in gully north of Archuleta Creek, 3.3 km southeast of Mount Hope. (See fig. 30.)
11. Gray densely welded Fish Canyon Tuff, "San Cristobal quadrangle; mouth of canyon of Texas Creek, at altitude of 9,050 feet" (Larsen

younger ash-flow sheets

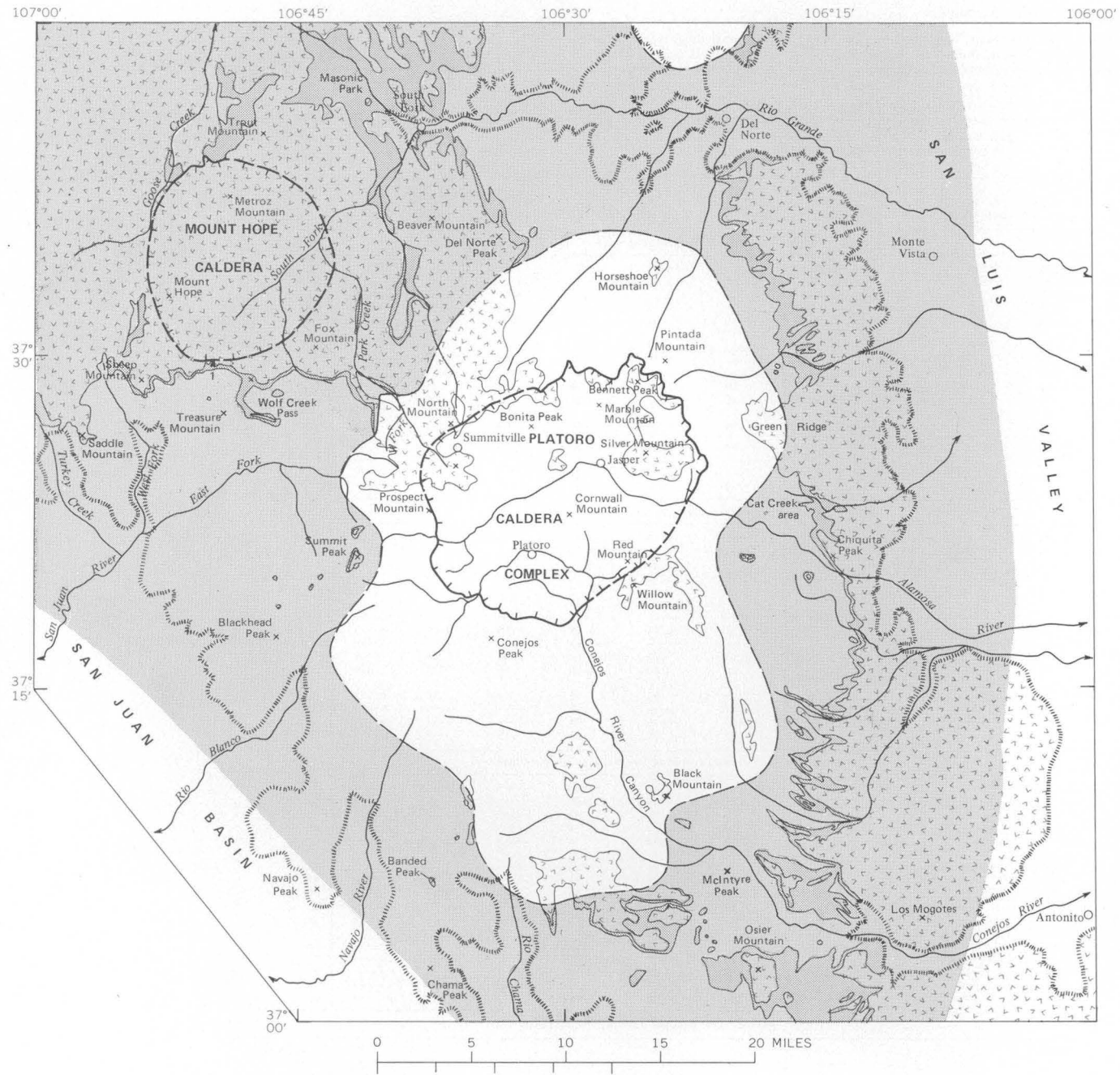
14 and 18 are from Olson, Hedlund, and Hansen (1968, table 1); analysis 13 is from unpublished data provided by W. R. Hansen; analyses 2-7 are by P. L. D. Elmore, Samuel Botts, Gillison Chloe, Lowell Artis, H. Smith, John Glenn, and James Kelsey. Major-oxide analyses by standard and 7 are by semiquantitative methods by J. C. Hamilton; analyses by quantitative methods are 9, 10, and 12 by J. D. Fletcher and 15-17

| Fish Canyon Tuff--Continued | | | | Carpenter Ridge Tuff | | | | | | | | Sample Field No. Lab. No. | |
|--|----------------------------|-------------------------|------------------------|-----------------------------|----------------------------|----------------------------|------------------------|--------------------------|--------------------------|--------------------------------|--|---------------------------------|--|
| Outflow--Continued | | | | | | | | | | | | | |
| 11 L+C 21-38 ----- | 12 66L-96-B W-168467 | 13 B6-62-39 ----- | 14 G-2384 152868 | 15 67L-133-G W-174427 | 16 65L-43-B W-168540 | 17 65L-33-B W-168541 | 18 G-3474 152866 | 19 65L-47 W-168539 | 20 L+C 21-47 ----- | | | | |
| Major oxides (weight percent), recalculated without H ₂ O and CO ₂ --Continued | | | | | | | | | | | | | |
| 66.93 | 68.7 | 70.2 | 70.6 | 60.6 | 66.2 | 71.6 | 71.9 | 73.8 | 74.80 | SiO ₂ | | | |
| 15.58 | 16.3 | 14.2 | 16.15 | 20.0 | 17.0 | 15.2 | 15.1 | 14.3 | 13.51 | Al ₂ O ₃ | | | |
| 2.52 | 2.3 | 3.6 | 1.7 | 3.2 | 3.3 | 2.2 | 1.4 | 1.0 | .98 | Fe ₂ O ₃ | | | |
| 1.14 | 1.2 | .36 | .16 | 1.2 | .33 | .16 | .23 | .45 | .33 | FeO | | | |
| .86 | .69 | 1.4 | .26 | 1.3 | .90 | .44 | .26 | .44 | ---- | MgO | | | |
| 3.74 | 3.0 | 2.7 | 1.4 | 5.2 | 3.5 | 1.9 | 1.2 | 1.5 | .77 | CaO | | | |
| 3.68 | 3.4 | 2.9 | 4.1 | 3.8 | 3.7 | 3.2 | 4.0 | 2.8 | 3.76 | Na ₂ O | | | |
| 4.63 | 3.4 | 4.1 | 4.9 | 3.5 | 4.4 | 4.9 | 5.4 | 5.4 | 5.65 | K ₂ O | | | |
| .50 | .44 | .40 | .3 | .60 | .44 | .30 | .23 | .25 | .20 | TiO ₂ | | | |
| .36 | .20 | .19 | .08 | .41 | .15 | .06 | .08 | .00 | ---- | P ₂ O ₅ | | | |
| .06 | .07 | .09 | .08 | .08 | .14 | .00 | .08 | .07 | ---- | MnO | | | |
| 100.00 | 100.00 | 100.13 | 99.93 | 99.89 | 100.06 | 99.96 | 99.88 | 100.01 | 100.00 | Total | | | |
| .56 | .57 | >1.6 | >.78 | 1.3 | .90 | .69 | .74 | .44 | ---- | H ₂ O+ | | | |
| .66 | .33 | >1.6 | >.78 | 1.7 | 1.2 | .91 | >.45 | .96 | .18 | H ₂ O- | | | |
| ---- | <.05 | .05 | .06 | <.05 | <.05 | <.05 | .16 | <.05 | ---- | CO ₂ | | | |
| Norms (weight percent)--Continued | | | | | | | | | | | | | |
| 20.04 | 27.53 | 30.40 | 24.9 | 13.05 | 19.66 | 29.83 | 24.94 | 33.19 | 29.79 | Quartz | | | |
| 27.34 | 19.84 | 24.15 | 29.0 | 20.74 | 25.98 | 28.92 | 32.13 | 31.93 | 33.41 | Orthoclase | | | |
| 31.12 | 30.99 | 24.46 | 34.8 | 32.32 | 31.14 | 26.74 | 34.07 | 23.29 | 31.77 | Albite | | | |
| 12.32 | 13.81 | 12.11 | 6.4 | 22.91 | 16.24 | 9.21 | 5.47 | 7.59 | 3.31 | Anorthite | | | |
| ---- | 1.56 | .54 | 1.7 | 1.55 | .20 | 1.32 | .59 | 1.12 | ---- | Corundum | | | |
| 1.61 | ---- | ---- | ---- | ---- | ---- | ---- | ---- | ---- | .21 | Wollastonite | | | |
| 2.13 | 1.72 | 3.47 | .65 | 3.34 | 2.24 | 1.09 | .65 | 1.09 | ---- | Enstatite | | | |
| ---- | ---- | ---- | ---- | ---- | ---- | ---- | ---- | ---- | ---- | Ferrosilite | | | |
| 2.40 | 2.90 | 2.94 | ---- | 2.53 | .25 | ---- | .34 | .94 | .49 | Magnetite | | | |
| .86 | .34 | 3.38 | 1.7 | 1.46 | 3.10 | 2.24 | 1.18 | .37 | .64 | Hematite | | | |
| .96 | .83 | .76 | .51 | 1.14 | .83 | .45 | .44 | .48 | .38 | Ilmenite | | | |
| ---- | ---- | ---- | ---- | ---- | ---- | ---- | ---- | ---- | ---- | Titanite | | | |
| ---- | ---- | ---- | .03 | ---- | ---- | .06 | ---- | ---- | ---- | Rutile | | | |
| .86 | .48 | .45 | .19 | .98 | .36 | .14 | .19 | ---- | ---- | Apatite | | | |
| Minor elements (parts per million)--Continued | | | | | | | | | | | | | |
| ---- | <20 | ---- | ---- | ---- | ---- | ---- | ---- | ---- | ---- | B | | | |
| ---- | 1200 | ---- | ---- | 13,000 | 4400 | 2400 | ---- | 680 | ---- | Ra | | | |
| ---- | 6 | ---- | ---- | <4 | <4 | <4 | ---- | <4 | ---- | Co | | | |
| ---- | 4 | ---- | ---- | 4 | 4 | 2 | ---- | 2 | ---- | Cr | | | |
| ---- | 24 | ---- | ---- | 10 | 13 | 8 | ---- | 8 | ---- | Cu | | | |
| ---- | 20 | ---- | ---- | 20 | 20 | 20 | ---- | 20 | ---- | Ga | | | |
| ---- | 7 | ---- | ---- | 8 | <4 | <4 | ---- | <4 | ---- | Ni | | | |
| ---- | 40 | ---- | ---- | 50 | 90 | ---- | ---- | 60 | ---- | Pb | | | |
| ---- | 8 | ---- | ---- | 10 | 8 | 6 | ---- | 5 | ---- | Sc | | | |
| ---- | ---- | ---- | ---- | <20 | <20 | ---- | <20 | ---- | ---- | Sn | | | |
| ---- | 260 | ---- | ---- | 1000 | 490 | 140 | ---- | 56 | ---- | Sr | | | |
| ---- | ---- | ---- | ---- | 40 | 60 | <20 | ---- | <20 | ---- | V | | | |
| ---- | 30 | ---- | ---- | <40 | <20 | 30 | ---- | 30 | ---- | Y | | | |
| ---- | 190 | ---- | ---- | 2 | ---- | ---- | ---- | ---- | ---- | Yb | | | |
| ---- | 960 | ---- | ---- | 960 | 400 | 330 | ---- | 220 | ---- | Zr | | | |
| Phenocrysts (volume percent)--Continued | | | | | | | | | | | | | |
| 18.0 | 20 | 19.9 | 28.0 | 27.9 | 11.6 | 4.9 | 5.5 | 0.2 | 4.0 | Plagioclase | | | |
| 6.0 | 5 | 4.8 | ---- | 2.4 | 4.4 | 4.8 | 2.5 | 4.7 | 2.5 | Sanidine | | | |
| 3.0 | 1.5 | 3.5 | ---- | ---- | ---- | ---- | ---- | ---- | ---- | Quartz | | | |
| 3.0 | 6 | 2.7 | 2.4 | 3.9 | 1.4 | .6 | .3 | .2 | .5 | Biotite | | | |
| ---- | ---- | ---- | .0 | 1.4 | ---- | ---- | ---- | ---- | ---- | Augite | | | |
| 3.0 | 2 | 2.3 | 1.4 | ---- | .6 | ---- | .3 | ---- | ---- | Hornblende | | | |
| .5 | .5 | .1 | .1 | ---- | ---- | ---- | ---- | ---- | ---- | Sphene | | | |
| 1.0 | 2 | 1.1 | 1.3 | 1.5 | .4 | .3 | .2 | .2 | .5 | Opaques | | | |
| 65.0 | 65 | 65.5 | 66.0 | 62.9 | 81.6 | 89.4 | 91.0 | 94.1 | 94.0 | Groundmass | | | |

SAMPLE DESCRIPTIONS—Continued

- and Cross, 1956, table 21, No. 39; beyond area of fig. 30).
12. Dark-gray cognate scoriaceous pumice block. Roedcut along U.S. Highway 160 along Pass Creek, at about 9,000 ft. (see fig. 30.)
13. Densely welded devitrified light-gray Fish Canyon Tuff. Anomalous high in Fe₂O₃ and MgO and low in both alkalis. Sapinero quadrangle: NE 1/4 SW 1/4 sec. 28, T. 48 N., R. 4 W. (beyond area of fig. 30.)
14. Massive light-brown devitrified Fish Canyon Tuff. Gateview quadrangle SE 1/4 SE 1/4 sec. 10, T. 47 N., R. 3 W. (Olson and others, 1968, table 1, No. 11; beyond area of fig. 30.)
15. Dark-gray scoria block (fig. 33C) from upper part of ash-flow sheet. (For analysis of bulk rock, see No. 16.) Measured section on west slope of Beaver Mountain, about 0.6 km northeast of Beaver Creek Reservoir spillway, at about 9,500 ft. (See fig. 31.)
16. Dark-brown densely welded devitrified mafic top of ash-flow sheet (fig. 33B). Same locality as No. 15.
17. Light-red-brown densely welded devitrified tuff from lower part of unit, just above basal vitrophyre zone. Same locality as No. 15, at about 9,250 ft.
18. Cinnamon-brown devitrified welded tuff. Gateview quadrangle, NE 1/4 SE 1/4 sec. 2, T. 46 N., R. 3 W. (Olson and others, 1968, table 1, No. 12; beyond area of fig. 31.)
19. Pale-purple densely welded devitrified tuff from lower part of unit. North side of upper Park Creek, on 10,600-ft knob, 0.9 km northeast of junction with West Fork. (See fig. 31.)
20. Light-brown devitrified welded tuff. "San Cristobal quadrangle, ridge west of Bennett Creek at altitude of 11,180 feet" (Larsen and Cross, 1956, table 21, No. 47; beyond area of fig. 31.)

PLATORO CALDERA COMPLEX, SAN JUAN MOUNTAINS, COLORADO



EXPLANATION

Outcrops shown by darker pattern, inferred original extent by lighter pattern.



Younger volcanic rocks

— Inferred original depositional margins — Dashed where approximate; queried where uncertain



Masonic Park Tuff

..... Limit of exposed volcanic rocks



Sample locality (table 6)

- - - Caldera wall (topographic) — Dashed where covered by younger rocks

FIGURE 26.—Outcrop area and inferred original depositional extent of the Masonic Park Tuff. Based on mapping by P. W. Lipman, 1965-67, 1970-71, and by T. A. Steven, 1965-66.

Peak, and at the head of Rio Chama. Although the Masonic Park Tuff in the southeastern San Juan Mountains is therefore rather similar in distribution to the Treasure Mountain Tuff, it extends much farther to the northwest, where it also accumulated to maximum thickness. The evidence for a source of the Masonic Park in the Mount Hope caldera seems compelling despite the somewhat eccentric distribution, as discussed in a later section. The Masonic Park therefore appears to have spread widely to the south and east on the flat plains underlain by Treasure Mountain units, but it lacked the momentum to ride up the outer slopes of the Platoro caldera area, which appears to have remained as a topographic high throughout the Oligocene ash-flow activity. In addition, volcanoes of Summitville Andesite may have presented barriers to the Masonic Park ash flows northwest of Platoro caldera, as indicated by the wedging out of these tuffs against andesite near the head of Park Creek (Platoro map).

LITHOLOGIC DESCRIPTION

The Masonic Park is petrologically uniform phenocryst-rich quartz latite, varying mainly in degree of welding. Where it is thickest, in the Masonic Park area, its cooling zonation is conspicuously compound—three major cliff-forming zones of red-brown densely welded tuff are separated by benches of less welded yellowish-brown tuff (fig. 27). In detail the zonation is more intricate, and many separate ash flows are clearly present. In contrast, the thinner sections of Masonic Park Tuff, along the edge of the San Luis Valley and elsewhere in the southern part of the volcanic field, generally approximate a simple cooling zonation, with the tuff only moderately densely welded in the interior of the sheet. In these areas the slight degree of welding of the Masonic Park results in great cavernous-weathering outcrops. Compound cooling is evident locally in this region, however, as along the Cat Creek road at the east edge of the Platoro map. Where basal parts of the sheet are exposed, welding has been insufficient to form a vitrophyre zone, and vapor-phase crystallization is typically well developed throughout the unit.

Over most of its extent the Masonic Park Tuff contains 40-50 percent phenocrysts (table 3), mostly plagioclase but accompanied by conspicuous biotite and augite. Sanidine is absent or extremely sparse; quartz and hornblende are absent. In distal portions of the sheet, especially near the Colorado-New Mexico line, total phenocryst content is lower—20-30 percent in the interior of the sheet—and at the top of the unit a winnowed shard-rich tuff contains only about 10 percent small fragmental phenocrysts (fig. 28). Small fragments of gray or red-brown andesite a few centimeters across are abundant and make up as much as 5 percent of the rock. These are especially conspicuous in the less welded zones.

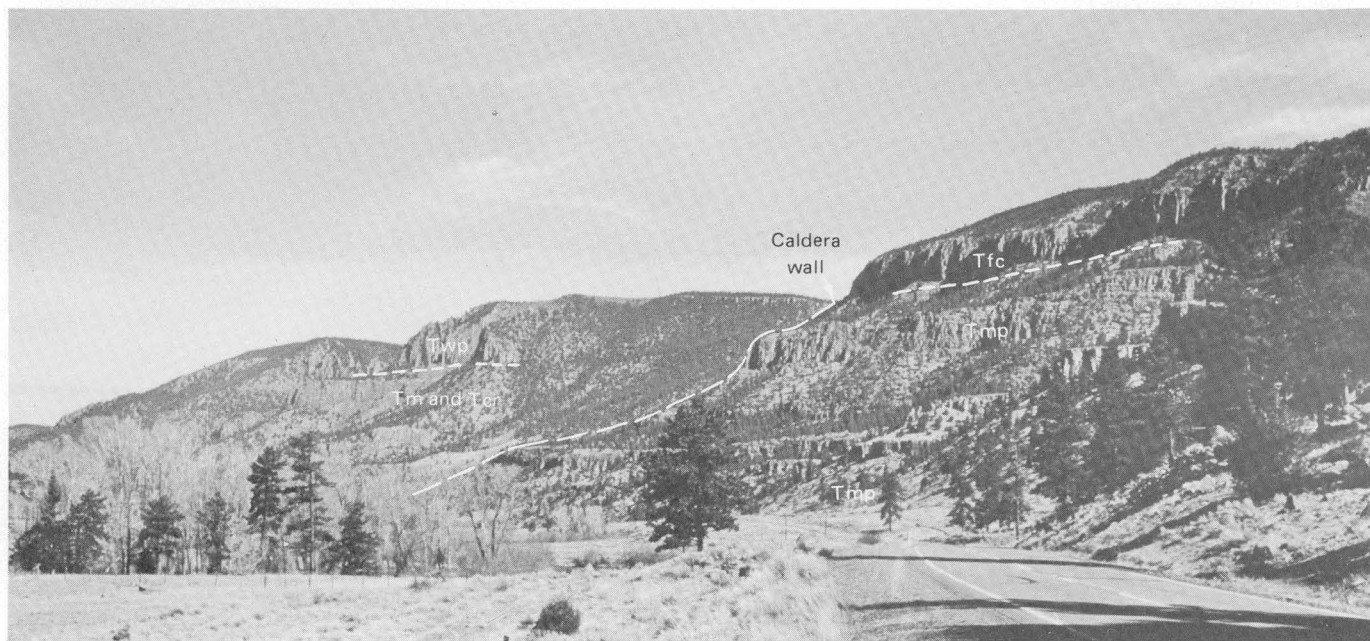


FIGURE 27.—Ash-flow sheets along the Rio Grande valley near Masonic Park. In foreground are Masonic Park Tuff (Tmp) overlain by Fish Canyon Tuff (Tfc) near the east wall of La Garita caldera. Up the valley, within the caldera, are Carpenter Ridge Tuff (Tcr), Mammoth Mountain Tuff (Tm), and Wason Park Tuff (Twp) that form the caldera fill. The compound cooling zonation of the Masonic Park Tuff is reflected by the alternation of benches and cliffs within this unit.

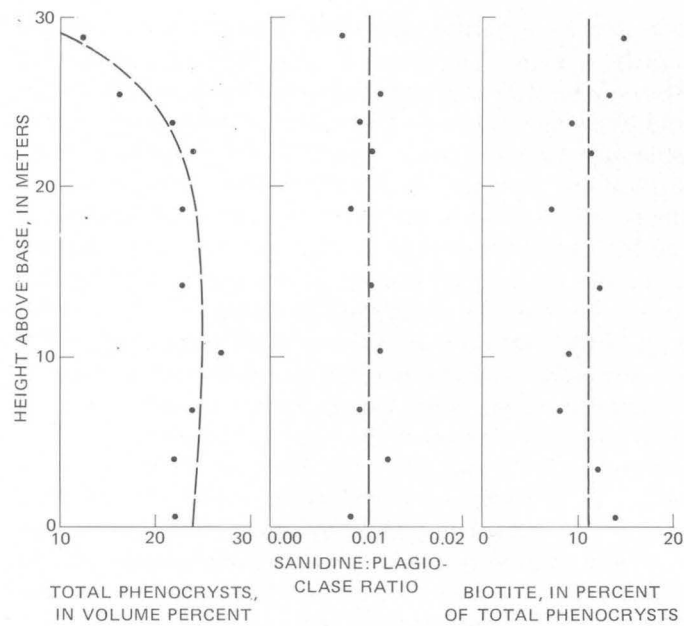


FIGURE 28.—Phenocryst variations in a section of the Masonic Park Tuff along Rio de los Pinos in New Mexico. Trends are shown by dashed lines. Near the top of the sheet, total phenocrysts (and average diameter of crystals) decrease, whereas proportions of phenocrysts remain fairly constant. This relation probably results from winnowing effects in far-traveled ash flows (here about 70 km from the caldera rim), with larger phenocrysts settling preferentially near the source, and fine ash and broken small phenocrysts concentrating in the moving ash flow (Lipman, 1967). Similar vertical variations, probably due to winnowing, also characterize the Wason Park Tuff (Ratté and Steven, 1967, fig. 17).

The single chemical analysis of the Masonic Park Tuff (table 6, No. 1) shows about 68 percent SiO₂. This sample contains fewer phenocrysts than average; a more typical phenocryst-rich sample might be slightly less silicic. However, the general petrologic uniformity of the Masonic Park suggests that any chemical variation is likely to be small and to be due more to sorting phenomena during eruption and emplacement (Fisher, 1966; Lipman, 1967, p. 321-322) than to compositional variations in the source magma.

The Masonic Park Tuff is generally similar in petrography to the La Jara Canyon Member of the Treasure Mountain but typically is more phenocryst rich and contains more augite. The augite tends to be replaced by carbonate and clay minerals, even where the rest of the rock seems unaltered.

In a few places south and west of the Mount Hope caldera—most notably northwest of Wolf Creek Pass and in upper Turkey Creek—crude bedding, defined by variations in size and abundance of pumices and phenocrysts, occurs within the welded lower few meters of the upper member (fig. 29). This bedded welded tuff is believed to represent agglutinated near-source ash fall, a

depositional process previously described for similar rocks of the lower tuff of the Treasure Mountain near the Platoro caldera rim.

The occurrence of bedded welded tuff of the Masonic Park near the rim of Mount Hope caldera is one of the criteria that indicate eruption of this unit from the Mount Hope caldera. Other evidence leading to this interpretation are: (1) the central position of the caldera, adjacent to the thickest accumulation of Masonic Park Tuff (fig. 26), (2) the intertonguing of Masonic Park Tuff with Sheep Mountain Andesite and other locally derived lavas near the rim of Mount Hope caldera, and (3) the stratigraphic constraints on the age of the caldera—in particular, the Mount Hope caldera must have formed just before eruption of the Fish Canyon Tuff (from the La Garita caldera), because it is filled by this tuff.



FIGURE 29.—Crudely bedded welded tuff near the base of the upper member of the Masonic Park Tuff, believed to represent near-source agglutinated ash fall. Bedding is defined by various sizes and abundance of pumice fragments and phenocrysts. Base of ash-flow sheet is indicated by arrows; note person (circled) for scale.

AGE AND MAGNETIC POLARITY

A single K-Ar age determined on biotite from the Masonic Park Tuff is 28.2 m.y. (Armstrong, 1969; Lipman and others, 1970), in excellent agreement with radiometric ages of underlying and overlying units. The remanent magnetic polarity determined in the field and in the laboratory seems to be everywhere reverse; low magnetic intensities, however, did complicate field interpretation of results from some weakly welded outcrops.

FISH CANYON TUFF

The Fish Canyon Tuff, a phenocryst-rich quartz latictic ash-flow sheet named by Olson, Hedlund, and Hansen (1968), is the most widespread (at least 15,000 km²) and voluminous (more than 3,000 km³) single ash-flow sheet in the San Juan volcanic field, and it ranks among the largest in the world (Smith, 1960a, fig. 3). The Fish Canyon was erupted about 27.8 m.y. ago (Steven and others, 1967; Lipman and others, 1970) from the great La Garita caldera (fig. 1), which is 35-40 km in diameter. Collapse of the La Garita caldera during the ash-flow eruptions permitted thick intracaldera accumulation of these tuffs, resulting in a unit analogous to the thick intracaldera-thin outflow association of the La Jara Canyon Member of the Treasure Mountain. The thick ash-flow sheet within the La Garita caldera, called the La Garita Quartz Latite (Steven and Ratté, 1964), is now known to be the intracaldera equivalent of the Fish Canyon Tuff and has been redefined as the La Garita Member of the Fish Canyon Tuff (Steven, Lipman, and Olson, 1974).

The Fish Canyon Tuff extends from north of the Gunnison River (Olson and others, 1968) southwest as far as the flanks of the Needle Mountains (Durango map) and southeast to Green Ridge (fig. 30). Within the La Garita caldera the La Garita Member is exposed to a thickness of nearly 1 km, with the top of the section eroded and the base exposed only around the margins of the caldera (Steven and Ratté, 1965).

Only the southeastern part of the vast area covered by the Fish Canyon is within the present mapped area (fig. 30). In the southeastern San Juan Mountains the Fish Canyon, with only local exceptions near its distal edges, rests on Masonic Park Tuff and is overlain by Carpenter Ridge Tuff. In places Huerto Andesite intervenes between the Fish Canyon and the Carpenter Ridge, and the Fish Canyon near its distal edges locally rests on units older than the Masonic Park, especially near topographically high parts of the Platoro caldera complex.

In the southeastern San Juan Mountains the Fish Canyon is much less extensive than the underlying Masonic Park Tuff, apparently because it was blocked by growing

volcanoes around the north margin of the Platoro caldera complex. The Fish Canyon Tuff wedges out slightly higher on the outer north slopes of the Platoro caldera complex than does the Masonic Park (fig. 26, 30). Unlike the Masonic Park, some Fish Canyon Tuff accumulated within the caldera complex, in the low northeastern part of the Platoro caldera moat that had previously been partly filled with upper units of the Treasure Mountain Tuff (figs. 23, 25). Only a single small patch of Fish Canyon Tuff is preserved south or east of the caldera complex, in a local erosional valley cut in Masonic Park Tuff (fig. 30), and it seems unlikely that any sizable volume of the Fish Canyon was ever deposited in this region. The main area of Fish Canyon along the San Luis Valley thins and wedges out north of Green Ridge, probably reflecting the growing accumulation of the volcanics of Green Ridge around the volcano centered at Cat Creek (described later). Similarly, northwest of the Platoro caldera, the Fish Canyon wedges out against a caldera-margin accumulation of the upper member of the Summitville Andesite, against which the Masonic Park and the Ra Jadero Member of the Treasure Mountain had earlier wedged out even farther from the caldera rim.

The maximum thickness of the Fish Canyon Tuff in the southeastern San Juan Mountains is in the topographic depression of the previously formed Mount Hope caldera (fig. 30), in the headwaters of the South Fork of the Rio Grande, where the tuff forms a single thick cooling unit continuously exposed from the valley bottom, at an elevation near 9,000 feet, to the top of Mount Hope, at 12,834 feet. Even with due allowance for a gentle northeastern dip, the exposed Fish Canyon here is nearly 1 km thick, even though the top of the ash-flow sheet has been eroded and the base is nowhere exposed within the caldera. The Fish Canyon Tuff thins abruptly across the Mount Hope caldera walls, and outside this caldera it is typically 20-200 m thick. Exceptional thicknesses of the Fish Canyon, as much as 500 m, also accumulated in downfaulted blocks at the head of the West Fork of the San Juan River (Steven and others, 1969).

The Fish Canyon Tuff is a phenocryst-rich quartz latite (table 6) that petrographically is perhaps the most distinctive ash-flow unit in the San Juan field. It contains 35-50 percent phenocrysts, including plagioclase, sanidine, quartz, biotite, hornblende, and accessory sphene. No other major ash-flow sheet in the field contains hornblende (and lacks augite) as the second most abundant mafic after biotite. The quartz phenocrysts, which are very rare in or absent from other quartz latictic tuffs of the field, are also distinctive: they occur as rounded pale amethystine pellets as much as 5 mm in diameter that are riddled with wormy glass inclusions whose texture is caused by resorption. The sanidine

PLATORO CALDERA COMPLEX, SAN JUAN MOUNTAINS, COLORADO

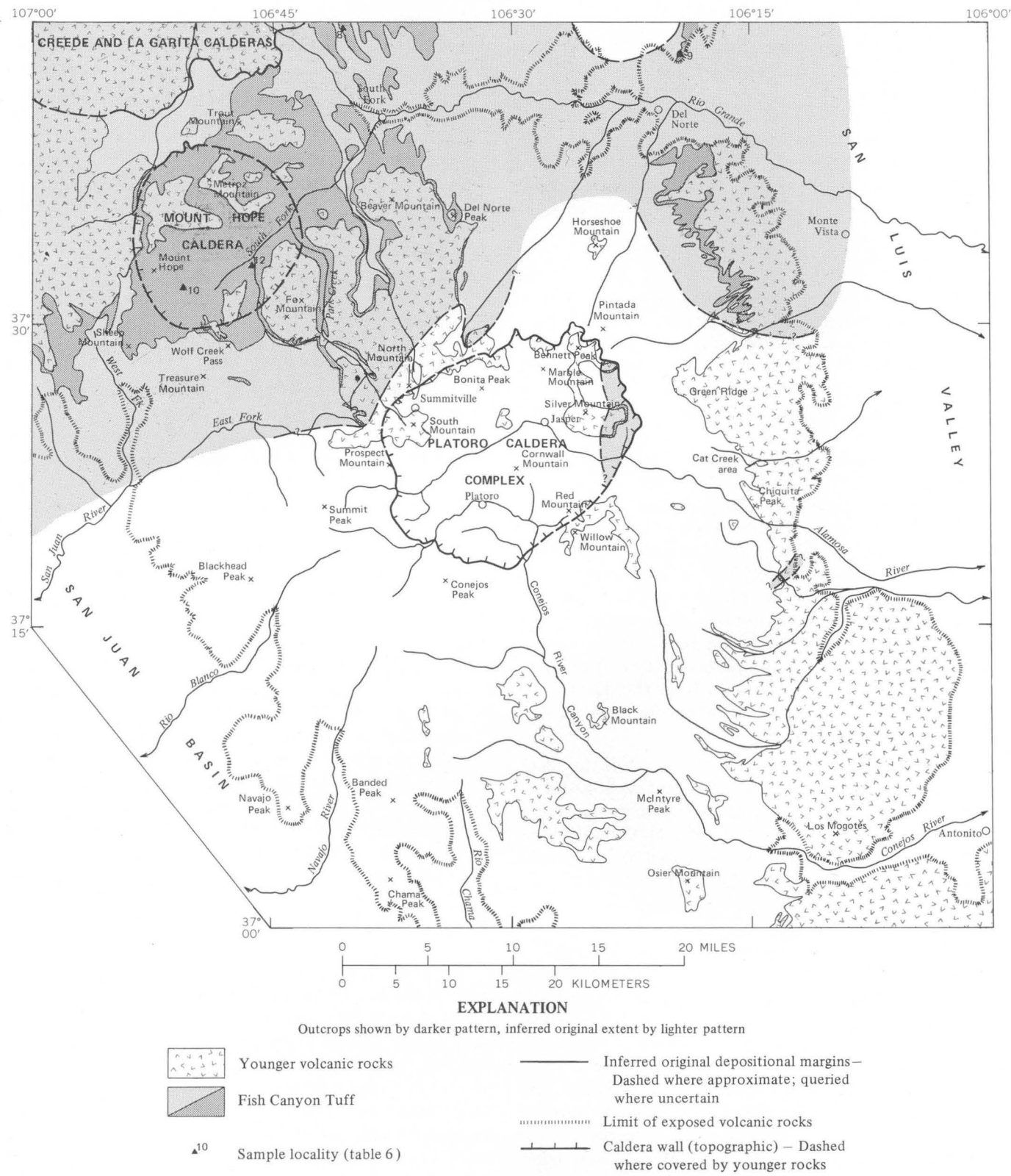


FIGURE 30.—Outcrop area and inferred original depositional extent of the Fish Canyon Tuff. Based on mapping by P. W. Lipman, 1965-67, 1970-71, and by T. A. Steven, 1965-66.

phenocrysts, which are exceptionally common in comparison with other quartz latitic tuffs of the San Juan field, are relatively potassic—X-ray and microprobe data for eight samples indicate compositions between Or_{67} and Or_{76} . Finally, the presence of abundant accessory sphene is unique.

Analyses of all the bulk-rock samples of the Fish Canyon from the southeastern and central San Juan Mountains, including those from the intracaldera tuffs, cluster between 66 and 68 percent SiO_2 ; one sample of a cognate block is slightly higher in SiO_2 (table 6, No. 12). Two samples from the Gunnison River area, near the north edge of the ash-flow sheet, contain more SiO_2 —as much as 70.6 percent (table 6, Nos. 13, 14)—possibly owing to winnowing of mafic phenocrysts during emplacement.

The Fish Canyon has normal remanent magnetic polarity (table 3).

CARPENTER RIDGE TUFF

The Carpenter Ridge Tuff, a phenocryst-poor rhyolitic ash-flow sheet named by Olson and others (1968), is probably the second largest ash-flow sheet in the San Juan field, surpassed only by the Fish Canyon Tuff. The Carpenter Ridge Tuff was erupted from the Bachelor caldera (fig. 1); its thick intracaldera equivalent, formerly called the Bachelor Mountain Rhyolite in the Creede district (Steven and Ratté, 1965), has been redefined as the Bachelor Mountain Member of the Carpenter Ridge Tuff (Steven, Lipman, and Olson, 1974). In the southeastern San Juan Mountains (fig. 31) the Carpenter Ridge Tuff generally rests on Fish Canyon Tuff or Huerto Andesite; locally near its distal margins it lies on lavas or volcaniclastic sedimentary rocks of the Los Pinos Formation, derived from the postcollapse volcanoes around the north margin of the Platoro caldera complex. Generally, the Carpenter Ridge is overlain by the Wason Park Tuff; beyond the area of deposition of the Wason Park, the Carpenter Ridge is overlain by the Los Pinos Formation or basalt flows of the Hinsdale Formation.

DISTRIBUTION AND THICKNESS

The Carpenter Ridge Tuff has a distribution very similar to that of the Fish Canyon, extending from north of the Gunnison River (Olson and others, 1968), southwest to the Needle Mountains area (Durango map), and southeast at least as far as the north slopes of Green Ridge (fig. 31). A small area of thin partly welded phenocryst-poor tuff, shown as Carpenter Ridge south of the Alamosa River (fig. 31), is of somewhat uncertain correlation; although this tuff has an appropriate phenocryst assemblage, it lacks the dense welding that characterizes the Carpenter Ridge Tuff elsewhere, even in similarly thin accumulations.

The outflow sheet of Carpenter Ridge Tuff is thin and uniform in thickness, having accumulated to more than 200-m thickness only in a few areas of rough fault-block topography such as at the head of the West Fork of the San Juan River (fig. 31). Within the Bachelor caldera, however, the equivalent Bachelor Mountain Member is more than 1 km thick (Steven and Ratté, 1965, p. 22), showing that collapse accompanied at least the later stages of eruption of the Carpenter Ridge Tuff.

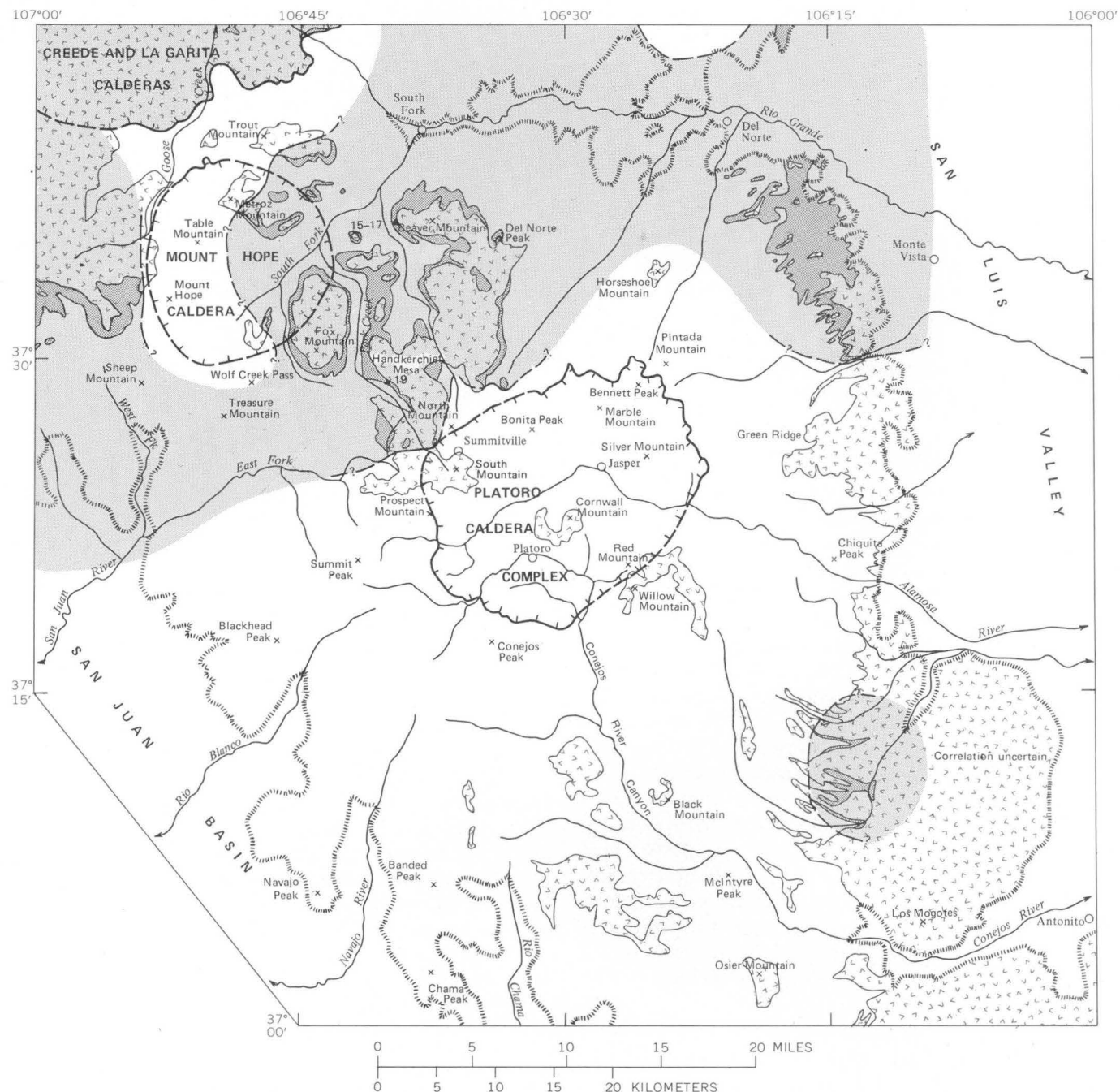
The Carpenter Ridge Tuff wedges out around the north outer slopes of the Platoro caldera complex, much like the preceding Fish Canyon, but slightly farther from the caldera rim (figs. 30, 31). Unlike the Fish Canyon Tuff, however, the Carpenter Ridge has not been found within this caldera. Although no caldera-margin lavas or derivative volcaniclastic sedimentary rocks have been found between the Fish Canyon and Masonic Park Tuffs, by the time of eruption of the Carpenter Ridge the caldera-margin volcanoes had grown sufficiently large that lavas and detrital material spread far enough to be preserved between the Fish Canyon and Carpenter Ridge Tuffs, especially north of North Mountain (Platoro map) and north of Green Ridge (Durango map). Thus, the contrast in distributions between the Fish Canyon and Carpenter Ridge Tuffs (figs. 30, 31) on the one hand, and the Masonic Park Tuff (fig. 26) on the other, is clearly tied by stratigraphic relations to marginal volcanic activity of the Platoro caldera complex.

Further local change in the topography is shown by the wedging out of the Carpenter Ridge against the Fish Canyon Tuff within the Mount Hope caldera (fig. 31; Durango map). This relation demonstrates that the Fish Canyon Tuff within Mount Hope caldera was uplifted and tilted between the times of deposition of these two units, apparently mainly by movement along a major fault up Beaver Creek (fig. 61); the Carpenter Ridge appears to wedge out depositinally against this fault scarp. In essence this movement represents a weak delayed resurgence of the Mount Hope caldera.

LITHOLOGIC DESCRIPTION

The Carpenter Ridge Tuff is typically a simple cooling unit, consisting mainly of densely welded red-brown tuff, almost everywhere having a black basal vitrophyre a few meters thick. Sections thicker than about 50 m commonly contain a well-developed central lithophysal zone, in which round or elliptical gas cavities average about 5 cm in diameter; in areas of lithophysal development, the welded devitrified tuff is commonly bleached to more pastel red, brown, or salmon colors. Where welding decreases near the top of the unit, the tuff is light gray owing to vapor-phase crystallization.

The Carpenter Ridge Tuff is readily distinguished



EXPLANATION

Outcrops shown by darker pattern, inferred original extent by lighter pattern



Younger volcanic rocks



Carpenter Ridge Tuff

17

Sample locality (table 6)

— Inferred original depositional margins — Dashed where approximate; queried where uncertain

..... Limit of exposed volcanic rocks

— Caldera wall (topographic) — Dashed where covered by younger rocks

FIGURE 31.—Outcrop area and inferred original depositional extent of the Carpenter Ridge Tuff. Based on mapping by P. W. Lipman, 1965-67, 1970-71, and by T. A. Steven, 1965-66.

from all other units in the southeastern part of the San Juan field by its abundant sanidine and by its low total phenocryst content. Phenocrysts in general constitute about 5 percent of the tuff and consist of subequal amounts of sanidine (Or_{65}) and plagioclase (An_{25-40}), accompanied by a minor amount of biotite and very sparse augite. Pumice fragments are abundant but small, the compacted lenses rarely being more than 5 cm long. Small intermediate-composition volcanic fragments are present but rare. The typical phenocryst-poor Carpenter Ridge Tuff contains about 73 percent SiO_2 (table 6) and is the most rhyolitic ash-flow sheet in the southeastern San Juan Mountains.

In the vicinity of Beaver Mountain, the Carpenter Ridge Tuff is about 120 m thick and displays atypical but extremely interesting variations in petrography and chemistry (figs. 32, 33). The lower part of the ash-flow sheet is the typical phenocryst-poor rhyolite described above (fig. 33A); however, from about 60 m above the

base to the top of the sheet, total phenocryst content gradually increases from about 5 percent to more than 25 percent (fig. 33B), the proportion of sanidine decreases, augite becomes abundant, and bulk-rock SiO_2 content decreases from about 73 to 66.5 percent. Large dark scoriaceous pumices become conspicuous (fig. 33C); these contain sparse sanidine, and the single analyzed sample has only 60.6 percent SiO_2 (table 6, No. 15). The phenocryst-poor rhyolitic pumices that characterize the lower part of the unit persist to the top of this section, however, and occur in the same samples as the dark, mafic pumices. The quartz laticic upper part of the Carpenter Ridge Tuff in this area is clearly a mixture of shards and pumice fragments ranging in composition from rhyolite to low-silica rhyodacite. Similar mechanical mixing during eruption and emplacement characterizes other such compositionally zoned ash-flow sheets (Lipman, 1967, p. 320-321).

Such compositional zonations in large ash-flow

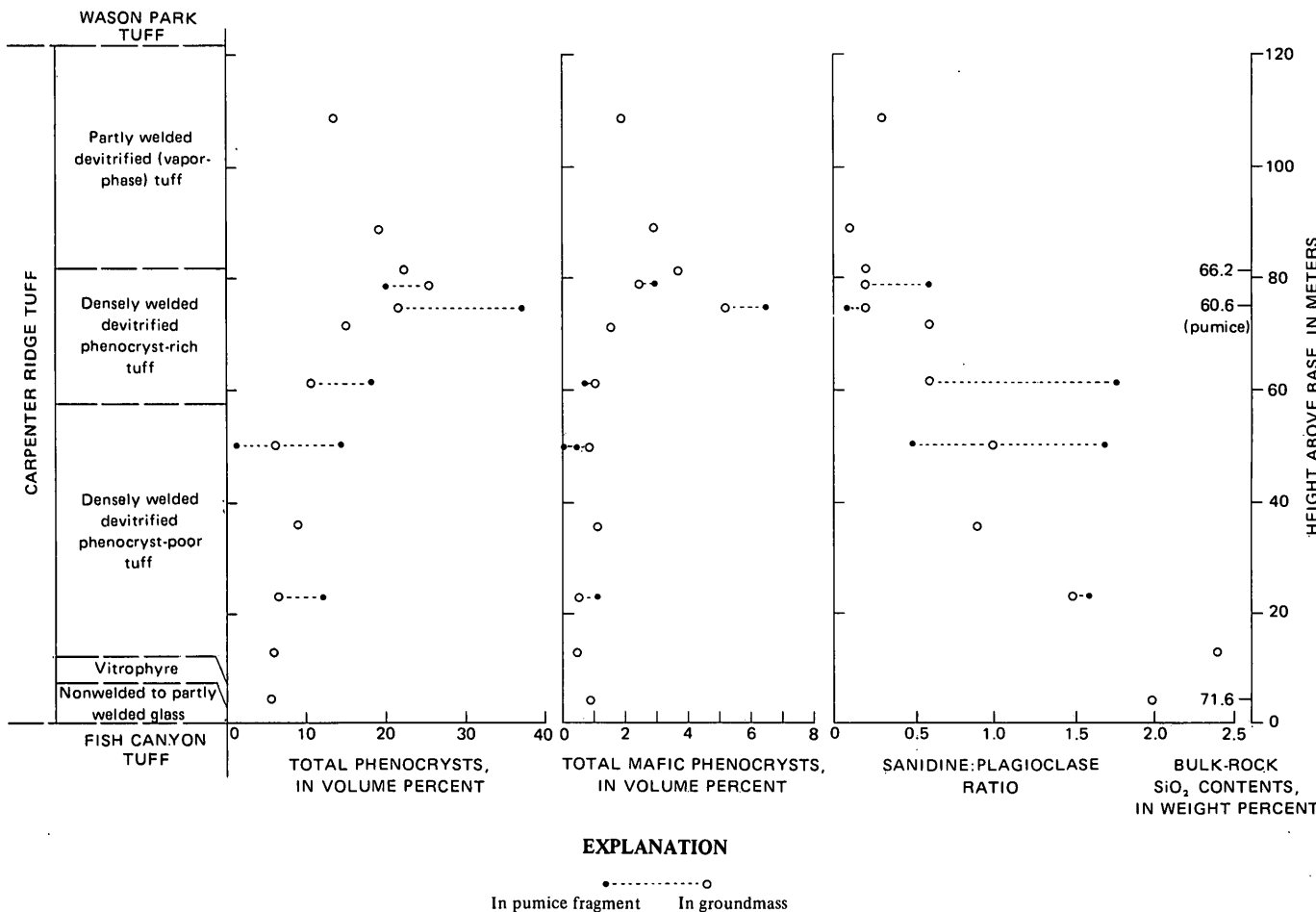


FIGURE 32.—Petrographic variations in a section of the Carpenter Ridge Tuff, southwest slope of Beaver Mountain. Total phenocrysts and mafics increase upward, whereas SiO_2 content and sanidine:plagioclase ratios decrease. Phenocryst contents of uppermost sample are anomalously low, owing to lesser welding and possibly also to winnowing effects. Pumices vary widely in phenocryst content and in places are clearly different in composition from enclosing groundmass.

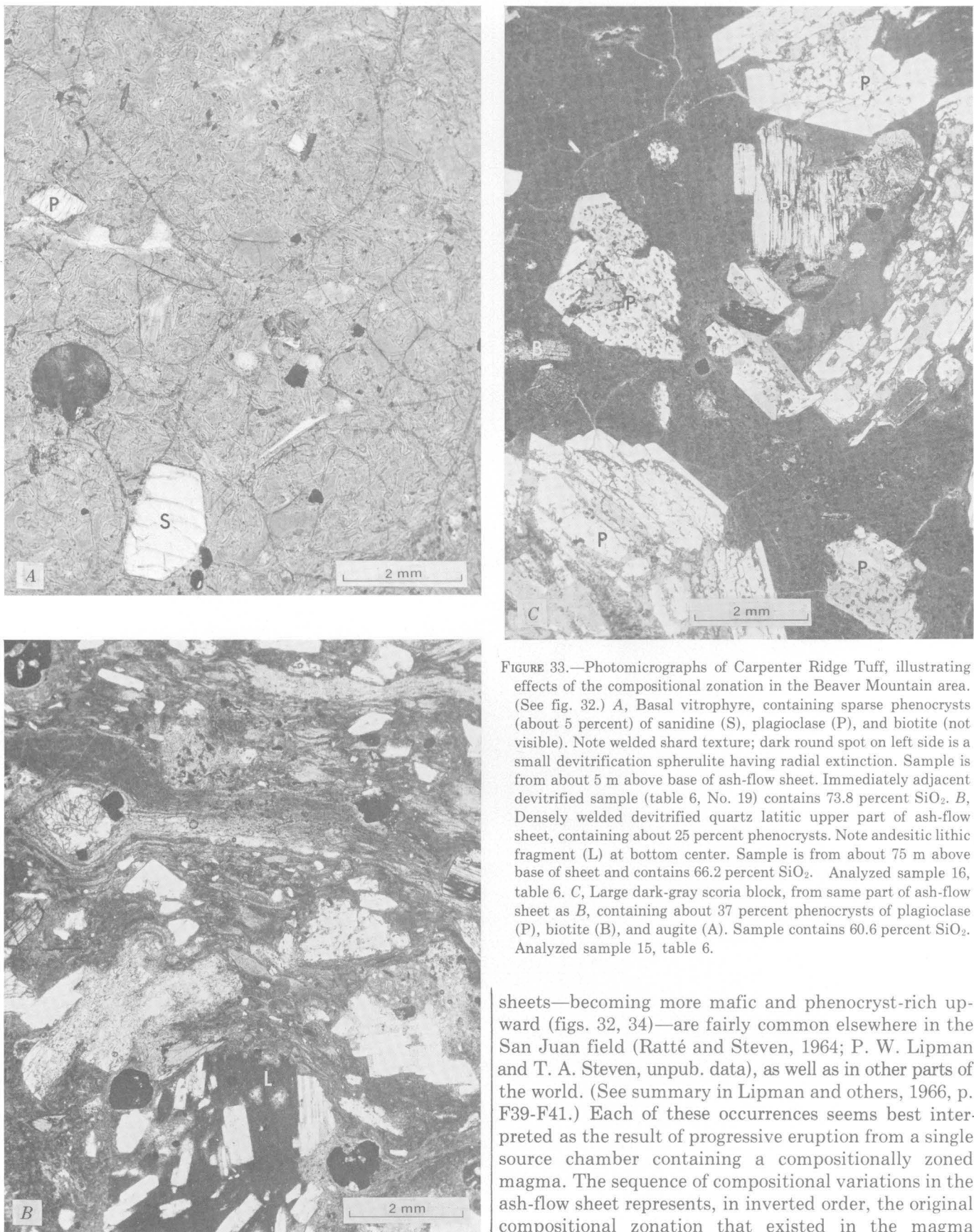


FIGURE 33.—Photomicrographs of Carpenter Ridge Tuff, illustrating effects of the compositional zonation in the Beaver Mountain area. (See fig. 32.) A, Basal vitrophyre, containing sparse phenocrysts (about 5 percent) of sanidine (S), plagioclase (P), and biotite (not visible). Note welded shard texture; dark round spot on left side is a small devitrification spherulite having radial extinction. Sample is from about 5 m above base of ash-flow sheet. Immediately adjacent devitrified sample (table 6, No. 19) contains 73.8 percent SiO₂. B, Densely welded devitrified quartz latitic upper part of ash-flow sheet, containing about 25 percent phenocrysts. Note andesitic lithic fragment (L) at bottom center. Sample is from about 75 m above base of sheet and contains 66.2 percent SiO₂. Analyzed sample 16, table 6. C, Large dark-gray scoria block, from same part of ash-flow sheet as B, containing about 37 percent phenocrysts of plagioclase (P), biotite (B), and augite (A). Sample contains 60.6 percent SiO₂. Analyzed sample 15, table 6.

sheets—becoming more mafic and phenocryst-rich upward (figs. 32, 34)—are fairly common elsewhere in the San Juan field (Ratté and Steven, 1964; P. W. Lipman and T. A. Steven, unpub. data), as well as in other parts of the world. (See summary in Lipman and others, 1966, p. F39-F41.) Each of these occurrences seems best interpreted as the result of progressive eruption from a single source chamber containing a compositionally zoned magma. The sequence of compositional variations in the ash-flow sheet represents, in inverted order, the original compositional zonation that existed in the magma

chamber at the time of eruption; for the Carpenter Ridge Tuff the original magmatic zonation was downward from phenocryst-poor rhyolite to phenocryst-rich rhyodacite. Although only a local feature of the Carpenter Ridge, the striking compositional zonation in the Beaver Mountain area demonstrates that even this most rhyolitic ash-flow sheet of the southeastern San Juan Mountains was closely associated with more mafic material in its magma chamber before eruption.

Although the outflow Carpenter Ridge Tuff and the intracaldera Bachelor Mountain Member are similar in phenocryst content and in remanent magnetic polarity, these two facies of a single ash-flow sheet so differ in general appearance that their equivalence is not readily apparent. The extreme dense welding and fluidal appearance (Ratté and Steven, 1967, figs. 4-7) of the dark-gray lower part (Willow Creek unit) of the intracaldera Bachelor Mountain Member is unknown outside the caldera in the red-brown Carpenter Ridge Tuff. Upper parts of the intracaldera Bachelor Mountain Member (Campbell Mountain and Windy Gulch units) contain abundant volcanic lithic fragments, in contrast to the paucity of such material in the outflow Carpenter Ridge. The intracaldera tuff has undergone pervasive extreme potassium metasomatism (Ratté and Steven, 1967, table 2), and therefore the two facies of the ash-flow sheet do not resemble each other chemically. Nevertheless, the equivalence of the two facies seems clearly established by the general distribution of the Carpenter Ridge Tuff around the Bachelor caldera, by similarities in phenocryst petrology and in paleomagnetism, and by similarity in stratigraphic posi-

tion both inside and outside the caldera with respect to the underlying Fish Canyon Tuff and the overlying Mammoth Mountain (table 1) and Wason Park Tuffs (Steven, Lipman, and Olson, 1974).

AGE AND MAGNETIC POLARITY

The Carpenter Ridge Tuff has not been dated radiometrically, but its age is bracketed by K-Ar determinations (Lipman and others, 1970) on the underlying Fish Canyon Tuff (27.8 m.y.) and on Mammoth Mountain Tuff (26.7 m.y.) that overlies it in the Creede area (table 1). The Carpenter Ridge Tuff has reverse remanent magnetic polarity.

WASON PARK TUFF

The Wason Park Tuff, named by Steven and Ratté (1964), is a generally densely welded ash-flow sheet of moderately phenocryst rich low-silica rhyolite, believed to have been erupted from a source now subsided beneath the Creede caldera (Ratté and Steven, 1967, p. H34). Because the Wason Park is a relatively minor unit in the southeastern San Juan Mountains, a separate distribution map has not been prepared. In this area, the Wason Park rests on Carpenter Ridge Tuff and is overlain by Snowshoe Mountain Tuff or by basalt flows of the Hinsdale Formation (Durango map). Where the Wason Park was partly confined by the wall of the La Garita caldera in the northwestern part of the mapped area (fig. 31), it is as much as 300 m thick, but scattered remnants that are preserved to the southeast as far as Wolf Creek Pass, Fox Mountain, and Beaver Mountain are generally no more than 50 m thick. Like the Carpenter Ridge Tuff (fig. 31), the Wason Park wedges out against the uplifted block of Fish Canyon Tuff within the Mount Hope caldera.

In the southeastern San Juan region the Wason Park Tuff appears to be a simple cooling unit. Where the unit is densely welded, a black vitrophyre 3-5 m thick near the base is overlain by brick red-brown tuff containing streaky light-gray pumice lenses as much as 50 cm long (Ratté and Steven, 1967, fig. 16). Less welded devitrified tuff near the top of the unit is gray, owing to vapor-phase crystallization; and where the Wason Park is thin near its depositional margins in the southeastern area, it is partly welded and is gray throughout.

The Wason Park contains 20-30 percent phenocrysts, mainly plagioclase (An_{25-40}), sanidine (about Or_{60}), biotite, and sparse augite. The plagioclase phenocrysts tend to be distinctively tabular, fairly unbroken, and parallel to the compaction foliation of the tuff. Foreign volcanic fragments are sparse, especially as compared to other ash-flow units already described. Seven chemical analyses of the Wason Park, listed by Ratté and Steven (1967, table 14), indicate 68-72 percent SiO_2 , on a volatile-free basis. In comparison with other ash-flow

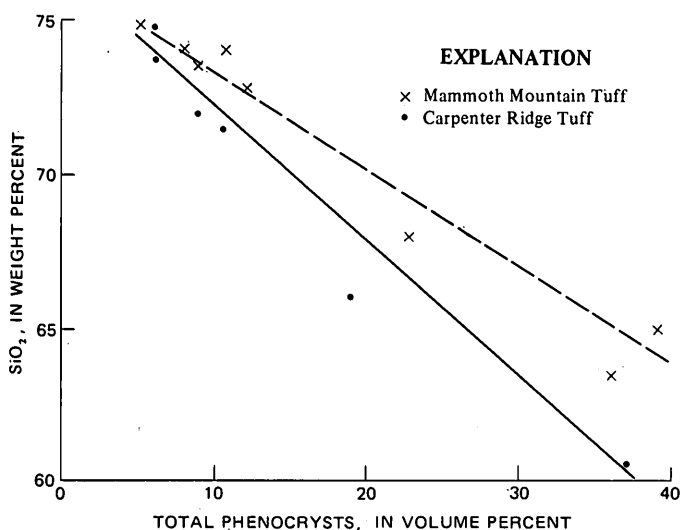


FIGURE 34.—Inverse correlation between SiO_2 and total phenocryst contents for two compositionally zoned ash-flow sheets of the San Juan volcanic field. Data from table 6, Ratté and Steven (1967), and P. W. Lipman (unpub. data). Approximate correlation trends drawn by inspection.

tuffs from the Creede area (Carpenter Ridge, Mammoth Mountain, and Snowshoe Mountain Tuffs), the Wason Park seems to be slightly higher in alkalis and lower in CaO, MgO, and total iron.

The age of the Wason Park is bracketed in the Creede district by ages of 26.7 m.y. on the underlying Mammoth Mountain Tuff and 26.4 m.y. on overlying lavas of the Fisher Quartz Latite (Lipman and others, 1970). The Wason Park Tuff has reverse remanent magnetic polarity.

SNOWSHOE MOUNTAIN TUFF

The Snowshoe Mountain Tuff (Steven and Ratté, 1964, 1965), the youngest ash-flow sheet in the central and eastern San Juan field, was erupted from Creede caldera a little more than 26.4 m.y. ago (Steven and others, 1967; Lipman and others, 1970). This ash-flow sheet accumulated to a thickness of at least 1,000 m (base not exposed) within Creede caldera as a result of subsidence concurrent with eruption (Steven and Ratté, 1965, p. 40, 59). By contrast, the outflow sheet is thin and weakly welded, and only a few patches have escaped erosion. The largest of these remnants is in the northwestern part of the area described in this report—at Handkerchief Mesa and on Trout, Beaver, and Fox Mountains (Durango map). In most of these places the Snowshoe Mountain Tuff has been protected from erosion by the capping basalt flows of the Hinsdale Formation. The Snowshoe Mountain Tuff rests on the Wason Park Tuff, except at the south end of Handkerchief Mesa (Platoro map), where it wedges between lavas and volcaniclastic sedimentary rocks of the Los Pinos Formation (fig. 35) that were eroded from lava domes around the north margin of Platoro caldera.

The outflow Snowshoe Mountain Tuff is a simple cooling unit of light-gray tuff 10-100 m thick that is rarely well exposed because it is only weakly welded. Where the tuff is best exposed, erosion along large crudely columnar joints has produced crumbling conical ribs ("tepees"). The outflow Snowshoe Mountain contrasts strikingly with the much thicker intracaldera part of this tuff sheet, which shows dense welding and compound cooling. These contrasts are analogous to those already described for the La Jara Canyon Member of the Treasure Mountain Tuff, the Fish Canyon Tuff, and the Carpenter Ridge Tuff within and outside their source calderas.

The Snowshoe Mountain Tuff is a phenocryst-rich quartz latite (table 3) containing common small angular red-brown or gray fragments of intermediate-composition volcanic rocks. In the outflow sheet, phenocrysts total about 40 percent; of this, about three-fourths are plagioclase (An_{30-50}) and the remainder is divided subequally among biotite, augite, Fe-Ti oxides, sanidine, and quartz. The presence of sanidine (Or_{71-75}) and quartz in a low-silica quartz latite (64-67 percent

SiO_2 ; Ratté and Steven, 1967, table 18) is notable and is in contrast with the phenocryst mineralogy of chemically similar quartz latites of the Treasure Mountain and Masonic Park Tuffs.

The Snowshoe Mountain Tuff can be only slightly older than the caldera-related ring lavas of Fisher Quartz Latite, well dated at 26.4 m.y. (Steven and others, 1967; Lipman and others, 1970). It has normal remanent magnetic polarity.

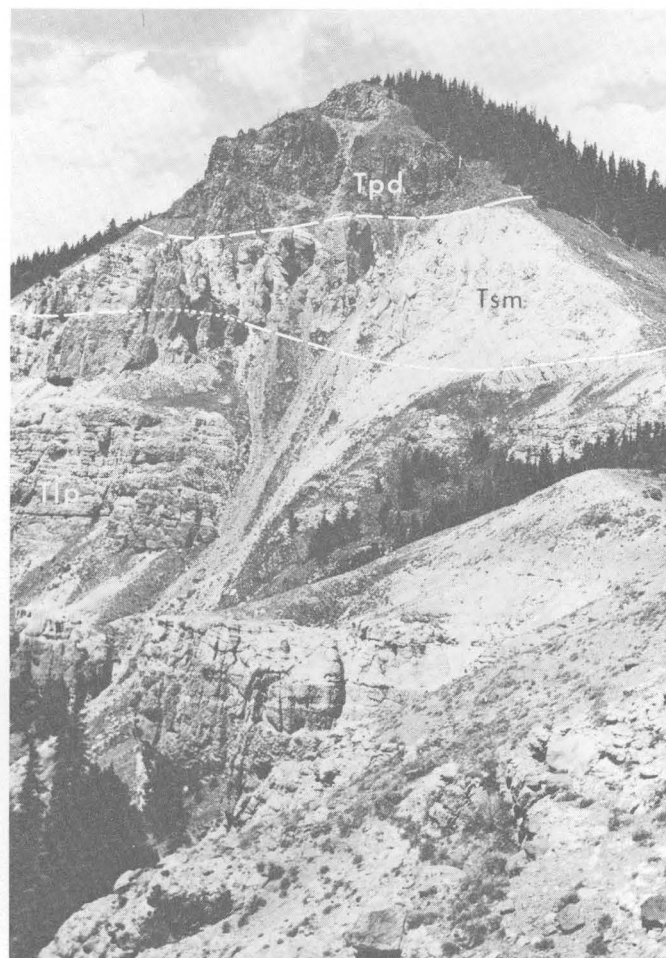


FIGURE 35.—Snowshoe Mountain Tuff, erupted from Creede caldera, interlayered with late volcanic products from the Platoro caldera complex. Light-gray slightly welded Snowshoe Mountain Tuff (Tsm) rests on volcaniclastic sediments of the Los Pinos Formation (Tlp) and is overlain by dark-gray lavas of the rhyodacite of Park Creek (Tpd). South end of Handkerchief Mesa. (See fig. 31.)

INTERLAYERED LAVA FLOWS

Andesitic to quartz latictic lava flows are interlayered with the younger ash-flow sheets at numerous horizons in the central San Juan Mountains (Durango map); only a few of these—those that are significant in the southeastern part of the field—are discussed briefly here.

SHEEP MOUNTAIN ANDESITE

The Sheep Mountain Andesite is a sequence of dark andesitic lavas, named by Larsen and Cross (1956). At the type locality northwest of Wolf Creek Pass (fig. 26), Sheep Mountain Andesite is interlayered with the members of the Masonic Park Tuff and apparently represents a local group of andesitic stratovolcanoes around the margins of the Mount Hope caldera. Although the Sheep Mountain as mapped by Larsen and Cross (1956) included andesitic rocks from volcanoes of various ages scattered widely over the San Juan field, the name "Sheep Mountain," to have any current utility, should be restricted to andesites in and near the type locality that are penecontemporaneous with the Masonic Park Tuff and that are related to evolution of the Mount Hope caldera. The name is therefore changed from Sheep Mountain Formation to Sheep Mountain Andesite. In this area Sheep Mountain flows and breccias occur below the lower member of the Masonic Park, between the two members, and above the upper member. The maximum thickness of the Sheep Mountain, about 250 m, is on the west slopes of Saddle Mountain (Wolf Creek Pass quadrangle).

The Sheep Mountain Andesite typically consists of lavas and flow breccias of dark andesite and perhaps some rhyodacite; interlayered with these are minor amounts of sedimentary rocks. Most of the lavas are nonporphyritic to sparsely porphyritic; small phenocrysts of plagioclase (An_{40-60}) and augite are the common types. The two analyses of Sheep Mountain lavas contain 56.1 and 57.3 percent SiO_2 (table 7).

Petrologically similar dark andesites that overlie the Masonic Park Tuff along the Continental Divide west of the Platoro caldera complex (Platoro map) are informally designated the andesite of Summit Peak. Although these flows lie at approximately the same stratigraphic position as the Sheep Mountain Andesite, they are most plausibly interpreted as part of the postcollapse volcanic activity related to the Platoro center.

HUEERTO ANDESITE

The Huerto Andesite, an assemblage of andesitic lava flows and associated breccias named by Larsen and Cross (1956, p. 143) and also described by Steven and Ratté (1965, p. 32-34) as the Huerto Formation, is locally present between the Fish Canyon and Carpenter Ridge Tuffs, mainly in the northwestern part of the mapped area (fig. 31). At the head of the West Fork of the San Juan River, these andesites buried an irregular fault-block topography and are locally as much as 500 m thick (Steven and others, 1969). In the South Fork of the Rio Grande the Huerto occurs discontinuously and is nowhere more than 50 m thick.

Typically, the Huerto consists of a succession of thin flows of distinctive porphyritic andesite that contains

tabular phenocrysts of calcic plagioclase (An_{55-65}) as much as 2 cm in diameter and that is virtually identical in petrography and chemistry to the platy-plagioclase andesite already described in the Conejos Formation (fig. 6). Huerto Andesite is dark gray, except for vesiculated upper and lower parts of flows which are red-brown owing to oxidation. Analyzed andesites of the Huerto contain 54-59 percent SiO_2 ; like the other platy-plagioclase andesites, they are characteristically higher in Al_2O_3 and lower in MgO than less porphyritic dark andesites of similar SiO_2 content in other units in the southeastern San Juan Mountains (table 7).

VOLCANICS OF TABLE MOUNTAIN

The volcanics of Table Mountain (Steven and Lipman, 1973) are a complex assemblage of lavas and breccias, ranging from dark fine-grained rhyodacites to lighter coarsely porphyritic quartz latites. They form a thick local accumulation between the Carpenter Ridge and Wason Park Tuffs northwest of the South Fork of the Rio Grande. These rocks were erupted from local vents near Table Mountain and farther to the southwest. Their maximum preserved thickness of about 500 m is on the west slopes of Table Mountain and near the head of Goose Creek.

LAVAS AND RELATED ROCKS
OF THE PLATORO CALDERA COMPLEX

The lavas and related rocks described in this section provide the main record of an intricate sequence of lengthy postcollapse igneous activity within and around the margins of the Platoro caldera complex (fig. 36). These rocks were emplaced over the interval 29-20 m.y. ago and are generally divisible into two groups: (1) older nonporphyritic to sparsely porphyritic dark andesite and rhyodacite, including the rhyodacite of Fisher Gulch, the members of the Summitville Andesite, the andesite of Summit Peak, and the major andesitic unit of the volcanics of Green Ridge; and (2) younger, more silicic lavas that characteristically contain large phenocrysts of feldspar as well as biotite and augite or hornblende—the upper rhyodacite unit of the volcanics of Green Ridge, the rhyodacite of Park Creek, the quartz latite of South Mountain, and the rhyolite of Cropsy Mountain. Concurrent intrusive rocks, including granitic stocks and outward-radiating andesitic to rhyolitic dikes, seem to mark cores of some of the same volcanoes whose dissected cone remnants are represented by the lavas. Interbedded volcaniclastic sedimentary rocks, including part of the Los Pinos Formation, record erosion of the primary volcanic constructional topography penecontemporaneously with its formation. Some general features of the postcollapse lavas and related rocks are summarized in table 8.

PLATORO CALDERA COMPLEX, SAN JUAN MOUNTAINS, COLORADO

TABLE 7.—Analyses of lava flows interlayered with the younger ash-flow sheets
 [Analysis 1 is by standard methods by C. L. Parker; other analyses are from Larsen and Cross (1956, tables 21, 23). Tr., trace]

| Sample----- Field No----- Lab. No----- | Sheep Mountain Andesite | | Huerto Andesite | | Volcanics of Table Mountain | |
|--|--|----------|-----------------|-------------|-----------------------------|--------------|
| | 1 S183A D100028 | 2 SV9 | 3 SC2391 | 4 SC2291 | 5 LaG1540 | 6 LaG1534 |
| | Major oxides (weight percent), recalculated without H ₂ O and CO ₂ | | | | | |
| SiO ₂ ----- | 56.11 | 57.33 | 54.89 | 58.19 | 60.17 | 60.76 |
| Al ₂ O ₃ ----- | 18.16 | 16.05 | 19.36 | 17.83 | 17.53 | 17.15 |
| Fe ₂ O ₃ ----- | 2.93 | 5.72 | 4.76 | 4.13 | 3.69 | 4.76 |
| FeO----- | 4.94 | 3.15 | 4.47 | 4.02 | 3.35 | 2.45 |
| MgO----- | 2.93 | 3.93 | 1.17 | 2.11 | 2.04 | 1.66 |
| CaO----- | 7.34 | 6.15 | 6.88 | 6.71 | 6.10 | 5.91 |
| Na ₂ O----- | 3.40 | 3.18 | 3.25 | 3.60 | 3.84 | 3.16 |
| K ₂ O----- | 2.25 | 2.84 | 3.03 | 2.03 | 2.03 | 2.82 |
| TiO ₂ ----- | 1.15 | 1.28 | 1.40 | .82 | .92 | .92 |
| P ₂ O ₅ ----- | .49 | .28 | .63 | .39 | .32 | .31 |
| MnO----- | .30 | .08 | .15 | .16 | ---- | .08 |
| TOTAL----- | 100.00 | 100.00 | 100.00 | 100.00 | 100.00 | 100.00 |
| H ₂ O+----- | .64 | ---- | .57 | .16 | .71 | .88 |
| H ₂ O----- | .27 | 1.4 | 1.19 | .94 | .17 | .60 |
| CO ₂ ----- | .72 | ---- | ---- | ---- | ---- | .00 |
| Norms (weight percent) | | | | | | |
| Quartz----- | 7.80 | 11.36 | 8.85 | 12.67 | 14.94 | 18.00 |
| Orthoclase----- | 13.27 | 16.79 | 17.88 | 12.00 | 12.00 | 16.65 |
| Albite----- | 28.80 | 26.88 | 27.48 | 30.41 | 32.46 | 26.75 |
| Anorthite----- | 27.65 | 21.15 | 29.32 | 26.51 | 24.63 | 24.28 |
| Wollastonite--- | 2.32 | 3.16 | .30 | 1.78 | 1.47 | 1.26 |
| Enstatite----- | 7.29 | 9.79 | 2.91 | 5.26 | 5.08 | 4.14 |
| Ferrosilite----- | 5.32 | ---- | 2.24 | 2.91 | 1.58 | ---- |
| Magnetite----- | 4.24 | 6.69 | 6.91 | 6.00 | 5.34 | 5.50 |
| Hematite----- | ---- | 1.11 | ---- | ---- | ---- | .97 |
| Ilmenite----- | 2.18 | 2.44 | 2.66 | 1.56 | 1.76 | 1.75 |
| Apatite----- | 1.15 | .65 | 1.49 | .91 | .77 | .76 |
| Phenocrysts (volume percent) | | | | | | |
| Plagioclase---- | 25 | 25 | 20 | 7 | 19 | 26 |
| Biotite----- | ---- | ---- | Tr. | Tr. | ---- | ---- |
| Hornblende----- | ---- | ---- | ---- | ---- | 8 | 2 |
| Augite----- | 9 | 9 | 1 | 2 | 1 | 2 |
| Hypersthene----- | 3 | 6 | 2 | Tr. | 2 | 3 |
| Olivine----- | 1 | 1 | 2 | Tr. | ---- | ---- |
| Opalines----- | 2 | 4 | 1 | 1 | 2 | 4 |
| Groundmass----- | 60 | 55 | 74 | 90 | 68 | 63 |

SAMPLE DESCRIPTIONS

- Gray andesite, containing abundant small (1-2 mm) phenocrysts in a fine-grained pilotaxitic groundmass. Pyroxenes are fresh, but olivine is altered to dark-brown iddingsite. Ridge between Goose and Leopard Creeks, at 9,950 ft, 2.5 km northeast of Lake Humphreys (Spar City quadrangle). Previously unpublished analysis provided by T. A. Steven.
- Platy-plagioclase andesite. Wolf Creek Pass quadrangle "in Beaver Creek, at an altitude of 9,000 feet" (Larsen and Cross, 1956, table 21, No. 7).
- Platy-plagioclase andesite. "San Cristobal quadrangle, south of Huerto Peak, at altitude of 12,000 feet" (Larsen and Cross, 1956, table 21, No. 10).
- Dense dark-gray andesite, containing "scattered white plagioclase tablets about 1 mm long" *** San Cristobal quadrangle, from the ridge west of the east fork of Woodfern Creek" (Larsen and Cross, 1956, table 21, No. 14).
- Dense gray hornblende rhyodacite. Spar City quadrangle, "shoulder west of Mount Hope at altitude of 12,500 feet" (Larsen and Cross, 1956, table 23, No. 2).
- Gray hornblende-pyroxene rhyodacite. Spar City quadrangle, "ridge east of Table Mountain, at altitude of 12,350 feet" (Larsen and Cross, 1956, table 23, No. 3).

The general petrologic progression of the postcollapse activity is toward more silicic types as age decreases (table 9): from voluminous dark andesites (56-59 percent SiO₂) to small scattered lava domes of porphyritic rhyolite (75-77 percent SiO₂) that are contemporaneous with nearby widespread flows of alkali olivine basalt. This postcollapse igneous activity at Platoro caldera therefore spans the regional transition from predominantly andesitic volcanism in the Oligocene to bimodal basalt-rhyolite suites in Miocene and Pliocene time (Lipman and others, 1970).

RHYODACITE OF FISHER GULCH

The rhyodacite of Fisher Gulch is a single thick biotite-plagioclase rhyodacite lava flow that represents one of the first major lava eruptions within the Platoro caldera after its collapse and resurgence. Although this rhyodacite flow is exposed only locally, over about 12 km² in the southeastern moat of Platoro caldera (fig. 36), it has been distinguished from the overlying Summitville Andesite because its distinctive phenocryst mineralogy and more silicic composition are petrologically transitional toward the Treasure Mountain Tuff. Where its

Platoro Caldera
--petrographic reference

| | Page |
|----------------------------|------------------------------|
| alteration, propylitic | 31 |
| andesite | 63 |
| Lithics | 38, 52 |
| porphyritic | 13 |
| apatite | 76 |
| aplite | 82 |
| augite | 13, 52, 63 73 |
| carbonate pseudomorph | 59 |
| reaction rim | 69, 85 |
| basalt | 93 |
| biotite | 52, 59(?), 69, 82, 85, 99 |
| oxidized | 73, 76 |
| to chlorite | 31 |
| compositional zonation | 52 |
| devitrification | 93 |
| devitrification spherulite | 52, 98 |
| disequilibrium | 73, 76 |
| flow layering | 93 |
| hornblende | 63 |
| oxidized margins | 63, 93 |
| hypersthene | 63, 85 |
| monzonite | 82, 85 |
| olivine | 93 |
| iddingsite | 99 |
| orthoclase | 82 |
| oxides | 63, 69, 99 |
| in basalt | 93 |

| | |
|-------------------------|--------------------|
| plagioclase | 52, 69, 99 |
| AN 35-45 | 73 |
| AN 40-45 | 82 |
| An 45-55 | 13 |
| glomeroporphritic | 76 |
| euhedral | 59 |
| replaced with carbonate | 29, 31, 82 |
| zoned | 63 |
| embayed | 76 |
| propylitic | 31 |
| quartz | 85, 99 |
| embayed | 73, 76, 93 |
| rhyodacite | 59, 63, 88 |
| rhyolite | 93 |
| sanidine | 52, 69, 73, 93, 99 |
| resoebed | 76 |
| euhedral | 93 |
| sphene | 76 |
| spherulite | 52 |
| textures | |
| pilotaxitic | 63, 69, 73, 76 |
| hyalopilitic | 63 |
| intergranular | 99 |
| perlitic | 73 |
| granophyric | 82 |
| phanero crystalline | 82 |
| skeletal | 93 |
| tuff | |
| shard rich | 29, 31 |
| vescile | 101 |
| vitrophyre | |
| welded tuff | 52 |
| basal | 52 |
| xenocryst, feldspar | 99 |

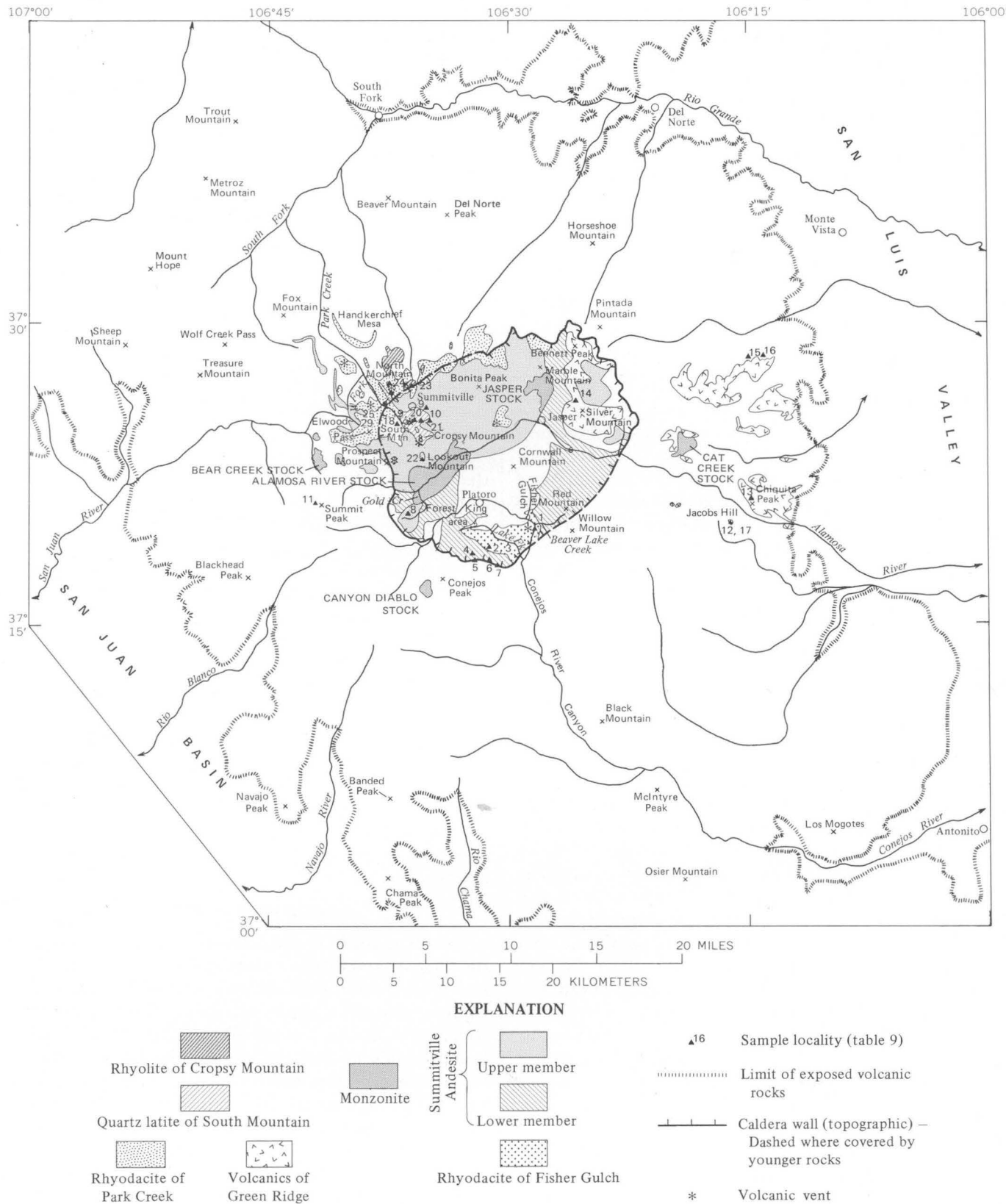


FIGURE 36.—Distribution of postcollapse lavas and related monzonitic intrusives of the Platoro caldera complex. Based on mapping by P. W. Lipman, 1965-67, 1970-71.

TABLE 8.—Summary of general features of lavas and related rocks of the Platoro caldera complex
[Rhyolitic lavas of the Hinsdale Formation are included for comparison]

| Rock unit | Approximate SiO ₂ content (percent) | Distinguishing phenocrysts | Total phenocrysts | Age (m.y.) |
|--|--|--|-------------------|--------------|
| Rhyolite of the Hinsdale Formation | 75-77 | Quartz, anorthoclase (Or ₄₃₋₄₅) | 1-15 | 4.8-21.9 |
| Rhyolite of Cropsy Mountain | 71-73 | Quartz, sanidine (Or ₆₅), hornblende | 10-25 | 20.2 |
| Quartz latite of South Mountain | 68-70 | Quartz, sanidine (Or ₇₅), hornblende | 20-35 | 22.8 |
| Rhyodacite of Park Creek | 60-64 | Biotite, augite | 20-30 | >25.8, <27.8 |
| Volcanics of Green Ridge: | | | | |
| Porphyritic rhyodacite unit | 60-66 | ... do | 20-30 | 27.4-27.8 |
| Andesite-rhyodacite unit | 58-62 | | (¹) | >27.4, <28.2 |
| Rhyolite unit | ?72 | | 5 | <28.2(?) |
| Summitville Andesite: | | | | |
| Upper member | 58-62 | | (¹) | >29.1 |
| Lower member | 56-60 | | (¹) | >29.1, <29.8 |
| Rhyodacite of Fisher Gulch | 62-64 | Biotite, augite | 10-20 | <29.8 |

¹ Small, sparse.

² Estimated.

base is exposed along the caldera wall, this flow rests on Conejos Formation; within the caldera, it lies on the La Jara Canyon Member or on thin tuffaceous sedimentary rocks that overlie the La Jara Canyon (Platoro map). The maximum exposed thickness of the rhyodacite of Fisher Gulch, about 350 m, is along the Lake Fork of the Conejos River (Platoro map), but the flow thins abruptly against the caldera wall and against the resurgent block. A small area of similar biotite-plagioclase rhyodacitic lava is exposed low within the caldera-fill sequence for a few hundred meters along the Alamosa River near the mouth of California Gulch (Platoro map), but equivalence of this lava flow to the main rhyodacite of Fisher Gulch is uncertain, owing to the gap of about 5 km between the two areas.

Most rhyodacite of Fisher Gulch is light to medium gray, but where oxidized, the rhyodacite is light red brown. Flow foliation, as defined by alternating light and dark layers and by mineral alignment, is well developed in much of this unit. In general, the flow foliation dips uniformly 10°-25°, but it steepens to nearly vertical where the rhyodacite was deposited against the south wall of the caldera (fig. 37). The foliation is also consistently steep (60°-90°) over an elliptical area of about 1 km² along the Conejos River just south of Fisher Gulch (Platoro map) that is thought to reflect the vent area. In detail, the foliation seems abruptly to fan outward to more gentle attitudes, as is characteristic of vent-dome complexes elsewhere (Williams, 1932).

The rhyodacite of Fisher Gulch contains about 20 percent phenocrysts, most of which are oscillatory-zoned plagioclase (An₃₀₋₅₀); biotite and sparse Fe-Ti oxides are the only other phenocrysts seen in most thin sections. Clinopyroxene was originally present, as indicated by carbonate pseudomorphs (fig. 37B); sparse augite was found in one sample from the vent area. Dark-gray andesitic inclusions, a few centimeters to a meter across, are locally abundant. Most of these inclusions are angular to subrounded, and in one area they are distinc-

tively rimmed by replacement carbonate (fig. 37A). At Big Lake at the head of the Lake Fork (Platoro map), andesitic inclusions and the rhyodacitic matrix are intricately intermixed in a marble-cake style that suggests that both components were mobile magmas at the time of mixing.

The rhyodacite of Fisher Gulch resembles the La Jara Canyon Member of the Treasure Mountain rather closely, both in general petrographic appearance and, especially, in the abundance of andesitic inclusions, which are rare in the other lava flows of the region. The large unbroken euhedral phenocrysts in the rhyodacite lava (fig. 37B) are diagnostic, however, in contrast to the smaller, broken phenocrysts of the ash-flow tuffs.

In chemical composition this unit is a typical rhyodacite: two fresh samples from the vent and the lava flow contain 62.5 and 63.8 percent SiO₂, respectively (table 9, Nos. 1, 2). Another analysis of the flow, from a zone of intense vapor-phase crystallization, seems high in SiO₂ content (66.4 percent) and is anomalous in several other oxides (high Fe₂O₃ and low CaO and Na₂O; table 9, No. 3).

SUMMITVILLE ANDESITE

The term Summitville Andesite is here applied to the thick local assemblage of dark sparsely porphyritic lavas and related rocks that accumulated within the Platoro caldera complex after collapse. The Summitville Andesite is divided into a lower member, which filled the Platoro caldera after eruption of the La Jara Canyon Member of the Treasure Mountain Tuff, and an upper member, which filled the Summitville caldera after eruption of the Ojito Creek and Ra Jadero Members.

The name Summitville Andesite was first proposed for almost the same sequence of rocks by Patton (1917, p. 35-38), who correctly noted its approximate stratigraphic equivalence to the Sheep Mountain Andesite elsewhere in the San Juan field. The name "Summitville" was subsequently abandoned by Larsen and Cross (1956, p. 124),

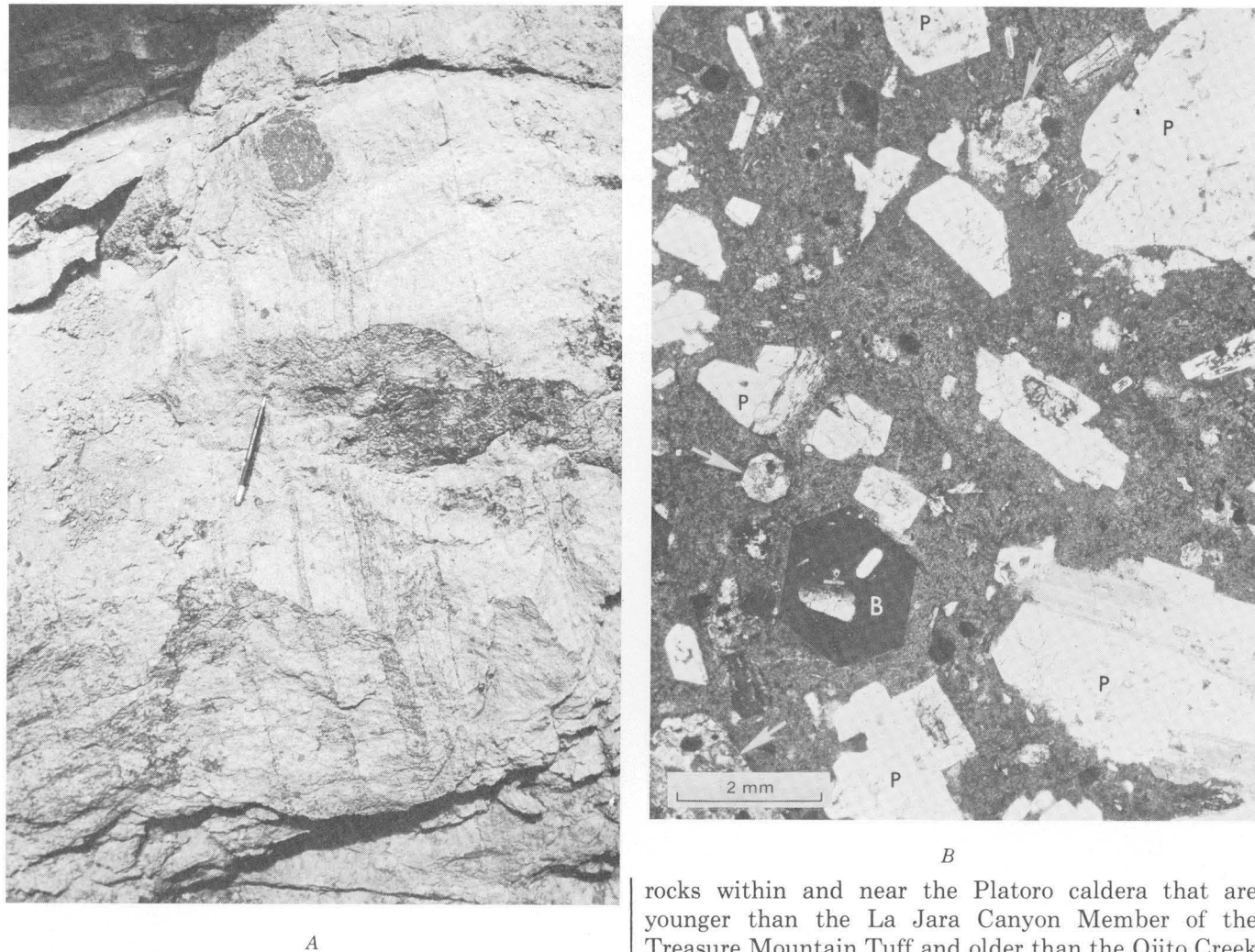


FIGURE 37.—Rhyodacite of Fisher Gulch. A, Steeply dipping flow layering where lava flow banked against the south caldera wall. Dark andesitic inclusions are irregularly rimmed by white replacement carbonate. Roadcut at 10,800 feet, along logging road above the Lake Fork, northeast ridge of Conejos Peak. B, Photomicrograph showing euhedral unbroken phenocrysts of plagioclase (P) and biotite (B). (Note textural contrast with compositionally similar welded tuff of the intracaldera La Jara Canyon Member, fig. 18.) Arrows indicate carbonate pseudomorphic after augite. Analyzed sample 2, table 9.

who, lacking knowledge of the significance of the Platoro and Summitville caldera structures, concluded that "****the great flows**** near Summitville to which the name Summitville andesite was applied, as well as the rhyolitic rocks underlying them and originally believed to belong to the Treasure Mountain****have been found to lie below the Treasure Mountain and to belong to the Conejos (formation)." Because the present study has shown that Patton was basically right and Larsen and Cross wrong, the term "Summitville Andesite" is a valid, useful name and is therefore reinstated.

The lower member of the Summitville Andesite is defined here to include the andesitic lavas and related

rocks within and near the Platoro caldera that are younger than the La Jara Canyon Member of the Treasure Mountain Tuff and older than the Ojito Creek Member; thus, in places the lower member is interlayered with the middle tuff of the Treasure Mountain. The upper member includes lavas within and near the Summitville caldera that are younger than the Ojito Creek Member of the Treasure Mountain Tuff and older than the Masonic Park Tuff.

DISTRIBUTION AND THICKNESS

As reinstated, the Summitville Andesite is a local sequence of andesitic lavas, breccias, and interlayered volcaniclastic sedimentary rocks that are confined to an area of about 500 km^2 in and near the Platoro caldera complex (fig. 36). Each member is exposed over a vertical distance of nearly 1 km within the Platoro and Summitville calderas, and original thickness must have been appreciably greater for each member, because the top is eroded and the base not exposed in the sections of maximum thickness. The original volume of the Summitville Andesite is difficult to estimate because of these exposure problems, but it must have been at least several hundred cubic kilometers, perhaps nearly 500 km^3 .

PLATORO CALDERA COMPLEX, SAN JUAN MOUNTAINS, COLORADO

TABLE 9.—Analyses of lava flows and

[Sample localities shown in fig. 36. Analyses 8, 11, and 14-16 are from Larsen and Cross 3); analyses 10 and 22 are from Patton (1917). All other major-oxide analyses are by John Glenn, and James Kelsey. Minor-element analyses by standard methods are Norma Rait; analyses 24-29 are by semiquantitative methods by J. L. Harris. >,

| | Rhyodacite of Fisher Gulch | Summitville Andesite | | | | | | | | Andesite of Summit Peak | Volcanics of Green Ridge | | | |
|--|----------------------------------|------------------------|------------------------|------------------------|-----------------------|-----------------------|--------------------------|--------------------------|-------------|-------------------------------|--------------------------|--------------|----------------------------|-------------------------|
| | | Lower member | | | | Upper member | | | | | Andesite-rhyodacite unit | | | |
| | | 1 71L-38 W176167 | 2 71L-17 W176165 | 3 71L-18 W176166 | 4 71J-1 W176170 | 5 71J-2 W176171 | 6 67L-126 D133704W | 7 67L-125 D133703W | 8 SV 136 | 9 SA-8 | 10 P 11 | 11 SV 115 | 12 66L-48-A W-168532 | 13 66L-7 W-168531 |
| Major oxides (weight percent), recalculated without H ₂ O and CO ₂ (original values listed separately below) | | | | | | | | | | | | | | |
| SiO ₂ ----- | 62.5 | 63.8 | 66.4 | 56.4 | 56.6 | 57.3 | 60.6 | 58.46 | 58.83 | 60.94 | 60.95 | 58.8 | 60.7 | 65.98 |
| Al ₂ O ₃ ----- | 18.3 | 17.2 | 16.8 | 17.9 | 17.4 | 17.0 | 17.4 | 17.77 | 18.30 | 17.50 | 15.53 | 17.2 | 17.0 | 16.76 |
| Fe ₂ O ₃ ----- | 2.0 | 2.9 | 5.2 | 2.7 | 4.0 | 5.0 | 3.2 | 4.57 | 3.30 | 3.94 | 3.27 | 3.5 | 2.6 | 2.95 |
| FeO----- | 2.2 | 2.3 | .70 | 5.5 | 4.5 | 3.4 | 2.8 | 3.51 | 3.04 | 1.98 | 3.14 | 3.9 | 3.7 | 1.28 |
| MgO----- | 1.5 | 1.4 | .73 | 3.2 | 3.1 | 3.1 | 2.3 | 2.82 | 2.41 | 2.11 | 2.60 | 3.0 | 3.0 | 1.20 |
| CaO----- | 4.3 | 3.8 | 2.0 | 6.4 | 6.3 | 5.6 | 5.0 | 4.61 | 5.91 | 5.58 | 5.01 | 6.4 | 5.5 | 3.71 |
| Na ₂ O----- | 4.0 | 3.8 | 3.0 | 3.4 | 3.4 | 3.6 | 3.9 | 3.52 | 3.70 | 3.48 | 4.11 | 2.8 | 3.3 | 3.39 |
| K ₂ O----- | 4.2 | 3.8 | 4.3 | 2.8 | 3.0 | 3.1 | 3.4 | 2.97 | 3.13 | 3.23 | 3.58 | 2.9 | 2.7 | 3.86 |
| TiO ₂ ----- | .73 | .72 | .74 | 1.1 | 1.1 | 1.2 | .92 | 1.40 | .84 | 1.00 | 1.06 | .97 | .88 | .59 |
| P ₂ O ₅ ----- | .17 | .16 | .16 | .41 | .41 | .43 | .39 | .37 | .42 | .11 | .75 | .30 | .48 | .21 |
| MnO----- | .11 | .09 | .07 | .15 | .16 | .11 | .14 | .00 | .11 | .13 | ----- | .10 | .09 | .06 |
| Total----- | 100.01 | 99.97 | 100.10 | 99.96 | 99.97 | 99.84 | 100.05 | 100.00 | 99.99 | 100.00 | 100.00 | 99.87 | 99.45 | 99.99 |
| H ₂ O+----- | .50 | .45 | 1.1 | .64 | 1.2 | .53 | .40 | .86 | 1.30 | .97 | .83 | .69 | .92 | 2.69 |
| H ₂ O----- | 1.1 | .55 | 1.6 | .76 | 1.1 | .57 | .91 | .63 | .32 | .60 | .43 | .41 | .18 | .44 |
| CO ₂ ----- | .20 | 1.6 | <.05 | <.05 | .75 | .18 | <.05 | 1.45 | .94 | 1.35 | ----- | <.05 | <.05 | ----- |
| Norms (weight percent) | | | | | | | | | | | | | | |
| Quartz----- | 11.86 | 17.05 | 27.60 | 6.64 | 8.06 | 9.37 | 12.06 | 13.44 | 10.07 | 17.68 | 11.69 | 13.39 | 14.85 | 22.33 |
| Corundum----- | ----- | .37 | 4.03 | ----- | ----- | ----- | ----- | 1.27 | ----- | 1.61 | ----- | ----- | ----- | .75 |
| Orthoclase----- | 24.70 | 22.44 | 25.58 | 16.79 | 17.64 | 18.55 | 19.81 | 17.56 | 18.50 | 19.42 | 21.17 | 17.32 | 16.24 | 22.83 |
| Albite----- | 33.64 | 32.13 | 25.29 | 28.34 | 28.74 | 30.85 | 32.67 | 29.77 | 31.25 | 29.93 | 34.76 | 23.94 | 27.57 | 28.68 |
| Anorthite----- | 19.60 | 17.76 | 8.64 | 25.31 | 23.40 | 20.79 | 20.17 | 20.43 | 24.11 | 18.57 | 13.35 | 25.52 | 23.65 | 17.06 |
| Wollastonite--- | .21 | ----- | ----- | 1.57 | 2.11 | 1.70 | .83 | ----- | 1.03 | ----- | 2.76 | 1.70 | .21 | ----- |
| Enstatite----- | 3.81 | 3.58 | 1.82 | 8.09 | 7.69 | 7.82 | 5.82 | 7.03 | 6.01 | 5.33 | 6.48 | 7.55 | 7.61 | 2.99 |
| Ferrosilite----- | 1.43 | .76 | ----- | 6.24 | 3.44 | .42 | 1.28 | .35 | 1.68 | ----- | 1.31 | 2.90 | 3.27 | ----- |
| Magnetite----- | 2.96 | 4.17 | .34 | 3.97 | 5.82 | 7.20 | 4.71 | 6.63 | 4.78 | 3.96 | 4.74 | 5.13 | 3.84 | 2.64 |
| Hematite----- | ----- | ----- | 4.92 | ----- | ----- | ----- | ----- | ----- | ----- | 1.28 | ----- | ----- | ----- | 1.13 |
| Ilmenite----- | 1.39 | 1.36 | 1.41 | 2.15 | 2.15 | 2.31 | 1.76 | 2.66 | 1.60 | 1.95 | 2.02 | 1.84 | 1.66 | 1.11 |
| Rutile----- | ----- | ----- | ----- | ----- | ----- | ----- | ----- | ----- | ----- | ----- | ----- | ----- | ----- | ----- |
| Apatite----- | .41 | .39 | .39 | .96 | .98 | 1.01 | .91 | .87 | .99 | .27 | 1.77 | .72 | 1.13 | .49 |
| Minor elements (parts per million) | | | | | | | | | | | | | | |
| B----- | ----- | ----- | ----- | ----- | ----- | ----- | ----- | ----- | ----- | ----- | ----- | 1200 | 1400 | ----- |
| Ba----- | 1000 | 920 | 800 | 720 | 520 | 920 | 1095 | ----- | ----- | ----- | ----- | ----- | ----- | ----- |
| Be----- | ----- | ----- | ----- | ----- | ----- | <2 | <2 | ----- | ----- | ----- | ----- | ----- | ----- | ----- |
| Ce----- | ----- | ----- | ----- | ----- | ----- | ----- | ----- | ----- | ----- | ----- | ----- | ----- | ----- | ----- |
| Co----- | 7 | 10 | 9 | 18 | 15 | 23 | 12 | ----- | ----- | ----- | ----- | 16 | 13 | ----- |
| Cr----- | 5 | 5 | 5 | 4 | 8 | 12 | 3 | ----- | ----- | ----- | ----- | 5 | 50 | ----- |
| Cu----- | 28 | 28 | 34 | 26 | 56 | 64 | 36 | ----- | ----- | ----- | ----- | 46 | 35 | ----- |
| Ga----- | 20 | 20 | 20 | 20 | 20 | 21 | 20 | ----- | ----- | ----- | ----- | 20 | 20 | ----- |
| La----- | 80 | 90 | 80 | 100 | 90 | 74 | 62 | ----- | ----- | ----- | ----- | ----- | ----- | ----- |
| Mo----- | 4 | ----- | ----- | 6 | ----- | <5 | <5 | ----- | ----- | ----- | ----- | ----- | ----- | ----- |
| Nb----- | 20 | 20 | 20 | 20 | 20 | 24 | 24 | ----- | ----- | ----- | ----- | ----- | ----- | ----- |
| Ni----- | 4 | 5 | 5 | 12 | 19 | <5 | ----- | ----- | ----- | ----- | ----- | 8 | 18 | ----- |
| Pb----- | 20 | 80 | <10 | 20 | 20 | <50 | <50 | ----- | ----- | ----- | ----- | 40 | 60 | ----- |
| Sc----- | 12 | 14 | 9 | 30 | 24 | 23 | 24 | ----- | ----- | ----- | ----- | 14 | 12 | ----- |
| Sn----- | ----- | ----- | ----- | ----- | <20 | <20 | ----- | ----- | ----- | ----- | ----- | <20 | <20 | ----- |
| Sr----- | 840 | 680 | 410 | 1200 | 960 | 520 | 440 | ----- | ----- | ----- | ----- | 1200 | 1000 | ----- |
| V----- | 60 | 90 | 80 | 180 | 180 | 200 | 120 | ----- | ----- | ----- | ----- | 180 | 120 | ----- |
| Y----- | 20 | 20 | 20 | 40 | 30 | 45 | 52 | ----- | ----- | ----- | ----- | 30 | 20 | ----- |
| Yb----- | 2 | 2 | 2 | 3 | 2 | 3 | 4 | ----- | ----- | ----- | ----- | ----- | ----- | ----- |
| Zr----- | 160 | 160 | 180 | 130 | 130 | 220 | 206 | ----- | ----- | ----- | ----- | 140 | 100 | ----- |
| Phenocrysts (volume percent) | | | | | | | | | | | | | | |
| Quartz----- | ----- | ----- | ----- | ----- | ----- | ----- | ----- | 9 | ----- | ----- | ----- | ----- | ----- | ----- |
| Sanidine----- | ----- | ----- | ----- | ----- | ----- | ----- | ----- | ----- | ----- | ----- | ----- | ----- | ----- | ----- |
| Plagioclase----- | 22.3 | 23.6 | 23 | 4 | 23.9 | 30.1 | 7.6 | 72 | ----- | ----- | 27 | 27.1 | 20.3 | 13 |
| Biotite----- | 4.9 | 5.2 | 5 | ----- | ----- | ----- | ----- | ----- | ----- | ----- | ----- | ----- | ----- | 2 |
| Hornblende----- | ----- | ----- | ----- | ----- | ----- | ----- | ----- | ----- | ----- | ----- | ----- | ----- | ----- | ----- |
| Augite----- | 2.1 | ----- | ----- | 1 | 7.2 | 5.7 | 2.9 | 7 | ----- | ----- | 5 | 5.2 | 4.3 | 1 |
| Hypersthene----- | ----- | ----- | ----- | ----- | 3.9 | 1.5 | 1.0 | 7 | ----- | ----- | 3.5 | 1.8 | 2.1 | 3 |
| Sphene----- | ----- | ----- | ----- | ----- | ----- | ----- | ----- | ----- | ----- | ----- | ----- | ----- | ----- | ----- |
| Opalines----- | 2.4 | 2.1 | 2 | ----- | 2.8 | 1.9 | 1.4 | 5 | ----- | ----- | 2 | 2.1 | .7 | 2 |
| Groundmass----- | 68.3 | 69.1 | 70 | 95 | 63.2 | 60.9 | 87.1 | ----- | ----- | ----- | 63 | 63.8 | 71.6 | 79 |

See page 62 for sample descriptions.

related rocks of the Platoro caldera complex

(1956, tables 21, 23); analyses 9, 18-21, and 23 are from Steven and Ratté (1960, tables 2, rapid methods by P. L. D. Elmore, Samuel Botts, Gillison Chloe, Lowell Artis, H. Smith, Nos. 1-5 by J. D. Fletcher, Nos. 6 and 7 by Harriet Neiman, and Nos. 12, 13, and 17 by more than; <, less than; Tr., trace)

| Volcanics of Green Ridge--Continued | | | Rhyolite of Cropsy Mountain | | | | | | | | | | | | | |
|---|--|---|--|--|--|--|--|--|---|---|--|--|---|--|--|------------------------------|
| Porphyritic rhyodacite unit | | Rhyodacite of Park Creek | Quartz Latite of South Mountain | | | Rhyolite flows | | Mix-lava complex at North Mountain | | | | | | | | |
| 15 Con 2 | 16 Con 606 | 17 66L-48-C W-168533 | 18 SM 244 139604 | 19 SA-2 A-153 | 20 SM 291 139603 | 21 SA-1 A 152 | P 39 ----- | 22 SM 23A1 139602 | 23 70L-139-C W174656 | 24 70L-159 W174660 | 25 70L-158-B W174659 | 26 70L-158-A W174658 | 27 70L-157 W174657 | 28 70L-161 W174661 | 29 70L-161 | Sample Field No. Lab. No. |
| Major oxides (weight percent), recalculated without H ₂ O and CO ₂ (original values listed separately below)--Continued | | | | | | | | | | | | | | | | |
| 60.84 16.41 5.82 .86 2.96 | 62.29 16.32 3.40 2.35 2.06 | 66.9 17.4 3.1 .77 .72 | 60.5 17.3 4.0 2.3 1.9 | 68.2 15.0 2.5 1.0 1.2 | 68.4 15.1 2.4 .54 .70 | 70.5 15.4 .65 .13 .44 | 70.73 14.64 14.6 .52 .85 | 72.3 14.6 1.3 .52 .62 | 64.0 17.1 4.0 .69 .54 | 64.9 16.8 4.06 .69 .51 | 64.7 15.8 3.7 .89 1.6 | 65.8 16.2 3.9 .65 .69 | 68.6 15.4 3.5 .36 .39 | 72.4 14.2 1.8 .49 .49 | SiO ₂ Al ₂ O ₃ Fe ₂ O ₃ FeO MgO | |
| 5.17 3.11 3.84 .73 .18 | 4.79 3.77 3.75 1.01 .27 | 3.8 3.7 2.6 .46 .36 | 5.7 3.7 3.0 .89 .52 | 3.2 3.7 4.2 .55 .39 | 2.8 4.0 4.3 .53 .41 | 1.4 4.1 4.4 .49 .32 | 2.36 4.29 4.66 .51 .18 | 1.63 3.8 4.7 .29 .27 | 2.8 5.0 4.3 .92 .51 | 2.7 4.6 4.3 .92 .48 | 3.5 4.3 4.1 .81 .39 | 2.5 4.7 4.2 .78 .36 | 2.03 4.4 4.3 .70 .26 | 1.5 3.9 4.6 .43 .11 | CaO Na ₂ O K ₂ O TiO ₂ P ₂ O ₅ | |
| .08 | .00 | .07 | .22 | .09 | .12 | .02 | .00 | .04 | .08 | .06 | .08 | .08 | .08 | .07 | .06 | MnO |
| 100.00 >.90 | 100.01 .12 | 99.88 .44 | 100.03 >1.3 | 100.03 .99 | 99.96 .55 | 100.01 >1.2 | 100.00 .59 | 100.07 >2.5 | 99.94 .63 | 100.00 .47 | 97.87 .94 | 99.86 .18 | 100.01 .73 | 99.98 .82 | Total H ₂ O+ H ₂ O- CO ₂ | |
| ----- ----- ----- <.05 | ----- 1.4 | ----- 1.99 | ----- 1.7 | ----- 0.00 | ----- ----- | ----- ----- | ----- 0.05 | ----- <.05 | ----- <.05 | ----- <.05 | ----- <.05 | ----- <.05 | ----- <.05 | ----- <.05 | | |
| Norms (weight percent)--Continued | | | | | | | | | | | | | | | | |
| 14.19 ----- 22.67 26.29 19.50 | 14.68 2.28 22.13 31.85 16.57 | 26.82 15.53 17.67 31.64 16.67 | 14.70 ----- 24.98 31.40 21.78 | 23.28 ----- 25.50 31.28 11.80 | 22.93 2.17 25.78 33.89 10.49 | 27.09 ----- 27.50 34.84 4.82 | 22.65 ----- 25.7 36.25 6.97 | 27.74 .97 27.70 31.90 6.36 | 13.1 .29 25.7 41.98 10.7 | 16.7 .78 25.2 38.7 10.5 | 15.6 1.5 24.4 36.7 11.5 | 17.0 .21 25.1 39.4 10.2 | 22.8 .57 25.1 36.9 8.3 | 28.6 .42 27.1 32.7 6.8 | Quartz Corundum Orthoclase Albite Anorthite | |
| 2.07 7.36 .92 | 2.25 5.12 4.64 | ----- 1.79 1.36 | 1.24 4.62 5.45 | .71 2.92 1.82 | .24 1.74 .83 | ----- 1.09 .39 | 1.48 2.11 .68 | ----- 1.55 ----- | 0.00 1.3 ----- | 0.00 1.3 ----- | 1.4 4.01 ----- | 0.00 1.7 ----- | ----- .96 ----- | Wollastonite Enstatite Ferrosilite Magnetite | | |
| 5.18 1.38 .43 | .20 1.92 .65 | 2.19 .88 .86 | .26 1.68 1.22 | 1.24 1.05 .93 | .41 .92 .77 | 2.15 .97 .44 | ----- .54 .63 | .65 1.6 1.2 | 4.05 1.6 1.1 | 4.06 1.6 1.1 | 3.2 1.5 1.1 | 3.9 1.5 .93 | 3.5 .92 .86 | 1.5 .81 .26 | Hematite Ilmenite Rutile Apatite | |
| Minor elements (parts per million)--Continued | | | | | | | | | | | | | | | | |
| ----- ----- ----- ----- ----- 8 5 14 20 ----- 8 70 5 420 860 50 30 150 | ----- 2300 ----- ----- ----- ----- ----- 100 15 20 ----- ----- ----- 1500 70 20 300 300 | ----- ----- ----- ----- ----- ----- ----- 100 15 150 ----- 15 0 15 10 10 10 1500 70 20 300 300 | ----- ----- ----- ----- ----- ----- ----- 70 10 100 100 100 30 30 300 300 | ----- 2000 1.5 500 10 100 100 150 150 1500 70 20 2 300 300 | ----- 2000 1.5 300 10 100 100 100 100 1500 70 20 2 300 300 | ----- 2000 1.5 500 10 100 100 100 100 1500 70 20 2 300 300 | ----- 2000 1.5 300 10 100 100 100 100 1500 70 20 2 300 300 | ----- 1500 2 300 10 100 100 100 100 1500 50 20 2 200 200 | ----- 1000 2 100 10 70 70 70 70 500 20 20 2 150 150 | B Ba Be Ce Co Cr Cu Ga La Mo Nb Ni Pb Sc Sn Sr V Y Yb Zr | | | | | | |
| Phenocrysts (volume percent)--Continued | | | | | | | | | | | | | | | | |
| ----- 25 5 1 3 2 3 2 3 2 60 | ----- 23 10 2 2 3.0 ----- 70 1.5 2.1 63.8 | ----- 24.9 6.2 3.0 ----- 70 80 | ----- 22 5 ----- 10 4 ----- 13 4 75 80 | 2 2 3 2 10 4 13 10 75 80 | 3 2 2 2 2 2 2 2 2 1.5 | 2 2 2 2 10 4 13 10 75 80 | 2.2 3.1 2.1 9.3 1 Tr. .8 .1 .7 81.7 | 0.2 .3 1 1 1 Tr. .8 .1 .2 98 | 0.1 .2 3.7 .2 .3 ----- .3 1 1 98 | 0.3 .8 6.5 1.5 15 1.5 1.5 1.5 1.5 1.5 | 1 1.5 6.5 15 15 15 15 15 15 1.5 | 2.5 3. 15 15 15 15 15 15 15 1.5 | 1.5 2.5 13.5 1.5 1.5 1.5 1.5 1.5 1.5 1.5 | Quartz Sanidine Plagioclase Biotite Hornblende Augite Hypersthene Sphene Opaques Groundmass | | |

TABLE 9.—Analyses of lava flows and related rocks of the Platoro caldera complex—Continued

- | SAMPLE DESCRIPTIONS | |
|---|---|
| 1. Dark-gray dense devitrified rock having steep obscure flow layering at vent area. Phenocrysts of plagioclase as much as 5 mm across are intricately zoned and resorbed; biotite is oxidized, and augite is partly replaced by carbonate. Platoro Road, along Conejos River, about 0.9 km north of junction with Beaver Lake Creek. | 15. Red-brown porphyritic rhyodacite, containing plagioclase phenocrysts as long as 2 cm. A clast in the Los Pinos Formation, almost certainly derived from the volcanics of Green Ridge. "North slope of Green Ridge, above Goat Ranch" (Larsen and Cross, 1956, table 23, No. 8). |
| 2. Dark dense lava, similar to No. 1, having steep well-developed flow layering (fig. 37A) where flow banked against caldera wall. Contains large inclusions of sparsely porphyritic andesite, with irregular rims of replacement carbonate along contacts. Groundmass is more finely devitrified than No. 1, and augite is completely replaced by carbonate (fig. 37B). At 10,800 ft, along logging road on northeast ridge of Conejos Peak, 1.6 km southeast of Big Lake. | 16. Gray glassy porphyritic rhyodacite, much like No. 15. Also a clast in the Los Pinos Formation. "Northeast slope of Green Ridge, ridge east of house, at altitude of 8,500 feet" (Larsen and Cross, 1956, table 21, No. 9). |
| 3. Pale-purplish-gray devitrified lava that is chalky because of intense vapor-phase crystallization. Composition appears anomalous: high in SiO_2 and Fe_2O_3 , and low CaO and Na_2O . About 100 m west of locality of No. 2 along the logging road. | 17. Red-brown porphyritic quartz latite. Contains phenocrysts of plagioclase as long as 1 cm in a dusty submicroscopically devitrified groundmass. Chemically anomalous: K_2O is low; CaO , P_2O_5 , and perhaps SiO_2 are high. South slope of Jacobs Hill, at about 9,300 ft. |
| 4. Dark-gray dense aphanitic andesite, containing small microphenocrysts of plagioclase less than 1 mm long and even smaller sparse augite microphenocrysts in a finely microcrystalline intergranular groundmass. At 11,400 ft, along Saddle Creek Road on northeast ridge of Conejos Peak, 1.4 km north of upper switchback. | 18. Dark-gray porphyritic rhyodacite. In addition to the large phenocrysts 3-10 mm across, the finely devitrified groundmass contains small plagioclase laths about 0.1-0.2 mm long that define a flow foliation. "Collected along the eastern branch of Park Creek due west of the summit of South Mountain" (Steven and Ratté, 1960, table 3, No. 1). |
| 5. Dense gray andesite, containing abundant plagioclase phenocrysts 1-2 mm in diameter and smaller pyroxenes in a very finely crystalline intergranular groundmass. About 200 m southeast of locality of No. 4, near crest of ridge along road. | 19. Gray porphyritic quartz latite, containing feldspar and quartz phenocrysts varying from one to several centimeters in diameter. Carbonate replaces feldspar phenocrysts, as well as groundmass. Modal estimate very approximate, because of coarse phenocryst size. "About 2,400 feet east of the summit of South Mountain" (Steven and Ratté, 1960, table 3, No. 3). |
| 6. Coarsely crystalline red-brown andesite. See fig. 38B for description and location. | 20. Gray porphyritic quartz latite, generally similar to No. 19. "Collected from within 200 feet" of No. 19 (Steven and Ratté, 1960, table 3, No. 2). |
| 7. Sparsely porphyritic dark andesite. See fig. 38A for description and location. | 21. Gray porphyritic quartz latite to rhyolite, in general similar to Nos. 19 and 20, but relatively free of carbonate. "The core of the South Mountain volcanic dome, collected from the nose of the ridge extending east from the Iowa mine workings at an altitude of about 11,700 feet" (Steven and Ratté, 1960, table 3, No. 4). |
| 8. Dark-gray fine-grained seriate andesite flow. "Gold Creek at an altitude of 11,400 feet" (Larsen and Cross, 1956, table 21, No. 3). | 22. Black vitrophyric rhyolite. "Contains sanidine, plagioclase, biotite, and hornblende in a fresh black glass. From Lookout Mountain" (Patton, 1917, p. 32). |
| 9. Dark-gray fine-grained dense andesite. Biotite occurs in finely granular aggregates and may be secondary. Other ferromagnesian minerals are completely altered, but clots of chlorite and carbonate probably are replacement products of augite. "Roadcut just east of the bridge across Wightman Fork and 500 feet west of the mouth of Cropsy Creek" (Steven and Ratté, 1960, table 2, No. 3). | 23. Black vitrophyric rhyolite. "Collected about two-thirds of the way up the south face of North Mountain" (Steven and Ratté, 1960, table 3, No. 6). |
| 10. Augite andesite, containing "plagioclase and augite phenocrysts in an altered groundmass that probably consisted of plagioclase, augite, and magnetite. From creek bed of Cropsy Gulch" (Patton, 1917, p. 31). | 24. Dark-gray phenocryst-poor rhyodacite. See fig. 45C for description. Near base of lava flow, at about 12,000 ft, above small pond 0.6 km northwest of west peak (12,568 ft) of North Mountain. |
| 11. Dark-gray dense plagioclase-pyroxene rhyodacite. "Higher in silica and potash than usual. The phenocrysts are variable in size and most of them are less than 1 mm long. West slope of Summit Peak, at an altitude of 12,800 feet" (Larsen and Cross, 1956, table 21, No. 8). | 25. Dark-gray phenocryst-poor rhyodacite, much like No. 24. Near base of flow, at about 12,375 ft, at saddle 0.4 km southwest of west peak (12,568 ft). |
| 12. Dark-gray dense andesite. See fig. 41C for description and location. | 26. Intermediate-composition phase, showing extreme disequilibrium. Well-developed flow layering, with abrupt local variations in phenocryst content. At 12,400 ft, along ridge 0.3 km southwest of west peak (12,568 ft). |
| 13. Dark-red-brown finely porphyritic rhyodacite. Texture much like No. 12, but phenocrysts are slightly larger—as much as 1 mm in diameter. At 9,400 ft, on northwest ridge of Chiquita Peak, about 0.3 km from summit. | 27. Intermediate-composition phase, showing phenocryst disequilibrium. See fig. 45B for sample description. Very similar to No. 26 but has higher phenocryst content; only 1.5 m from No. 26. |
| 14. Light-gray finely porphyritic rhyodacite to quartz latite. Described as devitrified, but analysis is problematic because of high H_2O . "The rock is seriate porphyritic, the larger phenocrysts are about 1 mm across, and they grade into submicroscopic crystals in the groundmass." "Saddle, ½ mile north of Silver Mountain" (Larsen and Cross, 1956, table 21, No. 16). | 28. Typical light-gray phenocryst-rich rhyolite. See fig. 45A for sample description. At 12,125 ft, southeast of main ridge, about 9.2 km from 12,410-ft spot elevation. |
| | 29. Dark-gray nearly vitrophyric margin of vent intrusive. At southwest contact on ridge, at about 11,925 ft. |

The two members of the Summitville Andesite are similar in general appearance and in composition; this similarity causes major mapping problems, because the members can only be reliably distinguished by stratigraphic relations with units of the Treasure Mountain Tuff. The Summitville Andesite also is similar in appearance and composition to the andesite of Summit Peak and, to a considerable extent, to intermediate-composition lavas of the Conejos Formation. Near the caldera complex, however, the Conejos Formation tends to be more propylitically altered than otherwise similar rocks of the Summitville Andesite.

Discrimination between the two members of Summitville Andesite is most confidently made in the eastern part of Platoro caldera, where upper units of the Treasure Mountain Tuff are present, and within the Summitville caldera, where the lower member of the Summitville Andesite is unlikely to be exposed. In the western parts of the caldera complex, especially south of the Alamosa River, division into lower and upper members is tenuous and is based mainly on the presence of some local intertonguing weakly welded ash-flow tuffs along Gold Creek that are uncertainly identified as the upper tuff and, possibly, the Ra Jadero Member of the Treasure Mountain (Platoro map).

The high stratigraphic position of some (probably rhyodacitic) lava flows and interbedded sedimentary rocks near the top of Red Mountain along the southeast rim of the Platoro caldera (Platoro map) suggests that

these rocks may be correlative with the andesite-rhyodacite unit of the volcanics of Green Ridge; but without firm evidence, such as control from the ash-flow stratigraphy, the rocks on Red Mountain have been tentatively included in the Summitville Andesite.

LITHOLOGIC DESCRIPTION

Lavas of the Summitville Andesite consist of sparsely porphyritic dark andesite and minor rhyodacite (fig. 38). Phenocrysts are generally less than 10 percent of the rock, are rarely more than 20 percent, and are typically small—2 mm or less. Tabular or blocky plagioclase (An_{35-55}), less abundant equant augite, and opaque oxides are the dominant phenocrysts; a few samples contain sparse hypersthene. Biotite and hornblende are rare. Seven samples of these lavas range in SiO_2 content from 56.4 to 60.9 percent (table 9, Nos. 4-10).

These petrologic features characterize especially the great sequence of lower member lavas exposed over a thickness of at least 500 m in the eastern caldera moat, along the Alamosa River canyon east of Jasper (Platoro map). At least 12 monotonously uniform sparsely porphyritic dark andesitic flows, each 10-40 m thick and traceable laterally for 100-1,000 m, constitute the bulk of this section and are separated by only minor andesitic sandstone interbeds.

The lower member is somewhat more variable in its other major accumulation, in the southwestern part of the Platoro caldera moat (Platoro map). The lowest flow

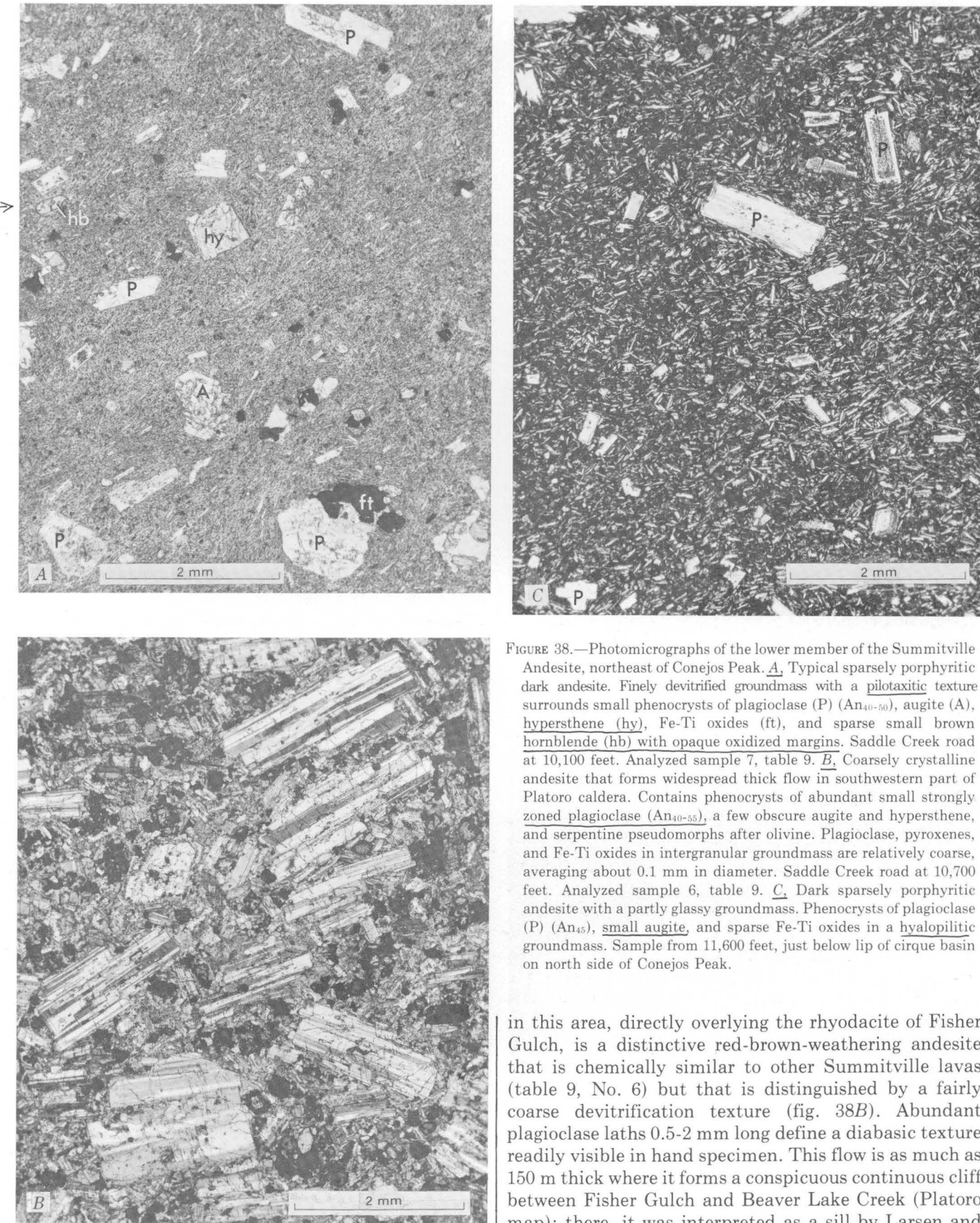


FIGURE 38.—Photomicrographs of the lower member of the Summitville Andesite, northeast of Conejos Peak. *A*, Typical sparsely porphyritic dark andesite. Finely devitrified groundmass with a pilotaxitic texture surrounds small phenocrysts of plagioclase (P) (An_{40-50}), augite (A), hypersthene (hy), Fe-Ti oxides (ft), and sparse small brown hornblende (hb) with opaque oxidized margins. Saddle Creek road at 10,100 feet. Analyzed sample 7, table 9. *B*, Coarsely crystalline andesite that forms widespread thick flow in southwestern part of Platoro caldera. Contains phenocrysts of abundant small strongly zoned plagioclase (An_{40-55}), a few obscure augite and hypersthene, and serpentine pseudomorphs after olivine. Plagioclase, pyroxenes, and Fe-Ti oxides in intergranular groundmass are relatively coarse, averaging about 0.1 mm in diameter. Saddle Creek road at 10,700 feet. Analyzed sample 6, table 9. *C*, Dark sparsely porphyritic andesite with a partly glassy groundmass. Phenocrysts of plagioclase (P) (An_{45}), small augite, and sparse Fe-Ti oxides in a hyalopilitic groundmass. Sample from 11,600 feet, just below lip of cirque basin on north side of Conejos Peak.

in this area, directly overlying the rhyodacite of Fisher Gulch, is a distinctive red-brown-weathering andesite that is chemically similar to other Summitville lavas (table 9, No. 6) but that is distinguished by a fairly coarse devitrification texture (fig. 38B). Abundant plagioclase laths 0.5-2 mm long define a diabasic texture readily visible in hand specimen. This flow is as much as 150 m thick where it forms a conspicuous continuous cliff between Fisher Gulch and Beaver Lake Creek (Platoro map); there, it was interpreted as a sill by Larsen and

Cross (1956, pl. 1, p. 106), presumably because of its thickness and coarse texture. However, the same flow or a texturally similar single flow is traceable nearly continuously to the west, up the Lake Fork to the north side of Conejos Peak (fig. 63), where it directly overlies the intracaldera La Jara Canyon Member and has a flow-brecciated basal contact.

Overlying this distinctive flow is a sequence of at least five flows in the Forest King area. There, the common sparsely porphyritic andesite flows (fig. 38A) are interlayered with darker andesitic flows characterized by a partly glassy pilotaxitic groundmass texture (fig. 38C). These partly glassy flows tend to form relatively thick local accumulations rather than laterally extensive sheets, and they are locally characterized by intricate closely spaced joints that define irregularly curved columns 0.5-1 m in diameter and 4-10 m in length. The bulbous shape, glassy textures, and irregular columnar jointing suggest that these lavas may have been deposited on wet sediments or in shallow water.

Unusual agglutinated andesitic breccias having steep foliations are preserved at the top of the section of Summitville Andesite along the southern caldera wall. These breccias seem to fringe the Summitville Andesite around the north side of Conejos Peak but are well exposed only on the lip of the major cirque basin on the north side of the peak (fig. 39A). There, the breccia forms the top and margin of an otherwise normal andesite flow, about 60 m thick, which was deposited against the Conejos Forma-

tion on the caldera wall. The breccia varies laterally and vertically from a weakly indurated mass containing monolithologic blocks of scoriaceous and dense lava, to an indurated compact breccia, to an extremely indurated breccia that has undergone flowage to such an extent that it appears flow layered (fig. 39B). All gradations occur both vertically and laterally within a few meters in continuous excellent exposures. The flow layering is very steep, varying from 50° to nearly 90° , and appears most plausibly to reflect draping and compaction against the steep caldera wall. This relation would only seem possible if these lavas were originally erupted outside the caldera, enabling brecciation, agglutination, and secondary flowage to take place as the lava cascaded over the wall of the caldera to the floor.

Where not intensely hydrothermally altered, most lavas of the upper member of the Summitville Andesite are little different in petrography from the abundant sparsely porphyritic lavas of the lower member. The best exposed sections, on Cornwalls Nose and along the Wightman Fork (Platoro map), are both more than 800 m thick. In these sections the flows differ from lavas of the lower member to the east in being thicker, less tabular or laterally traceable, and in places pervasively internally brecciated. (See detailed description in Steven and Ratté, 1960, p. 11-12.) These features suggest near-source deposition.

Interlayered with the typical sparsely porphyritic andesites in the upper member are more coarsely



A



B

FIGURE 39.—Features of lower member of Summitville Andesite along south wall of Platoro caldera. A, View of Conejos Peak from near the head of the Lake Fork. Upper part of Conejos Peak consists of hornblende rhyodacite lavas of the Conejos Formation that define the south wall of Platoro caldera. Lava flows in foreground and flooring the cirque basin on Conejos Peak are intracaldera lavas of the

lower member. Arrow indicates location of agglutinate breccia in B. B, Intensely flowed and compacted agglutinate breccia of lower member where it was deposited against steep slope of south caldera wall. This depositional foliation dips 70° - 90° . On lip of cirque basin at 11,800 feet on north side of Conejos Peak.

porphyritic dark lavas that contain phenocrysts of plagioclase (An_{30-50}) as much as 1 cm in diameter. Total phenocryst content of such flows varies from about 5 to 25 percent. In some flows the phenocrysts are heterogeneously distributed, with more phenocrysts concentrated in the interiors. These coarsely porphyritic lavas, although not studied chemically, are probably more silicic than typical Summitville Andesite. The coarsely porphyritic flows become more abundant upward in the lava sequence of the upper member between Wightman Fork and Marble Mountain (Platoro map), and they appear to constitute a transitional petrologic type between Summitville Andesite and the overlying coarsely porphyritic biotite-bearing rhyodacite of Park Creek. In the Bonito Peak-Marble Mountain area, some of the highest flows included in the upper member because they are interlayered with the more characteristic sparsely porphyritic andesite contain sparse phenocrystic biotite in addition to the ubiquitous plagioclase and augite. These are clearly transitional to the Park Creek unit and probably are rhyodacitic in composition.

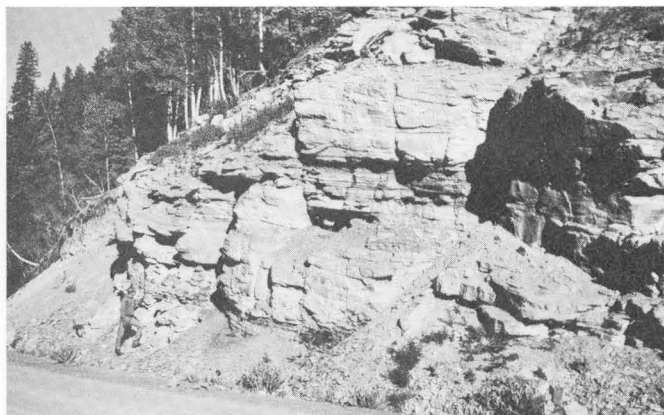
Upper member lavas that are exposed over a sizable area near the head of Park Creek (fig. 36) are different in lithology and thickness from those within the caldera. In the Park Creek area the upper member consists of only a few relatively thin flows that tend to be laterally persistent. In addition to the typical sparsely porphyritic andesite, a few flows of coarsely porphyritic platy-plagioclase andesite are similar to the common type described in the Conejos Formation (fig. 6) and also to the flows interlayered higher in the ash-flow sequence (Huerto Andesite). These outflow andesites of the upper member are well bracketed stratigraphically by the Ojito Creek and Ra Jadero Members of the Treasure Mountain Tuff (Platoro map), in contrast to the intracaldera lavas of the upper member, which lack well-defined stratigraphic relations with the upper members of the Treasure Mountain.

VOLCANICLASTIC ROCKS

About a fourth or a third of the Summitville Andesite consists of volcaniclastic sedimentary rocks, mainly gray sandstone and buff shale, that were eroded from the primary andesitic accumulations (fig. 40). These sedimentary rocks interfinger intricately with the lavas and breccias, and they could only easily be mapped separately on the Platoro map locally where they constitute most of the formation. Most of the sediments apparently were deposited in a deltaic environment, but some may represent shallow-water lake deposits. In places where clay-rich volcaniclastic rocks are interlayered with lavas of the Summitville Andesite, as, for example, high on the north side of Red Mountain (Platoro map), great landslides characteristically have developed.



A



B

FIGURE 40.—Intracaldera volcaniclastic sedimentary rocks of the Summitville Andesite. A, Volcaniclastic rocks at east caldera wall. Light-gray bedded tuffaceous sediments are deltaic or shallow-water lake deposits within caldera. Distant timbered slopes are andesitic lavas and mudflow breccias of Conejos Formation on caldera wall. Outcrops high on caldera wall (arrow) here consist of agglutinated bedded ash fall material that appears to have been welded as it was deposited, presumably because of proximity to its source. Alamosa River road, just west of Ranger Creek. B, Intracaldera sandstone and shale containing plant remains. Rito Gato, along Platoro Reservoir road.

The southeast caldera moat, north of Red Mountain, apparently contained the thickest accumulation of intracaldera sediments; about 300 m is preserved there. These sedimentary rocks interfinger to both the northeast and the southwest with intermediate-composition lavas. To the northwest the sedimentary rocks originally lapped against the Cornwall Mountain resurgent block of the intracaldera La Jara Canyon Member of the Treasure Mountain Tuff; this contact was subsequently modified by faulting. Toward the resurgent block, the predominantly sandstone deposits coarsen and grade into monolithologic fanglomerate breccia containing blocks of the La Jara Canyon

Member that are as much as 1 m in diameter and that represent the gray partly welded top of the ash-flow sheet. This relation demonstrates that the resurgent block was already a structural and topographic high when the lower member of the Summitville Andesite filled the caldera moat.

Poorly preserved, fragmented carbonized plant remains have been found in the intracaldera sedimentary rocks in several places: most abundantly along roadcuts and streams near the mouth of Rito Gato (fig. 40B) and in a few small slumped outcrops along Beaver Lake Creek at an elevation of about 10,050 feet (Platoro map). Preliminary study by Estella Leopold of the U.S. Geological Survey (written commun., 1972) indicated that rocks from the Beaver Lake Creek locality (U.S.G.S. paleobot. loc. D4772, samples A-E; NE $\frac{1}{4}$ sec. 1, T. 35 N., R. 4 E., elev. 10,000 ft) contain an excellently preserved pollen assemblage. The main forms recognized are:

- Pinus*
- Picea*, large form
- Selaginella* cf. *S. densa*
- Typha* cf. *T. angustifolia*
- Ephedra* cf. *E. nevadensis*, cf. *E. torreyana*, and an *Ephedra* species typical of White River Group
- Chenopodiaceae undet. and *Sarcobatus*
- Acer* cf. *A. negundo*
- cf. *Juniperus*
- cf. *Salix*
- Ulmaceae, p4 and p5
- Abies* cf. *A. venusta*
- Cruciferae?
- cf. *Parthenocissus*
- Carya*?
- Acrostichium* type
- Dodonaea*?
- Juglans* or *Pterocarya*
- Juglans*
- Compositae? (contaminant?)

Leopold reported that "this flora is intermediate in aspect between flora of the Florissant Lake Beds (lower Oligocene) and flora of the Creede Formation (uppermost Oligocene). It is more diverse than the Creede flora and yet resembles the flora at Creede more than it does that of the Florissant Lake Beds. It is certainly Oligocene and probably late Oligocene in age."

Exceptionally tuffaceous intracaldera sandstones and conglomerates that have been extremely silicified to white, buff, and light-purple dense slabby rocks occur along the divide just within the east wall of the Summitville caldera, where they have been the cause of the misleading name of "Marble Mountain" on topographic maps. These rocks, which apparently originated as tuffaceous deltaic or lake deposits, differ conspicuously from sedimentary rocks of the lower member to the east, outside the caldera, that are of andesitic provenance. This contrast in sediment types, in conjunction with

significant local differences in lava types, marks the topographic wall of the Summitville caldera. Marble Mountain is the only place where this topographic boundary is preserved within the Platoro caldera complex. Elsewhere, the margin of the Summitville caldera is marked by the Cornwall fault, which represents the structural boundary of the caldera rather than its topographic wall, or is covered by postcaldera lavas.

SOURCE VENTS

Most of the source vents for the lavas of the Summitville Andesite are poorly understood. Two main lava accumulations of the lower member, in the eastern Platoro caldera moat along the lower Alamosa River and in the southwestern moat northwest of Conejos Peak (fig. 36), are separated by the thick accumulation of volcanoclastic sedimentary rocks northeast of Red Mountain. The eastern accumulation clearly interfingers with sediments to the east toward the caldera wall, and the thickness of individual flows appears to increase to the west, right up to truncation by the younger Summitville caldera. These lavas probably represent the east flank of a large intracaldera andesitic stratovolcano, whose core is farther to the west, within the Summitville caldera area. Like the eastern accumulation, the southwestern accumulation of lavas of the lower member has no exposed source within the Platoro caldera. The source could have been to the north, within the area that later collapsed to form the Summitville caldera, or it could have been outside the caldera, as is perhaps suggested by the relations on the north side of Conejos Peak (fig. 39). Possibly, the Canyon Diablo stock (fig. 36) marks the dissected core of a volcano from which these lavas were erupted.

The eruptive source of the lavas of the upper member is equally obscure. Thickness, local lateral irregularity, and chaotic brecciation of upper member lavas in the Cornwalls Nose-Wightman Fork area suggest that these lavas are not far from their source and that they perhaps constitute part of a cone complex. Measurements of flow attitudes are too few and inconsistent to make this conclusion firm, however, and the extreme alteration to the northwest along the Alamosa River further impedes interpretation. Tentatively, the 29.1-m.y. Alamosa River stock is interpreted as the central intrusive of an eroded volcano source for the main mass of the intracaldera upper member lavas. This interpretation is based mainly on appropriateness of compositions (andesitic \equiv monzonitic), radiometric age (older than Masonic Park Tuff), and location (intrusive into the thick chaotic near-source portion of the upper member lavas).

AGE AND MAGNETIC POLARITY

The lower member of the Summitville Andesite is younger than 29.8 m.y., the well-established age of the underlying La Jara Canyon Member of the Treasure

Mountain Tuff. Much of the thick section of the upper member of the Summitville Andesite is intruded by and therefore older than the 29.1.-m.y. Alamosa River stock (Lipman and others, 1970). A few topographically and stratigraphically high patches of the upper member might be slightly younger than 29.1 m.y. but cannot be younger than 28.2 m.y., the date on the overlying Masonic Park Tuff.

Both lower and upper members of the Sunmitville Andesite seem to be characterized by normal magnetic polarities, as indicated by preliminary determinations on 12 separate flows (M. C. Beck, Jr., and James Diehl, written commun., 1971).

ANDESITE OF SUMMIT PEAK

The andesite of Summit Peak is named for a small group of scattered erosional remnants of intermediate-composition lavas and breccias that overlie the Masonic Park Tuff along the continental divide west of the Platoro caldera complex. Because these lavas cap the volcanic sequence wherever they are exposed, their exact age is uncertain, as is their correlation with intermediate-composition lavas interlayered with the ash-flow sequence elsewhere. The andesite of Summit Peak is similar in lithology and is approximately equivalent in age to the andesite-rhyodacite unit of the volcanics of Green Ridge on the opposite side of the caldera, and it appears to represent approximately similar postcollapse caldera-margin igneous activity.

The Summit Peak rocks may also be equivalent to flows of Sheep Mountain Andesite that interfinger with and overlie the Masonic Park Tuff to the west near Wolf Creek Pass. However, because the andesite of Summit Peak is restricted to the west margins of the Platoro caldera complex and has a close spatial association with the upper member of the Summitville Andesite, it is most validly considered as a continuation of the Summitville Andesite activity. The Summit Peak flows and the Sheep Mountain Andesite are difficult to distinguish lithologically, although the andesite of Summit Peak may be slightly more silicic on the average and may include more rhyodacite. North of Summit Peak, where the Masonic Park Tuff wedges out, the formation assignment of several small isolated hills of andesitic rocks is tenuous (Platoro map).

By far the thickest accumulation of this unit is at Summit Peak, where at least 10 flows form an aggregate thickness of about 200 m. Most of these flows are andesite that contains 10-20 percent small phenocrysts of plagioclase and augite, but some are probably rhyodacite. The only chemical analysis of the andesite of Summit Peak (table 9, No. 11) is clearly andesitic. One flow of porphyritic platy-plagioclase andesite is similar to the distinctive rock type that is so abundant in the Conejos Formation (fig. 6); this platy-plagioclase flow is

one of the rare recurrences of that type within the post-collapse lava sequence of the Platoro caldera complex, although it is the dominant lithology of the Huerto Andesite within the ash-flow sequence farther to the northeast.

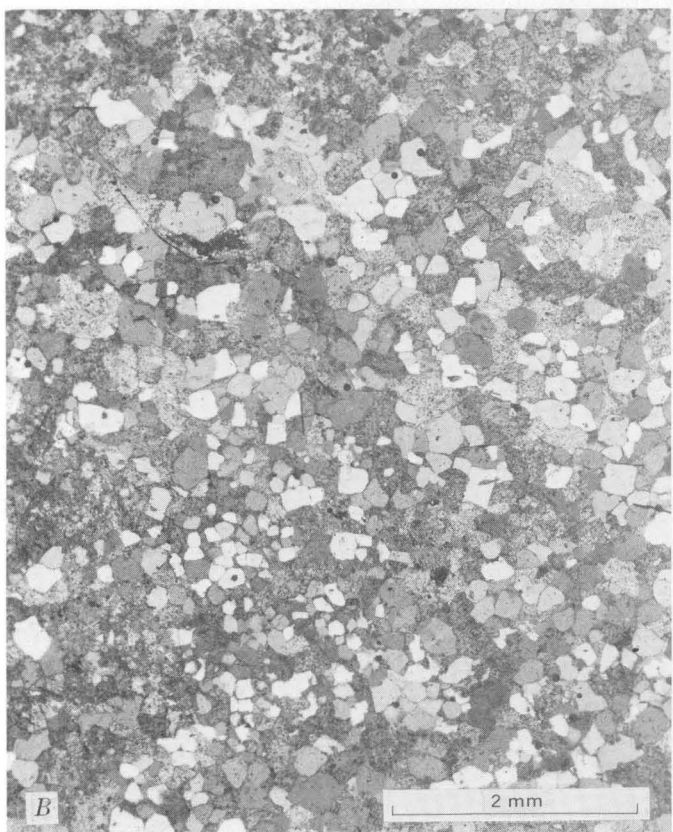
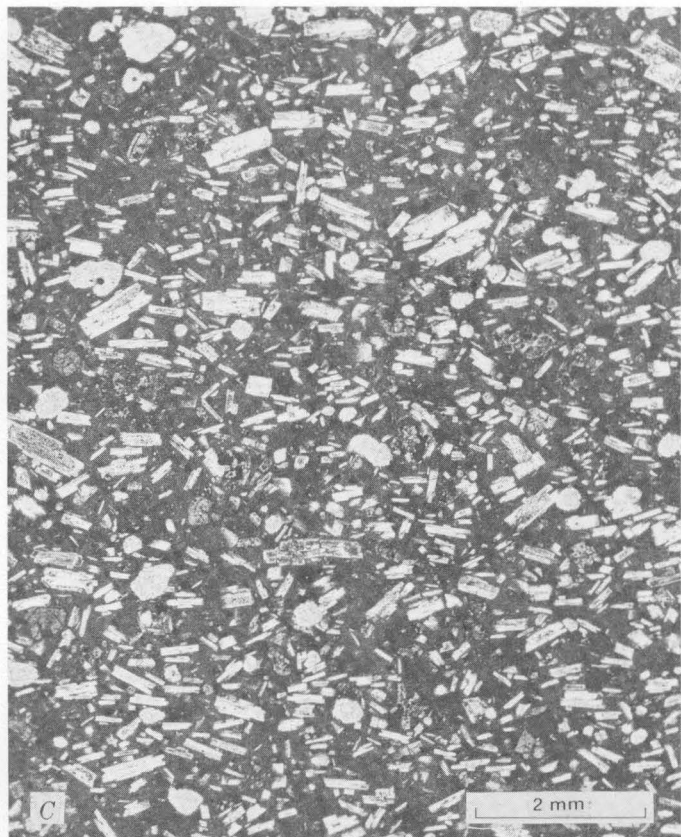
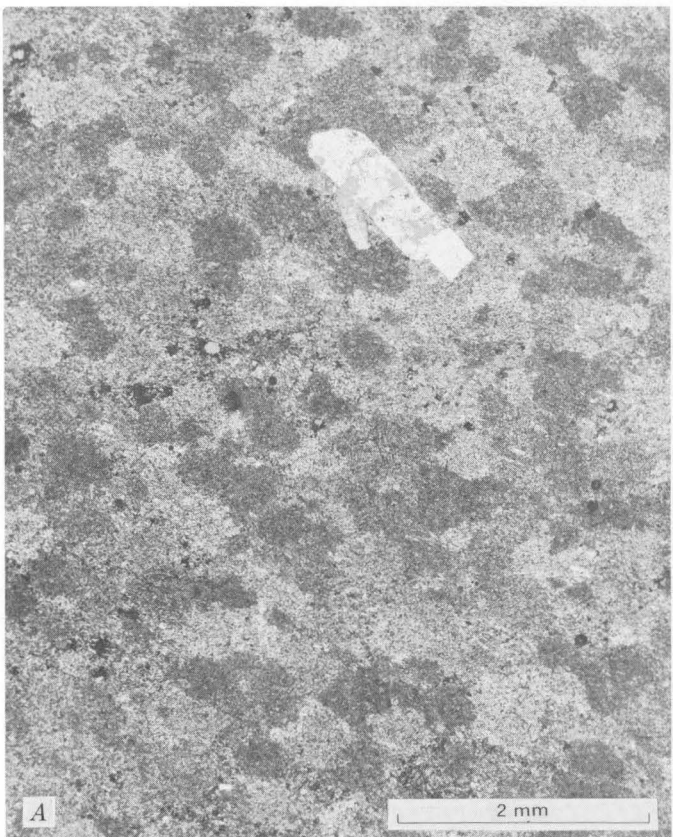
VOLCANICS OF GREEN RIDGE

The volcanics of Green Ridge are a heterogeneous accumulation of lava flows and breccias, ranging in composition from andesite to rhyolite. These rocks represent the erosional remnants of a stratovolcano, as much as 25 km in basal diameter, that developed near the east rim of the Platoro caldera complex (fig. 36). This postulated former stratovolcano is called the Cat Creek volcano, because it appears to be centered at the Cat Creek stock, which is interpreted as the intrusive core of the volcano. The volcanics of Green Ridge appear to have originally dipped outward 5°-15° from this central area; at present, dips are steeper on the east and more nearly horizontal on the west, as a result of 5°-10° regional eastward tilting of the southeastern San Juan Mountains toward the San Luis Valley. Three informal subdivisions recognized within the volcanics of Green Ridge are, in ascending sequence: the rhyolite unit, the andesite-rhyodacite unit, and the porphyritic rhyodacite unit. These three units are separately mapped on the Platoro map but not on the maps accompanying this report.

RHYOLITE UNIT

The rhyolite unit of the volcanics of Green Ridge consists of buff to white phenocryst-poor rhyolitic lava, flow breccia, and minor pumiceous tuff. It seems to represent the initial and areally most restricted activity of the Cat Creek volcano. It is preserved only over a few square kilometers near the head of Cat Creek, where it forms parts of the walls and roof of the Cat Creek stock at the core of the volcano (Platoro map).

Within about 100 m of the Cat Creek stock, the rhyolite has been recrystallized to dense blocky hornfels (fig. 41A, B) that crops out as erosion-resistant cliffs and jagged ribs; elsewhere, the rhyolite breaks down readily to small flakes and scree and is therefore poorly exposed on subdued slopes. Primary structural features of the rhyolite are obscure in the well-exposed hornfels because of recrystallization, but elsewhere the rhyolite is characterized by fine flow layers a few millimeters to a few centimeters thick. The flow layering is broadly subhorizontal but is highly irregular locally and has not been studied in detail. Many outcrops are of monolithologic breccia, consisting of blocks a few centimeters to at least 1 m in diameter that probably resulted from flow brecciation of the lava. Rarely, near the base of the rhyolite where the rhyolite rests on the Conejos Formation, thin beds of lapilli tuff of similar rhyolitic composition seem to have resulted from explosive ash and pumice eruptions.



The basal contact of the rhyolite is irregular, showing about 200 m of exposed relief; this indicates either that the rhyolite covered very rugged erosional topography or, more likely, that the rhyolite is intrusive in its lower parts and constitutes the remnants of an intrusive-extrusive vent-dome complex. The entire area of rhyolite seems plausibly to have been a single lava dome, although the fragmentary exposures, hornfelsic recrystallization and brief nature of this study make this conclusion only tentative.

The rhyolite contains only about 1 percent phenocrysts (fig. 41A). These are typically small, no more than 1 mm in diameter, and are plagioclase (An_{20-30}) accompanied by sparse flakes of biotite. The rhyolite unit has not been analyzed chemically, but petrographic similarity to analyzed phenocryst-poor rhyolitic lavas in the San Juan field, such as the rhyolite of Summer Coon volcano (Lipman, 1968, table 1, Nos. 4-6), suggests that the rhyolite unit of the volcanics of Green Ridge contains 70-72 percent SiO_2 .

The rhyolite is younger than the Conejos Formation and older than the Cat Creek stock. Unlike upper units of the volcanics of Green Ridge, the rhyolite cannot be related directly in age to the sequence of ash-flow sheets, because it is nowhere in contact with them. Clasts of petrographically similar rhyolite in the Los Pinos Formation, where the Los Pinos overlies the Masonic Park Tuff and is covered by the andesite-rhyodacite unit in the Green Ridge area, suggest that the rhyolite formed a topographic high that was being eroded at this time. In addition, the distribution of the rhyolite unit, restricted to the core of the volcano, indicates that emplacement of the rhyolite unit was the initial activity of this volcano and probably occurred after deposition of the 28.2-m.y. Masonic Park Tuff.

FIGURE 41 (left).—Photomicrographs of characteristic rock types of volcanics of Green Ridge. A, Rhyolite unit, about 300 m west of contact with monzonite stock, South Cat Creek. Single small phenocryst of plagioclase (An_{25}) is surrounded by cryptocrystalline groundmass that displays a mottled texture probably due to weak contact metamorphism. B, Rhyolite unit, about 1 m from contact with monzonite stock, South Cat Creek. Phenocrysts are not recognizable; rock has been recrystallized to a fine microcrystalline mosaic of plagioclase, sanidine, and quartz. C, Andesite-rhyodacite unit, south slope of Jacobs Hill at about 9,350 feet. Finely devitrified dark groundmass having a pilotaxitic texture surrounds abundant microphenocrysts of plagioclase (An_{40-45}), augite, Fe-Ti oxides, and serpentine pseudomorphs after olivine that are surrounded by reaction rims of finely granular augite. Analyzed sample 12, table 9. D, Porphyritic rhyodacite unit. Finely devitrified interior of thick flow contains about 30 percent phenocrysts of plagioclase (P), biotite (B), augite (not visible), olivine (not visible), and Fe-Ti oxides (ft). Northeast side of Green Ridge at about 9,200 feet. Radiometrically dated sample (Lipman and others, 1970, table 4, No. 5).

ANDESITE-RHYODACITE UNIT

The andesite-rhyodacite unit of the volcanics of Green Ridge consists of dark-gray to red-brown lavas and breccias of finely porphyritic andesite and rhyodacite. This unit constitutes much of the exposed volcanics of Green Ridge near Chiquita Peak and in the Green Ridge area, as well as all the probably correlative rocks in the Silver Mountain-Bennett Peak area to the west (fig. 36). Although correlation of the rocks of this western area with the Cat Creek volcano is uncertain and some of these lavas may have been derived from a local center near Silver Mountain, the rocks are included in the andesite-rhyodacite unit on the basis of generally similar lithology and age.

The andesite-rhyodacite unit overlies the Masonic Park Tuff in the Chiquita Peak-Green Ridge area, whereas the approximately equivalent rocks to the west, in the Silver Mountain-Bennett Peak area, are above the Fish Canyon Tuff within the Platoro caldera. In both areas, volcaniclastic sedimentary rocks of the Los Pinos Formation locally lie between ash-flow tuffs and overlying lavas (fig. 42). North of Green Ridge, the conglomerate of the Los Pinos Formation that occurs between the Fish Canyon and Carpenter Ridge Tuffs (Durango map) contains clasts that apparently were derived from the andesite-rhyodacite unit, as well as from the overlying porphyritic rhyodacite unit. In the Chiquita Peak and Green Ridge areas, the andesite-rhyodacite unit is capped by the porphyritic rhyodacite unit and in places also by basalt flows of the Hinsdale Formation.

Most of the andesite-rhyodacite unit was erupted before the porphyritic rhyodacite, but these two lithologies locally interfinger. At Jacobs Hill just southwest of Chiquita Peak (fig. 36) a thin flow of porphyritic rhyodacite (not shown on the Platoro map) occurs beneath the andesite-rhyodacite unit. A similar interfingering may occur near the crest of Chiquita Peak, east of the detailed Platoro map area.

Included in the andesite-rhyodacite unit are many somewhat petrographically varying lava flows and breccias. Individual lava flows are typically 10-20 m thick, although a single thick flow on the southeast side of Silver Mountain is at least 125 m thick. Interbedded volcaniclastic sedimentary rocks seem to be minor. Some of the flows are nonporphyritic, but most contain 5-15 percent small phenocrysts (mostly about 1 mm in diameter), mainly of plagioclase (An_{30-50}) and augite. An exceptional flow on the west slope of Bennett Peak contains about 25 percent phenocrysts of plagioclase (An_{40-55}), augite, hypersthene, and Fe-Ti oxides. Some lavas that appear megascopically nonporphyritic actually contain abundant microphenocrysts of plagioclase and pyroxene no more than 0.5 mm in diameter (fig. 41C).

Three chemical analyses of this unit vary from 58.8 to

almost 66 percent SiO_2 , calculated volatile free; however, the highest SiO_2 value is an old analysis (Larsen and Cross, 1956, table 21, No. 16) that shows more than 3 percent H_2O (table 9, No. 14), and it may be anomalous. Petrographic comparisons with other analyzed intermediate-composition lava flows from the southeastern San Juan area suggest that most samples of this unit would contain between about 57 and 64 percent SiO_2 .

At Green Ridge the age of the andesite-rhyodacite unit is bracketed by the underlying 28.2-m.y. Masonic Park Tuff and by the overlying porphyritic rhyodacite unit, dated at about 27.4 m.y. (Lipman and others, 1970). At the time of eruption of the 27.8-m.y. Fish Canyon Tuff, the Cat Creek volcano appears to have been sufficiently large to interfere with spreading of this ash-flow sheet to the south, as already discussed, yet intermediate-composition lavas of the andesite-rhyodacite unit continued to erupt after emplacement of the Fish Canyon, as indicated by the relations at Silver Mountain.

PORPHYRITIC RHYODACITE UNIT

The porphyritic rhyodacite unit of the volcanics of Green Ridge consists of a few thick light-gray lava flows of coarsely porphyritic rhyodacite and minor quartz latite. The porphyritic rhyodacite is exposed mainly along the crest and on the northeast slopes of Green Ridge; smaller patches are preserved on the northwest ridge of Chiquita Peak, on Jacobs Hill, and on the high double knob about 5 km farther west (fig. 36). In various places, the porphyritic rhyodacite overlies volcaniclastic sedimentary rocks of the Los Pinos Formation derived from early activity of the Cat Creek volcano, overlies and interfingers with the andesite-rhyodacite unit of the volcanics of Green Ridge, and is overlain by basalt flows of the Hinsdale Formation.

The porphyritic rhyodacite is characterized by 25-40 percent large phenocrysts, including plagioclase (An_{30-45}) grains as long as 1 cm, biotite, and hornblende or augite (fig. 41D). The augite-bearing lavas contain a second type of mafic phenocryst, identified as olivine in one nearly glassy sample, but these phenocrysts are generally altered completely to fine-grained serpentine-type minerals. Three analyses of this unit range from 60.8 to 66.9 percent SiO_2 (table 9, Nos. 15-17). The two samples that are relatively low in SiO_2 are actually clasts from the Los Pinos Formation (Larsen and Cross, 1956, p. 191); these contain augite and are petrographically similar to the flow that caps Green Ridge. In contrast, the single analyzed augite-free hornblende-bearing sample is distinctly more silicic and is a quartz latite. The change, at about 65 percent SiO_2 , from augite to hornblende as the second most abundant mafic after biotite in the coarsely porphyritic lavas also occurs in many of the lavas around Summitville.



FIGURE 42.—Volcaniclastic sedimentary rocks of the Los Pinos Formation overlain and fused by a thick nonporphyritic andesite or rhyodacite lava flow of the volcanics of Green Ridge (arrows indicate base of flow). South side of Silver Mountain, at 11,700 feet. Note person for scale.

RHYODACITE OF PARK CREEK

The rhyodacite of Park Creek is a new name for the predominantly porphyritic biotite-bearing assemblage of thick lavas, flow breccias, and minor pyroclastic rocks that were erupted as lava-dome complexes around the northwest margin of the Summitville caldera after its final collapse. This rhyodacite is similar in petrology and age to the porphyritic rhyodacite unit of the volcanics of Green Ridge, just described, and the two units are distinguished mainly by their separate areas of accumulation, which reflect separate sources. The rhyodacite of Park Creek essentially consists of the rocks described by Steven and Ratté (1960, p. 14-18) as the rhyodacite lavas of the lower member of the Fisher Quartz Latite, but use of the name Fisher Quartz Latite was subsequently restricted to lavas and breccias that are localized around the Creede caldera and that postdate the ash-flow se-

quence there, leaving the Summitville assemblage without a formal designation (Steven and Ratté, 1965, p. 43-44).

The lavas of the rhyodacite of Park Creek are concentrated along the northern and western topographic walls of the Summitville caldera, and they are especially thick and well exposed in upper Park Creek (fig. 36). These lavas rest partly on the upper member of the Summitville Andesite within the caldera and partly on older rocks of the caldera wall that range from the Conejos Formation to the younger ash-flow sheets. North and northeast of the caldera rim the rhyodacite of Park Creek interfingers with and overlies volcaniclastic sedimentary rocks of the Los Pinos Formation that formed by nearly contemporaneous erosion and reworking of the rhyodacitic lavas. Locally, the rhyodacite of Park Creek is overlain by distinctly younger rocks, such as the quartz latite of South Mountain, the rhyolite of Cropsy Mountain, and the basaltic lavas of the Hinsdale Formation.

Individual flows of the rhyodacite of Park Creek are as much as 150 m thick, especially where well exposed along the continental divide west of Summitville. Each flow typically contains a basal flow breccia a few meters thick that is overlain by a thick dark-gray vitrophyre zone as much as 10 m thick (fig. 65) and then by generally structureless lighter gray devitrified rock in the interior and upper parts of the flow. Flow layering is well developed only near the basal vitrophyre and near the top of the flow, where it tends to be steeply inclined. (See Christiansen and Lipman, 1966, fig. 3.) The geometry of many individual flows is complex, owing to emplacement on irregular topography adjacent to the caldera wall. In general, individual flows were not separated in the field, because exposures and time were limited.

Three vent structures were recognized for the rhyodacite of Park Creek; additional vents probably are present but are covered by younger volcanic rocks or are simply obscure owing to poor exposure. The largest vent feature is a mass of intrusive rhyodacite porphyry, about 3 km long and almost 1 km wide, that is well exposed along the divide between the East and West Forks of Park Creek about 5 km northwest of the caldera rim (fig. 36). This body, which has the form of a thick stubby sill dipping about 40°-50° to the northeast, is localized by the Summitville fault, a major fault on the northeast side of the Elwood Creek fault zone (fig. 61). The intrusive porphyry is continuous to the southwest into a thick extrusive flow, characterized by gently dipping flow layering (Platoro map), which differs only slightly in appearance from intrusive parts of the vent complex; compared with the flow, the intrusive is slightly lighter in color owing to coarser groundmass crystallization and is slightly more massive, less clearly flow layered, and more regularly jointed. This intrusive and the fault that

localized it have tilted the welded tuffs of its roof to near vertical dips along Park Creek (Platoro map, cross section D-D').

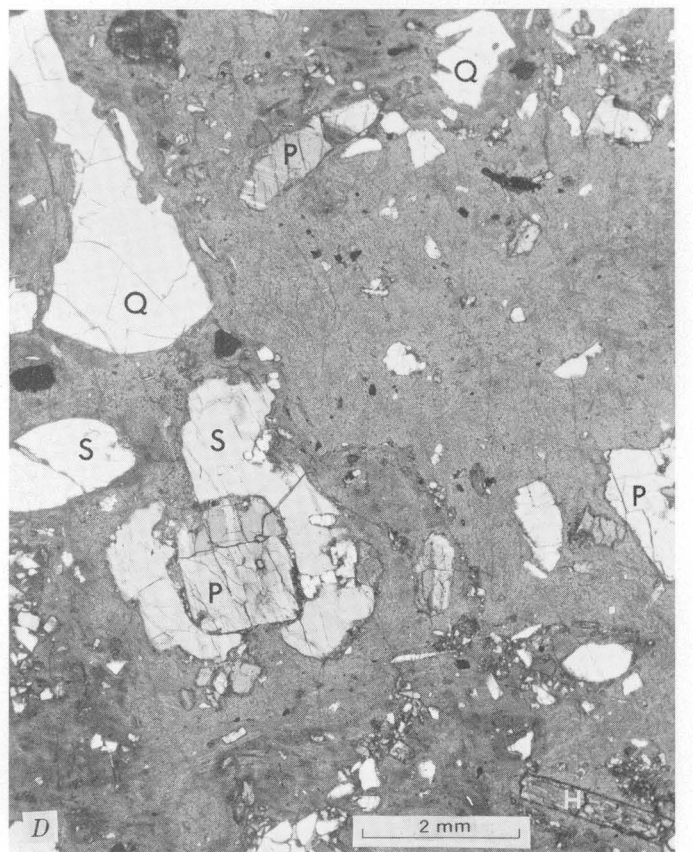
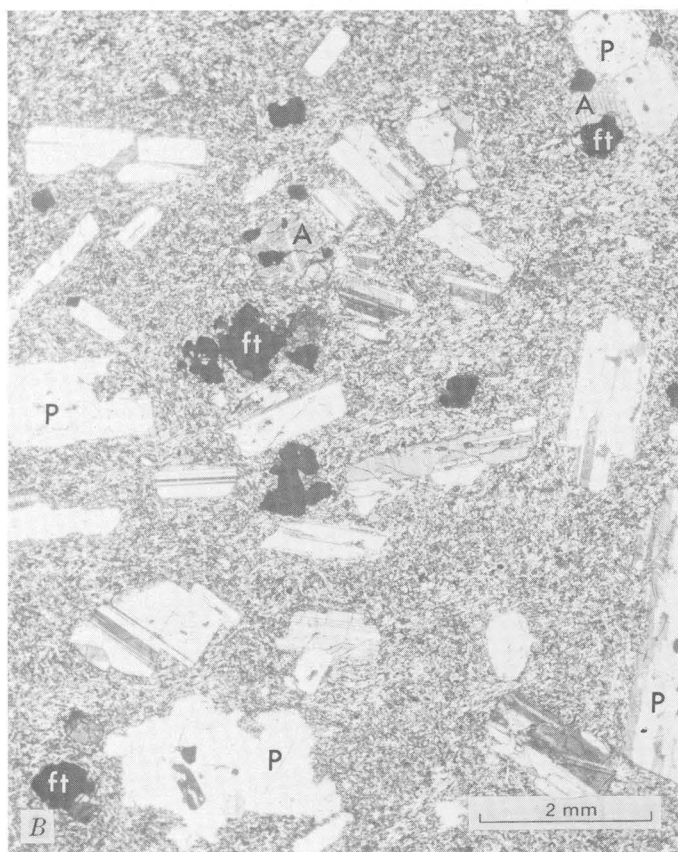
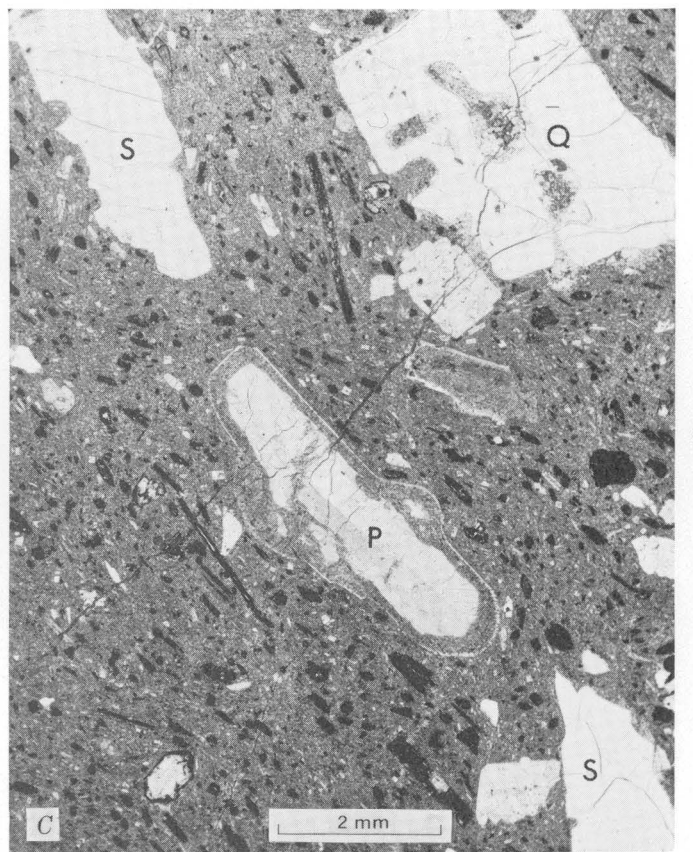
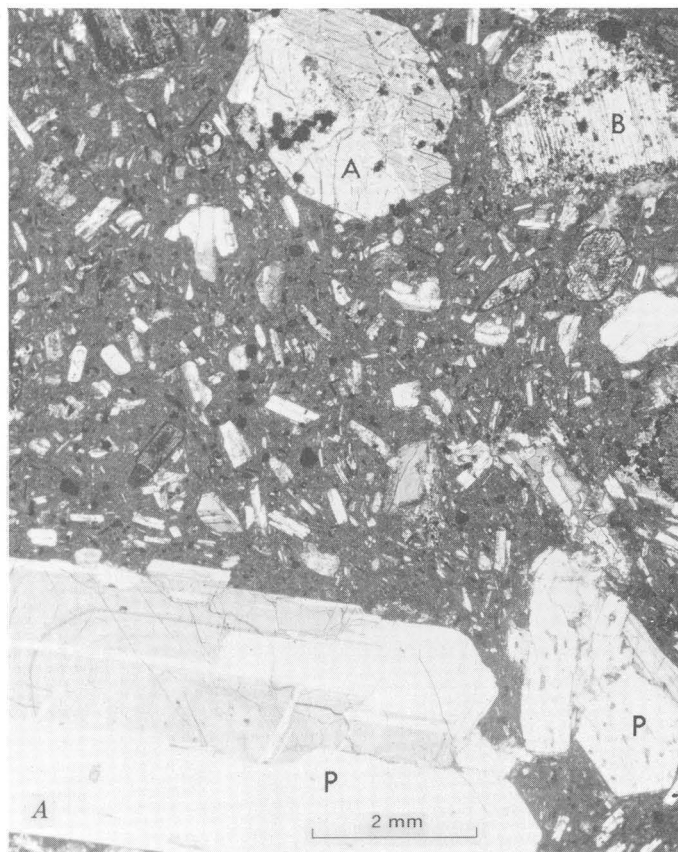
A similar but smaller vent was the source of the isolated patch of lava between Summitville and Jasper (fig. 36). The western end of this body is clearly intrusive, cutting steeply through lavas of the upper member of the Summitville Andesite, but it merges with gently dipping flow-layered lavas on the crest of the ridge (Platoro map). Because this body contains sparse large sanidine phenocrysts in association with both hornblende and augite, especially in its intrusive part, and is petrographically transitional toward typical quartz latite of South Mountain, its correlation with the rhyodacite of Park Creek is uncertain.

A third rather different vent structure, which forms a steep hill near the northwest caldera rim (elev. 11,874 feet; Platoro map), apparently is the eroded remnant of a pyroclastic cone. Here, layers of irregularly outward dipping bedded agglutinated tuff alternate with variably indurated monolithologic breccia that consists of blocks of rhyodacite.

The rhyodacite of Park Creek typically contains about 20-30 percent phenocrysts (fig. 43A). Blocky plagioclase (An_{30-50}) crystals as much as 10 mm in diameter constitute 75-90 percent of total phenocrysts and are accompanied by lesser amounts of biotite, augite, and Fe-Ti oxides. Hornblende is rarely present instead of augite. Quartz and sanidine are absent or very sparse. The petrography of this unit is described in more detail by Steven and Ratté (1960, p. 17).

The rhyodacite of Park Creek can generally be distinguished from Summitville Andesite by the presence of biotite and larger more abundant plagioclase phenocrysts; it differs from the quartz latite of South Mountain in paucity of quartz and sanidine and in the general presence of augite rather than hornblende as the second mafic. However, in a few atypical lava flows included in this unit for convenience, the phenocrysts are few and small, and biotite is sparse (fig. 43B); such rocks occur high in the unit, above the Snowshoe Mountain Tuff at the south end of Handkerchief Mesa (fig. 35), and also low in the unit, along the upthrown side of the fault zone west of Elwood Pass (Platoro map). These rocks seem to be more mafic than the typical coarsely porphyritic rhyodacite and are petrographically transitional toward Summitville Andesite. Within the caldera, especially, there may be no significant depositional hiatus between Summitville and Park Creek volcanic activity: as previously noted, porphyritic sparsely biotitic local lavas of transitional composition and texture are also interlayered with the upper member of the Summitville Andesite near the northern rim of the caldera complex.

The rhyodacite of Park Creek has not been dated



radiometrically, but its age can be approximated by reference to other units. The lowest flows outside the caldera complex are above the Fish Canyon Tuff (27.8 m.y., table 3) and below the Carpenter Ridge Tuff (>26.7 m.y., table 3). Lower lavas of the Park Creek unit that are petrographically transitional toward Summitville Andesite may represent yet earlier activity than any of the flows that can be stratigraphically related to the ash-flow sequence outside the caldera. Upper flows of this unit overlie the Snowshoe Mountain Tuff (>26.4 m.y.) at the south end of Handkerchief Mesa (fig. 35), and other late flows are cut by a sanidine porphyry dike in Schinzel Meadows that has been dated at 25.8 m.y. (Lipman and others, 1970, table 4, No. 6). The rhyodacite of Park Creek is also overlain by the quartz latite of South Mountain, dated at 22.8 m.y., as is discussed later.

Thus, most of the rhyodacite of Park Creek seems to have been erupted between about 28 and 26 m.y. ago, but significantly earlier or later activity is possible.

QUARTZ LATITE OF SOUTH MOUNTAIN

The name "quartz latite of South Mountain" is given to a coarsely porphyritic lava dome and related rocks at least 300 m thick, near the west rim of the Summitville caldera (fig. 36). Although this body covers an area of only about 5 km², it is of special interest as the host rock of the Summitville ore body. The quartz latite of South Mountain was discussed by Steven and Ratté (1960) but was referred to as the quartz latitic lavas of the lower member of the Fisher Quartz Latite, a usage subsequently abandoned by these authors. The quartz latite of South Mountain rests partly on dark lavas of the upper member of the Summitville Andesite and partly on the porphyritic rhyodacite of Park Creek. Because these

rocks—the quartz latite of South Mountain—were described in detail by Steven and Ratté (1960, p. 18-22, 33-34) only the general features of this unit and a few new interpretations are summarized here.

Where least altered, the quartz latite of South Mountain is a light-gray thoroughly devitrified massive lava in which crude flow layering is discernible locally; primary volcanic features of much of the main body at South Mountain have been obscured by intense acid-sulfate alteration. This quartz latite typically contains 20-30 percent phenocrysts, consisting of sanidine (Or_{75-77}), plagioclase (An_{20-40}), quartz, biotite, and hornblende (fig. 43C). Although broadly similar in appearance to the underlying rhyodacite of Park Creek, this unit is distinguishable by the presence of sanidine, quartz, and, generally, hornblende rather than augite. Rounded and resorbed phenocrysts locally indicate disequilibrium relations (fig. 43C). The quartz latite of South Mountain is especially coarsely porphyritic over an area about 1 km in diameter, just south of Summitville (fig. 36; Steven and Ratté, 1960, pl. 2), where the sanidine phenocrysts—commonly showing Carlsbad twinning—are as long as 5 cm. Some of these sanidines are rounded by resorption and are rimmed by sodic plagioclase, resulting in a rapakivi texture. This area was interpreted by Steven and Ratté (1960, p. 33-34) as the core of the lava dome, overlying the vent. Their interpretation has been confirmed by recent exploratory drilling that demonstrates that this coarse porphyry extends downward below any plausible projection, based on the exposed marginal contacts of the body, were it interpreted as a simple lava flow.

An outlying area of sanidine-quartz-hornblende quartz latite, along the east side of upper Park Creek (Platoro map; Steven and Ratté, 1960, p. 24), has been included in the quartz latite of South Mountain because of general petrologic similarity and because it is hydrothermally altered and intruded by unaltered porphyry that is interpreted as a vent of the rhyolite of Cropsy Mountain. It is not clear whether these Park Creek outcrops are a marginal remnant of the dome centered at South Mountain or whether they represent nearly contemporaneous accumulation from a separate source.

Also assigned to this unit are lavas and flow breccias at the south end of Cropsy Mountain (Steven and Ratté, 1960, p. 18-19) that contain a sanidine-plagioclase-biotite-augite phenocryst assemblage and that seem petrographically transitional toward the rhyodacite of Park Creek. These rocks apparently are local accumulations around a separate vent.

The quartz latite of South Mountain seems to contain about 68-70 percent SiO_2 (table 9, Nos. 19-21), but two of the three analyses contain abundant CO_2 , making precise interpretation difficult.

FIGURE 43. (left).—Photomicrographs of typical lavas of the late viscous domes around the margins of the Summitville caldera. A, Typical rhyodacite of Park Creek. Large phenocrysts of plagioclase (P) (An_{45-48}), augite (A), and biotite (B) with oxidized margins are set in a matrix of microphenocrysts of the same minerals and groundmass. Prominent nose at head of Park Creek, east of Summitville-Stunner road at about 11,400 feet. B, Rhyodacite of Park Creek, mafic type. Biotite phenocrysts are absent; about 25 percent small phenocrysts of plagioclase (P), augite (A), and Fe-Ti oxides (ft) are surrounded by fine-grained groundmass with pilotaxitic texture. South end of Handkerchief Mesa, overlying the Snowshoe Mountain Tuff. (See fig. 35.) C, Quartz latite of South Mountain. Large phenocrysts, some showing disequilibrium relations, are resorbed embayed quartz (Q), sanidine (S), rounded plagioclase (P) with dusty marginal inclusions, and abundant smaller dark oxidized biotite and hornblende. Northeast shoulder of Cropsy Mountain at about 12,200 feet. D, Rhyolite of Cropsy Mountain. Large rounded and embayed phenocrysts of quartz (Q), sanidine (S) around plagioclase (P), green hornblende (H), and brown biotite (not visible) in perlitic glassy groundmass containing abundant microlites that define swirlly flow foliation. Basal vitrophyre, from saddle east of North Mountain, at about 12,300 feet.

The age of the main lava dome at South Mountain is about 22.8 m.y., as indicated by K-Ar determinations on phenocrystic biotite (22.8 m.y.) and sanidine (22.9 m.y.) from a seemingly unaltered sample near the east margin of the dome (Mehnert and others, 1973). The petrographically transitional augite-bearing quartz latite at the south end of Cropsy Mountain may be appreciably older, however, because it may correlate with a dike of generally similar sanidine-quartz porphyry about 3 km to the west which contains carbonate pseudomorphs after augite and which has yielded a biotite K-Ar age of 25.8 m.y. (Lipman and others, 1970, table 4, No. 6).

RHYOLITE OF CROPSY MOUNTAIN

The youngest coarsely porphyritic lava flows in the Summitville area, named the rhyolite of Cropsy Mountain, are petrographically similar to but slightly more silicic than the quartz latite of South Mountain (table 8). These rocks were described as the upper member of the Fisher Quartz Latite by Steven and Ratté (1960, p. 22-25, 34-36) but later were excluded from the Fisher Quartz Latite (Steven and Ratté, 1965, p. 43-44; Lipman and others, 1970, p. 2341-2342). The rhyolite of Cropsy Mountain is everywhere unaltered, in striking contrast to the widespread alteration of the underlying rocks, including the Summitville Andesite, rhyodacite of Park Creek, and quartz latite of South Mountain.

The rhyolite of Cropsy Mountain is exposed as discontinuous erosional remnants which cap the ridge from South Mountain to Lookout Mountain and which cover larger areas around North Mountain (fig. 36). In most and perhaps all these places, the rhyolite of Cropsy Mountain is a single flow of uneven thickness. Variation in thickness is due to irregular preeruption topography and to erosion of the flow top. On Cropsy Mountain the exposed thickness of the unit is typically 50-75 m, but north of North Mountain a single flow is at least 300 m thick. Even though only one flow is present at each locality, several distinct flows are likely, as indicated by variations in petrology and by recognition of several areally separated vents.

These flows are characterized by a basal dark-gray to black vitrophyre, 5-10 m thick, overlain by light-gray or pink devitrified rhyolite. Where the base is best exposed, as on the west face of Lookout Mountain (fig. 44), the vitrophyre is underlain by a few meters of flow breccia in which dark-gray dense blocks and lighter colored vesiculated blocks are enclosed in a white tuffaceous matrix. Flow layering, defined by variations in devitrification, is typically distinct in lower and upper parts of the flow. In lower parts of the flow the layering generally dips gently, but locally it is intricately flow folded; inclined ramp structures characterize upper parts of the flow in most outcrops.

The rhyolite of Cropsy Mountain is fairly uniform in phenocryst petrology, except for the rocks related to the vent west of North Mountain described later. Typically, the rhyolite contains 20-30 percent phenocrysts of sanidine (Or_{65}), plagioclase (An_{15-30}), quartz, biotite, and hornblende. The sanidine phenocrysts are large and blocky and show conspicuous Carlsbad twinning; quartz

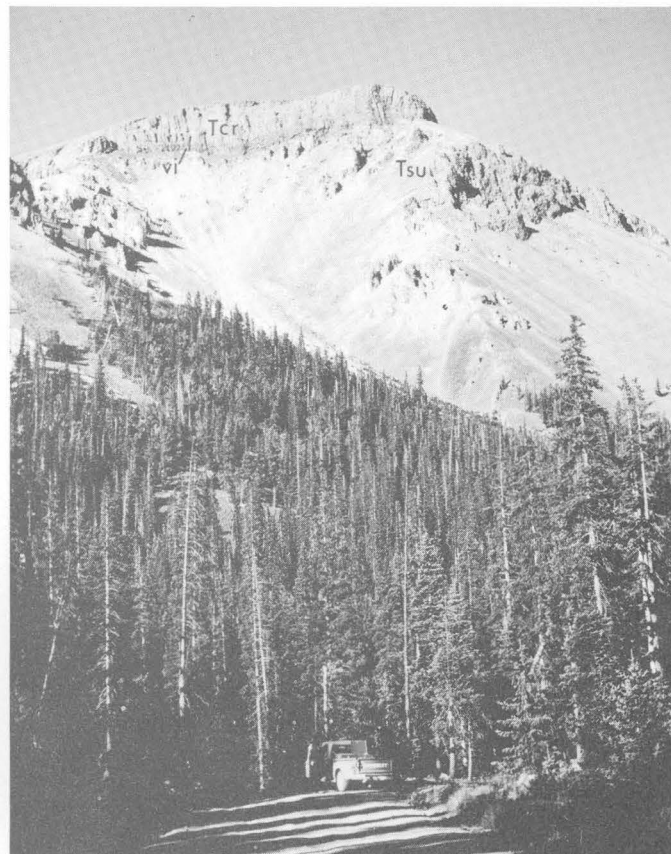


FIGURE 44.—Rhyolite of Cropsy Mountain (Tcr). Single thick flow, 20.2 m.y. old, has a distinct dark basal vitrophyre (vi) and rests unconformably on hydrothermally altered lavas of the upper member of the Summitville Andesite (Tsu). Lookout Mountain as seen from the Stunner-Summitville road, just west of Iron Creek.

occurs as rounded resorbed pellets. This assemblage is similar to that of the quartz latite of South Mountain, except that both feldspars are somewhat more sodic.

Three vent structures related to eruption of the rhyolite of Cropsy Mountain have been recognized: (1) on the west shoulder of South Mountain, (2) at Sheepshead near Prospect Mountain, and (3) west of North Mountain. Shallow intrusives of similar petrography probably fed other vents, the surficial parts of which have been eroded. Such probable intrusive equivalents of the rhyolite of Cropsy Mountain are described in a separate section, however, because of the difficulty in distinguishing many of them from intrusives related to the quartz latite of South Mountain.

The vent on the west shoulder of South Mountain is represented by an arcuate dike with steeply dipping flow foliation that either merges with or cuts extrusive rhyolite of Cropsy Mountain at the ridge crest; this feature is described in more detail by Steven and Ratté (1960, p. 35).

The vent at Sheepshead is largely intrusive at the present erosional level; it consists of a stubby funnel-shaped dike that bulges outward on its southeastern side where it apparently approached the surface. In petrographic appearance it is identical to the flow on Cropsy Mountain. The Sheepshead vent intrusion is fresh rock, in contrast to the surrounding intensely altered lava flows of the Summitville Andesite.

Perhaps the most interesting vent structure—and the only one examined in detail during this study—apparently formed at the crest of a pyroclastic cone and is exposed on the prominent shoulder west of North Mountain. Here, a steeply dipping elliptical intrusive mass, characterized by roughly concentric steeply dipping flow layering, is continuously traceable upward into a subhorizontal flow of unaltered lava more than 100 m thick that lies on hydrothermally altered rhyodacite of Park Creek (Platoro map). Especially interesting are conspicuous compositional heterogeneities in both the intrusion and the lava flow. The most striking variation seen in the field is in total phenocryst content, which varies from only about 2 percent to at least 25 percent (fig. 45), both within the flow and in the vent. In the vent intrusion, concentric shells that consist of light-gray or pink devitrified rock and that differ by 5-10 percent in total phenocryst content are separated by black vitrophyre zones 1-2 m thick. In the surface flow, the phenocryst content varies both vertically and laterally. Lowest phenocryst contents are near the base of the flow, especially at distances of more than a few hundred meters from the vent. The phenocryst content generally increases upward in the flow, although adjacent subhorizontal flow layers in the interior locally vary discernibly in total phenocryst content. In upper parts of the flow, where layering generally defines steeply inclined ramp structures and is intricately contorted in detail, phenocryst heterogeneities from layer to layer are especially conspicuous.

Rocks of this complex that contain the fewest phenocrysts, only about 2 percent (fig. 45C), are dark gray and have a conspicuously slabby jointing due to trachytic groundmass texture. The sparse scattered phenocrysts, consisting of quartz, plagioclase, sanidine, biotite, and hornblende, are small—mostly 0.5 mm or less—and irregular in outline owing to resorption. Among the phenocrysts are a few curious euhedral hexagonal inclusion-filled crystals as much as 0.8 mm in diameter that seem to be apatite. The feldspars are cloudy, owing to small glass inclusions, and some

plagioclase crystals have clear rims of more calcic composition. These rocks are rhyodacitic in composition, containing 64-65 percent SiO_2 (table 9, Nos. 24, 25).

The phenocryst-rich rocks (fig. 45A), which have 20-25 percent phenocrysts (table 9, Nos. 28, 29), are distinctly more silicic, containing as much as 72.4 percent SiO_2 —about typical for the rhyolite of Cropsy Mountain. Quartz and feldspar phenocrysts in these rocks also show some rounding, resorption, and dusty inclusions, but these features are relatively minor. The phenocrysts are as much as 1 cm in diameter, much larger than phenocrysts in the phenocryst-poor parts of the complex. These rocks are texturally within the normal range of the rhyolite of Cropsy Mountain.

Intermediate compositional and textural types (fig. 45B; table 9, Nos. 26, 27) are the most abundant. These types are typically flow layered, and phenocryst size changes conspicuously from layer to layer.

The heterogeneous textures and compositions within the vent and related flow at North Mountain clearly demonstrate mixing of magmas of significantly different compositions before eruption. A rough calculation indicates that the groundmass compositions of the more silicic rocks of the complex (table 9, Nos. 28, 29) are even more silicic than the bulk compositions, as is typical for porphyritic volcanic rocks in the San Juan field (Larsen and Cross, 1956, figs. 53-56) and elsewhere. The compositional differences between phenocryst-poor rhyodacite and phenocryst-rich rhyolite cannot be due to the different phenocryst contents. It is also not clear whether the observed compositional extremes truly represent the end-member compositions of the magma before mixing, or whether the observed end members are themselves partial mixes of even more extreme initial compositional contrasts. A mixed-lava complex of silicic rhyolite and basalt, described in the section on the Hinsdale Formation, formed at the south end of Handkerchief Mesa at about the same time as the mixed-lava complex at North Mountain.

The rhyolite of Cropsy Mountain has been well dated at the type area at 20.2 m.y., as indicated by concordant K-Ar determinations on sanidine, plagioclase, biotite, and hornblende phenocrysts from the same sample (Steven and others, 1967; Lipman and others, 1970), but the rocks assigned to this unit in the North Mountain area could possibly be somewhat different in age.

In both petrology and age the rhyolite of Cropsy Mountain is transitional toward the Miocene and Pliocene silicic alkali rhyolites of the Hinsdale Formation (table 11), but its position marginal to the Summitville caldera and its petrographic affinities with older coarsely porphyritic lavas indicate that it is part of the postcollapse lava sequence of the Platoro-Summitville center.

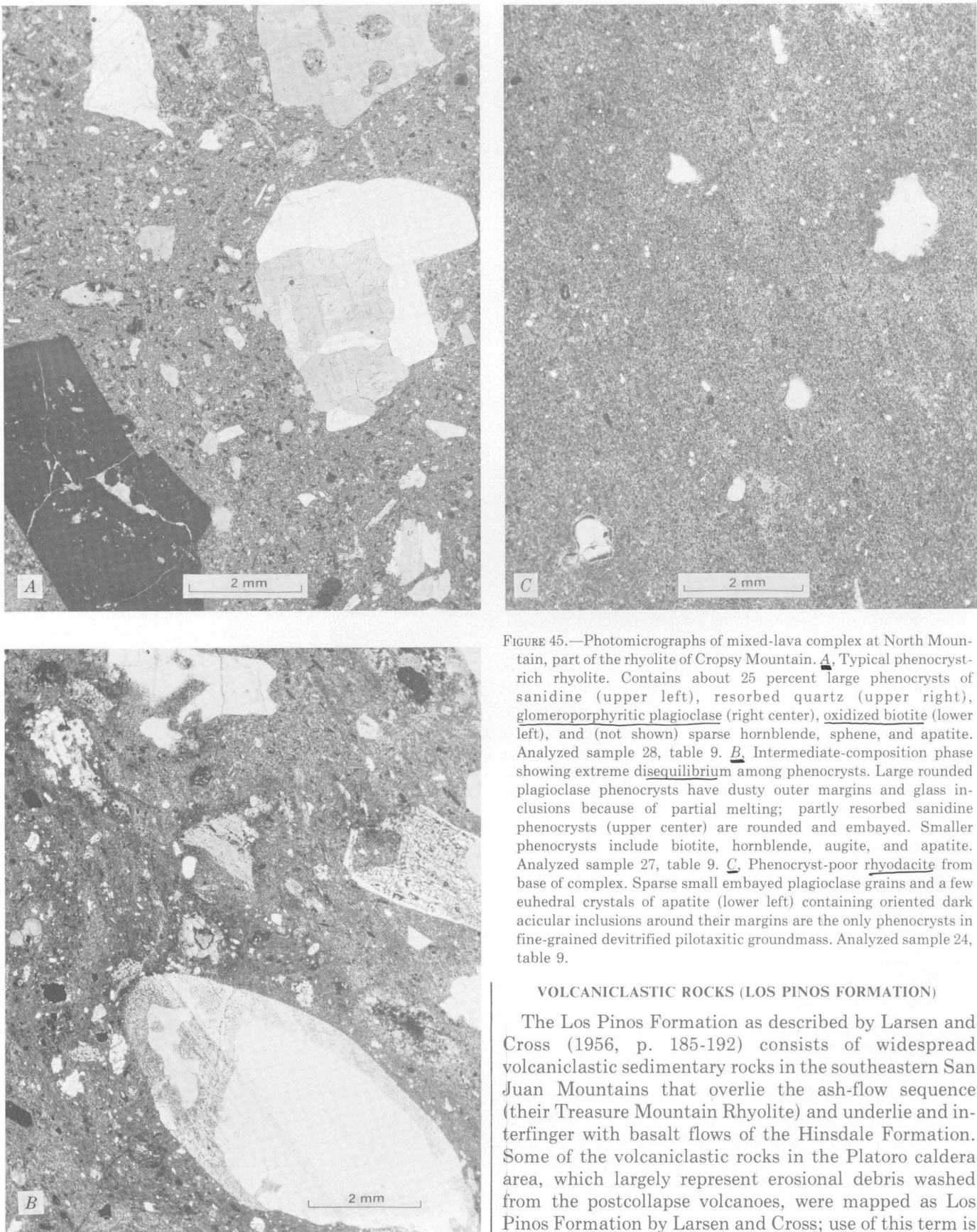


FIGURE 45.—Photomicrographs of mixed-lava complex at North Mountain, part of the rhyolite of Cropsy Mountain. *A*, Typical phenocryst-rich rhyolite. Contains about 25 percent large phenocrysts of sanidine (upper left), resorbed quartz (upper right), glomeroporphyritic plagioclase (right center), oxidized biotite (lower left), and (not shown) sparse hornblende, sphene, and apatite. Analyzed sample 28, table 9. *B*, Intermediate-composition phase showing extreme disequilibrium among phenocrysts. Large rounded plagioclase phenocrysts have dusty outer margins and glass inclusions because of partial melting; partly resorbed sanidine phenocrysts (upper center) are rounded and embayed. Smaller phenocrysts include biotite, hornblende, augite, and apatite. Analyzed sample 27, table 9. *C*, Phenocryst-poor rhyodacite from base of complex. Sparse small embayed plagioclase grains and a few euhedral crystals of apatite (lower left) containing oriented dark acicular inclusions around their margins are the only phenocrysts in fine-grained devitrified pilotaxitic groundmass. Analyzed sample 24, table 9.

VOLCANICLASTIC ROCKS (LOS PINOS FORMATION)

The Los Pinos Formation as described by Larsen and Cross (1956, p. 185-192) consists of widespread volcaniclastic sedimentary rocks in the southeastern San Juan Mountains that overlie the ash-flow sequence (their Treasure Mountain Rhyolite) and underlie and interfinger with basalt flows of the Hinsdale Formation. Some of the volcaniclastic rocks in the Platoro caldera area, which largely represent erosional debris washed from the postcollapse volcanoes, were mapped as Los Pinos Formation by Larsen and Cross; use of this term is

herein continued, even though the Los Pinos Formation in the type locality farther south seems to consist mainly of younger material derived from other centers. Discussion of the postcaldera lavas and related rocks in terms of two groups—the near-source accumulations that formed volcanic cones or lava domes and the surrounding aprons of volcanic sedimentary rocks—is thus parallel to previous discussion of the early intermediate-composition lavas and breccias of the Conejos Formation in terms of a vent facies and a volcaniclastic facies.

In the Platoro map area, aprons of volcaniclastic sedimentary rocks of approximately similar age are marginal both to the Cat Creek volcano (volcanics of Green Ridge) east of the caldera and to the accumulation of the rhyodacite of Park Creek in the Summitville area.

The sedimentary sequence derived from the Cat Creek volcano was mapped by Larsen and Cross (1956) as part of the Los Pinos Formation (as were most of the lavas here included in the volcanics of Green Ridge). In the Cat Creek-Green Ridge area the volcaniclastic sedimentary rocks generally rest on Masonic Park Tuff and are overlain by younger lavas of the Cat Creek volcano (fig. 46). North of Green Ridge and farther from the volcanic center, however, some of these volcaniclastic rocks are interlayered with the ash-flow sequence, between the Fish Canyon and Carpenter Ridge Tuffs (Durango map).

In contrast, in the Summitville area, marginal volcaniclastic sedimentary rocks derived from the rhyodacite of Park Creek were not previously mapped separately from the rhyodacite, although they are similar in age, lithology, and genesis to rocks of the Los Pinos Formation to the east. These rocks are extensive in the Park Creek and Beaver Creek drainages (Platoro map), where they are exposed below the rhyodacite of Park Creek near the caldera rim and where they interfinger with the ash-flow sequence away from the volcanic centers. As in the Green Ridge area, the volcaniclastic rocks here occur between the Fish Canyon and Carpenter Ridge Tuffs, and higher tongues of similar volcaniclastic rocks wedge below and above the Snowshoe Mountain Tuff at the south end of Handkerchief Mesa (fig. 35).

Farther south, the Los Pinos Formation occurs mainly as a widespread eastward-thickening alluvial wedge that overlies the ash-flow sequence and that is interlayered with Miocene and Pliocene basalt flows of the Hinsdale Formation. These rocks appear to have accumulated as

great coalescing alluvial fans along the east front of the San Juan Mountains; accumulation was a response to eastward tilting of the Oligocene volcanic sequence concurrent with structural development of the San Luis Valley graben system (Lipman and Mehnert, 1969). Although these Los Pinos rocks are therefore younger than the Oligocene volcaniclastic accumulations near the Platoro caldera complex, both areas of the Los Pinos Formation are generally similar in lithology and therefore are difficult to separate except where control is provided by radiometrically dated interlayered basalt flows. In the southern San Juan region contrasting lithologies of clasts in the Los Pinos Formation reflect derivation from local centers south of the Platoro caldera complex, such as the one along the continental divide at the head of Elk Creek (fig. 13) and others farther south (Butler, 1971, p. 295-297).

The Los Pinos Formation is weakly indurated and therefore rarely well exposed. Areas underlain by the Los Pinos Formation are typically characterized by subdued topography mantled by cobbles and boulders that were weathered out of conglomeratic units. Accordingly, conglomeratic rocks seem at first to be exceptionally abundant in the Los Pinos Formation, but the sparse good exposures show that most of the unit consists of poorly indurated volcaniclastic sandstones commonly containing abundant tuffaceous material. Two thin nonwelded white ash-flow sheets, each about 5 m thick, are exposed in an exceptionally fine cut along the lower Conejos River, just south of Los Mogotes (Durango map).

The Los Pinos Formation includes upper Oligocene, Miocene, and Pliocene rocks. The oldest part of the formation is probably the volcaniclastic sequence that is interlayered with the ash-flow sequence between the Fish Canyon (27.8 m.y.) and Carpenter Ridge (>26.7 m.y.) Tuffs around the north and east sides of the Platoro center. In northern New Mexico, a local rhyolitic ash-flow tuff interbedded with conglomerates of the Los Pinos Formation has been dated at 25.9 m.y. (Bingler, 1968, p. 36). Southeast of the Platoro caldera complex, sedimentary rocks of the Los Pinos Formation are interlayered with basalt flows of the Hinsdale Formation, one of which has been dated at 17.7 m.y., and the upper part of the Los Pinos Formation intertongues with Hinsdale basalt of the Los Mogotes volcano, which seems to be about 5 m.y. old (Lipman and others, 1970).



FIGURE 46.—Diagrammatic cross section through the Cat Creek volcano, showing general relations between volcanics of Green Ridge (black) and surrounding apron of volcaniclastic rocks of the Los Pinos Formation (stippled). As the volcano grew, lavas spread over an enlarging area, so in local sections the lavas generally overlie the peneccontemporaneous volcaniclastic sedimentary rocks.

INTRUSIVE ROCKS

Intrusive rocks in the southeastern San Juan region, consisting of numerous andesitic to rhyolitic dikes and scattered larger granitic stocks, tend to cluster around and radiate out from the Platoro caldera complex (fig. 47). Although some of these intrusives can be linked to individual units of the caldera-related lavas described in the preceding sections, the intrusive rocks are described separately because the precise volcanic associations of many are ambiguous.

GRANITIC INTRUSIONS

About 10 granitic stocks, ranging in size from less than 0.5 to at least 5 km across, intrude the volcanic sequence near the Platoro caldera complex, and several large laccolithic granitic bodies are localized along the boundary between the Conejos Formation and prevolcanic rocks along the southwest margin of the San Juan Mountains (fig. 47). Although these rocks were considered to be related to the Conejos Formation by Larsen and Cross (1956, p. 104-105), most of the stocks around the Platoro area are younger than the Treasure Mountain Tuff, as discussed below.

These bodies consist mainly of texturally variable monzonite, in places transitional into diorite or granodiorite (table 10). Locally, the granitic rocks are equigranular, but most are porphyritic, with plagioclase the conspicuous phenocryst. Two pyroxenes are also typically present as early-formed euhedral minerals; these tend to be variably altered, the hypersthene to chlorite or serpentine and the augite to chlorite, carbonate, or tremolite. Interstices between plagioclase and pyroxenes are characteristically occupied by various amounts of quartz and orthoclase—in places with a tendency toward granophytic intergrowths—and by biotite and Fe-Ti oxides. Because good brief petrographic descriptions of many of these rocks are given by Larsen and Cross (1956, p. 104-110), the following short discussions of the individual bodies concentrate on the major compositional and textural variations. These intrusives were studied only briefly; several that are well exposed and internally complex are deserving of more detailed investigation.

ALAMOSA RIVER STOCK

The Alamosa River stock (fig. 47, loc. A) is the largest of the granitic intrusives, about 3 by 7 km, and is elongate to the northeast, apparently owing to emplacement along the Cornwall fault (fig. 61). Contacts are steep, except in the Alum Creek-Bitter Creek area (Platoro map), where the north contact dips broadly outward and has many irregular apophyses.

South of the Alamosa River, the stock consists of little-altered fine- to medium-grained equigranular monzonite (fig. 48A); it is fairly uniform in texture but varies in composition from about 57 to 62 percent SiO_2

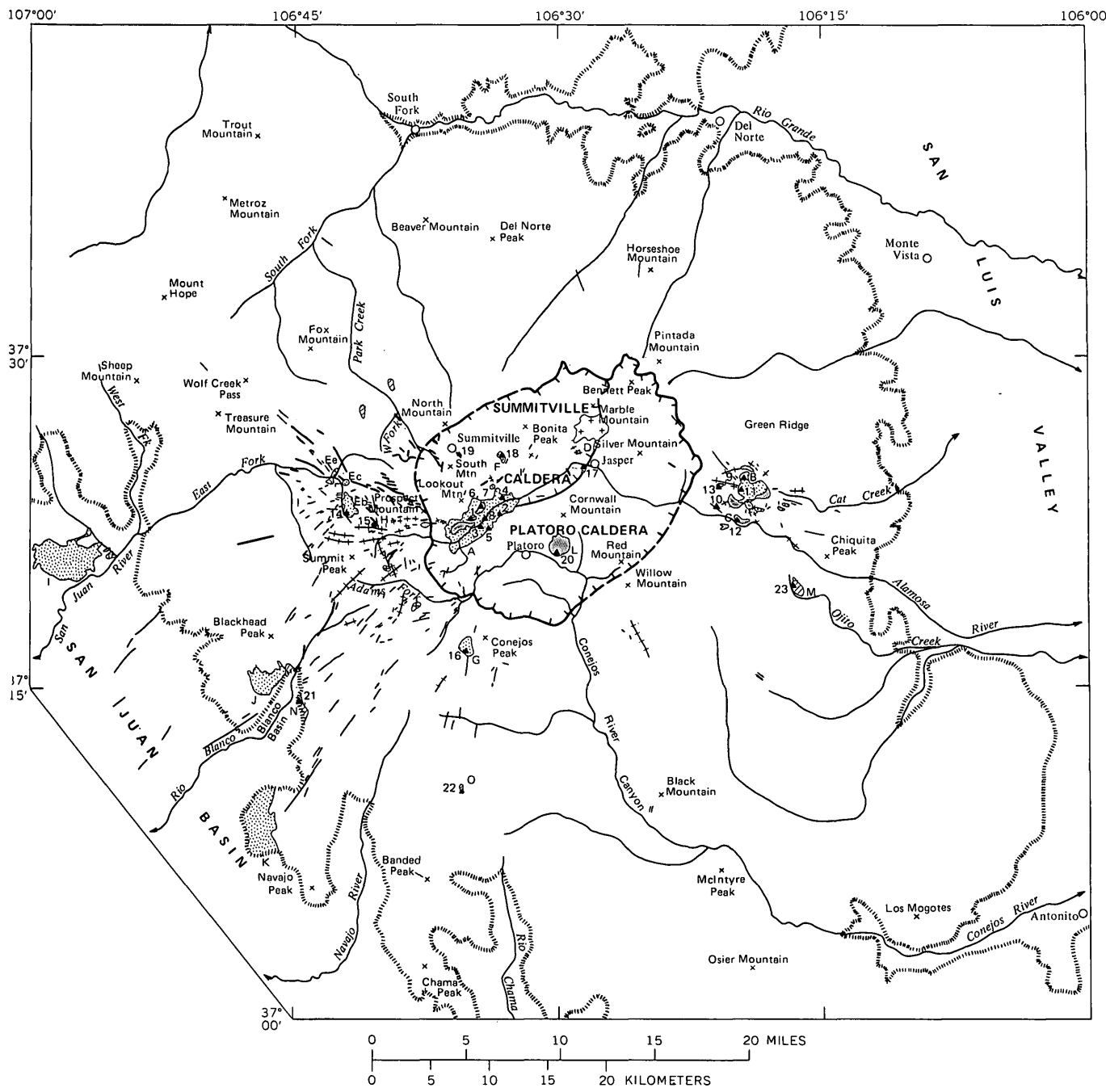
(table 10, Nos. 2-5). In contrast, the northwestern part of the intrusion is texturally and compositionally complex and is also the locus of intense hydrothermal alteration (fig. 61). In this area a separately mapped porphyritic phase is distinctly more silicic (about 65 percent SiO_2 ; table 10, Nos. 6, 7) than the equigranular monzonite and varies greatly in texture; the average size of phenocrysts ranges from only slightly larger than the equigranular grains of the monzonite to at least 1 cm, and the ground-mass texture ranges from aphanitic to phaneritic (fig. 48B, C). The most aphanitic parts of the porphyritic phase generally are intensely hydrothermally altered, so relations with the other porphyritic types are obscure. The porphyritic phase is at least locally intrusive into the equigranular monzonite, as first recognized by Calkin (1971, p. 237), but in the southwestern part of the stock the porphyritic phase grades into equigranular monzonite. Although several porphyritic phases of different ages may be present, it seems preferable to regard them all as late phases of the Alamosa River stock, rather than as a separate intrusive, as suggested by Calkin (1971).

An even more silicic phase of the Alamosa River stock (71 percent SiO_2 ; table 10, No. 8) is represented by late irregular aplite veins, rarely more than 10 cm thick, that locally have chilled margins against the monzonite (fig. 48D).

Many of the dikes in the western part of the mapped area radiate outward from the area of the Alamosa River stock and seem to be closely related to it. These dikes are described in the section on porphyro-aphanitic intrusions.

The Alamosa River stock intrudes the intracaldera La Jara Canyon Member; it also seems to be partly structurally controlled by the Cornwall fault that bounds the Summitville caldera on its south side (fig. 61), suggesting that the stock may be younger than the Ojito Creek and Ra Jadero Members of the Treasure Mountain as well. Biotite from a sample of the equigranular monzonite (fig. 48A; table 10, No. 2) yielded a K-Ar age of 29.1 m.y., which is compatible with all available geologic and geochronologic constraints (Lipman and others, 1970).

Exposures of equigranular monzonite of the Alamosa River stock at elevations of over 12,000 feet along the divide between the Alamosa and Conejos Rivers present a significant paleotopographic problem. This position must be close to the regional late Oligocene land surface, as marked by the level of ash-flow sheets of the Treasure Mountain Tuff on adjacent high ridges (Platoro map). Reasonably, even a shallow subvolcanic intrusive could have been emplaced and cooled at such a high level only if it were covered by a thick local volcanic accumulation that stood significantly above the regional terrain. Thus, intrusion of the Alamosa River stock



EXPLANATION

| | | | |
|---|---------------------|-----------------|--|
| [Monzonite pattern] | Rhyodacite porphyry | ▲ ²⁰ | Sample locality (table 10) |
| [Quartz latite and rhyolite porphyry pattern] | Andesite porphyry | | Limit of exposed volcanic rocks |
| [Blank] | | - - - - | Caldera wall (topographic) — Dashed where covered by younger rocks |
| [Blank] | | | |

FIGURE 47.—Distribution of major groups of intrusive rocks in the southeastern San Juan Mountains. Based on mapping by P. W. Lipman 1965-67, 1970-71. A, Alamosa River stock. B, Cat Creek stock. C, Terrace Reservoir laccolith. D, Jasper stock. E, Bear Creek stock cluster; Eb, Bear Creek stock; Ec, Crater Creek stock; Ee, Elwood Creek stock. F, Wightman Fork stock. G, Canyon Diablo stock. H, Cataract Creek stock. I, Jackson Mountain laccolith. J, V Mountain laccolith. K, Squaretop laccolith. L, Cornwall Mountain stock. M, Ojito Creek plug. N, Blanco Basin sill. O, Trail Lake plug.

PLATERO CALDERA COMPLEX, SAN JUAN MOUNTAINS, COLORADO

TABLE 10.—Analyses of intrusive

[Sample localities shown in fig. 47. Analyses 3 and 19 are from Patton (1917). All other Chloe, Lowell Artis, H. Smith, John Glenn, and James Kelsey. Minor-element No. 22 by J. L. Harris; by quantitative methods are Nos. 2, 6, 7, 9-14, Harriet Neiman. <, less than]

| Sample----- Field No----- Lab. No----- | Alamosa River stock | | | | | | | | Intrusive complex at Cat Creek | | | | | |
|---|---------------------|--------------|----------|--------------|-------------|---------------|---------------|-------------|--------------------------------|--------------|----------------|--------------|--------------|-------|
| | 1 71L-34 | 2 67L-113 | 3 P57 | 4 66L-155 | 5 ST-128 | 6 ACL-2363 | 7 ACL-2964 | 8 71L-31 | 9 70L-16 | 10 70L-10 | 11 70L-14-A | 12 66L-51 | 13 70L-11 | |
| | W176169 | W174423 | ----- | W168451 | W168450 | W174424 | W174425 | W176168 | W174432 | W174429 | W174431 | W174426 | W174430 | |
| Major oxides (weight percent), recalculated with H ₂ O and CO ₂ (original values listed separately below) | | | | | | | | | | | | | | |
| SiO ₂ ----- | 56.5 | 56.6 | 60.32 | 59.9 | 61.7 | 64.9 | 65.3 | 70.9 | 59.6 | 61.4 | 63.2 | 66.2 | 66.2 | 66.2 |
| Al ₂ O ₃ ----- | 17.0 | 16.8 | 14.67 | 16.5 | 16.2 | 15.5 | 16.0 | 14.3 | 18.1 | 17.55 | 16.7 | 17.1 | 17.1 | 17.1 |
| Fe ₂ O ₃ ----- | 4.8 | 4.5 | 5.14 | 3.05 | 3.5 | 3.8 | 2.8 | 1.4 | 3.7 | 3.4 | 2.7 | 2.2 | 2.5 | 2.5 |
| FeO----- | 4.6 | 3.8 | 3.03 | 3.9 | 2.97 | 2.0 | 2.4 | .93 | 2.9 | 1.9 | 2.6 | 1.7 | 1.5 | 1.5 |
| MgO----- | 3.7 | 3.6 | 2.92 | 3.3 | 2.5 | 1.5 | 1.5 | .66 | 2.4 | 2.1 | 2.1 | 1.3 | 1.1 | 1.1 |
| CaO----- | 5.4 | 6.1 | 4.52 | 5.5 | 3.99 | 4.3 | 3.9 | .88 | 5.07 | 5.9 | 4.05 | 3.9 | 3.4 | 3.4 |
| Na ₂ O----- | 3.7 | 3.3 | 3.91 | 3.5 | 3.6 | 3.6 | 3.3 | 2.8 | 4.2 | 3.2 | 3.7 | 3.7 | 3.97 | 3.97 |
| K ₂ O----- | 2.8 | 2.8 | 4.21 | 2.9 | 4.1 | 3.6 | 3.6 | 6.9 | 3.1 | 3.3 | 3.5 | 2.9 | 3.3 | 3.3 |
| TiO ₂ ----- | 1.0 | .91 | .99 | .90 | .97 | .54 | .57 | .52 | .36 | .72 | .81 | .53 | .54 | .54 |
| P ₂ O ₅ ----- | .30 | .48 | .12 | .40 | .29 | .31 | .27 | .47 | .38 | .34 | .34 | .23 | .22 | .22 |
| MnO----- | .22 | .13 | .13 | .17 | .29 | .12 | .11 | .06 | .11 | .12 | .11 | .09 | .09 | .09 |
| TOTAL----- | 100.02 | 99.02 | 99.94 | 100.02 | 100.11 | 100.17 | 99.75 | 99.82 | 99.92 | 99.93 | 99.81 | 99.85 | 99.92 | 99.92 |
| H ₂ O+----- | 2.1 | 1.0 | .76 | .70 | 1.5 | 1.4 | .80 | .63 | .77 | 1.4 | .55 | 1.8 | 1.3 | 1.3 |
| H ₂ O----- | .33 | .25 | .09 | .28 | .44 | .27 | .30 | .33 | .43 | .23 | .19 | .71 | .26 | .26 |
| CO ₂ ----- | .29 | <.05 | .04 | .05 | .18 | <.05 | <.05 | <.05 | <.05 | 1.6 | <.05 | 1.0 | .24 | .24 |
| Norms (weight percent) | | | | | | | | | | | | | | |
| Quartz----- | 7.12 | 10.4 | 10.3 | 12.3 | 13.5 | 20.7 | 21.3 | 26.34 | 9.2 | 16.1 | 16.4 | 23.2 | 22.4 | 22.4 |
| Corundum----- | ----- | ----- | ----- | ----- | ----- | ----- | ----- | 1.68 | ----- | ----- | ----- | ----- | ----- | ----- |
| Orthoclase----- | 16.53 | 16.8 | 24.8 | 17.4 | 24.2 | 21.03 | 21.5 | 41.15 | 18.3 | 19.5 | 20.9 | 17.2 | 19.3 | 19.3 |
| Albite----- | 31.57 | 28.4 | 33.1 | 29.3 | 30.3 | 28.3 | 23.91 | 35.9 | 27.1 | 31.7 | 31.7 | 33.6 | 33.6 | 33.6 |
| Anorthite----- | 21.36 | 22.3 | 10.1 | 20.7 | 15.9 | 15.7 | 17.8 | 1.26 | 21.2 | 23.8 | 17.8 | 18.1 | 15.2 | 15.2 |
| Wollastonite----- | 1.42 | 2.02 | 4.8 | 1.6 | .82 | 1.5 | ----- | ----- | .61 | 1.3 | ----- | ----- | ----- | ----- |
| Enstatite----- | 9.29 | 8.8 | 7.3 | 8.1 | 6.1 | 3.8 | 3.8 | 1.63 | 5.9 | 5.1 | 5.3 | 3.4 | 2.8 | 2.8 |
| Ferrosilite----- | 3.13 | 1.95 | ----- | 3.4 | 1.5 | .00 | 1.4 | ----- | 1.8 | ----- | 1.4 | .55 | ----- | ----- |
| Magnetite----- | 6.91 | 6.5 | 7.4 | 4.4 | 5.04 | 5.4 | 4.1 | 1.67 | 5.4 | 4.6 | 3.96 | 3.2 | 3.7 | 3.7 |
| Hematite----- | ----- | ----- | .03 | ----- | ----- | .04 | ----- | .26 | ----- | 2.1 | ----- | ----- | .02 | ----- |
| Ilmenite----- | 1.97 | 1.73 | 1.9 | 1.7 | 1.8 | 1.02 | 1.07 | 1.00 | .69 | 1.4 | 1.5 | 1.0 | 1.03 | 1.03 |
| Titanite----- | ----- | ----- | ----- | ----- | ----- | ----- | ----- | ----- | ----- | ----- | ----- | ----- | ----- | ----- |
| Rutile----- | ----- | ----- | ----- | ----- | ----- | ----- | ----- | ----- | ----- | ----- | ----- | ----- | ----- | ----- |
| Apatite----- | .71 | 1.13 | .29 | .94 | .68 | .72 | .65 | 1.12 | .91 | .81 | .81 | .54 | .53 | .53 |
| Minor elements (parts per million) | | | | | | | | | | | | | | |
| Ag----- | ----- | ----- | ----- | 0.5 | 0.3 | ----- | ----- | ----- | ----- | ----- | ----- | ----- | ----- | ----- |
| Ba----- | 2200 | ----- | 1000 | 1000 | 1900 | 1900 | 1900 | ----- | 2500 | 2200 | 2800 | 2800 | 2600 | 2600 |
| Be----- | 7 | ----- | 3 | 3 | <2 | <2 | <2 | ----- | <2 | <2 | <2 | <2 | <2 | <2 |
| Ce----- | ----- | ----- | 100 | 100 | ----- | ----- | ----- | ----- | ----- | ----- | ----- | ----- | ----- | ----- |
| Co----- | 20 | ----- | 20 | 15 | 13 | 8 | ----- | 28 | 10 | 10 | 6 | 7 | 7 | 7 |
| Cr----- | 110 | ----- | 50 | 10 | 11 | 22 | ----- | 200 | 27 | 22 | 7 | 8 | 8 | 8 |
| Cu----- | 15 | ----- | 70 | 30 | 50 | 60 | ----- | 23 | 24 | 34 | 22 | 13 | 20 | 20 |
| Ge----- | 30 | ----- | 15 | 15 | 10 | 20 | ----- | 20 | 20 | 40 | 20 | 20 | 20 | 20 |
| La----- | ----- | ----- | 100 | 100 | ----- | ----- | ----- | ----- | ----- | ----- | ----- | ----- | ----- | ----- |
| Mo----- | ----- | ----- | 7 | 7 | ----- | ----- | ----- | ----- | ----- | ----- | ----- | ----- | ----- | ----- |
| Nb----- | ----- | ----- | 7 | 5 | ----- | ----- | ----- | ----- | ----- | ----- | ----- | ----- | ----- | ----- |
| Ni----- | 14 | ----- | 30 | 15 | 18 | 10 | ----- | 19 | 9 | 15 | 8 | 10 | 10 | 10 |
| Pb----- | ----- | ----- | 200 | 30 | ----- | ----- | ----- | ----- | ----- | ----- | ----- | ----- | ----- | ----- |
| Sc----- | 24 | ----- | 15 | 15 | 14 | 11 | ----- | 21 | 14 | 12 | 8 | 10 | 10 | 10 |
| Sr----- | 1000 | ----- | 500 | 500 | 4300 | 480 | ----- | 480 | 360 | 320 | 440 | 340 | 340 | 340 |
| V----- | 200 | ----- | 150 | 100 | 80 | 90 | ----- | 200 | 100 | 90 | 40 | 30 | 30 | 30 |
| Y----- | <40 | ----- | 50 | 30 | <40 | <40 | ----- | <40 | <40 | <40 | <40 | <40 | <40 | <40 |
| Yb----- | 6 | ----- | 3 | 3 | 3 | 3 | ----- | <2 | 3 | <2 | <2 | <2 | <2 | <2 |
| Zr----- | 380 | ----- | 300 | 300 | 260 | 300 | ----- | 170 | 120 | 160 | 150 | 190 | 190 | 190 |
| Phenocrysts (volume percent) | | | | | | | | | | | | | | |
| Quartz----- | ----- | 4.7 | ----- | 3.8 | 5 | 10 | 10 | 23.9 | 3.1 | ----- | 5.8 | ----- | ----- | ----- |
| Orthoclase----- | ----- | 15.1 | ----- | 21.3 | 20 | 25 | 25 | 52.4 | 13.9 | ----- | 24.5 | ----- | ----- | ----- |
| Plagioclase----- | 9 | 51.2 | ----- | 50.2 | 55 | 45 | 45 | 18.7 | 53.4 | 26.4 | 43.1 | 19.7 | 20 | 20 |
| Biotite----- | ----- | 5.2 | ----- | 2.7 | 10 | 7 | ----- | 3.1 | ----- | 3.0 | 4.1 | 3 | 3 | 3 |
| Hornblende----- | ----- | ----- | ----- | ----- | ----- | ----- | ----- | ----- | ----- | ----- | ----- | ----- | ----- | ----- |
| Augite----- | 2 | 14.3 | ----- | 13.2 | 10 | 5 | 10 | 2.1 | 11.7 | 5.3 | 13.7 | 2.2 | 5 | 5 |
| Hypersthene----- | ----- | 4.7 | ----- | 6.1 | 5 | ----- | ----- | ----- | 8.2 | ----- | 4.8 | ----- | ----- | ----- |
| Opalites----- | 1 | 4.8 | ----- | 3.3 | 5 | 3 | 2.9 | 4.5 | 3.1 | 4.2 | 2.2 | 2 | 2 | 2 |
| Groundmass----- | 88 | ----- | ----- | ----- | ----- | ----- | ----- | ----- | 65.2 | ----- | 71.8 | 70 | 70 | 70 |

See page 82 for sample descriptions.

rocks of the Platora caldera area

major-oxide analyses are by rapid methods by P. L. D. Elmore, Samuel Botts, Gillison
 analyses by semiquantitative methods are Nos. 4, 5, and 15 by H. W. Worthing and
 and 23 by Norma Rait, Nos. 1, 8, and 16-18 by J. D. Fletcher, and No. 20 by

| Bear Creek stock | Cataract Creek stock | Canyon Diablo stock | Jasper stock | Wightman Fork stock | Porphyro-aphanitic intrusives | | | | | | Sample No. Field No. Lab. No. |
|---------------------------|----------------------|-------------------------|-------------------------|-------------------------|-------------------------------|--------------------------|------------|----------------------------|-------------------------|--|-------------------------------------|
| 14 67L-86-B W174428 | 15 66B-13A | 16 71J-59 W176175 | 17 70L-95 W176184 | 18 70L-91 W176183 | 19 P12 | 20 68L-110 D133706 | 21 GL-8 | 22 66L-244-C W168070 | 23 66L-15 W168529 | | |

Major oxides (weight percent), recalculated without H₂O and CO₂ (original values listed separately below)--Continued

| | | | | | | | | | | |
|-------|--------|-------|-------|--------|--------|--------|-------|-------|-------|--------------------------------|
| 58.9 | 59.1 | 62.5 | 61.6 | 56.6 | 66.25 | 66.5 | 67.3 | 67.4 | 67.5 | SiO ₂ |
| 17.1 | 17.3 | 17.4 | 15.9 | 17.4 | 15.52 | 17.1 | 15.7 | 16.2 | 16.4 | Al ₂ O ₃ |
| 2.7 | 3.9 | 6.0 | 3.7 | 3.3 | .67 | 3.1 | 2.4 | 3.1 | 2.2 | Fe ₂ O ₃ |
| 5.4 | 3.2 | .24 | 3.1 | 5.3 | 3.11 | .80 | 1.8 | .97 | 1.0 | FeO |
| 3.1 | 2.9 | 1.1 | 2.8 | 3.4 | 1.99 | 1.1 | 1.5 | 1.2 | 1.1 | MgO |
| 5.1 | 5.8 | 4.9 | 4.2 | 7.0 | 4.03 | 2.7 | 2.4 | 3.2 | 3.6 | CaO |
| 3.2 | 3.99 | 3.6 | 3.4 | 3.1 | 3.19 | 3.8 | 4.0 | 4.3 | 3.9 | Na ₂ O |
| 2.9 | 2.6 | 3.0 | 4.0 | 2.6 | 4.01 | 4.1 | 4.0 | 2.4 | 3.5 | K ₂ O |
| 1.0 | .63 | .69 | .87 | 1.1 | .77 | .60 | .55 | .73 | .40 | TiO ₂ |
| .38 | .43 | .27 | .17 | .33 | .38 | .12 | .24 | .29 | .22 | P ₂ O ₅ |
| .16 | .25 | .16 | .12 | .16 | .08 | .08 | .08 | .08 | .04 | MnO |
| 99.94 | 100.10 | 99.86 | 99.86 | 100.09 | 100.00 | 100.00 | 99.97 | 99.87 | 99.86 | TOTAL |
| 1.2 | 1.3 | .49 | 1.0 | 1.6 | 1.44 | 1.0 | .63 | .43 | .26 | H ₂ O+ |
| .56 | .57 | .23 | .27 | .33 | .80 | .82 | .23 | .42 | .23 | H ₂ O- |
| <.05 | .39 | <.05 | <.05 | .15 | 3.75 | .62 | <.05 | <.05 | <.05 | CO ₂ |

Norms (weight percent)--Continued

| | | | | | | | | | | |
|-------|-------|-------|-------|-------|-------|-------|-------|-------|-------|--------------|
| 11.9 | 10.5 | 18.42 | 13.35 | 9.08 | 20.31 | 21.65 | 21.56 | 25.01 | 22.28 | Quartz |
| ----- | ----- | ----- | ----- | ----- | ----- | 1.89 | .90 | 1.22 | .78 | Corundum |
| 17.5 | 15.1 | 17.86 | 23.94 | 14.50 | 23.67 | 24.25 | 23.74 | 14.32 | 20.86 | Orthoclase |
| 26.7 | 33.8 | 30.69 | 29.13 | 25.96 | 26.98 | 32.12 | 34.00 | 36.73 | 33.28 | Albite |
| 22.8 | 21.7 | 22.35 | 15.96 | 26.42 | 16.19 | 12.43 | 10.38 | 14.12 | 16.56 | Anorthite |
| ----- | 1.8 | ----- | 1.68 | 2.48 | .54 | ----- | ----- | ----- | ----- | Wollastonite |
| 7.6 | 7.1 | 2.76 | 7.06 | 8.40 | 4.96 | 2.81 | 3.75 | 3.02 | 2.76 | Enstatite |
| 6.3 | 2.02 | ----- | 1.54 | 5.51 | 4.03 | ----- | .57 | ----- | ----- | Ferrosilite |
| 4.0 | 5.6 | ----- | 5.29 | 4.75 | .97 | 1.12 | 3.50 | 1.28 | 2.21 | Magnetite |
| ----- | ----- | 6.04 | ----- | ----- | ----- | 2.30 | ----- | 2.25 | .69 | Hematite |
| 1.9 | 1.2 | .86 | 1.65 | 2.14 | 1.47 | 1.13 | 1.05 | 1.38 | .77 | Ilmenite |
| ----- | ----- | .26 | ----- | ----- | ----- | ----- | ----- | ----- | ----- | Titanite |
| ----- | ----- | .13 | ----- | ----- | ----- | ----- | ----- | ----- | ----- | Rutile |
| .89 | 1.02 | .64 | .41 | .78 | .90 | .29 | .57 | .69 | .53 | Apatite |

Minor elements (parts per million)--Continued

| | | | | | | | | | | |
|-------|------|-------|-------|-------|-------|-------|-------|-------|-------|-------|
| ----- | 0.5 | ----- | ----- | ----- | ----- | ----- | ----- | ----- | ----- | Ag |
| 2200 | 1000 | 970 | 640 | 560 | 880 | ----- | 700 | 1500 | ----- | Ba |
| <2 | 3 | ----- | ----- | ----- | <2 | ----- | 2 | ----- | ----- | Be |
| ----- | 100 | ----- | ----- | ----- | ----- | ----- | 300 | ----- | ----- | Ce |
| 16 | 15 | 10 | 20 | 22 | 6 | ----- | 15 | 7 | Co | ----- |
| 19 | 10 | 7 | 70 | 3 | 3 | ----- | 30 | 8 | ----- | Cr |
| 57 | 15 | 18 | 68 | 88 | 9 | ----- | 20 | 16 | ----- | Cu |
| 20 | 15 | 20 | 20 | 20 | 19 | ----- | 20 | 20 | ----- | Ga |
| ----- | 100 | 100 | 90 | 100 | 50 | ----- | 100 | ----- | ----- | La |
| ----- | 3 | 4 | ----- | ----- | ----- | ----- | ----- | ----- | ----- | Mo |
| ----- | 3 | 20 | 30 | 20 | 23 | ----- | 10 | ----- | ----- | Nb |
| 14 | 7 | 4 | 24 | 9 | <5 | ----- | 30 | 6 | ----- | Ni |
| ----- | 70 | 20 | 20 | 20 | <50 | ----- | 7 | <20 | ----- | Pb |
| 17 | 10 | 21 | 20 | 30 | 8 | ----- | 20 | 7 | ----- | Sc |
| 570 | 700 | 850 | 600 | 1240 | 510 | ----- | 1000 | 550 | ----- | Sr |
| 160 | 100 | 50 | 140 | 240 | 65 | ----- | 70 | 40 | ----- | V |
| <40 | 30 | 30 | 30 | 30 | 38 | ----- | 20 | 30 | ----- | Y |
| 4 | 3 | 3 | 2 | 3 | 2 | ----- | 2 | ----- | ----- | Yb |
| 180 | 200 | 200 | 300 | 130 | 260 | ----- | 150 | 240 | ----- | Zr |

Phenocrysts (volume percent)--Continued

| | | | | | | | | | | |
|-------|-------|-------|-------|-------|-------|-------|-------|------|-------|-------------|
| 6.5 | ----- | ----- | 5.8 | ----- | ----- | ----- | 3 | 2.1 | ----- | Quartz |
| 21.5 | ----- | ----- | 28.7 | ----- | ----- | ----- | 5 | 6.3 | ----- | Orthoclase |
| 48.1 | 30 | 52 | 42.6 | 65 | 25 | ----- | 25 | 28.5 | ----- | Plagioclase |
| 3.0 | ----- | ----- | ----- | ----- | 2 | ----- | 4 | 4.2 | ----- | Biotite |
| ----- | 15 | ----- | ----- | ----- | ----- | ----- | 2 | .5 | ----- | Hornblende |
| 12.9 | ----- | 7 | 12.3 | 20 | 5 | ----- | ----- | 1.6 | ----- | Augite |
| 4.0 | ----- | ----- | 4.7 | 10 | ----- | ----- | 1 | .7 | ----- | Hypersthene |
| 4.3 | 5 | 6 | 5.9 | 5 | 3 | ----- | 60 | 57.7 | ----- | Opaque |
| ----- | 50 | 35 | ----- | ----- | 65 | ----- | 60 | 57.7 | ----- | Groundmass |

TABLE 10.—Analyses of intrusive rocks of the Platoro caldera area—Continued

SAMPLE DESCRIPTIONS

1. Greenish-gray porphyritic andesite. See fig. 48C for sample description and location.
2. Gray medium-grained monzonite. See fig. 48A for sample description and location.
3. Monzonite. "Contains orthoclase, plagioclase, quartz, pyroxene, and biotite. Anomalous- ly high in K₂O and low in Al₂O₃ and P₂O₅. Near sawmill above Stunner" (Patton, 1917, p. 31-32).
4. Relatively coarse grained monzonite. Petrographically generally similar to No. 2. Augite is fairly fresh, but orthopyroxene is pseudomorphed to chlorite and serpentine. Biotite grains are small, irregular, and interstitial with quartz and orthoclase. Roadcut on Alamosa River road, just east of Bitter Creek.
5. Gray fine-grained monzonite. Feldspars are cloudy, biotite is absent, and pyroxenes are thoroughly altered—augite to tremolite, and hypersthene to chlorite. Scattered grains of secondary epidote as much as 0.2 mm in diameter; also some secondary carbonate. Roadcut on north side of Stunner Pass, at about 10,200 ft.
6. Porphyritic quartz monzonite from drill hole. See fig. 48B for sample description and location.
7. Porphyritic quartz monzonite from 2,964-ft depth in drill hole in Alum Creek. Sample provided by W. S. Calkin. Petrographically similar to No. 6.
8. Light-gray aplite vein in monzonite. See fig. 48D for sample description and location.
9. Dark-gray fine-grained fresh monzonite. Slightly porphyritic; plagioclase tablets 1-2 mm long are set in matrix of plagioclase and mafics averaging about 0.5 mm in diameter. Quartz and orthoclase are interstitial. Augite is fresh, but hypersthene is altered to chlorite. Anomalously low in TiO₂. Along North Fork Cat Creek, at 9,250 ft.
10. Gray porphyritic rhyodacite dike. Plagioclase phenocrysts are as much as 4 mm long; augite is largely replaced by carbonate. Anomalously low in Fe and slightly high in CaO (note high CO₂). Northwest side of Negro Gulch, at about 9,500 ft.
11. Gray medium-grained equigranular monzonite. Petrographically much like No. 4. Along South Fork Cat Creek, at 9,150 ft.
12. Light-gray porphyritic quartz latite from Terrace Reservoir laccolith. Collected from talus above Alamosa River road, at northwest end of laccolith.
13. Greenish-gray porphyritic quartz latite. Blocky plagioclase phenocrysts are as much as 5 mm across and relatively fresh; mafic minerals that apparently originally included both biotite and augite are completely replaced by chlorite, epidote, and carbonate. North side of South Fork Cat Creek, at about 9,450 ft.
14. Medium-grained equigranular monzonite. Much like Nos. 4 and 11, but hypersthene is only slightly altered. East side of Bear Creek, at about 11,800 ft.
15. Porphyro-aphanitic facies of monzonite, containing abundant elongate phenocrysts of plagioclase and hornblende as much as 1.3 mm long in a fine-grained granular groundmass. Northwest shore of the small lake within the area of the stock.
16. Granodiorite porphyry, containing abundant plagioclase laths that range in length from less than 0.1 mm to 3 mm. Presence of fine-grained granular groundmass is only evident in thin section. Rim of cirque basin, at about 12,200 ft, 0.3 km northwest of unnamed lake at head of Canyon Diablo.
17. Medium-grained equigranular monzonite. Petrographically much like No. 4, but both pyroxenes are altered, and orthoclase is extensively sericitized. Striking granophytic interstitial textures. Edge of beaver-pond dam, about 150 m east of abandoned Miser mill site, south of the Alamosa River at Jasper.
18. Fine-grained equigranular diorite. A few percent plagioclase phenocrysts as much as 3 mm long are set among groundmass grains that have an average diameter of about 0.5 mm. Augite is partly altered to tremolite, and hypersthene has been completely replaced by chlorite. Wightman Fork road, at 10,350 ft.
19. Porphyritic quartz latite dike. "Contains phenocrysts of glassy sanidine, plagioclase, quartz, and biotite in a very fine grained groundmass. From dike in Cropsy Gulch" (Patton, 1917, p. 31).
20. Porphyritic quartz latite from Cornwall Mountain stock. Plagioclase phenocrysts are blocky and as much as 6 mm in diameter; mafics are completely altered, with sericitic replacing biotite and carbonate pseudomorphing augite. Fine granular groundmass (average diameter 0.05 mm) is about two-thirds sanidine and one-third quartz. West fork of Robinson Gulch, at about 10,600 ft.
21. Porphyritic quartz latite sill. Northeast side of Blanco Basin, east of Squaretop Mountain. Previously unpublished analysis provided by David Gottfried.
22. Light-gray porphyritic quartz latite plug. Plagioclase phenocrysts (An₂₀₋₃₀) are as much as 1 cm in diameter; similar sanidine and somewhat smaller quartz are rounded and embayed. Hornblende is nearly opaque from exsolved Fe-Ti oxides. Modal estimate is only a rough approximation because of large phenocrysts. Anomalously low in K₂O. 1 km north of Trail Lake, at about 12,200 ft (fig. 13).
23. Light-gray porphyritic quartz latite. Petrographically similar to No. 22, except for presence of augite and generally less severe oxidation of mafic phenocrysts. East side of Ojito Creek road, at 8,700 ft.

seems best interpreted as a final stage in the evolution of an upward-moving body of magma, which, at a lower crustal level, had earlier fed volcanic eruptions to form a large stratovolcano. Perhaps, the lavas of the upper member of the Summitville Andesite, which are similar in composition to the monzonite, are preserved remnants of the lower northern flank of this volcano within the Summitville caldera.

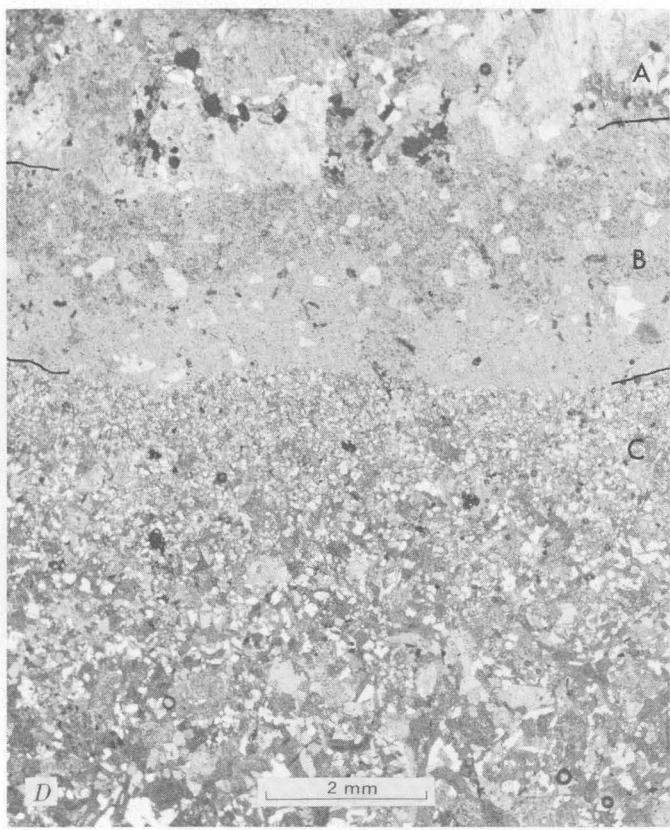
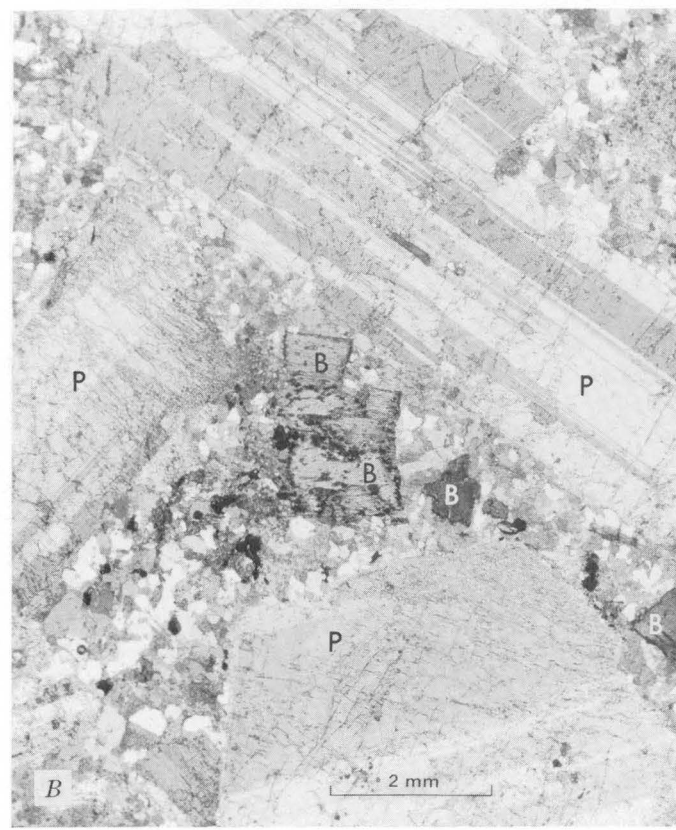
CAT CREEK STOCK

The Cat Creek stock, the large intrusive complex centered about 3 km east of the Platoro caldera rim (fig. 47, loc. B), is thought to represent the intrusive core of the volcano that erupted the volcanics of Green Ridge. This intrusive complex has a texturally uniform core, about 3 km in diameter, consisting of fine-grained equigranular monzonite (60-63 percent SiO₂; table 10, Nos. 9, 11); the core is enclosed by a finer grained porphyritic margin around the south and east sides of the stock and is flanked in other directions by scattered satellite laccolithic bodies of similar porphyry (fig. 47). The marginal porphyry is too highly altered to determine its original composition, but two of the satellite laccoliths are compositionally transitional between rhyodacite and quartz latite (table 10, Nos. 12, 13)—distinctly more silicic than the equigranular monzonite of the core.

The Terrace Reservoir laccolith (fig. 47, loc. C), south of the major exposure of the Cat Creek stock, is a biotite-augite-plagioclase porphyry (table 10, No. 12). It has been cut through by the Alamosa River (fig. 47) and is well exposed on both north and south walls of the valley.

Outcrops south of the river are near the edge of the laccolith, where it wedges out completely from a thickness of about 75 m, and provide the best exposures of the roof of the intrusion. North of the river, where the laccolith bulges to as much as 250 m of exposed thickness, the roof has been largely eroded. In this area, the subhorizontal basal contact of the laccolith is well exposed; the resis-

FIGURE 48 (right).—Photomicrographs of rocks of the Alamosa River stock. A, Medium-grained equigranular monzonite from summit of Telluride Mountain. Euhedral plagioclase (P), (An₄₀₋₄₅) and altered pyroxenes, with interstices filled by large biotite (B) and orthoclase (O) or by granophytic quartz-orthoclase intergrowths. Analyzed sample 2, table 10; biotite from this sample has been dated radiometrically at 29.1 m.y. (Lipman and others, 1970, table 4, No. 9). B, Porphyritic quartz monzonite from 2,363-foot depth in drill hole in Alum Creek. Sample provided by W. S. Calkin. Large plagioclase phenocrysts (P) (An₃₅₋₄₀) and small biotites (B) in a phanerocrystalline sugary-textured groundmass intergrowth of quartz and alkali feldspar. Analyzed sample 6, table 10. C, Porphyritic andesite from roadcut, Stunner-Summitville road at 10,100 feet elevation, stream crossing south of Lookout Mountain. An exceptionally mafic part of the rhyodacite porphyry phase of the stock. Large plagioclase phenocrysts (An₃₅₋₄₀) are marginally altered to carbonate in fine-grained groundmass; pyroxene phenocrysts (not visible) are pseudomorphed by epidote and carbonate. This rock type is typically much more altered than this sample indicates. Analyzed sample 1, table 10. D, Chilled border of aplite vein, in contact with fine-grained equigranular monzonite, from bridge abutment across the Alamosa River at Stunner. The fine-grained monzonite (A) is sharply truncated by a selvage of microcrystalline porphyry (B) that contains small phenocrysts of plagioclase and orthoclase. This porphyry, in turn, is sharply truncated by fine-grained aplite that becomes coarser toward interior of vein (C). Coarse aplite consists of subequal amounts of quartz and orthoclase, accompanied by a few percent plagioclase. Analyzed sample 8, table 10.



tant rocks of the intrusion form the overhanging upper walls of caves along the contact, just a short distance above the main Alamosa River roadway.

The wallrocks of the intrusive complex at Cat Creek are lavas and breccias of the Conejos Formation and, around much of the central stock, the rhyolite unit of the volcanics of Green Ridge. Although the marginal contacts of the central stock vary widely in attitude, generally moderate outward dips indicate that the present level of exposures is close to the original top of the rather irregularly shaped stock. Over a sizable area, especially along the ridge between Deer Creek and the North Fork of Cat Creek (Platoro map), the contact between the equigranular monzonite and the overlying recrystallized rhyolite (fig. 41B) clearly forms the roof of the stock.

The Cat Creek stock and related rocks have not been dated radiometrically, but their age can be inferred with some confidence if their correlation with the volcanics of Green Ridge is valid. Although the monzonitic rocks nowhere intrude the ash-flow sequence, the area of alteration that extends outward from the central stock (fig. 61) has—contrary to Larsen and Cross (1956, p. 110)—intensely affected the units of the Treasure Mountain Tuff, including the Ra Jadero Member, especially in the tributary of Cat Creek known as “The Canyon” (Platoro map). Furthermore, dikes that radiate from the central stock in Cat Creek (fig. 47) intrude the Treasure Mountain and Masonic Park Tuffs, as well as the overlying volcanics of Green Ridge (Platoro map). These relations, in conjunction with the focal position of the monzonite stock with respect to the outward-dipping volcanics of Green Ridge, favor an interpretation of the Cat Creek stock as intrusive into its comagmatic volcanics, an interpretation analogous to that developed for the Alamosa River stock. A similar paleotopographic argument, requiring the presence of a thick volcanic cover over the Cat Creek stock during its emplacement, also applies. These relations all suggest emplacement of the Cat Creek stock toward the end of eruption of the volcanics of Green Ridge, about 27 to 27.5 m.y. ago.

JASPER STOCK

The Jasper stock, a subequant body about 2 km across centered just north of the old mining district of Jasper (fig. 47, loc. D), is erosionaly exposed very near the level of its roof. The walls of the stock dip 30°-50° outward along much of the east and west sides, and where the northern contact is well exposed at the head of Burnt Creek (Platoro map), it is broadly flat, although irregular in detail. The stock is lithologically heterogeneous including porphyritic monzonite, porphyritic biotite rhyodacite, and fine-grained sparsely porphyritic intrusive rocks of andesitic composition and

texture. These diverse rock types are seemingly intergradational; but exposures are mostly poor and relations are widely obscured by intense hydrothermal alteration (fig. 61). The intrusive nature of the andesite, which is petrographically similar to many adjacent lavas of the Summitville Andesite, is evident from crosscutting contact relations, especially where the wallrocks have volcaniclastic textures. The margins of the stock consist mainly of the andesitic rocks; the porphyritic monzonite is exposed only locally in the interior, especially along the ridge between Jasper and Burnt Creeks (Platoro map). Monzonitic rocks would probably be more abundant deeper within the stock. Emplacement of the stock seems to be localized by the eastern ring-fault zone of the Summitville caldera (fig. 61), and the small dike-like body of monzonite exposed south of the alluvium around Jasper (fig. 47) may be a southern extension of the Jasper stock along this fault zone.

The Jasper stock, like the 29.1-m.y. Alamosa River stock, is younger than the Summitville caldera, as indicated by its intrusion along the ring-fracture zone. Also, the stock cannot be younger than about 28 m.y., as indicated by relations east of Spring Creek; there, the lower member of the Summitville Andesite has been hydrothermally altered by the Jasper stock but is unconformably overlain by the unaltered andesite-rhyodacite unit of the volcanics of Green Ridge (Platoro map). The 27.8-m.y. Fish Canyon Tuff occurs along this unconformity farther to the east, at the southeast end of Silver Mountain (Platoro map). Like the Alamosa River stock, the Jasper stock may be a subvolcanic intrusive related to an eroded vent for the upper member of the Summitville Andesite, which occurs as a chaotic near-source accumulation in adjacent parts of the Summitville caldera, as at Cornwalls Nose and in the Wightman Fork area.

BEAR CREEK STOCK CLUSTER

The Bear Creek stock is a steep-sided body of monzonite that is spectacularly exposed vertically for nearly 1 km on the rugged castellated ridge between Bear and Crater Creeks (fig. 47, loc. Eb). Satellitic to the northwest and north are two smaller stocks that are less well exposed at the mouth of Elwood Creek and east of lower Crater Creek (fig. 47, locs. Ee and Ec).

These three seemingly related stocks vary widely in texture: from exceptionally coarse equigranular monzonite (fig. 49A), to rather fine-grained equigranular monzonite (fig. 49B), to porphyritic monzonite (fig. 49C). Each of the three stocks locally shows this diversity of textures; relations among the different textural types have not been determined adequately but appear to be gradational, with porphyritic phases concentrated near contacts. The Bear and Crater Creek stocks seem to consist mainly of equigranular monzonite of variable

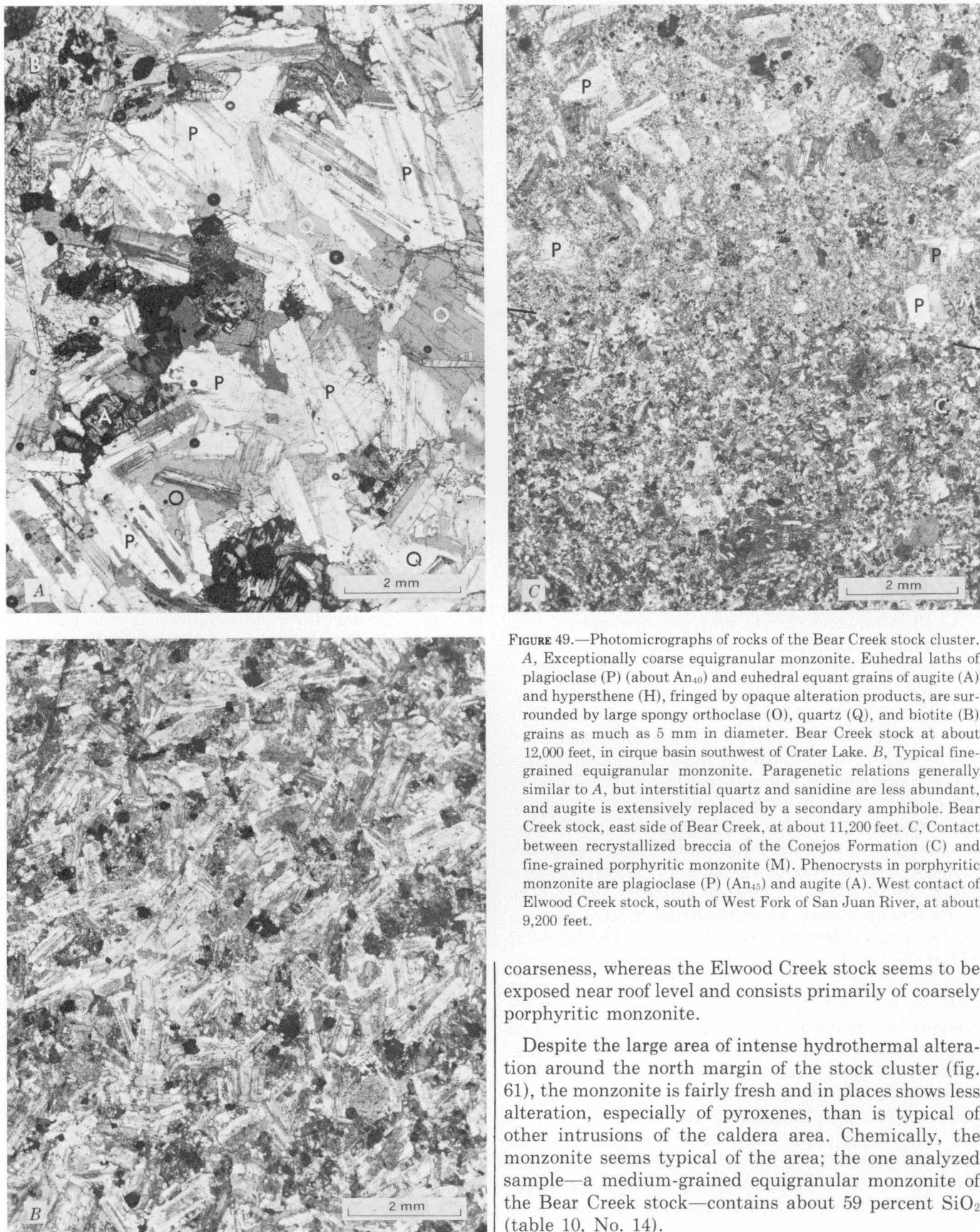


FIGURE 49.—Photomicrographs of rocks of the Bear Creek stock cluster. A, Exceptionally coarse equigranular monzonite. Euhedral laths of plagioclase (P) (about An₄₀) and euhedral equant grains of augite (A) and hypersthene (H), fringed by opaque alteration products, are surrounded by large spongy orthoclase (O), quartz (Q), and biotite (B) grains as much as 5 mm in diameter. Bear Creek stock at about 12,000 feet, in cirque basin southwest of Crater Lake. B, Typical fine-grained equigranular monzonite. Paragenetic relations generally similar to A, but interstitial quartz and sanidine are less abundant, and augite is extensively replaced by a secondary amphibole. Bear Creek stock, east side of Bear Creek, at about 11,200 feet. C, Contact between recrystallized breccia of the Conejos Formation (C) and fine-grained porphyritic monzonite (M). Phenocrysts in porphyritic monzonite are plagioclase (P) (An₄₅) and augite (A). West contact of Elwood Creek stock, south of West Fork of San Juan River, at about 9,200 feet.

coarseness, whereas the Elwood Creek stock seems to be exposed near roof level and consists primarily of coarsely porphyritic monzonite.

Despite the large area of intense hydrothermal alteration around the north margin of the stock cluster (fig. 61), the monzonite is fairly fresh and in places shows less alteration, especially of pyroxenes, than is typical of other intrusions of the caldera area. Chemically, the monzonite seems typical of the area; the one analyzed sample—a medium-grained equigranular monzonite of the Bear Creek stock—contains about 59 percent SiO₂ (table 10, No. 14).

The age of the Bear Creek and related stocks cannot be determined closely from field relations, but these monzonites seem to be among the youngest of the caldera area. The wallrocks are mainly lavas and breccias of the Conejos Formation, but the south margin of the Bear Creek stock intrudes the La Jara Canyon Member of the Treasure Mountain Tuff (contrary to the observations of Larsen and Cross 1956, p. 107). The three stocks also appear to be intruded along and are largely younger than the Elwood Creek fault system, which, to the east, offsets lavas of the rhyodacite of Park Creek (fig. 61, 65). No satisfactory younger limit can be placed on the age of these intrusives, however.

OTHER STOCKS

A small irregular intrusive exposed for less than 1 km² along the upper Wightman Fork (fig. 47, loc. F) consists of fairly uniform and unaltered fine-grained dark-gray phanerocrystalline rock that is slightly more mafic than other granitic stocks of the caldera area, containing only 56.6 percent SiO₂ (table 10, No. 18). The walls of the Wightman Fork intrusive converge upward, as shown by good exposures on the rugged northeast side of the stream valley (Platoro map). The exposed level appears to represent the upper part of a body that may increase in size downward, possibly to connect with the northeast end of the Alamosa River stock, which is exposed in Bitter Creek just across the divide to the west.

An elliptical stock of light-gray porphyro-aphanitic to equigranular monzonite, intrusive into lavas and breccias of the Conejos Formation, is well exposed in glaciated terrane over an area of about 2 km² at the cirque head of Canyon Diablo southwest of Conejos Peak (fig. 47, loc. G). This body, which has been examined only briefly, seems to lack the hydrothermal alteration that is associated with most other monzonitic stocks of the caldera area. A petrologically diverse swarm of intermediate-composition porphyro-aphanitic dikes that are well exposed on the cirque rim (Platoro map) are confined to the interior of this stock and may represent a late phase of the same igneous activity. The Canyon Diablo stock is slightly more silicic than most other monzonites of the caldera area, containing about 62.5 percent SiO₂ (table 10, No. 16). An age more precise than post-Conejos cannot be determined for the Canyon Diablo stock by field relations. Relations of the Summitville Andesite on the north side of Conejos Peak indicate an eruptive source outside the caldera to the southwest (fig. 39 and related text discussion) and suggest the possibility that this stock may be the subvolcanic core of another center for the intracaldera andesitic lavas.

A small stock about half a kilometer across, at the head of Cataract Creek (fig. 47, loc. H), is well exposed in glaciated terrane at the level of its roof and is relatively little altered. This stock is texturally heterogeneous

and ranges from plagioclase-augite porphyry having a greenish-gray aphanitic groundmass to equigranular fine-grained gray monzonite distinguished by the presence of hornblende in addition to augite and biotite. This is the only hornblende-bearing monzonite in the area. Chemically, this monzonite (table 10, No. 15) is little different from the nearby hornblende-free Bear Creek stock (table 10, No. 14). The Cataract Creek stock is intrusive into the Treasure Mountain Tuff, to a level at about the base of the La Jara Canyon Member. Detached roof remnants of recrystallized La Jara Canyon Member float within the stock at about the same level at which this tuff unit occurs in the walls, indicating that the stock was emplaced passively and did not significantly bulge its roof. Numerous related dikes cut the Cataract Creek stock and extend outward from it—many more than could be shown on the Platoro map.

Three large laccolithic bodies of fine-grained dark granitic rock are each exposed over several square kilometers along the southwest margin of the San Juan Mountains: at Jackson Mountain, V Mountain, and Squaretop (fig. 57, locs. I, J, K). These bodies are localized near the contact between the Conejos Formation and prevolcanic rocks. They were examined cursorily during this study, and little can be added to the descriptions given by Larsen and Cross (1956, p. 104-106). They may be somewhat more mafic than the granitic rocks near the Platoro caldera, as indicated by a single analysis from the V Mountain laccolith (Larsen and Cross, 1956, table 21, No. 2) that shows about 56 percent SiO₂. None of these intrusions has been dated radiometrically, and no very significant constraints can be placed on their ages from the field relations, other than that they are younger than basal Conejos Formation.

PORPHYRO-APHANITIC INTRUSIONS

Radiating out to the west from several of the granitic intrusions, especially the Alamosa River stock (fig. 47), are numerous dikes of porphyro-aphanitic texture that range in composition from andesite to rhyolite. Similarly textured intrusive rocks also occur locally as plugs and a few small stocks.

ANDESITIC ROCKS

Dark-gray dikes, commonly containing small phenocrysts of plagioclase and augite or plagioclase and hornblende but lacking biotite, are probably mostly andesitic in composition, although chemical analyses are lacking. A few of these may be sufficiently silicic to be rhyodacites, as judged from petrographic comparisons with analyzed lavas. Most of the andesitic dikes are narrow—rarely more than a few meters thick—and they are typically poorly exposed and are traceable along strike for only short distances. Many additional dikes of this group undoubtedly were overlooked in field map-

ping, in contrast to the more conspicuous silicic types, most of which are thought to have been mapped. In exceptionally good exposures, as where the country rocks are weakly consolidated mudflow breccia, a few individual andesitic dikes have been traced for at least 1 km.

The andesitic dikes form a well-developed radial system around the Cat Creek stock and are especially numerous around the west side of the Alamosa River stock (fig. 47). The andesitic dikes are the most numerous and widespread type in the Platoro area, and they extend outward farther than the more silicic types. The andesitic group of dikes seems to merge at the southwest margin of the volcanic field with the well-known swarm of mafic dikes that extends along the east edge of the San Juan Basin for at least 75 km, as far south as northern New Mexico (fig. 1).

The andesitic dikes are likely of several ages, which can only locally be satisfactorily distinguished. Many of them are undoubtedly part of the prolonged postcollapse igneous events around the margins of the Platoro caldera complex, especially the radial dikes around the Cat Creek and Alamosa River stocks. Some of these dikes have conspicuous petrographic similarities to nearby intermediate-composition lavas, such as the andesite-rhyodacite unit of the volcanics of Green Ridge east of the caldera complex, or the andesite of Summit Peak to the west. Other andesitic dikes are almost certainly related to the Conejos Formation, however, and these are difficult to identify confidently because of the similar lithologies. Best candidates for dikes of Conejos age are some with the distinctive platy-plagioclase texture (fig. 6) typical of many Conejos lavas, and also a few divergently trending east-west dikes in the western headwaters of the upper Conejos River that seem to be crudely radial to the Adams Fork volcano of Conejos age (fig. 7).

Two small plugs on opposite sides of the Adams Fork (Platoro map) may also be of Conejos age, especially the southern one that is intrusive into the flank of the Adams Fork cone. This plug consists of dense dark non-porphyritic rock that would be taken for an andesitic flow were it not exposed in crosscutting relations over a vertical distance of at least 250 m. The other plug, a light-gray porphyritic monolithologic intrusion breccia that is well exposed on the ridge crest between the Adams Fork and the head of the Alamosa River (Platoro map), is of less certain age.

RHYODACITIC ROCKS

Light gray or greenish-gray dikes and a few sills (fig. 50), which contain phenocrysts of biotite in addition to plagioclase and augite or hornblende, are probably mostly rhyodacitic, although some may be low-silica quartz latite. The phenocrysts in these biotite-bearing dikes are

typically larger than those in the andesitic dikes, and plagioclase crystals in some attain a diameter of at least 1 cm. The rhyodacitic dikes are thicker than andesitic ones—commonly 5-10 m or more—and they are better exposed and more continuous along strike. Several rhyodacitic dikes at the head of the Alamosa River (fig. 47), are continuously exposed for about 3 km.

The rhyodacitic dikes are probably entirely related to postcaldera volcanism, because this compositional type is rare in the Conejos Formation. Rhyodacitic dikes that radiate outward from the Cat Creek stock are similar in petrography to the porphyritic margins of this stock and to the satellitic laccoliths that have already been mentioned; these intrusive rocks may be comagmatic with the porphyritic rhyodacite unit of the volcanics of Green Ridge. Similarly, the dikes of this type in the Summitville area are probably related to eruption of the rhyodacite of Park Creek, and the great concentration of rhyodacitic dikes in the upper Alamosa River area (fig. 47) suggests that a large volcanic accumulation of porphyritic rhyodacite may once have been erupted there.

A subequant stock of biotite-bearing porphyry about 2 km across, which is petrographically similar to the rhyodacitic dikes, intrudes the intracaldera welded tuff of the La Jara Canyon Member on Cornwall Mountain (fig. 47, loc. L). This stock is compositionally transitional toward quartz latite (table 10, No. 20) and is similar in petrography and chemistry to the intracaldera La Jara Canyon (compare table 4, Nos. 5, 6), which represents the last volcanism from the caldera during collapse. This similarity, together with the central location of the stock in the resurgent block, suggests that the stock is a cupola of the magma body that caused resurgence. This interpretation, discussed more fully in the section on the Platoro caldera, is illustrated in cross sections of the Platoro map (sections C-C' and D-D').

A similar stock of much-altered porphyry characterized by a rather variable phenocryst content is rather poorly exposed at the south foot of Prospect Mountain and seems to be at the focus of the great concentration of rhyodacitic dikes along the upper Alamosa River (fig. 47; Platoro map).

Many of the best exposed intrusives of biotite rhyodacite porphyry (and also more silicic porphyritic bodies) are characterized by dark phenocryst-poor margins (fig. 50). In some of the intrusives, such phenocryst-poor margins may be due to flowage differentiation (Bhattacharji and Smith, 1964). In others, the abundance of mafic groundmass minerals in the marginal zone, as compared with the interior (fig. 50B, C), suggests the possibility of significant compositional differences within the magmas that formed different parts of a single intrusive.

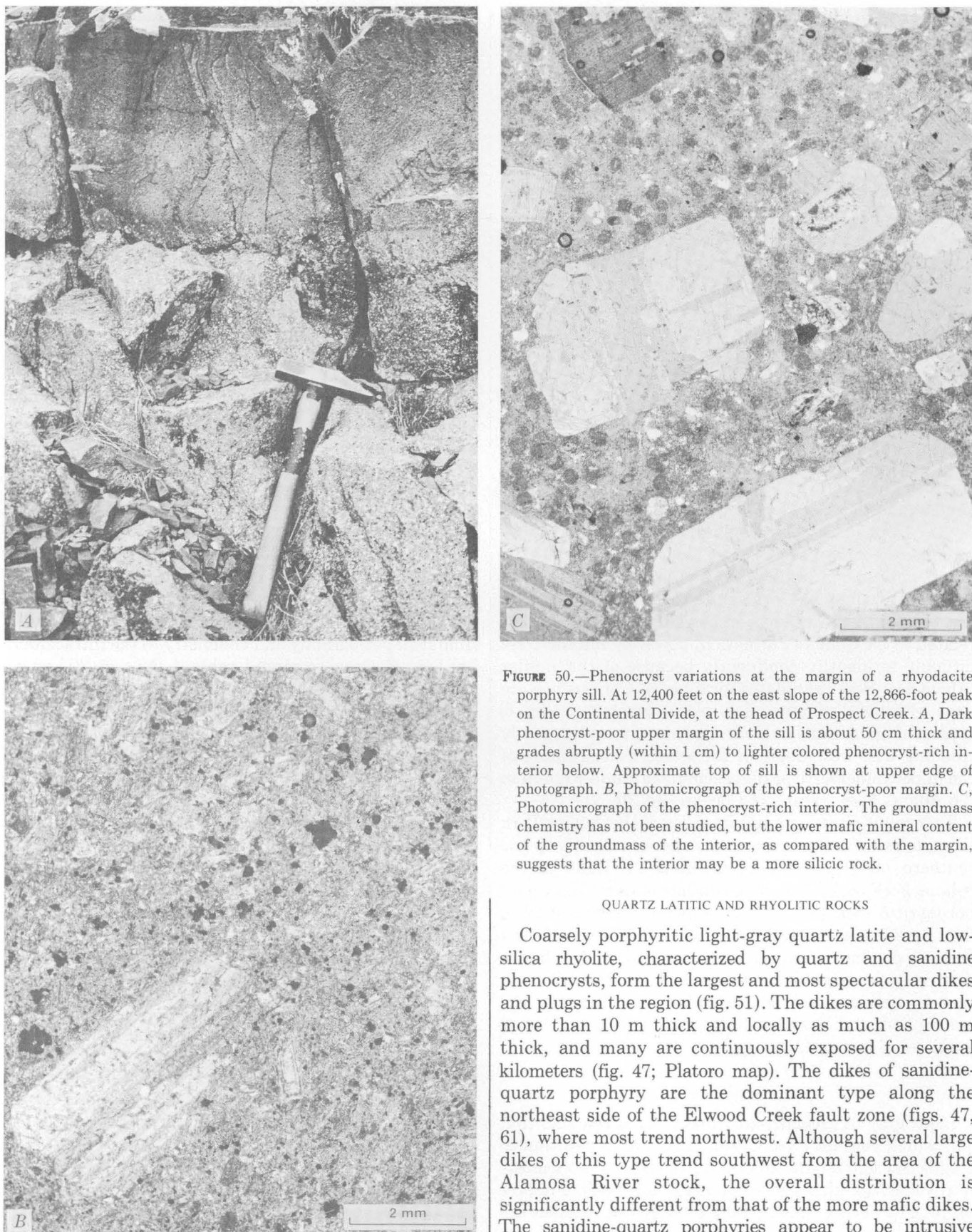


FIGURE 50.—Phenocryst variations at the margin of a rhyodacite porphyry sill. At 12,400 feet on the east slope of the 12,866-foot peak on the Continental Divide, at the head of Prospect Creek. *A*, Dark phenocryst-poor upper margin of the sill is about 50 cm thick and grades abruptly (within 1 cm) to lighter colored phenocryst-rich interior below. Approximate top of sill is shown at upper edge of photograph. *B*, Photomicrograph of the phenocryst-poor margin. *C*, Photomicrograph of the phenocryst-rich interior. The groundmass chemistry has not been studied, but the lower mafic mineral content of the groundmass of the interior, as compared with the margin, suggests that the interior may be a more silicic rock.

QUARTZ LATITIC AND RHYOLITIC ROCKS

Coarsely porphyritic light-gray quartz latite and low-silica rhyolite, characterized by quartz and sanidine phenocrysts, form the largest and most spectacular dikes and plugs in the region (fig. 51). The dikes are commonly more than 10 m thick and locally as much as 100 m thick, and many are continuously exposed for several kilometers (fig. 47; Platoro map). The dikes of sanidine-quartz porphyry are the dominant type along the northeast side of the Elwood Creek fault zone (figs. 47, 61), where most trend northwest. Although several large dikes of this type trend southwest from the area of the Alamosa River stock, the overall distribution is significantly different from that of the more mafic dikes. The sanidine-quartz porphyries appear to be intrusive



FIGURE 51.—Typical exposure of large quartz latite porphyry dike, about 40 m thick (for scale, note the truck parked near the left contact of the dike). Poorly exposed wallrock is upper member of Summitville Andesite. Biotite from this dike has yielded a K-Ar age of 25.8 m.y. (Lipman and others, 1970, table 4, No. 6). Summitville-Stunner road, at South Fork of Iron Creek in Schinzel Meadows.

equivalents of both the quartz latite of South Mountain and the rhyolite of Cropsy Mountain, but these rocks are so similar that further subdivision is at present impractical.

A few exceptionally well exposed dikes have spectacular marginal grooves along their contacts that plunge gently to moderately toward the area of the Alamosa River stock (fig. 52). Many of these dikes also have marginal vitrophyre zones—a feature rarely observed in the more mafic dikes.

Most of the larger sanidine-quartz latitic and rhyolitic intrusives are some distance outside the caldera complex (fig. 47). An elliptical quartz latitic plug about 1 km across, containing sparse large sanidine and quartz, intrudes the outflow Treasure Mountain Tuff along lower Ojito Creek (fig. 47, loc. M). This plug is structurally interesting because it acted as a piston that punched up its roof (probably lower tuff of the Treasure Mountain overlain by upper lava unit of the Conejos Formation) and also locally deflected upward the welded tuff wallrocks adjacent to the intrusive contact (Platoro map). This plug consists of quartz latite that contains



FIGURE 52.—Wall of large quartz latite porphyry dike displaying low-angle flow grooves. The grooves are 5-10 cm deep and about 25-50 cm apart; the plunge of the grooves and the strike of the dike are to the northeast, toward the area of the Alamosa River stock. At about 12,600 feet, on the west slope of the 12,866-foot peak on the Continental Divide, at the head of Prospect Creek.

about 67 percent SiO₂ (table 10, No. 23); it seems chemically and petrographically intermediate between the other porphyritic rhyodacites and quartz latites of the caldera complex.

In upper Park Creek, along the northeastern side of the Elwood Creek fault zone, a small steep-sided plug on the north side of the valley and a stubby inclined sill on the south side both consist of exceptionally light colored porphyry that contains abundant rounded quartz and small sanidine phenocrysts. Chemical analyses are not available, but these rocks seem to be exceptionally silicic, perhaps transitional to the Hinsdale rhyolite type.

At Sheepshead, just east of Prospect Mountain (Platoro map), a small plug of unaltered quartz-sanidine porphyry about 300 m across intrudes intensely hydrothermally altered Summitville Andesite. It seems petrographically identical to the rhyolitic lava flow on Lookout Mountain (fig. 44) and is almost certainly an example of an intrusive genetically related to the rhyolite of Cropsy Mountain. A much smaller plug of this type, only about 40 m across, crops out on the west slope of Lookout Mountain.

To the southwest, on the east side of Blanco Basin (fig. 47, loc. N), a large sill at least 100 m thick of typical quartz latite porphyry (table 10, No. 21) is poorly exposed beneath landslide deposits. Prior to erosion, it probably was continuous across the valley to the north with a petrographically similar irregular body which has the shape of a stubby dike that flattens downward into a sill-like orientation.

Farther to the southeast, near Trail Lake northeast of Banded Peak (figs. 13; 47, loc. O), a small plug of porphyritic quartz latite (67 percent SiO₂; table 10, No. 22) that contains large sanidine and quartz phenocrysts intrudes the ash-flow sequence as well as basalt flows of the Hinsdale Formation. This is the only place where a sanidine-quartz intrusive can be shown by field relations to be younger than Hinsdale basalt, although late porphyritic lavas of the caldera margin and basalt flows have overlapping radiometric ages in the Summitville area.

The porphyritic quartz latite and rhyolite intrusives are phenocryst rich (15-40 percent) except along borders, where some bodies are depleted in phenocrysts, as are the rhyodacites already discussed (fig. 50). Glassy margins of some of these intrusives have very intricate textures that indicate major phenocryst-groundmass disequilibrium. Sanidine phenocrysts are in places as much as 10 cm long; some are ovoid in outline, riddled with small glassy inclusions, and mantled by rims of sodic plagioclase (An₁₀₋₁₅). The quartz phenocrysts typically show remnants of bipyramidal outline but are rounded

and embayed by resorption. In addition to sanidine and quartz, these rocks contain smaller phenocrysts of sodic plagioclase (An₁₀₋₂₅), biotite, Fe-Ti oxides, and, commonly, hornblende. A few contain augite in place of, or in addition to, hornblende. Available analyses of the sanidine-quartz intrusives show a range of only 67 to 68 percent SiO₂ (table 10, Nos. 21-23), all near the compositional range of the quartz latite of South Mountain. Phenocryst variations (abundant quartz and sanidine) indicate that at least some sanidine-quartz intrusives, such as the plugs in upper Park Creek and at Prospect Mountain (Sheepshead), are more silicic and are similar to the rhyolite of Cropsy Mountain, to which many of the intrusives seem likely related.

In the rare places where cross-cutting contacts with other dikes can be observed, the sanidine porphyry dikes are invariably the youngest. Biotite from one dike has been dated at 25.8 m.y. (fig. 51; Lipman and others, 1970, table 4, No. 6). The close relations of other intrusives of this type with the 22.8-m.y. quartz latite of South Mountain and with the 20.2-m.y. rhyolite of Cropsy Mountain indicate that the sanidine porphyry dikes were emplaced over a time span of several million years.

LATE BASALT AND RHYOLITE (HINSDALE FORMATION)

Miocene and Pliocene volcanic activity in the southeastern San Juan region produced a widespread but thin veneer of basaltic lavas, with which are associated local rhyolite lavas and tuffs that are high in silica and alkalis. This basalt-rhyolite association contrasts markedly with the voluminous intermediate to silicic Oligocene lavas and ash-flow tuffs that make up most of the San Juan volcanic field. This contrast was implied by Larsen and Cross (1956), who placed all the late basalt and rhyolite of the San Juan region together in a single unit, the Hinsdale Formation. Usage of the term "Hinsdale Formation" is continued here, even though new radiometric and chemical data show that the postcollapse porphyritic lavas around the margins of the Platoro caldera complex bridge the transition from the intermediate-composition eruptions to the bimodal (basalt-rhyolite) associations. This upper Cenozoic bimodal volcanic association is believed to reflect fundamental aspects of the evolution of the San Juan Mountains and adjacent regions (Lipman and others, 1970; Christiansen and Lipman, 1972).

BASALTIC LAVAS

Although dark-gray basaltic lavas of the Hinsdale Formation are present over most of the southeastern San Juans only as scattered erosional remnants that cap high mesas (fig. 53), they appear originally to have con-

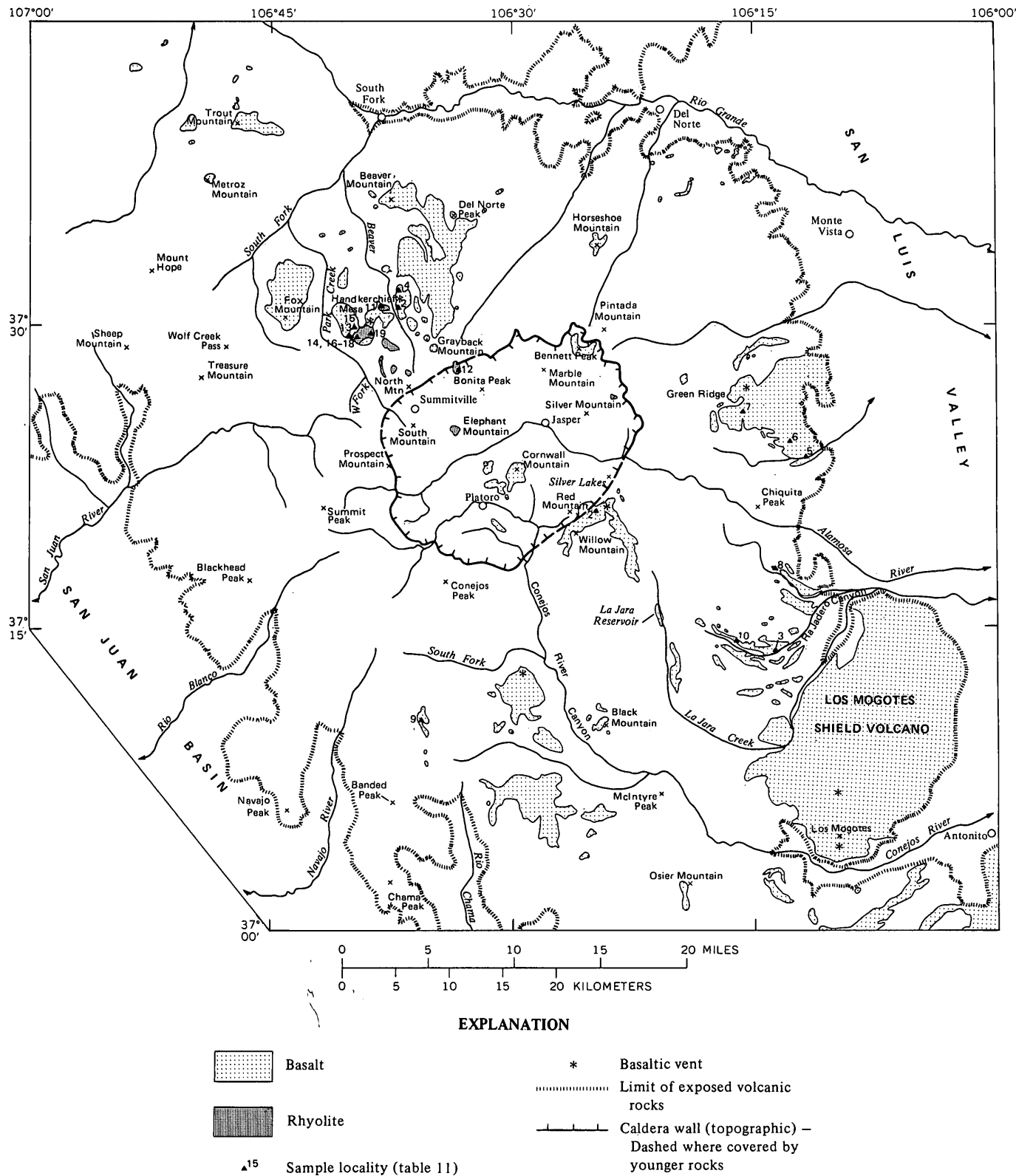


FIGURE 53.—Distribution of basaltic and rhyolitic lavas of the Hinsdale Formation. Based on mapping by P.W. Lipman, 1965-67, 1970-71.

stituted a widespread veneer over much of the region. At various places the basalt flows rest on most of the older units, and along the east front of the San Juan Mountains they interfinger with volcaniclastic rocks of the Los Pinos Formation. Individual flows are 5-50 m thick, but most are no more than 10 m thick. The thickest flows apparently represent ponded valley fillings. In places, as many as 15 thin flows with only minor interbedded sediments are exposed in cliff sections no more than 100 m high, as at Del Norte Peak, east of Red Mountain, and along the south flank of Los Mogotes shield volcano where it is cut by the Conejos River (fig. 53).

Patches of basaltic lava flows from near Red Mountain to south of the La Jara reservoir (fig. 53; Platoro map) were named the latite of Red Mountain and were mistakenly interpreted as Quaternary in age by Larsen and Cross (1956, p. 207). This age was assigned because these lavas were interpreted as having flowed down the modern drainage of La Jara Creek. More detailed mapping has demonstrated, however, that these basalts are preserved along the downthrown side of the La Jara Reservoir fault (fig. 61) and that a distinctive sequence of three flows east of the reservoir, that decreases upward in olivine phenocrysts, correlates across the fault with basalts mapped as Hinsdale Formation both by Larsen and Cross (1956, pl. 1) and in this study (Platoro map).

Vent areas for the basaltic lavas are mostly obscure, but a notable exception is the relatively young and little eroded Los Mogotes shield at the southeast edge of the area (fig. 53). Vent areas that lack surviving constructional form are distinguishable mainly by thick accumulations of bedded red-brown cinders and scoria blocks. In places these beds show primary dips of as much as 25° (fig. 60A), and constitute eroded remnants of cinder cones. Such cinder accumulation marking vent areas have been recognized in the Handkerchief Mesa-Beaver Creek area, south of the mouth of the South Fork of the Conejos River, at Horse Park at the east end of Green Ridge, and along the ridge east of Red Mountain (fig. 53). East of Red Mountain, at the head of the large Silver Lakes landslide scar (Platoro map), a central basaltic plug is surrounded by outward-dipping interbedded lava flows and cinders. (The reddish-brown beds interlayered with lavas on Red Mountain proper are not, as thought by Larsen and Cross (1956, p. 207), bedded cinders of a basaltic crater; rather, they are tuffaceous sandstones and conglomerates of the Platoro caldera fill that owe their conspicuous color to baking by an overlying intermediate-composition flow of Summitville Andesite.)

The Hinsdale basalts in the southeastern San Juan region appear to have erupted intermittently over much of Miocene and Pliocene time (Lipman and others, 1970). A basalt flow near Beaver Creek north of Summitville (fig. 53), believed to represent an old part of the

Hinsdale Formation because it predates associated silicic volcanism, yielded a whole-rock K-Ar age of 23.4 m.y. A basalt flow interlayered low in the Los Pinos Formation along La Jara Creek gave a whole-rock age of 17.7 m.y. A high flow and a dike from the relatively little eroded Los Mogotes shield volcano yielded ages of 4.7 and 5.3 m.y., respectively.

Although Pleistocene basalts do not appear to be present in the southeastern San Juan Mountains, young basalt flows in the Tusas Mountains of northern New Mexico that have been called the Brazos Basalt by Doney (1968) are only slightly eroded and are probably Pleistocene in age (Larsen and Cross, 1956; Bingler, 1968); these basalts are similar in petrography and chemistry to older basalts of the Hinsdale Formation to the north (Lipman, 1969).

Despite this great range in age, all late basaltic rocks of the southeastern San Juan region (and for that matter, the entire volcanic field) have generally similar petrography and chemistry. These basalts are typically dense and fine grained (fig. 54A); they contain small phenocrysts of olivine, commonly altered to iddingsite, and in places sparse phenocrysts of plagioclase or diopsidic augite. The groundmass of all the rocks consists of fine-grained plagioclase, olivine, and augite; the texture is typically intergranular but tends toward pilotaxitic in some of the most silicic lavas.

Rounded xenocrysts of quartz jacketed by finely granular augite, and of oligoclase mantled by andesine or labradorite, occur sparsely in many of the flows and abundantly in a few (Larsen and others, 1938; Lipman, 1969, pl. 2; Doe and others, 1969). The origin of these xenocrysts is in doubt. They may have been derived from Precambrian plutonic rocks (Doe and others, 1969); they may represent disequilibrium remnants from high-pressure crystallization in the upper mantle (Nicholls and Carmichael, 1971); or they may have resulted from mixing with phenocryst-bearing rhyolitic magma as discussed under "Mixed Lavas."

The basaltic rocks contain 50-59 percent SiO_2 (table 11). Most of the more silicic rocks contain abundant xenocrysts, suggesting that they represent contaminated lavas originally of more mafic composition. All the basalts are high in K_2O and in total alkalis. Even the basalts lowest in silica typically contain more than 1 percent K_2O , and this oxide is as high as 3-4 percent in some of the relatively silicic xenocystic basaltic andesites. Total alkalis range from 4 to 8 percent (fig. 55). Such high sodium and potassium contents apparently are characteristic of most upper Tertiary basaltic rocks from the Basin and Range and the Southern Rocky Mountains provinces (Moore, 1962; Leeman and Rodgers, 1970). A plot of total alkalis against silica for basalts of the Hinsdale Formation from the southeastern San Juan volcanic field shows that these basalts fall in the range of

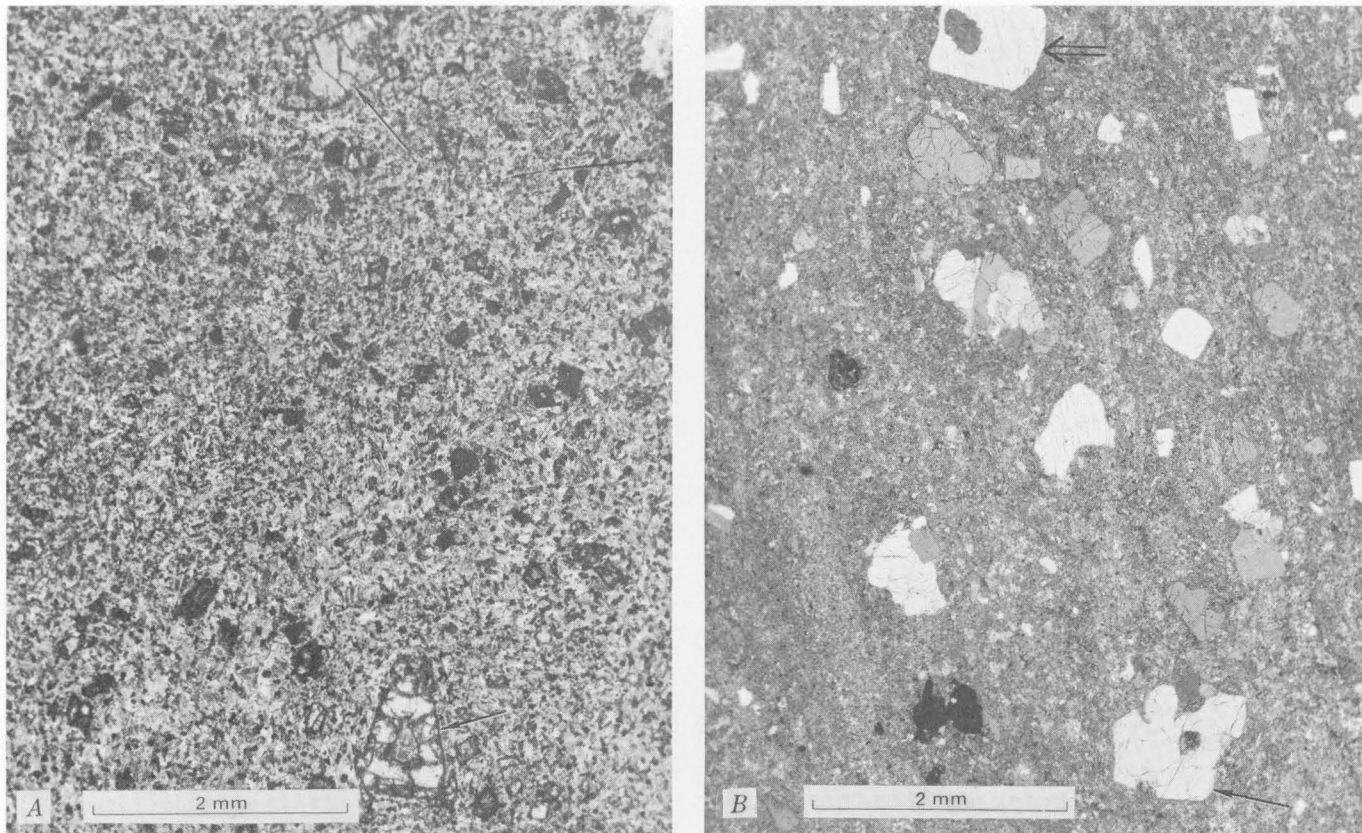


FIGURE 54.—Photomicrographs of common basalt and rhyolite types of the Hinsdale Formation. *A*, Dense basaltic lava, containing a few small olivine phenocrysts (arrows) in a fine-grained groundmass of plagioclase, olivine, augite, and Fe-Ti oxides. Phenocryst at the bottom is skeletal. High lava flow on west rim of Handkerchief Mesa, just north of the mixed-lava complex. Analyzed sample 13, table 11. *B*, Silicic alkali rhyolite, containing small phenocrysts of sodic

sanidine (Or_{40}), quartz, and sparse plagioclase, biotite, and Fe-Ti oxides. Single arrow indicates resorbed quartz phenocryst that shows remnant bipyramidal outline. Double arrow indicates euhedral sanidine enclosing rounded grain of sodic plagioclase (An_{15}) in extinction position. Sample is devitrified and displays weak flow layering. East side of rhyolite plug dome at Grayback Mountain. Analyzed sample 12, table 11.

to end
plag Sanidine

alkali basalts of Hawaii (fig. 55). In contrast, nearby upper Pliocene basalts of the southern San Luis Valley and the Rio Grande rift (Servilleta Formation) are much lower in alkalis and are tholeiitic in composition (fig. 55; Aoki, 1967; Lipman, 1969).

RHYOLITIC LAVAS AND TUFFS

Rhyolites of the Hinsdale Formation are petrologically distinctive white or light-gray rocks which are high in silica and alkalis and which are characterized by phenocrysts of quartz and sodic alkali feldspar. These contrast with the Oligocene rhyolites, which are lower in silica, contain both plagioclase and sanidine phenocrysts, and generally lack phenocrystic quartz.

Two major accumulations of rhyolitic rocks of the Hinsdale Formation have been recognized: one around the Summitville caldera (fig. 53) and the other around the Lake City caldera in the northwestern part of the volcanic field (fig. 1; Durango map). The rhyolites around the Summitville caldera form several small lava domes, each as thick as 200 m but nowhere covering

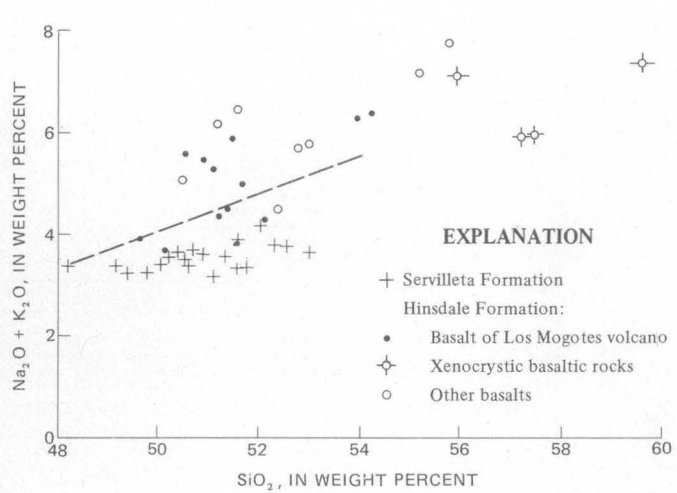


FIGURE 55.—Total alkalis and SiO_2 for basalts of the southeastern San Juan Mountains (Hinsdale Formation) and the northern end of the Rio Grande depression (Servilleta Formation). Dashed line is boundary between alkalic and tholeiitic basalts of Hawaii (Macdonald and Katsura, 1964). Analyses are from table 11 and from Aoki (1967) and Lipman (1969 and unpub. data).

PLATORO CALDERA COMPLEX, SAN JUAN MOUNTAINS, COLORADO

TABLE 11.—Analyses of basaltic and

[Sample localities shown in fig. 53. Analyses 6 and 7 are from Larsen and Cross (1956, table 25). Other major-oxide analyses are by rapid methods by titrative spectrographic analyses by J. D. Fletcher; other analyses

| Sample----- Field No----- Lab. No----- | Basalt | | | | | | | Xenocrystic basalt | | |
|---|--|--------------------------|------------------------|------------------------|------------------------|---------------------|------------|------------------------|---------------------------|---------------------------|
| | 1 67L-107-B W169529 | 2 70L-31-B W174433 | 3 66L-26 W168066 | 4 65L-32 W168063 | 5 66L-98 W168425 | 6 Con21 ----- | 7 ----- | 8 66L-20 W168065 | 9 66L-244-A W168069 | 10 66L-27 W168423-B |
| | Major oxides (weight percent), recalculated without H ₂ O and CO ₂ (original values listed separately below) | | | | | | | | | |
| SiO ₂ ----- | 50.5 | 51.2 | 52.4 | 52.8 | 53.0 | 55.43 | 55.89 | 57.4 | 57.5 | 59.6 |
| Al ₂ O ₃ ----- | 15.3 | 15.6 | 14.6 | 17.7 | 15.5 | 15.85 | 14.98 | 14.5 | 15.3 | 16.3 |
| Fe ₂ O ₃ ----- | 4.5 | 4.7 | 4.6 | 5.9 | 4.4 | 4.58 | 4.31 | 3.0 | 3.5 | 2.0 |
| FeO----- | 6.2 | 5.4 | 7.0 | 4.1 | 5.6 | 4.60 | 4.25 | 4.9 | 4.6 | 4.6 |
| MgO----- | 7.5 | 6.6 | 6.4 | 4.1 | 5.3 | 4.19 | 3.92 | 5.7 | 4.8 | 2.8 |
| CaO----- | 7.9 | 7.5 | 8.1 | 7.6 | 7.4 | 6.70 | 6.39 | 6.7 | 6.3 | 5.4 |
| Na ₂ O----- | 3.6 | 4.6 | 3.1 | 3.5 | 3.5 | 3.90 | 4.38 | 3.5 | 3.8 | 4.3 |
| K ₂ O----- | 1.5 | 1.6 | 1.3 | 2.2 | 2.3 | 3.32 | 3.38 | 2.4 | 2.2 | 3.1 |
| TiO ₂ ----- | 1.8 | 1.8 | 1.8 | 1.4 | 2.0 | 1.46 | 1.41 | 1.3 | 1.3 | 1.2 |
| P ₂ O ₅ ----- | .87 | .75 | .42 | .52 | .66 | ----- | .99 | .39 | .38 | .55 |
| MnO----- | .18 | .16 | .07 | .14 | .16 | .06 | .12 | .12 | .11 | .07 |
| TOTAL----- | 99.85 | 99.91 | 99.79 | 99.96 | 99.82 | 100.09 | 100.02 | 99.91 | 99.79 | 99.92 |
| H ₂ O+----- | 1.80 | 1.0 | .54 | .72 | .56 | .13 | .72 | .43 | .44 | .75 |
| H ₂ O----- | .65 | .71 | .36 | .88 | .40 | .61 | .42 | .47 | .46 | .65 |
| CO ₂ ----- | <.05 | <.05 | <.05 | .09 | .05 | ----- | ----- | .21 | <.05 | <.05 |
| CIPW norms (weight percent), from recalculated analyses | | | | | | | | | | |
| Quartz----- | ----- | ----- | 3.84 | 4.71 | 2.69 | 2.18 | 2.85 | 6.87 | 7.77 | 7.89 |
| Corundum----- | ----- | ----- | ----- | ----- | ----- | ----- | ----- | ----- | ----- | ----- |
| Orthoclase----- | 9.16 | 9.63 | 7.81 | 13.29 | 13.71 | 19.63 | 19.97 | 14.34 | 13.12 | 18.61 |
| Albite----- | 30.59 | 38.78 | 26.66 | 29.40 | 29.88 | 32.94 | 37.01 | 29.94 | 32.45 | 36.11 |
| Anorthite----- | 20.91 | 17.13 | 21.89 | 26.00 | 19.69 | 15.77 | 11.26 | 16.40 | 18.08 | 15.90 |
| Wollastonite--- | 5.38 | 6.40 | 6.57 | 3.39 | 5.25 | 7.28 | 5.84 | 5.90 | 4.36 | 3.02 |
| Enstatite----- | 13.78 | 5.60 | 15.95 | 10.18 | 13.32 | 10.42 | 9.77 | 14.10 | 12.06 | 7.09 |
| Ferrosilite----- | 3.71 | 1.13 | 6.21 | .51 | 3.68 | 2.37 | 2.14 | 4.65 | 3.65 | 4.84 |
| Forsterite----- | 3.50 | 7.63 | ----- | ----- | ----- | ----- | ----- | ----- | ----- | ----- |
| Fayalite----- | 1.04 | 1.69 | ----- | ----- | ----- | ----- | ----- | ----- | ----- | ----- |
| Magnetite----- | 6.59 | 6.79 | 6.63 | 8.59 | 6.44 | 6.64 | 6.24 | 4.40 | 5.12 | 2.95 |
| Hematite----- | ----- | ----- | ----- | ----- | ----- | ----- | ----- | ----- | ----- | ----- |
| Ilmenite----- | 3.33 | 3.48 | 3.47 | 2.72 | 3.83 | 2.76 | 2.67 | 2.50 | 2.49 | 2.32 |
| Rutile----- | ----- | ----- | ----- | ----- | ----- | ----- | ----- | ----- | ----- | ----- |
| Apatite----- | 2.05 | 1.78 | .99 | 1.23 | 1.55 | ----- | 2.33 | .93 | .91 | 1.30 |
| Minor elements (parts per million) | | | | | | | | | | |
| Ba----- | 680 | 3200 | 500 | 700 | 1000 | ----- | ----- | 700 | 700 | 1500 |
| Be----- | ----- | <2 | ----- | <1 | 2 | ----- | ----- | <1 | <1 | 1 |
| Ce----- | ----- | ----- | 100 | 100 | ----- | ----- | ----- | 100 | 300 | ----- |
| Co----- | 28 | 10 | 50 | 30 | 70 | ----- | ----- | 50 | 30 | 50 |
| Cr----- | 240 | 5 | 200 | 15 | 70 | ----- | ----- | 200 | 200 | 70 |
| Cu----- | 76 | 36 | 70 | 50 | 30 | ----- | ----- | 100 | 50 | 30 |
| Ga----- | 20 | 10 | 10 | 15 | 70 | ----- | ----- | 10 | 150 | 30 |
| La----- | ----- | ----- | 70 | 100 | 100 | ----- | ----- | 70 | 70 | 100 |
| Mo----- | ----- | ----- | 3 | 3 | ----- | ----- | ----- | 3 | 3 | ----- |
| Nb----- | ----- | ----- | 10 | 7 | 10 | ----- | ----- | 10 | 10 | 10 |
| Ni----- | 110 | 10 | 300 | ----- | 150 | ----- | ----- | 300 | 150 | 70 |
| Pb----- | ----- | ----- | 20 | 15 | 500 | ----- | ----- | 15 | 7 | 700 |
| Sc----- | 24 | 11 | 30 | 30 | 150 | ----- | ----- | 20 | 20 | 70 |
| Sn----- | ----- | ----- | ----- | ----- | 70 | ----- | ----- | ----- | ----- | 150 |
| Sr----- | 1400 | 200 | 700 | 1500 | 3000 | ----- | ----- | 700 | 1000 | 2000 |
| V----- | 190 | 90 | 200 | 200 | 150 | ----- | ----- | 200 | 200 | 150 |
| Y----- | 60 | <40 | 50 | 50 | 50 | ----- | ----- | 50 | 30 | 30 |
| Yb----- | ----- | <2 | 5 | 5 | 5 | ----- | ----- | 5 | 3 | 3 |
| Zr----- | 140 | 130 | 100 | 150 | 300 | ----- | ----- | 200 | 200 | 400 |
| Phenocrysts (volume percent) | | | | | | | | | | |
| Quartz----- | ----- | ----- | Tr. | ----- | ----- | ----- | ----- | 2 | 1 | Tr. |
| Sanidine----- | ----- | ----- | ----- | ----- | ----- | ----- | ----- | Tr. | 1 | ----- |
| Plagioclase----- | ----- | Tr. | ----- | 24.4 | ----- | 1 | 1 | 3 | 2 | ----- |
| Biotite----- | ----- | ----- | ----- | ----- | ----- | ----- | ----- | ----- | ----- | ----- |
| Hornblende----- | ----- | ----- | ----- | ----- | ----- | ----- | ----- | ----- | ----- | ----- |
| Augite----- | ----- | ----- | ----- | 7.3 | ----- | 1 | 1 | 1 | 1 | 5 |
| Olivine----- | 5 | ----- | 5 | 2.4 | 5 | ----- | ----- | 4 | 5 | Tr. |
| Opales----- | ----- | ----- | ----- | 1.1 | ----- | 1 | 1 | ----- | ----- | ----- |
| Groundmass----- | 95 | 100 | 95 | 64.8 | 95 | 97 | 97 | 90 | 90 | 95 |

See page 96 for sample descriptions.

rhyolitic lavas of the Hinsdale Formation

P. L. D. Elmore, Samuel Botts, Gillison Chloe, Lowell Artis, H. Smith, John Glenn, and James Kelsey. Minor-element analyses 1, 2, and 12 are quantified by semiquantitative methods by J. C. Hamilton. Tr., trace]

| Rhyolite | | Mixed-lava complex of Handkerchief Mesa | | | | | | | | Sample Field No. Lab. No. |
|---|--|---|------------------------------------|-------------------------------------|------------------------------------|------------------------------------|------------------------------------|---|---|---------------------------------|
| 11 65L-161-A W168067 | 12 70L-115-B W176185 | 13 70L-146-B W174649 | 14 70L-147-C W174651 | 15 70L-148 W174654 | 16 70L-147-D W174652 | 17 70L-147-E W174653 | 18 70L-147-A W174650 | 19 70L-151 W174655 | | |
| Major oxides (weight percent), recalculated without H ₂ O and CO ₂ (original values listed separately below)--Continued | | | | | | | | | | |
| 76.2 .32 .44 .15 | 76.6 .65 .32 .08 | 51.6 16.2 4.1 5.7 | 56.0 16.0 4.4 4.1 | 63.3 15.9 3.05 2.2 | 64.8 16.1 2.5 1.6 | 67.8 16.1 2.4 .60 | 68.0 15.8 2.2 .69 | 70.5 15.3 2.2 .2 | SiO ₂ Al ₂ O ₃ Fe ₂ O ₃ FeO | |
| .69 4.1 4.8 .11 .02 | .23 4.4 4.3 .06 .00 | 7.4 3.8 2.7 1.9 .64 | 6.4 3.98 3.2 .63 .37 | 4.4 4.2 3.96 .04 .47 | 2.9 4.3 5.1 .78 .19 | 1.7 4.5 5.5 .54 .13 | 1.6 4.7 5.5 .5 .14 | 1.2 4.03 5.5 .42 .06 | CaO Na ₂ O K ₂ O TiO ₂ P ₂ O ₅ | |
| .14 | .10 | .18 | .19 | .12 | .11 | .08 | .10 | .10 | MnO | |
| 100.07 .04 .16 <.05 | 100.04 .31 .14 <.05 | 99.82 1.2 1.0 <.05 | 99.97 .68 .92 <.05 | 99.94 .81 .29 <.05 | 99.88 1.0 .63 <.05 | 99.90 .37 .63 <.05 | 99.80 .66 .29 <.05 | 99.85 .55 .15 <.05 | TOTAL H ₂ O+ H ₂ O- CO ₂ | |
| CIPW norms (weight percent), from recalculated analyses--Continued | | | | | | | | | | |
| 35.00 .70 26.84 32.46 3.27 | 33.63 .89 25.53 37.40 1.15 | 0.00 0.00 15.8 32.2 19.3 | 2.4 .00 18.7 33.7 16.5 | 12.8 .00 23.4 35.2 13.1 | 13.2 .00 30.1 36.2 9.6 | 16.2 .00 32.7 38.3 7.3 | 15.6 .00 32.8 40.1 5.5 | 22.9 .63 32.7 34.1 5.6 | Quartz Corundum Orthoclase Albite Anorthite | |
| .38 .63 ---- ---- ---- | .20 .14 2.3 4.4 1.5 | 5.5 7.7 3.2 .00 .00 | 5.4 11.7 1.7 .00 .00 | 2.3 5.8 3.8 .00 .00 | 1.5 1.4 .00 .00 .00 | .15 1.4 .00 .00 .00 | .64 1.4 .00 .00 .00 | .00 .85 .00 .00 .00 | Wollastonite Enstatite Ferrosilite Forsterite Fayalite | |
| .47 ---- .21 ---- .05 | .94 .00 .11 .00 1.5 | 5.96 .00 3.7 .00 .87 | 6.4 .00 1.2 .00 1.1 | 4.4 .00 .08 .00 .46 | 3.3 .24 1.5 .00 .46 | .63 1.98 1.03 .00 .31 | 1.08 1.5 1.95 .00 .33 | .00 2.2 .64 .09 .14 | Magnetite Hematite Ilmenite Rutile Apatite | |
| Minor elements (parts per million)--Continued | | | | | | | | | | |
| 30 7 100 ---- ---- | 28 18 ---- 50 150 | 1500 1 200 30 200 | 1000 1 100 30 70 | 2000 1.5 500 15 50 | 1500 3 500 10 10 | 1500 3 500 10 10 | 1500 3 500 15 15 | 1000 5 500 5 5 | Ba Be Ce Co Cr | |
| 3 200 70 7 50 | 4 30 70 3 110 | 20 15 100 15 10 | 20 15 70 5 10 | 50 15 150 5 20 | 10 15 150 3 20 | 5 15 150 5 20 | 7 10 150 5 20 | 7 10 150 5 20 | Cu Ga La Mo Nb | |
| ---- 300 ---- 30 10 10 | 70 30 20 16 | 100 7 100 15 2000 | 100 15 70 10 1500 | 30 10 150 10 2000 | 30 10 150 10 700 | ----- 10 150 5 700 | ----- 15 150 7 700 | ----- 15 15 5 200 | Ni Pb Sc Sn Sr | |
| ---- 20 2 100 | 20 3 2 130 | 150 30 3 200 | 100 30 3 200 | 70 30 3 200 | 50 30 3 200 | 30 30 3 300 | 30 30 3 300 | 20 20 2 200 | V Y Yb Zr | |
| Phenocrysts (volume percent)--Continued | | | | | | | | | | |
| ---- | 2.9 6.3 ---- ---- ---- | 0.2 1.7 ---- ---- ---- | ---- | 0.5 3.2 3.2 .8 ---- | 0.8 7.5 7.4 .7 ---- | 0.6 7.4 .5 .8 ---- | 1.1 3.4 3.2 .8 ---- | Quartz Sandaline Plagioclase Biotite Hornblende | | |
| ---- | ---- | .9 4.1 1.2 88.7 | ---- | 1 3.6 ---- | .9 6 .9 85.8 | 1.1 Tr. 1.1 85.4 | 1.1 ---- | .2 ---- | Augite Olivine Opalines Groundmass | |
| 100 | 95.9 | 93.6 | 99 | 91.2 | 85.8 | 85.4 | 90.8 | | | |

TABLE 11.—Analyses of basaltic and rhyolitic lavas of the Hinsdale Formation—Continued

- SAMPLE DESCRIPTIONS
1. Dark-gray dense olivine basalt. Euhedral small olivine phenocrysts, mostly less than 1 mm in diameter and partly altered to iddingsite, are set in a very fine grained intergranular groundmass. Cliffs east of Beaver Creek, north end of Upper Beaver Meadow, at about 10,500 ft.
 2. Dark-gray dense olivine basalt. Consists of intergranular fine intergrowth of olivine, augite, and plagioclase. Only a few dusty resorbed plagioclase xenocrysts are as much as 1 mm in diameter. Conspicuous light-gray mottling on weathered surfaces is due to concentration of slightly coarser plagioclase in the groundmass. Lip of landslide headwall, 2.0 km northeast of Red Mountain, at 11,000 ft.
 3. Vesicular gray olivine basalt. Olivine phenocrysts are as much as 2 mm in diameter, euhedral with a tendency toward skeletal outlines, and marginally altered to iddingsite. Groundmass texture is intergranular but tends toward diktytactic: equant grains of augite, olivine, and opaques are between plagioclase laths about 0.5 mm long; interstices are filled by dusty brownish tachylitic material. One xenocryst of quartz in thin section is jacketed by rind of finely granular augite. Mouth of Ra Jadero Canyon, at about 8,400 ft.
 4. Exceptionally porphyritic gray basalt, containing abundant plagioclase laths 1-2 mm long, equant augite phenocrysts as much as 4 mm in diameter, and smaller altered olivines. Talus along Beaver Creek road, 0.2 km west of Race Creek.
 5. Dark-gray dense basaltic andesite. Small euhedral or skeletal olivine phenocrysts, mostly 1-2 mm in diameter and partly altered to iddingsite, are set in a relatively coarse pilotaxitic groundmass that contains plagioclase laths as much as 0.5 mm long. Southeast side of Green Ridge, along Cat Creek road, at about 8,100 ft.
 6. Vesicular black basalt. "The few phenocrysts are about 0.5 mm across. From northeast shoulder of Green Ridge, half way to top" (Larsen and Cross, 1956, table 25, No. 6).
 7. Similar to sample 6. No location given, other than Green Ridge (Larsen and Cross, 1956, table 25, No. 7).
 8. Gray vesicular xenocystic basaltic andesite. Xenocrysts of quartz as much as 5 mm across are embayed and rimmed by augite plagioclase forms anhedral grains 1-3 mm in diameter; clear cores (about An_{20}) are surrounded by a wormy, partly melted zone and, in places, by a more calcic overgrowth that forms a clear rim on the wormy zone. (For photomicrograph, see Lipman, 1968, pl. 2.) Ridge crest, about 0.7 km east of junction between Hot Creek and Ojito Creek.
 9. Dense gray xenocystic basaltic andesite, much like No. 8. At small pond, 0.7 km north of Trail Lake.
 10. Gray slabby andesite, containing elongate vesicles. Sparse resorbed xenocrysts of quartz. Augite phenocrysts, as much as 3 mm in diameter, are set in pilotaxitic groundmass. Ridge crest, north of Ra Jadero Canyon, at about 9,200 ft.
 11. Obsidian cores ("apache tears"), collected from glassy perlitic flow breccia, rhyolite of Beaver Creek. Contains less than 1 percent microphenocrysts of plagioclase (avg diameter about 0.1 mm). Dated sample (Lipman and others, 1970, table 5, No. 7). At about 11,400 ft, on north side of hill reaching altitude of 11,529 ft.
 12. Light-gray rhyolite, containing resorbed phenocrysts of quartz and sodic sanidine in finely devitrified flow-layered groundmass (fig. 54B). At 12,400 ft, on prominent rib, east side of Grayback Mountain.
 13. Fine-grained dense black basalt. Underlies mixed-lava complex. Petrographically much like No. 1. From main gully on southwest side of Handkerchief Mesa, at about 11,000 ft (fig. 54A).
 14. Basaltic phase of mixed-lava complex. See fig. 59B for description. At about 11,300 ft, 0.3 km southeast of locality of No. 13.
 15. Dark-gray nonporphyritic vesicular rhyodacite. Flow appears to overlie the mixed-lava complex along its northwest side. Contains about 1 percent microphenocrysts of augite that average about 0.5 mm in diameter. At about 11,400 ft, along north mesa rim, 0.9 km northeast of locality of No. 13.
 16. Typical gray xenocystic interior of main flow. Much like No. 8. Same locality as No. 14.
 17. Light-gray phenocryst-rich lower part of main flow. Resorbed feldspars and quartz are as much as 55 mm in diameter. Downhill from locality of No. 14, at about 11,100 ft.
 18. Scoriferous red-brown top of upper flow. Phenocrysts petrographically very similar to No. 17. Uphill from locality of No. 14, at about 11,400 ft.
 19. Light-gray rhyolitic phase. See fig. 59A for description. Northeast rim of Handkerchief Mesa, at about 11,700 ft, 0.5 km southwest of Poage Lake.

more than 1 km² in outcrop area. These erosional remnants tend to be preserved near their vents, and vent structures are exposed for three of the bodies—at Elephant and Grayback Mountains within the Platoro map area and at the head of Beaver Creek just to the north.

The Beaver Creek body, which intrudes nearly contemporaneous lower Miocene basalt of the Hinsdale Formation (Lipman and others, 1970), is perhaps the most interesting. The lowest exposures of this rhyolite are beds of crudely sorted pumice and ash fall that have primary dips of 15°-25° away from the vent area. At the vent, a steeply dipping dike of flow-layered devitrified rhyolite extends upward (fig. 56), flattens, and merges at the original surface of the pyroclastic cone with subhorizontally flow layered lava (fig. 57). At the base of the

lava flow, overlying the pyroclastic cone, is several tens of meters of poorly sorted unstratified flow breccia. A conspicuous cooling zonation is evident within the flow breccia. The lower zone consists of loose glassy blocks that become indurated and compacted upward to form a vitrophyre zone of hydrated gray perlite in which outlines of fragmental blocks are still faintly visible. Within the perlite are preserved scattered remnant nodules of nonhydrated black obsidian ("apache tears") and red-brown spherulites that mark the inception of devitrification (fig. 58). The spherulites increase upward in size and abundance and eventually coalesce to form completely devitrified rhyolite near the base of the originally fluidal lava, which is marked by well-defined subhorizontal flow layering (fig. 57).

Devitrified rhyolite of the Hinsdale Formation is a petrographically uniform light-gray, light-pink, or white chalky rock containing 10 percent or less small phenocrysts (1-2 mm in diameter) of quartz and alkali feldspar in subequal amounts, accompanied by minor biotite, sphene, and Fe-Ti oxides (fig. 54B). The quartz occurs as variably rounded and resorbed bipyramidal euhedra, and the alkali feldspar is sodic sanidine (Or_{40-45}). Two of the flow domes at the head of Beaver Creek contain sparse small phenocrysts of sodic plagioclase (about An_{15}), commonly enclosed in alkali feldspar phenocrysts (fig. 54B). These rocks are the most silicic in the volcanic field; the few available analyses show 76-77 percent SiO_2 (table 11, Nos. 11-12).

The only dated rhyolite of the Hinsdale Formation near the Platoro caldera complex, from the Beaver Creek vent-dome complex (figs. 56-58), has yielded an age of 21.9 m.y. by K-Ar analysis on obsidian and a date of 21.2 m.y. by fission-track methods. This rhyolite is partly intrusive into 23.4-m.y. basalt of the Hinsdale Formation



FIGURE 56.—Feeder dike for the Beaver Creek vent-dome complex is the ridge in foreground; it intrudes basalt flows of the Hinsdale Formation that form the mesa rims on both sides of the rhyolite.

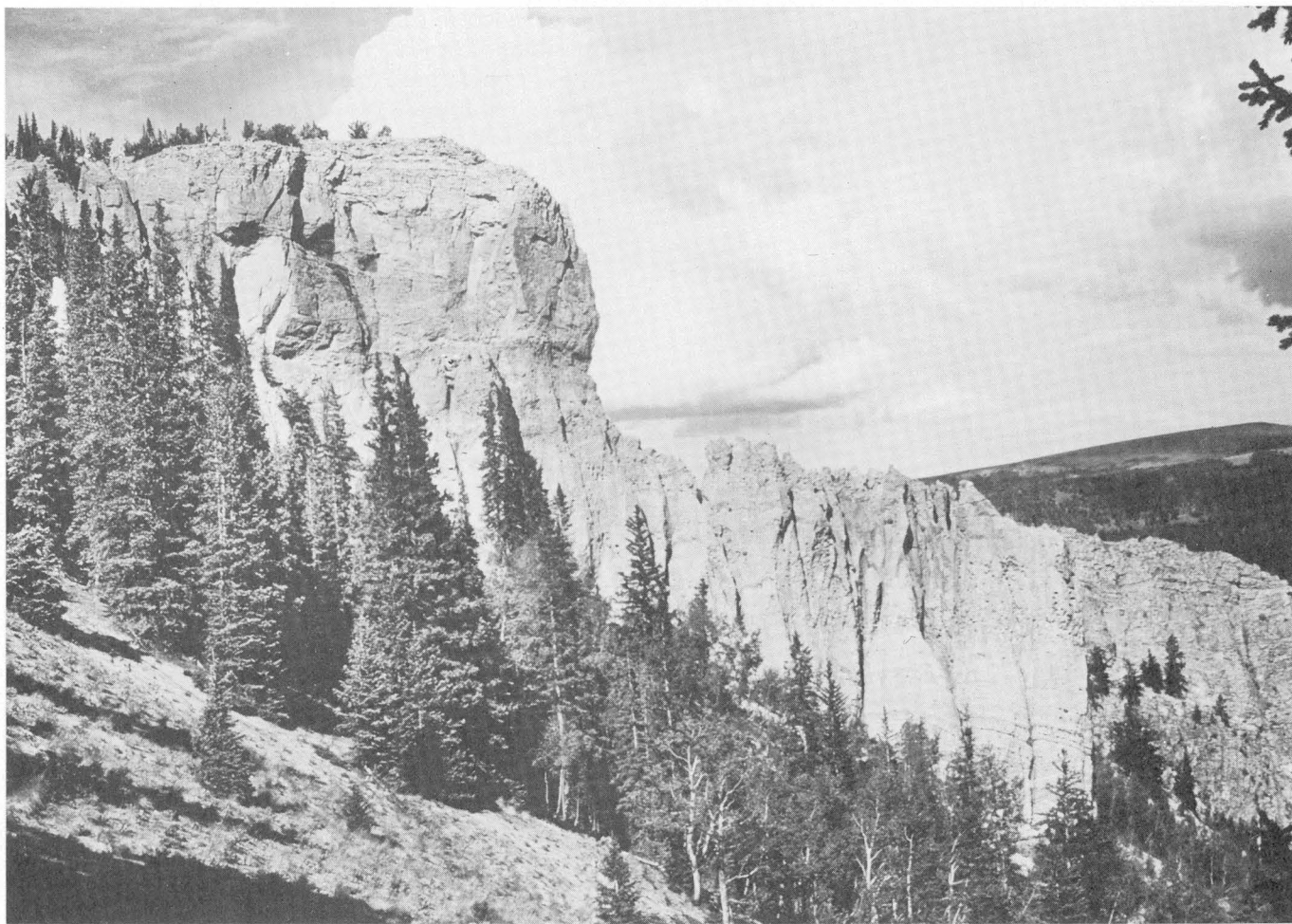


FIGURE 57.—Depositional units of the Beaver Creek vent-dome complex. Lowest visible dipping layers are bedded pumice fall of the pyroclastic cone. These are overlain by unstratified massive flow breccia, the upper part of which has been fused to a dark vitrophyre by the overlying lava flow, itself devitrified and subhorizontally flow layered. On the back side of this outcrop, the flow-layered lava is continuous into the steeply dipping vent dike (fig. 56), which cuts down through the dipping pumice fall of the pyroclastic cone.

(Lipman and others, 1970). The petrologically related rhyolite near the Lake City caldera (Sunshine Peak Tuff) in the northwestern part of the volcanic field has yielded similar K-Ar ages ranging from 22.0 to 22.9 m.y. (H. H. Mehnert, written commun., 1971), but a petrologically similar rhyolitic lava flow near No Agua, N. Mex., at the southeastern edge of the San Juan field, has a fission-track age of only 4.8 m.y. (Lipman and others, 1970).

MIXED LAVAS

At two localities near the Platoro caldera area, the rhyolitic and basaltic lavas of the Hinsdale Formation are intimately intermingled, forming rhyolite-basalt mixed-lava complexes that are similar to the well-known complex on Gardiner River in Yellowstone National Park (Wilcox, 1944). The smaller of the Platoro occurrences, on the northwest slope of Cornwall Mountain, is largely covered by talus and landslide deposits and hence was not studied in detail. The other mixed-lava

complex, however, is superbly exposed along the steep slopes of Handkerchief Mesa (fig. 53; Platoro map).

The Handkerchief Mesa mixed-lava complex occupies a broad northeast-trending paleovalley about 1 km wide, near the south end of Handkerchief Mesa (Platoro map), and it is well exposed on cliffs about 150 m high on both southwest and northeast sides of the mesa. Exposures are generally poor on the flat mesa top. Before eruption of the mixed lavas, this area had been a center for basaltic eruptions of the Hinsdale Formation, as indicated by dissected basaltic cinder cones on the northeast side of the mesa, some of which show primary dips as great as 20° (fig. 60A). On the southwest side of the mesa, a sequence of four or five rather typical fine-grained dense Hinsdale basalt flows underlies the mixed lavas (fig. 54A; table 11, No. 13). The rhyolitic Beaver Creek vent-dome complex (figs. 56-58) lies only about 1 km north of the Handkerchief Mesa mixed-lava complex, but age relations between these two bodies are unclear.

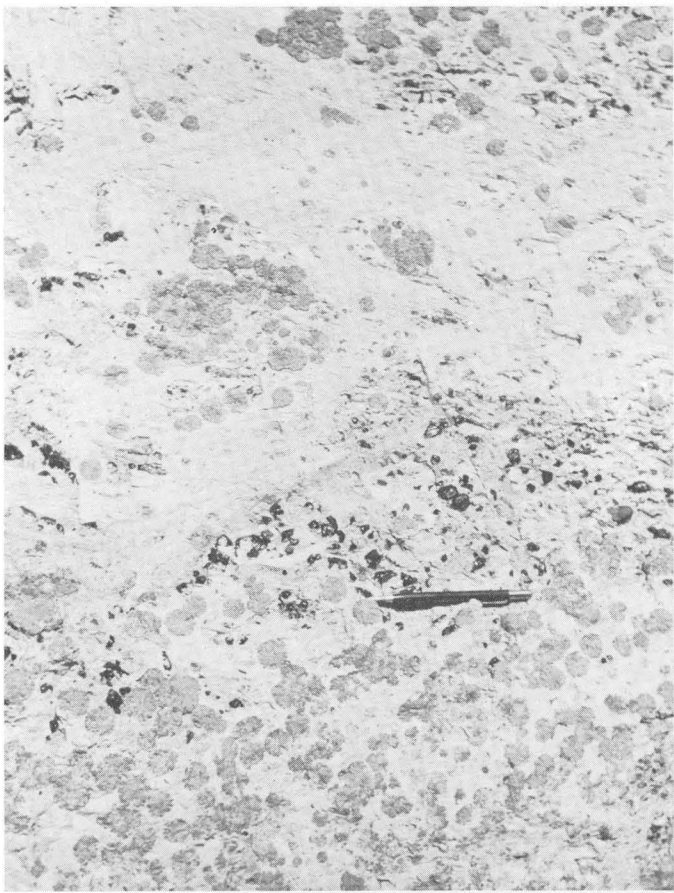


FIGURE 58.—Upper part of the vitrophyric zone of the Beaver Creek vent-dome complex. Initial stage of devitrification is development of scattered red-brown spherulites, 1-3 cm in diameter, commonly nucleated around a feldspar phenocryst. Gray hydrated perlite surrounding the spherulites contains scattered black nonhydrated obsidian nodules ("apache tears").

Relations are simplest on the southwest side of the mesa, where the main body of mixed lava forms a mass 100 m thick, interpreted as a flow, that is overlain by a flow 20 m thick having a scoriaceous top and a well-exposed basal flow breccia. Each flow, though heterogeneous in detail, tends to become more mafic and darker upward. The rhyolitic rock is light to medium gray and contains about 10 percent phenocrysts, including fairly large (up to 3 mm in diameter) sanidine, plagioclase, and quartz phenocrysts, accompanied by small biotite and augite (fig. 59A). All phenocrysts are rounded, resorbed, and generally texturally complex. In the higher, more mafic parts of these flows the feldspar and quartz phenocrysts become smaller and sparser and even more intricately resorbed (fig. 59B). The most mafic parts contain olivine and lack biotite. On the southeast side of the mesa, these compositional variations are generally gradational, and sharply bounded internal contacts are absent. In places, however, swirlly flow layering is defined by variations in

color, phenocryst content, and, presumably, chemical composition. Locally, both flows contain angular to rounded well-defined masses of sparsely porphyritic dark basalt (table 11, No. 14); these inclusions vary in size from a few centimeters (fig. 59C) to at least 5 m. Except for the mafic inclusions and local flow layering, however, these rocks are texturally and compositionally within the spectrum of xenocystic basaltic lavas of the Hinsdale Formation.

In contrast, on the northeast side of Handkerchief Mesa, chaotically heterogeneous relations in the mixed-lava complex are superbly exposed in the cliffs above Poage Lake (Platoro map), where the complex is intrusive into preexisting basaltic cinder cones (fig. 60A). Here, the relatively homogeneous intermediate-composition rocks that constitute the bulk of the mixed lavas on the other side of the mesa are sparse, and more obviously rhyolitic or basaltic types predominate. Abrupt compositional discontinuities occur every few meters in most outcrops, and no masses of relatively homogeneous rock are sufficiently large to be mapped, even on a 1:24,000 map scale.

Near the margins of the complex, light-gray rhyolitic dikes, sills, and irregular bodies a few centimeters to at least 10 m thick intricately vein bedded basaltic cinders of the local precomplex cinder cones (fig. 60A, B). These rhyolitic intrusives are completely devitrified, and the larger bodies have caused fusion, induration, local flowage, and peculiar patchy recrystallization effects in the bedded cinder deposits. In contrast, some of the smaller rhyolitic intrusives intricately intruded the basaltic cinders but did not significantly modify the textual features (fig. 60C, D).

The Handkerchief Mesa mixed-lava complex shows the same kinds of compositional and textural relations, as described by Wilcox (1944) for the complex on Gardiner River, that indicate that both the basalt and the rhyolite were simultaneously mobile and at least partly liquid at the time of eruption. Perhaps the most significant evidence for mixing is (1) the disequilibrium xenocrysts of quartz and alkali feldspar in the basalt that are identical to the phenocrysts of Hinsdale rhyolite and (2) the augite crystals of the rhyolite that resemble phenocrysts in basaltic phases of the complex. Although gradations are complete from basaltic to rhyolitic compositions, the end members are less extreme than typical rhyolitic and basaltic lavas of the Hinsdale Formation, suggesting that no completely uncontaminated magma has survived in the complex. Inclusions of basalt are preserved in rhyolitic matrix but never the reverse, as would be predicted from the lower solidus temperature of a rhyolitic melt. At the intrusive parts of the complex near Poage Lake, basalt inclusions that were derived from the country-rock cinder cones can be difficult to distinguish from basalt that was mobile

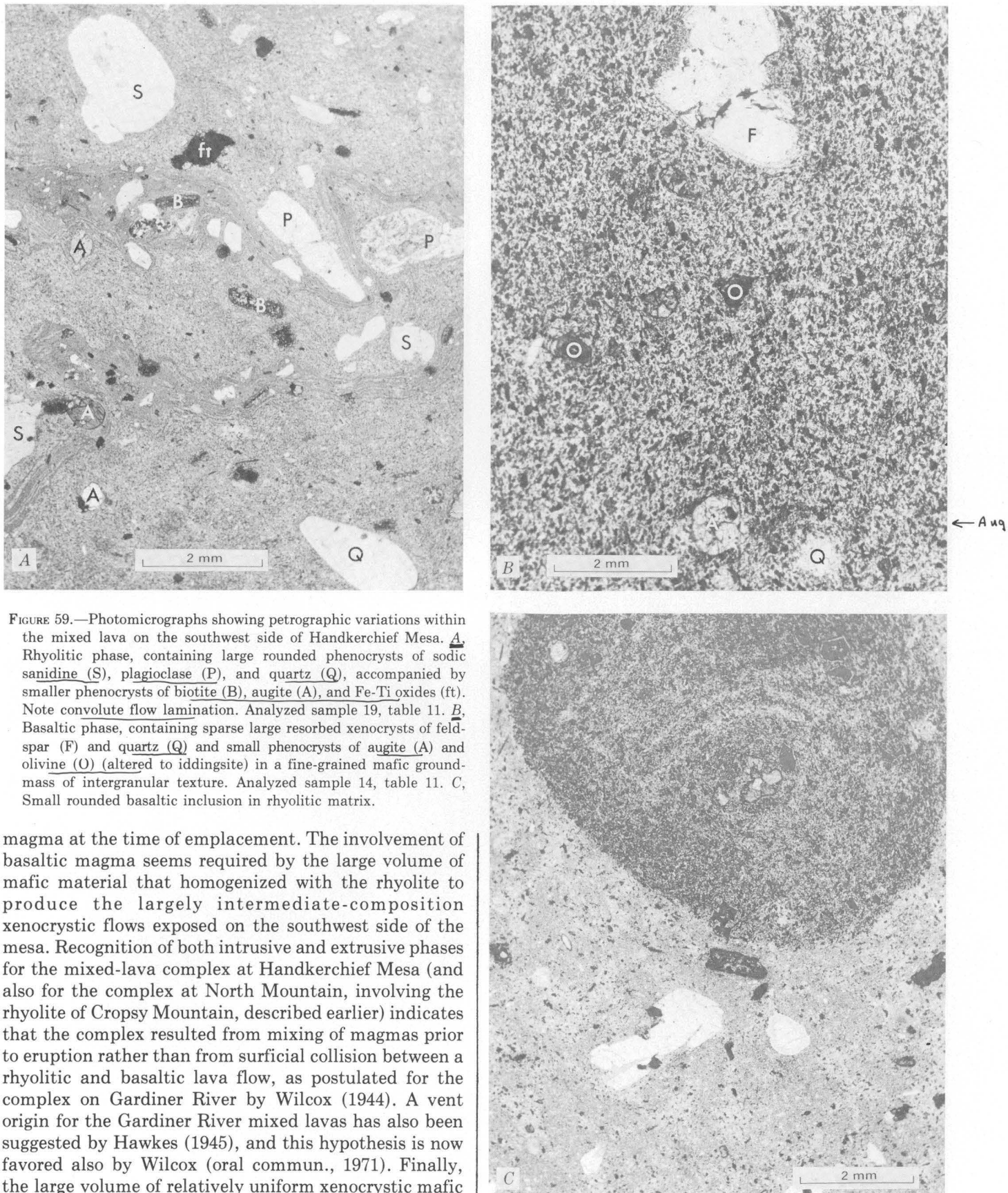


FIGURE 59.—Photomicrographs showing petrographic variations within the mixed lava on the southwest side of Handkerchief Mesa. *A*, Rhyolitic phase, containing large rounded phenocrysts of sodic sanidine (S), plagioclase (P), and quartz (Q), accompanied by smaller phenocrysts of biotite (B), augite (A), and Fe-Ti oxides (ft). Note convolute flow lamination. Analyzed sample 19, table 11. *B*, Basaltic phase, containing sparse large resorbed xenocrysts of feldspar (F) and quartz (Q) and small phenocrysts of augite (A) and olivine (O) (altered to iddingsite) in a fine-grained mafic groundmass of intergranular texture. Analyzed sample 14, table 11. *C*, Small rounded basaltic inclusion in rhyolitic matrix.

magma at the time of emplacement. The involvement of basaltic magma seems required by the large volume of mafic material that homogenized with the rhyolite to produce the largely intermediate-composition xenocystic flows exposed on the southwest side of the mesa. Recognition of both intrusive and extrusive phases for the mixed-lava complex at Handkerchief Mesa (and also for the complex at North Mountain, involving the rhyolite of Cropsy Mountain, described earlier) indicates that the complex resulted from mixing of magmas prior to eruption rather than from surficial collision between a rhyolitic and basaltic lava flow, as postulated for the complex on Gardiner River by Wilcox (1944). A vent origin for the Gardiner River mixed lavas has also been suggested by Hawkes (1945), and this hypothesis is now favored also by Wilcox (oral commun., 1971). Finally, the large volume of relatively uniform xenocystic mafic

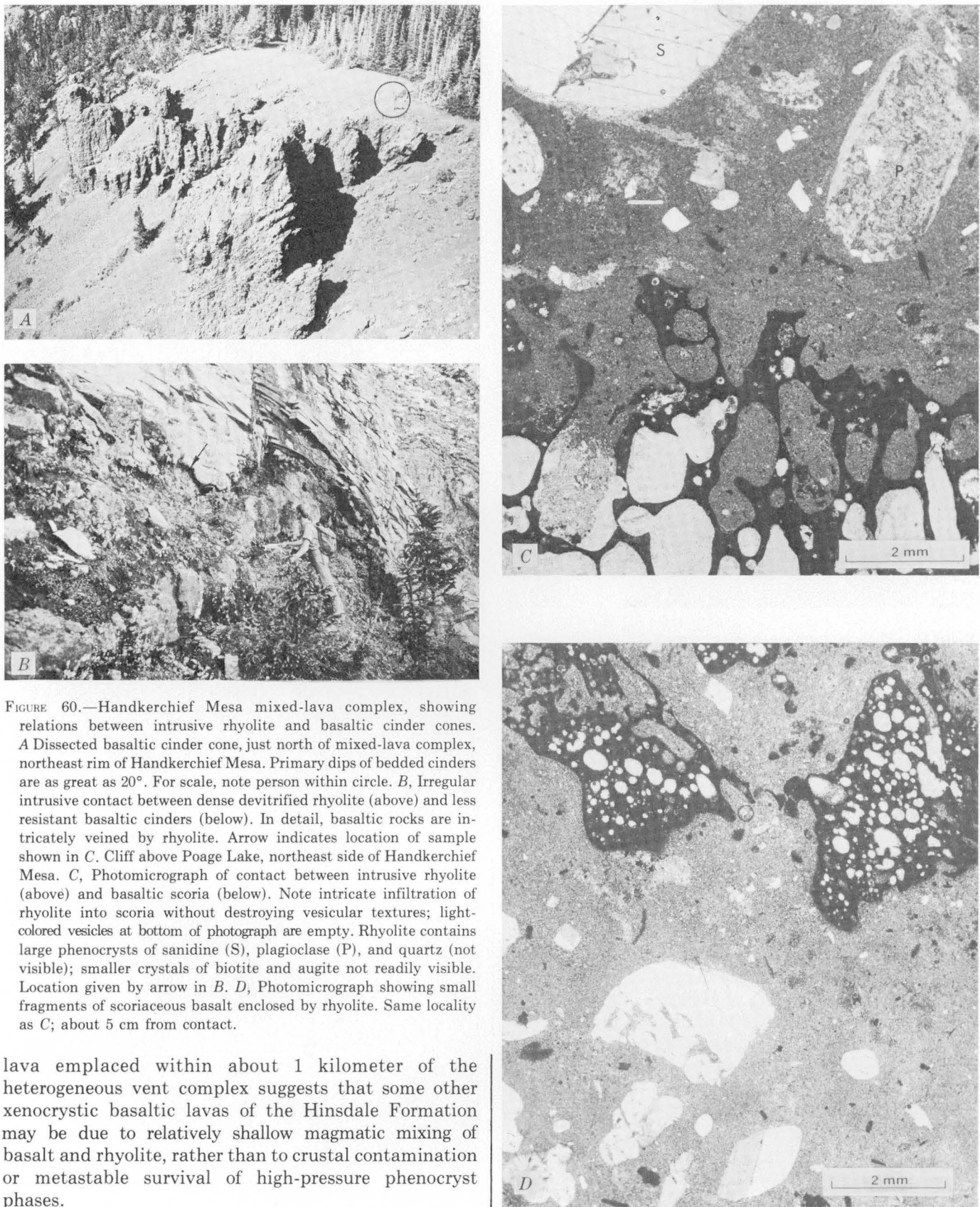


FIGURE 60.—Handkerchief Mesa mixed-lava complex, showing relations between intrusive rhyolite and basaltic cinder cones. *A*, Dissected basaltic cinder cone, just north of mixed-lava complex, northeast rim of Handkerchief Mesa. Primary dips of bedded cinders are as great as 20°. For scale, note person within circle. *B*, Irregular intrusive contact between dense devitrified rhyolite (above) and less resistant basaltic cinders (below). In detail, basaltic rocks are intricately veined by rhyolite. Arrow indicates location of sample shown in *C*. Cliff above Poage Lake, northeast side of Handkerchief Mesa. *C*, Photomicrograph of contact between intrusive rhyolite (above) and basaltic scoria (below). Note intricate infiltration of rhyolite into scoria without destroying vesicular textures; light-colored vesicles at bottom of photograph are empty. Rhyolite contains large phenocrysts of sanidine (S), plagioclase (P), and quartz (not visible); smaller crystals of biotite and augite not readily visible. Location given by arrow in *B*. *D*, Photomicrograph showing small fragments of scoriaceous basalt enclosed by rhyolite. Same locality as *C*; about 5 cm from contact.

lava emplaced within about 1 kilometer of the heterogeneous vent complex suggests that some other xenocystic basaltic lavas of the Hinsdale Formation may be due to relatively shallow magmatic mixing of basalt and rhyolite, rather than to crustal contamination or metastable survival of high-pressure phenocryst phases.

SURFICIAL DEPOSITS

Surficial deposits were mapped in the Platoro caldera area only where they are sufficiently thick and widespread to obscure the bedrock geology. Units distinguished on the Platoro map include glacial moraine, glacial outwash gravels, landslide deposits, rock glaciers, talus, colluvium, alluvial-fan deposits, and alluvium.

STRUCTURAL EVOLUTION

Pre-Tertiary structural features of the San Juan Mountains are little known because of widespread cover by younger volcanic rocks. The major Tertiary structures over most of the region are volcanic in origin and include numerous large calderas (fig. 1) that collapsed as a result of the voluminous ash-flow eruptions and the associated postsubsidence doming and faulting. In the southeastern area, however, these volcanic structures, largely of Oligocene age, are overprinted by later Cenozoic block faulting related to development of the Rio Grande rift depression in the San Luis Valley to the east (fig. 1, 61).

PRE-TERTIARY STRUCTURES

Pre-Tertiary structural features in the southeastern San Juan Mountains, although incompletely known, are significant to interpretation of some later Tertiary structures that seem to follow similar trends. Laramide deformation, which was superimposed on Precambrian and middle Paleozoic features (Muehlberger, 1960), began in the Late Cretaceous and probably continued until early Eocene time (Dunn, 1964). The major structures formed at this time are anticlinal and block-fault uplifts, similar to those elsewhere in the southern Rocky Mountains, including the Uncompahgre arch, Needle Mountains uplift, and Brazos arch (fig. 1; Kelley, 1957). These uplifts apparently partly or completely coalesced to produce a major northwest-trending highland almost 500 km long (King, 1969), although relations have been largely obscured along the middle sector by the Tertiary San Juan volcanic field. In the southeastern San Juan Mountains, Mesozoic sedimentary rocks that were folded during Laramide deformation underlie the Tertiary sequence along the southwest margin of the volcanic field. The axis of the main Laramide highland lay farther to the northeast under the volcanic cover, as indicated by the few small outcrops of Precambrian rocks along the lower Conejos River, the more widespread Precambrian exposures to the south in New Mexico, and the abundant Precambrian detritus in the prevolcanic Animas and Blanco Basin Formations.

TERTIARY VOLCANIC STRUCTURES

After erosion of the Mesozoic sedimentary cover from the Laramide uplifts and after concurrent fluvial deposition of the Blanco Basin Formation around margins of

these highlands, large-scale volcanism broke out—probably in early Oligocene time—over much of the southern Rocky Mountain region (Steven and Epis, 1968).

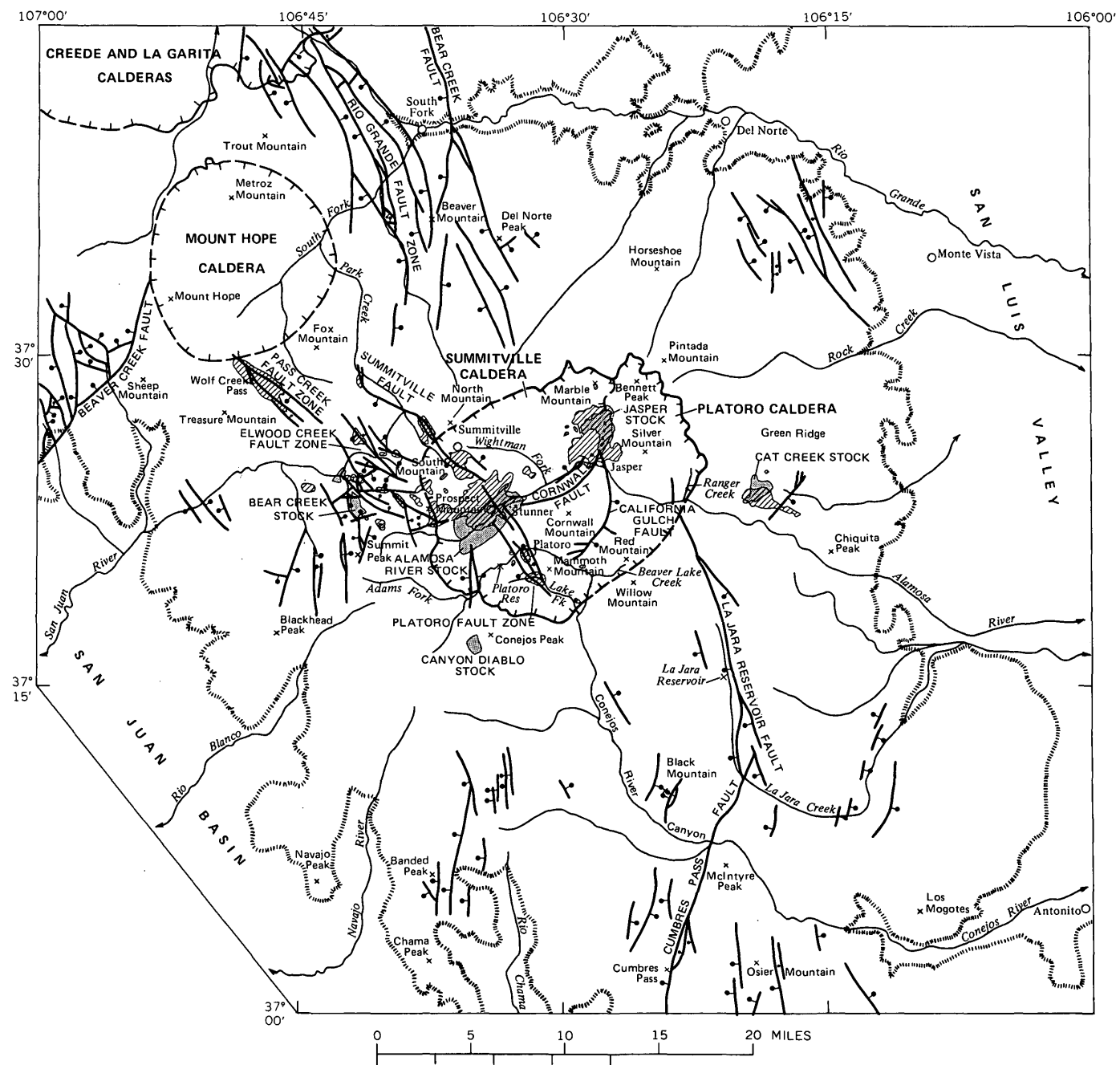
In the San Juan field, which constitutes the largest single erosional remnant of this middle Tertiary volcanism, major activity began about 35 m.y. ago (Lipman and others, 1970) when many stratovolcanoes began to form by eruptions scattered over most of the area of the now-preserved volcanic field. These eruptions were overwhelmingly intermediate in composition, consisting mainly of andesitic and rhyodacitic lavas that now form the vent facies of the Conejos and related formations. Some volcanoes were very large, with basal diameters of as much as 20 km and original heights of at least 3 km. Basins and valleys between these volcanoes were filled by mudflow and other volcaniclastic deposits washed from the primary volcanic structural features. These early intermediate-composition rocks constitute about two-thirds of the volume of the entire middle Tertiary activity in the San Juan field. Where now exposed, the vent and volcaniclastic facies together average about 1 km in thickness, and reconstructions of original distribution indicate that great additional volumes of these rocks have been removed by erosion.

During the early intermediate-composition activity, areas that were subsequently to be sites of the first calderas—such as the San Juan-Uncompaghre (Lipman and others, 1973), Bonanza (Burbank, 1932; Knepper and Marrs, 1971), and Platoro areas—were volcanic highlands marked by clusters of andesitic stratovolcanoes. Ash-flow tuffs are rare through most of the early intermediate sequence, but near the top of the sequence in the Platoro area, a change in the volcanic activity was premonished by eruption—from within the cluster of andesitic volcanoes there—of the rhyodacitic tuff of Rock Creek, the first sizable ash-flow sheet in the southeastern San Juan Mountains.

SAN JUAN CALDERA CLUSTER

The major middle Tertiary structural features of the San Juan field are the 14 or more calderas (fig. 1) and the related doming and faulting that resulted from eruption of the ash-flow sequence (table 1). The calderas range in diameter from less than 10 to almost 50 km (Durango map), and the largest caldera, La Garita, collapsed as a result of eruption of the most voluminous ash-flow sheet, the Fish Canyon Tuff. The volume of erupted material is roughly proportional to the size of related collapse, as seems to be generally true (Smith, 1960a, p. 834).

A few of the San Juan calderas are simple collapse depressions that were subsequently filled by younger volcanic materials, but most are resurgent calderas (Smith and Bailey, 1968) in which renewed magmatic



EXPLANATION

- | | | | |
|---------------------|--|---------------|---|
| [Hatched Box] | Hydrothermal alteration | [Dotted Line] | Limit of exposed volcanic rocks |
| [Cross-hatched Box] | Monzonite stocks | [Solid Line] | Caldera wall (topographic) – Dashed where concealed |
| [Dashed Line] | Fault – Dotted where concealed. Bar and ball on downthrown side | | |

FIGURE 61.—Distribution of faults, stocks, and areas of hydrothermal alteration in the southeastern San Juan Mountains. Based on mapping by P. W. Lipman, 1965-67, 1970-71, and by T. A. Steven, 1965-66.

pressure after collapse caused uplift of the central part of the caldera. The principal elements of little-eroded calderas of this type are a topographic wall and rim, a central mountain representing the floor of the caldera typically uplifted to heights as great or greater than the rim, and a moatlike structural valley between. The topographic walls of the calderas are characteristically scalloped by arcuate reentrants that resulted from landsliding and slumping shortly after initial caldera collapse. The actual structural boundary of caldera collapse is rarely exposed but lies approximately beneath the sedimentary or volcanic fill in the moat. The best preserved example of a simple resurgent caldera of this type in the San Juan field is the Creede caldera (fig. 62) (Steven and Ratté, 1965; Ratté and Steven, 1967). The older calderas of the San Juan field are variably complicated by later features, such as overlapping younger calderas, fill by younger volcanic units, faulting, and erosional modifications. All of these tend to cut across and obscure primary topographic and structural elements of the calderas.

PLATORO CALDERA

The Platoro caldera originated by collapse about 30 m.y. ago as a result of eruption of ash flows to form the La Jara Canyon Member of the Treasure Mountain Tuff. The northwestern part of the caldera has been complicated by further collapse that formed the Summitville caldera during eruption of later ash-flow sheets of the Treasure Mountain Tuff. The Platoro caldera is crudely rectangular, about 18 by 23 km, and trends northeast (fig. 61). The core of the caldera was resurgently uplifted,

shortly after collapse, to form the Cornwall Mountain resurgent block that is still topographically high, but otherwise the primary elements of the caldera are no longer well expressed topographically.

Eruption of the La Jara Canyon Member from Platoro caldera concurrent with subsidence is clearly indicated by several kinds of evidence. The La Jara Canyon tuffs were deposited more or less uniformly around the caldera, except for gaps related to preexisting topography. The La Jara Canyon was the first major ash-flow sheet in the southeastern San Juan region large enough to cause major caldera collapse, yet the Platoro caldera existed as a depression before completion of these eruptions, as shown by local plastering of the La Jara Canyon Member across the outer caldera walls (figs. 63, 64) and by the thick intracaldera accumulation of these tuffs. Within and near the caldera, the La Jara Canyon is more propylitically altered and more densely welded and contains more abundant and larger lithic fragments, all features that indicate near-source deposition.

PREMONITORY VOLCANISM

Stages in the development of Platoro caldera can be readily described in terms of the stages outlined by Smith and Bailey (1968) for resurgent calderas in general. Stage 1 in the resurgent-caldera cycle—regional tumescence—refers to magma insurgence, broad doming, and initial formation of a ring-fracture system.

Direct structural evidence of tumescence is absent in the Platoro area, which was by this time a constructional topographic highland of clustered andesitic



FIGURE 62.—View of Creede caldera from the north, showing central resurgent dome, outer topographic wall, and structural moat. Rio Grande has excavated the soft lacustrine caldera fill of Oligocene age that filled the moat. From Ratté and Steven (1967, color frontispiece).

stratovolcanoes. Indeed, such evidence is rare at resurgent calderas (Smith and Bailey, 1968, p. 636), with the notable exception of Timber Mountain caldera in Nevada (Christiansen and others, 1965). However, the initial events in development of Platoro caldera—the premonitory eruption of biotite-bearing quartz latitic and rhyolitic ash flows to form the lower tuff of the Treasure Mountain—seem to reflect the rise of silicic magma to a shallow crustal level for the first time in the area. Such rise of magma must be the basic condition for tumescence and doming.

In addition, development of the intermediate-composition volcano cluster of Conejos age and the eruption of the rhyodacitic ash-flow tuff of Rock Creek may well reflect earlier stages of tumescence. The inferred locations of vents for the clustered early andesitic volcanoes in the Platoro area are all close to the margins of the subsequent caldera collapse (fig. 5). This distribution may have been an early manifestation of broad insurgence and the resultant ring-fracture formation over a rising andesitic magma body that was subsequently to differentiate and feed the caldera-forming eruptions. A close relation between the andesitic lavas and more silicic ash-flow activity has already been inferred, and the development of several large early calderas of the San Juan field—Platoro, San Juan, Uncompahgre, and Bonanza—over clusters of andesitic stratovolcanoes seems significant in interpreting the origin and development of the ash-flow magmas.

ASH-FLOW ERUPTIONS AND CALDERA COLLAPSE

Ash-flow eruptions and caldera collapse represent both stage 2 and stage 3 of the resurgent-caldera cycle of Smith and Bailey (1968), but at Platoro caldera the stages overlapped too complexly to be discussed separately.

At some optimum time, for reasons not well understood but perhaps related to progressive effects of the premonitory ash-flow eruptions of the lower tuff, the ring-fracture zone became sufficiently well established to trigger eruption of much more voluminous ash flows. Once these culminating eruptions began, they produced numerous ash flows so rapidly that no evidence of erosion between flows has anywhere been observed, and only locally was interruption sufficient to permit development of even partial cooling breaks.

Because most of the early andesitic volcanoes had been extensively eroded and the intervening basins filled with the resultant detritus, these ash flows were able to spread 30-40 km in all directions from the ring-fracture zone, depositing approximately 350 km^3 of tuff (estimated by use of model in fig. 20) as the outflow sheet of the La Jara Canyon Member (fig. 14). This great single cooling unit of phenocryst-rich quartz latitic ash-flow tuff originally covered an area of nearly $5,000 \text{ km}^2$.

Before completion of these rapid and voluminous eruptions, drainage of much of the magma chamber caused the chamber roof to collapse along the ring-fracture zone and become a downdropped central cauldron block.

As a result of ash-flow eruptions continuing concurrently with caldera collapse, the later ash flows were largely ponded within the caldera; they wedge out part way up the outer walls (fig. 63). In a few low sectors of the caldera wall, the outflow sheet was deposited on the upper part of the wall and was draped over the rim (fig. 64). Within the caldera these tuffs accumulated to a thickness in excess of 800 m, as indicated by exposures on the resurgent block near Jasper from the valley bottom almost to the crest of Cornwall Mountain. The total original volume of the intracaldera tuff of the La Jara Canyon is estimated at 235 km^3 (fig. 20), although this figure is very approximate because the base of this accumulation is exposed only near its edges at the outer caldera walls. The intracaldera tuffs were somewhat more mafic and phenocryst rich than the initially erupted tuffs that formed the widespread thin outflow sheet. These differences probably reflect sorting during eruption, as well as limited preeruption magma differentiation that was similar in origin to the more extensive fractionation described for other ash-flow sheets in the San Juan field (fig. 34; Ratté and Steven, 1964).

The concurrence of eruption and collapse at the Platoro caldera clearly differs from the timing of these events at other carefully studied areas, such as the Valles caldera in New Mexico, where the last erupted units are no thicker inside the caldera than outside, demonstrating that eruption was virtually complete before major subsidence occurred (Smith and Bailey, 1968, p. 638). In the San Juan volcanic field, caldera collapse contemporaneous with eruption appears to have been a common process; other thick intracaldera accumulations of ash-flow tuff that demonstrate concurrent eruption and collapse are the Snowshoe Mountain Tuff at Creede caldera, the Carpenter Ridge Tuff at Bachelor caldera, and the Fish Canyon Tuff at La Garita caldera (table 3). Similar relations prevail at the San Luis and Lake City calderas (fig. 1; Durango map) and at several calderas in southern Nevada (Christiansen and others, 1965; Byers and others, 1969). Collapse probably occurs concurrently only with ash-flow eruptions of very large volume; in some such eruptions initial collapse appears to have coincided approximately with abrupt compositional changes in the ash-flow sheets (Lipman and others, 1966, p. F24-F25; Byers and others, 1969, p. 86).

The overlapping timing between eruption of the La Jara Canyon ash flows and collapse of the caldera shows that the collapse resulted from the withdrawal of magma, with the emptied part of the magma chamber being filled by the subsided block. This timing also

suggests that the volume of collapse should approximate the volume of erupted magma, as has been shown for other calderas of this type (Smith, 1960a, p. 834). A minimum volume of collapse at Platboro caldera can be estimated if the resurgent block, as bounded by the arcuate California Gulch fault on the southeast and by the hinge line of the Platboro fault zone on the southwest (fig. 61), is assumed to coincide approximately with the outline of original block subsidence before subsequent enlargement of the caldera by slumping and landsliding. This geometry suggests an original diameter of the subsided block of about 12 km and an original area of about 110 km², including the northwest sector, which subsequently collapsed into the Summitville caldera. The total vertical collapse of Platboro caldera, about 2.5 km, was estimated from the combined thickness of the postresurgence lavas within the caldera (about 1 km at Red Mountain) and the intracaldera La Jara Canyon Member (assumed to be 1.5 km; fig. 20). The resultant

calculated volume of collapse, 275 km³, is less than the crude approximation of the initial volume of the La Jara Canyon, 500-1,000 km³, or, preferably, 580 km³ (table 5). Alternatively, the volume of collapse can be calculated by using a cone-shaped model and by assuming collapse across the entire 20-km rim-to-rim diameter of the caldera; for a 2.5-km maximum subsidence at the center of the cone, the volume of collapse would be about 400 km³, still appreciably less than the estimated 580 km³ of the La Jara Canyon Member, although perhaps a not unreasonable agreement, considering the assumptions involved. An additional factor, not considered, is the probability that the precollapse andesitic volcano cluster within the caldera area had a mean elevation that was higher than the caldera rim; a mean excess height of these volcanoes of only 0.5 km could account for the entire discrepancy.

The caldera wall must have been modified by landsliding during collapse of the main cauldron block.



FIGURE 63.—View of Conejos Peak from Hillman Park road, showing densely welded cliff-forming ash-flow tuff of the La Jara Canyon Member (*T_{lj}*) within the caldera in depositional contact against the south caldera wall. All rocks at right side of photograph are lavas and breccias of Conejos Formation (*T_c*). Top rim, above La Jara Canyon Member within caldera, is intracaldera lava flow of the lower member of the Summitville Andesite (*T_{sl}*).



FIGURE 64.—South slope of Prospect Mountain, above Lake de Nolda, showing depositional relations at west wall of Platoro caldera. Subhorizontal units of Conejos Formation (T_c) and lower tuff (T_{tl}) of Treasure Mountain Tuff are truncated by topographic wall of caldera, over which La Jara Canyon Member (T_{lj}) is draped. Compaction foliations in the La Jara Canyon are as high as 60° on steepest slopes. Inside the caldera, subhorizontal dark lavas of the Summitville Andesite (T_s) lap out against the dipping welded tuffs of the La Jara Canyon Member.

The main ring-fracture collapse would have initially formed a steep-walled depression, at least 1 kilometer deep, into which the steep walls subsequently slumped, as indicated by large lobate scars and by shallow dips of the outer walls. A particularly large slump scar, more than 5 km across, is evident in the Bennett Peak area (fig. 61; Platoro map), and smaller scallops are evident elsewhere around the rim; such features are also characteristic of other large calderas, such as Valles in New Mexico (Smith and others, 1970), Timber Mountain in Nevada (Christiansen and others, 1965), and Creede in Colorado (Steven and Ratté, 1965, pl. 1). Dips on the outer walls of Platoro caldera are gentle (9° - 31°) at all localities (table 12) where the caldera wall has been preserved below the Summitville Andesite and is now exposed by erosion.

The paucity of landslide-derived megabreccia interlayered with or overlying the intracaldera La Jara Canyon is surprising, inasmuch as such deposits are sub-

stantial in otherwise analogous calderas such as Timber Mountain (Christiansen and others, 1965, p. B46), Creede (Steven and Ratté, 1965, p. 42), and Lake City (Lipman and others, 1973, p. 640). The necessary conclusion would seem that most slumping and landsliding at Platoro caldera occurred before deposition of the intracaldera La Jara Canyon Member at the levels now exposed, and such an interpretation is illustrated in the cross sections that accompany the map of the caldera

TABLE 12.—Measurements of slopes of Platoro caldera walls (from Platoro map)

| Position of wall | Locality | Vertical exposure (m) | Dip (degrees) |
|--------------------------|-------------------------------|-----------------------|---------------|
| North side | Bennett Mountain | 200 | 9 |
| Northeast side | Rock Creek | 110 | 10 |
| East side | Lower Alamosa River | 500 | 28-31 |
| Southwest side | Upper Conejos River (fig. 63) | 500 | 19 |
| West side | Upper Alamosa River | 150 | 29 |

(Platoro map, sections C-C'; D-D'). One small patch of monolithologic andesitic crackle breccia of landslide origin, derived from the Conejos Formation, is exposed as a lens (too thin to be shown on the geologic map) beneath the intracaldera La Jara Canyon along the southwest caldera wall just north of the Adams Fork of the Conejos River. These landslide deposits are the only recognized unit within the caldera that are likely to represent stage 4 of Smith and Bailey's resurgent-caldera cycle—preresurgence sedimentation and volcanism. No preresurgence volcanic activity has been identified within the caldera.

RESURGENT UPLIFT

The thick tuffs of the La Jara Canyon Member within the Platoro caldera are topographically and structurally high as a result of uplift of a central block shortly after caldera collapse; this uplift represents stage 5 of the resurgent-caldera cycle. Early resurgence is demonstrated by the presence of monolithologic talus breccias which are derived from the weakly welded upper part of the intracaldera La Jara Canyon and which intertongue with lavas of Summitville Andesite adjacent to the resurgent block. Such talus breccias are especially well exposed at the head of California Gulch and in an isolated outcrop on the east slope of Mammoth Mountain, opposite the mouth of Fisher Gulch.

The Platoro caldera differs in structure from other known resurgent calderas, where resurgence has resulted in formation of a fairly complete structural dome (fig. 62; Smith and Bailey, 1968). At Platoro caldera, the resurgence uplifted a block that dips 10°-25° homoclinally to the southwest and that is bounded on its east side by the arcuate California Gulch fault (fig. 61). This normal fault has a large displacement that accommodated most of the resurgent uplift, as indicated by the adjacent early-formed talus breccias and fanglomerates. The minimum displacement along the California Gulch fault is at least 900 m, as indicated by the differences in level between the top of the intracaldera La Jara Canyon Member, where exposed in the caldera moat barely above the level of the Alamosa River east of Jasper, and the highest exposures of this tuff on the resurgent block on Cornwall Mountain (Platoro map). The California Gulch fault splays and seems to decrease in displacement to the southwest. Additional curved faults, concave to the northwest and north and related to resurgent uplift, are probably buried beneath the rhyodacite of Fisher Gulch and the Summitville Andesite on the south side of the caldera. Any such concealed faults could not have displacements as large as the California Gulch fault. These arcuate faults probably mark the ring-fracture system along which subsidence occurred, because the La Jara Canyon Member on the main resurgent block is unfaulted and appears to have been

deposited over a core area that retained coherence during caldera collapse. The northwestern part of the resurgent block is missing, however, having caved into the younger Summitville caldera by collapse along the Cornwall fault (fig. 61).

On the southwest side of the resurgent block, the intracaldera La Jara Canyon tuff is almost continuously traceable across the filled caldera moat and has at most only small fault displacement. Dips of the tuff define a synclinal sag at the caldera moat; the tuff dips off the resurgent block and then rises again toward the depositional wedge-out on the caldera wall. This relation is well exposed along the Lake Fork of the Conejos River, where the moat-filling rhyodacite of Fisher Gulch covers the intracaldera tuff only for a distance of about half a kilometer east of Big Lake, and exposures of the intracaldera tuff are near the top of the unit, as indicated by the prevalence of weakly welded punky tuff. A similar relation is spectacularly exposed in the Platoro Reservoir area along the upper Conejos River, where weakly welded intracaldera tuff dips toward the moat from both the outer caldera wall (fig. 64) and the resurgent block, and the trough of the moat is filled by subhorizontal lavas and volcaniclastic rocks of Summitville Andesite. Here, the northwest-trending Platoro fault zone (fig. 61) approximately marks the hinged margin of the resurgent block, even though the faults of this zone have displacements limited to a few tens of meters, and at least some of this displacement occurred significantly later than uplift of the resurgent block.

The cause of the asymmetrical resurgence at Platoro caldera, in contrast to the typical domical uplift at other resurgent calderas (fig. 62; Smith and Bailey, 1968), is uncertain, but it may be related to asymmetry of the preceding subsidence. As already noted, the northeastern part of the Platoro caldera moat seems to have collapsed deeper than other areas, as indicated by the accumulation there of upper ash-flow units of the Treasure Mountain Tuff and the Fish Canyon Tuff, which are not found elsewhere within the caldera. This is not unique; mildly asymmetrical subsidence has been documented at Timber Mountain caldera (Carr and Quinlivan, 1968, p. 102), and a strongly asymmetrical trapdoor type of subsidence is evident for the Silverton and Cochetopa Park calderas in the San Juan field (fig. 1; Lipman and others, 1973, p. 640; T. A. Steven, written commun., 1971). At Platoro caldera, the side that subsided the most deeply also achieved the greatest resurgent uplift. This relation would favor a hydrostatic rebound hypothesis (Smith and Bailey, 1968, p. 648) for the origin of resurgent uplift at Platoro.

POSTRESURGENCE VOLCANISM

After resurgence was virtually complete, the rhyodacite of Fisher Gulch and the lavas of the lower

member of the Summitville Andesite accumulated within the caldera moat and lapped unconformably onto the uplifted central block. This volcanism marks the beginning of stage 6 of the resurgent-caldera cycle. The thick rhyodacite lava flow of Fisher Gulch was clearly erupted from within the caldera, along the southeastern ring-fracture zone; it represents a typical ring lava dome, similar to lava domes recognized at most other resurgent calderas. The sources of the andesitic lavas are less certain. Some may have flowed down the caldera walls into the moat from volcanoes beyond the rim, as indicated by relations already described in the Conejos Peak area (fig. 39). Elsewhere, as at the thick accumulation just east of Jasper, the source probably lay within the caldera, in this case to the west near the fault margin of the younger Summitville caldera. These lavas are 600-800 m thick in several parts of the Platoro caldera moat; where best preserved near Red Mountain against the southeast wall, they are almost 1 km thick.

These andesitic lavas represent a continuation of the same type of volcanic activity that characterized the Conejos Formation, with which they are readily confused in the field. Continued andesitic volcanic activity during ash-flow eruptions characterizes other parts of the San Juan volcanic field as well, and this relation is significant in reconstructing the petrologic evolution of the volcanism, as discussed later.

These intracaldera lavas are interlayered with and overlie shallow-water lake and deltaic sedimentary rocks in several areas, most notably near Rito Gato and Beaver Lake Creeks in the southwestern caldera moat and near Ranger Creek in the eastern part of the caldera (fig. 40). Association of postresurgence volcanism with lake sediments and caldera fill is characteristic of resurgent calderas (Smith and Bailey, 1968, p. 641).

The postresurgence evolution of the Platoro caldera was interrupted or ended by development of the Summitville caldera, although in a sense the post-collapse volcanism around the younger caldera forms a continuum with the postresurgence activity of Platoro caldera, especially in terms of compositional evolution of the lavas. Notably lacking, however, from the postresurgence activity around the Platoro caldera before development of the Summitville structure is any indication of hydrothermal alteration or solfataric activity that would be representative of stage 7, terminal activity of the resurgent-caldera cycle.

SUMMITVILLE CALDERA

Several features indicate the probable existence of a late collapse, here described as the Summitville caldera, related to upper units of the Treasure Mountain Tuff within the northwestern part of the Platoro caldera (fig. 61). The Ojito Creek and Ra Jadero Members were erupted after the moat of the Platoro caldera was nearly

filled by lavas of the lower member of the Summitville Andesite, because these tuffs are found within the caldera only in a few places above thick accumulations of andesitic lavas (Platoro map). The Ojito Creek and Ra Jadero tuffs are nearly coextensive with the La Jara Canyon Member and must have been erupted from the same general area. Although the volumes of these upper two members are much less than the volume of the La Jara Canyon, on the order of 50 and 120 km³, respectively (table 5), they are sufficiently large to indicate the likelihood of associated caldera collapse (Smith, 1960a, fig. 3). In addition to the volume and general distribution of the ash-flow tuffs, the interpretation of the Summitville caldera is based mainly on (1) the Cornwall fault, which is thought to represent the main ring-fracture fault on the southeast side of the caldera, (2) fragmentary exposures of the topographic wall, especially on the northeast side, and (3) the concentration of late igneous activity and mineralization around the caldera margins. Many aspects of the development of this caldera are poorly understood, however, because of the thick intracaldera fill (upper member of Summitville Andesite), the absence of postcollapse resurgence that might have exposed internal structures, and the extensive late intrusion and hydrothermal alteration.

The Summitville caldera is inferred to have collapsed twice, once after eruption of the Ojito Creek Member and again after the Ra Jadero. This interpretation is based on the hypothesis that both units are sufficiently large to have caused collapse, but recurrent collapse cannot be demonstrated from the structural features of the caldera. Near the northwest rim of the caldera, in upper Park Creek, the upper member of Summitville Andesite intervenes between the Ojito Creek and Ra Jadero Members and seemingly is continuous back into the western area of intracaldera andesite, indicating major caldera-fill volcanism at this time. In contrast, any lava erupted after Ra Jadero-related collapse seems to have been confined to the caldera area, because andesite has been recognized overlying this unit near the caldera rim.

ARCUATE FAULTING

The most conspicuous expression of the Summitville caldera is the arcuate northeast-trending Cornwall fault, first described and named by Patton (1917, p. 62). This fault truncates the central resurgent block of intracaldera La Jara Canyon tuff and juxtaposes lavas of the Summitville Andesite against the block for more than 800 m of elevation. Although the position, shape, and offset of this fault are thus anomalous with respect to the geometry of the Platoro caldera, features of the fault can be reasonably interpreted as an expression of the bounding ring-fracture zone on the southeast side of the Summitville caldera (fig. 61).

This fault cannot be a simple ring structure, against which the upper member of the Summitville Andesite was deposited unconformably after caldera collapse; appreciable renewed movement took place along the break after deposition of the adjacent andesite. The Summitville Andesite is locally altered, and about 25 cm of gouge occurs along the contact in the single outcrop where the actual fault zone is exposed, at about 11,400 feet just west of the prominent rib 1.5 km southeast of Cornwalls Nose. Significant downward displacement of the Summitville Andesite, along the Cornwall fault and also along a parallel fault to the north (fig. 61), seems required by the low position of the rhyodacite of Park Creek east of Wightman Fork (fig. 36), which seems to have accumulated in a structural depression. Paucity of detritus interlayered with the exposed Summitville Andesite—detritus that could have been derived from the adjacent intracaldera La Jara Canyon—also argues against interpretation of the contact as a simple depositional unconformity against a faultline scarp. Therefore, if the Cornwall fault originated as a ring fracture of the Summitville caldera, as seems likely, significant additional displacement occurred after the caldera was filled by Summitville Andesite.

Movement on the Cornwall fault appears to have been largely or entirely complete by the time of emplacement of the 29.1-m.y. Alamosa River stock and the approximately contemporaneous Jasper stock, both of which appear to be localized by the fault zone. This timing, predating eruption of the next succeeding major ash-flow sheet, the 28.1-m.y. Masonic Park Tuff, brackets the development of the Cornwall fault in the same narrow time span as indicated for the eruption of the Ojito Creek and Ra Jadero Members.

TOPOGRAPHIC WALL

About a 180° sector of the topographic wall of the Summitville caldera appears to have survived erosion, mainly on the north and northwest sides. Because the fill of Summitville caldera lacks good stratigraphic markers, such as the ash-flow units that so clearly define the Platoro caldera walls (figs. 63, 64), the wall is mostly defined by a boundary between lavas of the Conejos Formation and lithologically similar intracaldera andesite. Much of the wall is difficult to locate precisely, and exposures are poor in several key areas.

Relations are clearest on the northeast side, near Marble Mountain, despite the fact that both caldera wall and caldera fill seem to be members of the Summitville Andesite. In this area, mapped as upper member is a distinctive sequence of interlayered sparsely and coarsely porphyritic lavas overlain by the silicified white bedded tuff of Marble Mountain. These rocks lap unconformably onto a markedly different sequence of lavas and volcaniclastics of the lower member of the

Summitville Andesite on the caldera wall to the east. In comparison with lower member andesites in the Platoro caldera, the upper member lavas within the Summitville caldera tend to be exceptionally thick, poorly stratified, and highly brecciated. Also, flows containing large phenocrysts of plagioclase are more abundant in the upper member than in the lower member.

West of Marble Mountain, the caldera wall is mostly concealed by surficial deposits and by thick viscous flows of the rhyodacite of Park Creek that cover rough topography interpreted as the caldera margin. A small patch of outflow La Jara Canyon Member resting on Conejos Formation along the Summitville-Del Norte road just north of the Platoro map area (fig. 14; Durango map) provides a key northern constraint on the location of the caldera wall in this sector.

In a small area just east of North Mountain, the Summitville caldera wall seems to be marked by the contact between dark sparsely porphyritic andesite, which is continuous over a large area to the south and is considered typical of the upper member of Summitville Andesite, and the underlying more altered red-brown lavas, which contain abundant small phenocrysts of plagioclase, augite, and, in places, hornblende and which are interpreted as part of the Conejos Formation.

The location of the caldera wall southwest of Summitville is uncertain. Both caldera wall and caldera fill seem to be members of the Summitville Andesite, but the contact is obscured by intense hydrothermal alteration. The contact between members of Summitville Andesite, shown southwest of the Alamosa River stock (fig. 36), is tenuous because it depends on uncertain identification of locally intervening weakly welded ash-flow tuffs within the Platoro caldera as the Ra Jadero Member and the upper tuff of the Treasure Mountain.

POSTCOLLAPSE VOLCANISM

Perhaps the most interesting feature of the evolution of the Summitville caldera is the prolonged sequence of postcollapse volcanism and related alteration and mineralization, beginning with the filling of the caldera to overflowing by the upper member of the Summitville Andesite. Whereas only minor silicic postcollapse volcanism and alteration occurred around margins of the main Platoro caldera, a complex sequence of postcollapse igneous activity continued for almost 10 m.y. around margins of the Summitville caldera. Structural features of the younger caldera and associated igneous activity also seem to have localized most of the major alteration and mineralization in the southeastern San Juan Mountains, as discussed in the section on economic significance. Postcollapse intermediate to silicic lava flows and related intrusives, localized around margins of the Summitville caldera,

were emplaced over the interval 29-20 m.y., with dated events at 29.1 m.y. (Alamosa River stock), between 27.8 and 26.7 m.y. (lower flows of rhyodacite of Park Creek that wedge between Fish Canyon and Carpenter Ridge Tuffs), <26.5 (upper rhyodacite of Park Creek that overlies the Snowshoe Mountain Tuff), 25.8 m.y. (dated dike of quartz latite porphyry), 22.8 m.y. (quartz latite of South Mountain), and 20.2 m.y. (rhyolite of Cropsy Mountain). More extensive dating of the voluminous postcaldera lavas and intrusives would likely disclose additional events. Isopach maps of the young ash-flow sheets that were erupted from other calderas northwest of Platoro (fig. 1) show variations in distribution and thickness in the Platoro area (figs. 26, 30, 31) that correlate with the growing constructional topography of these caldera-margin volcanoes.

CALDERA-RELATED REGIONAL FAULTING

Within the region of the San Juan caldera cluster, three major fault-graben systems trend northwest, between or tangential to several of the major calderas (Durango map). These include the Clear Creek graben that tangentially connects the west sides of Creede and San Luis calderas (Steven, 1967), the Rio Grande fault zone that runs from the northeast side of Creede caldera across the La Garita caldera wall toward the north side of the Summitville caldera (fig. 61), and the Pass Creek-Elwood Creek-Platoro fault system that connects Mount Hope caldera with the Platoro caldera complex (fig. 61). Locally determinable ages of faulting show that these major zones had lengthy histories of recurrent movement, but their initiation and much of their total displacement seem to have occurred approximately contemporaneously with ash-flow activity and major caldera collapse. From a broad perspective, these fault zones appear to reflect attenuation related to a *general resurgence* of the roof of the composite batholith that is inferred to underlie the entire caldera cluster (Plouff and Pakiser, 1972), in contrast to the *specific resurgences* of individual calderas, each of which is inferred to overlie a shallow cupola of the batholith.

RIO GRANDE FAULT ZONE

The Rio Grande fault zone consists of several major northwest-trending faults, extending about 50 km from the southeast flank of the La Garita Mountains (Steven and Ratté, 1965) to south of Del Norte Peak (fig. 61). These faults, though clearly diminishing in displacement to the southeast, probably extend even farther, perhaps to the rim of the Platoro caldera complex, but they are concealed beneath surficial deposits and are lost in areas of poor exposure on the heavily timbered north slopes of the caldera. In the South Fork area and along the Rio Grande to the northwest, this fault zone forms a well-defined graben followed by the river, with offsets of as much as 350 m on

individual faults, but the graben is asymmetrical, and the general sense of displacement along the zone is a downdrop of the region to the southwest.

The Rio Grande fault zone appears to have been recurrently active over a period of at least 5 m.y. in late Oligocene and early Miocene time. At the northwest end of the zone, the major faults along the flank of the La Garita Mountains coincide closely with the margin of the Bachelor caldera, where it caved away the southwest flank of the La Garita resurgent dome during eruption of the Carpenter Ridge Tuff (26.7-27.8 m.y.), and these faults probably originated then (Steven and Ratté, 1965, p. 61). A little farther to the southeast, these faults offset the Nelson Mountain Tuff that immediately preceded eruption of the Snowshoe Mountain Tuff and associated formation of the Creede caldera (table 1). Some faults of the Rio Grande zone predate and are covered by the great lava dome of Fisher Quartz Latite along the Creede caldera rim at Wagonwheel Gap, which is dated at 26.5 m.y. (Armstrong, 1969; Lipman and others, 1970). Southeast of South Fork in the Beaver Mountain area, the entire ash-flow sequence—including the outflow Snowshoe Mountain Tuff—is faulted; but at least some of the faults are overlain by basalt flows of the Hinsdale Formation that show no offset (Durango map). At the southeast end of the zone around Del Norte Peak, however, Hinsdale basalts—including the one dated at 23.4 m.y.—are offset as much as 50 m.

PASS CREEK-ELWOOD CREEK-PLATORO FAULT SYSTEM

The Pass Creek-Elwood Creek-Platoro fault system (fig. 61) consists of a geometrically complex group of faults, characterized by northwest trends, that extends about 35 km from the margin of Mount Hope caldera across the southwest side of the Platoro caldera complex. As just described for the Rio Grande fault zone, different ages of movement along different parts of the system can also be documented here. The Pass Creek-Elwood Creek-Platoro fault system is also of particular interest in the evolution of the Platoro caldera complex because it localized much of the postcollapse igneous activity and the associated alteration and mineralization (fig. 61).

The Pass Creek zone, at the northwest end of the system, consists of only a few faults that define a small graben. Several dikes follow these faults (fig. 47) and widespread weak hydrothermal alteration in and close to the graben affects rocks as young as the Fish Canyon Tuff. The major displacement along these faults appears to be younger than the 27.8-m.y. Fish Canyon but older than the Huerto Andesite (>26.7 m.y.), which unconformably covers a faultline scarp at least 75 m high along the major northwestern fault of this zone.

The Elwood Creek zone includes some of the most intricate and largest displacement faults in the San Juan volcanic field (fig. 65). About 15 faults of irregular trend

extend outward from the west side of the Summitville caldera and define a stubby complex graben that terminates near the Bear Creek stock, where most of these faults tend to converge (fig. 61). At this focal area the cumulative displacement of the graben faults is at a maximum; the La Jara Canyon Member, exposed along the bottom of lower Crater Creek (Platoro map), is downdropped as much as 550 m. This area is also a locus for intrusion of monzonite, hydrothermal alteration, and sulfide mineralization. In contrast to the complex fault pattern on the southwest side of the graben, the bounding faults on the northeast side tend to be a more regular series of antithetic normal faults, with displacements down to the southwest. These faults extend toward but apparently do not quite join faults of the Pass Creek zone. Some faults in this graben system may have been initiated during subsidence of the Summitville caldera, as suggested by major downdropping of an area just to the west of the caldera,

especially the large triangular block west of Prospect Mountain (fig. 61). However, much of the displacement around Elwood and Crater Creeks is clearly younger than the 27.8-m.y. Fish Canyon Tuff, the undated rhyodacite of Park Creek (fig. 65), and the Carpenter Ridge Tuff (>26.7 m.y.).

In a real sense, the Summitville fault is part of the boundary system on the northeast side of the Elwood Creek fault zone. It forms a well-defined continuous structure for 15 km from Park Creek to the Alamosa River and merges to the southeast with the Platoro fault zone for another 10 km (fig. 61). Interpretation based on cross sections suggests that at least one more fault of similar geometry is buried by younger rocks farther to the northeast (Platoro map, section *D-D'*). The Summitville fault in the upper Park Creek area has a maximum displacement of 300-350 m, down to the southwest, but its location near the buried margin of the Summitville caldera suggests that it may have begun as



FIGURE 65.—Faulted ridge east of Crater Creek, showing displacement in thick rhyodacite of Park Creek well defined by offset of the dark-colored basal vitrophyre. This area is near the focus of maximum displacement on the Elwood Creek fault zone. On near ridge, lavas of the upper member of the Summitville Andesite rest on weakly welded light-gray tuff at the top of the La Jara Canyon Member. Arrow indicates large dike of quartz latite porphyry. View is to the north from 12,866-foot peak on the Continental Divide at the head of Prospect Creek.

part of the caldera ring-fault system and may have had an original displacement in the opposite sense. An even earlier inception of the Summitville fault is hinted by onlap relations of Treasure Mountain Tuff against lavas of the Conejos Formation on the upthrown side of the fault east of Lost Mine Creek in the upper Park Creek drainage (Platoro map). These relations are not conclusive because this buried topography of Conejos age does not necessarily have to be fault related. In upper Park Creek the major movement on the Summitville fault is clearly younger than the Carpenter Ridge Tuff (26.7-27.8 m.y.), which is tilted to near-vertical dips in the vicinity of the fault (Platoro map). The major movement probably preceded deposition of the overlying volcaniclastics of the Los Pinos Formation and the interlayered 26.4-m.y. Snowshoe Mountain Tuff (fig. 35). If so, it is slightly younger than the principal movement in the Pass Creek zone. Substantially younger movement farther southeast along the Summitville fault is probably indicated by displacement of the 22.8-m.y. quartz latite of South Mountain, which was erupted from a vent localized near the fault (Steven and Ratté, 1960, pl. 2). Near Summitville the quartz latite of South Mountain is displaced only slightly; on the southeast side of South Mountain it is offset as much as 100 m, but this estimate is complicated by the possibility that the lava dome was deposited against an existing faultline scarp in this area. Steven and Ratté (1960, p. 37) suggested movement of the Summitville fault following emplacement of the 20.2-m.y. rhyolite of Cropsy Mountain, but evidence for this age of movement seems inconclusive: one key area between South Mountain and Cropsy Mountain is exposed entirely as talus and solifluction debris, and the faulted lavas assigned to this unit west of North Mountain by Steven and Ratté (1960, pl. 2) seem equally plausibly interpreted as a correlative of the quartz latite of South Mountain or as a representative of some intermediate stage of activity. In this area, the mixed-lava complex at North Mountain, correlated with the rhyolite of Cropsy Mountain by Steven and Ratté and also in this report, was clearly erupted from a vent localized along the Summitville fault, but the complex itself is unfaulted.

The main Summitville fault seems to end north of the Alamosa River, but near its terminus, en echelon faults of the Platoro fault zone appear. Faults in the Platoro zone, as in other parts of the system, trend northwestward and define an asymmetrical graben that is regionally downdropped to the southeast. These faults, though important loci for alteration and mineralization, seem to have relatively small offsets that decrease to the southeast. At the pass between Stunner and Platoro, the easternmost and largest fault of the zone displaces the contact between the La Jara Canyon Member and the Summitville Andesite at least 100 m; in

contrast, along the ridge south of Platoro, no fault of this zone has more than 50 m of offset (Platoro map). Faults of the Platoro zone are younger than the 29.1-m.y. Alamosa River stock, but no satisfactory minimum age limit is determinable from the field relations.

LATE CENOZOIC EXTENSIONAL FAULTING

In the southern and eastern parts of the San Juan Mountains, the northwest-trending zones of normal faulting that were active during the time of caldera formation merge with generally more northward-trending normal faults. Many of these faults offset basalt flows of the Hinsdale Formation and seem to be late Cenozoic structures related to regional eastward tilting of the volcanic field toward the San Luis Valley.

Most of these late faults trend N. 20° E. to N. 30° W. and tend to be high-angle normal faults having small displacements down to the west. These faults define a well-developed antithetic pattern; the dominant sense of displacement is opposite to the eastward dip of the volcanic strata, and similar stratigraphic levels are repeatedly exposed. Offsets as small as 10 m have been mapped where possible (fig. 13; Durango map) to define the style of deformation. Few of the faults have displacements greater than 50 m, with the notable exception of the La Jara Reservoir-Cumbres Pass fault system that extends about 45 km from near the southeast rim of Platoro caldera to the New Mexico line (fig. 61) and beyond for an additional 8 km south (Bingler, 1968). This fault system has about 250 m of displacement east of La Jara Reservoir and about 300 m of displacement at Cumbres Pass, although between these places near the Conejos River the system diminishes to a large monoclinal flexure with no more than 10-20 m of actual fault displacement.

Other areas in which faulting of this style has been recognized are south of Del Norte, near La Jara Creek, around Osier Mountain, and around Banded Peak (fig. 61). The north-trending faults west of Summit Peak may also be part of this association; the age of movement, however, cannot be proved, because young basalts are absent there. Because these faults are mostly of small displacement, they have been recognized mainly where the stratigraphically well-controlled ash-flow sequence has been preserved. Similar faults were surely missed during mapping of the large areas underlain by the lithologically monotonous lavas and breccias of the Conejos Formation.

The age of this faulting has yet to be tightly established, but in all the areas mentioned above, except for Summit Peak, basalts of the Hinsdale Formation are faulted. Dated basalts as young as 4.7 m.y. and as old as 17.7 m.y. (Lipman and others, 1970) are cut by these faults, and the dated basalts are underlain by older flows that are too altered for reliable radiometric age deter-

minations to be made. The regional basaltic volcanism encompassed much and perhaps all of Miocene and Pliocene time (Lipman and others, 1970). Tilting and faulting also continued throughout much of the late Cenozoic, as indicated by progressively steeper dips of the older basalt flows along the southeast margin of the San Juan field and by eastward thickening of the intervening alluvial wedges of Los Pinos Formation. The merging of the late Cenozoic faults with the older caldera-related fault systems to the northwest also suggests that some caldera-related faults were reactivated at various later times to accommodate extensional deformation. This is suggested especially by the contrast between the northwest end of the Rio Grande fault zone, which seems to have been dormant after 26.5 m.y., and the southeast end, where 23.4-m.y. basalt flows were involved in the faulting.

The antithetic pattern of this late faulting is characteristic of extensional deformation, as is the block faulting of the Basin and Range province (Nolan, 1943; Thompson, 1960; Stewart, 1971). This, together with the regional eastward tilting of the southeastern San Juan region toward the San Luis Valley, suggests that the block faulting and eastward tilting are marginal manifestations of downdropping and rifting of the San Luis Valley segment of the Rio Grande depression. The Rio Grande depression is a major rift structure (Chapin, 1971) that is a local expression of widespread late Cenozoic crustal extension in western North America (Hamilton and Myers, 1966). The San Luis Valley segment of this structure is as much as 50 km across and may contain as much as 10 km of upper Cenozoic sedimentary fill, as indicated by gravity data (Gaca and Karig, 1966).

ALTERATION AND MINERALIZATION

In recent years it has become increasingly clear that most major ore deposits of the San Juan Mountains, such as those near Creede, Silverton-Telluride-Ouray, and Lake City, are closely related to the large calderas that collapsed as a result of the voluminous ash-flow eruptions in Oligocene time (Steven and Ratté, 1965; Luedke and Burbank, 1968; Steven and Lipman, 1968; Lipman and others, 1973). The Summitville-Platoro district seemed to be an exception (Steven and Ratté, 1960; Steven, 1968), but recognition of the Platoro caldera and of the sequence of igneous events related to its development has provided at least partial answers to the major questions concerning the localization of the mineral deposits of the Summitville-Platoro district and nearby mineralized areas.

Mineralization at Summitville and in certain nearby areas is now known to be closely related to intrusive and extrusive centers localized along marginal ring structures formed during the compound subsidence of the

Platoro caldera complex. Outlying mineralization was controlled mainly by outward-extending fracture zones. The localization of mineralization in these zones is thus closely comparable to that of other highly mineralized areas in the central and western San Juan Mountains (Steven, 1968; Luedke and Burbank, 1968). Although no detailed investigations of individual mining districts were undertaken in the present study, the structural relations and the timing of ore deposition at individual mineralized areas are reinterpreted in terms of the evolving caldera complex.

SUMMITVILLE DISTRICT

The alteration and mineralization at Summitville represent a late stage in the complex sequence of related igneous and hydrothermal episodes along the western margin of the Summitville caldera. As described by Steven and Ratté (1960), the gold-silver-copper ore in the Summitville district was deposited in a very shallow volcanic environment within a then recently erupted volcanic dome of coarsely porphyritic lava—the 22.8-m.y. quartz latite of South Mountain. Both the vent-dome complex and the associated alteration and mineralization are near the intersection of the Summitville fault with the buried ring-fracture zone of the Summitville caldera (fig. 61). The Summitville fault lies along the northeast margin of the Pass Creek-Elwood Creek-Platoro fault system; the Summitville ore deposit, as well as the major mineralization in the Stunner and Platoro districts to the southeast, is situated approximately at intersections of this regional fault system with ring-fracture zones of the Platoro caldera complex.

The ore at Summitville occurs in intensely altered pipes and irregular tabular masses of quartz-alunite rock that replaced the quartz latite along northwest-trending fracture zones. Metallic minerals, chiefly pyrite and enargite, fill irregular vugs that formed by local intense leaching of the quartz-alunite rock. The quartz-alunite masses are surrounded successively by soft argillically altered envelopes (illite-kaolinite zone) and by pervasively propylitized rocks (montmorillonite-chlorite zone). The alteration was interpreted by Steven and Ratté (1960) to have resulted from shallow solfataric activity similar to that associated with recent volcanism.

The close spatial association between hydrothermal alteration and ore deposition within the core of the lava dome, directly overlying the vent, indicates that the mineralization was closely related to and followed shortly after emplacement of the quartz latite. This interpretation is supported by isotopic age data, which show that the emplacement of the quartz latite and the alteration and mineralization were coincident at about 22.5 m.y. within the limits of analytical precision (Mehnert and others, 1973).

STUNNER AND GILMORE DISTRICTS

As described by Patton (1917, p. 98-101), quartz-pyrite veins with ore shoots containing gold and silver tellurides were deposited locally in the Stunner and Gilmore districts within variably altered monzonite of the Alamosa River stock. The veins near Stunner strike generally northwest and dip steeply; they lie along small faults and fractures at the northern end of the Platoro fault zone. This vein mineralization is largely limited to the south side of the Alamosa River and is less well developed in the more intensely altered rock north of the river. In contrast, the mineralogically similar veins of the Gilmore district, also south of the river, strike N. 30°-40° E. and are in little-altered monzonite. These quartz veins have localized the breakaway zones of slump blocks on the steep north slopes of the Gilmore district (Patton, 1917, p. 57-60), and major slumping has impeded both geologic studies and mineral development.

In the Stunner area, the north margin of the Alamosa River stock and much adjacent wallrock are intensely altered. Calkin (1967, p. 123; 1971) noted that the porphyritic phase of the Alamosa River stock (which he called the "Alum Creek Porphyry") is the focus of the most intense hydrothermal alteration. This porphyritic phase contains locally anomalous quantities of several metals (Calkin, 1967, p. 144-146) and in places is cut by numerous closely spaced quartz veinlets containing abundant pyrite and sparse molybdenite.

Some dikes and plugs of coarse porphyry similar to that in the quartz latite dome at Summitville cut both the Alamosa River stock and the adjacent altered rock, and these in turn were variously altered (Calkin, 1967, p. 74). Sharp and Gualtieri (1968) described zoned concentrations of lead, copper, molybdenum, and zinc near one of these porphyry dikes.

PLATORO DISTRICT

Most veins in the Platoro district are persistent north-northwest-trending quartz-pyrite veins in the thick mass of intracaldera La Jara Canyon Member exposed on the resurgent block of Platoro caldera. Local ore shoots on these veins, containing gold tellurides and silver sulfosalts (Patton, 1917, p. 89-96), supplied most of the ore produced in early mining in the district. Although most of the La Jara Canyon tuff within the caldera is propylitically altered, hydrothermal alteration related to mineralization is restricted to local argillic zones flanking the quartz-pyrite veins (fig. 61). Mineralization in the Platoro district was recently studied by Bird (1972).

The veins in the Platoro district are about on strike with some of the stronger veins in the Stunner district to the north, and both sets of veins follow the Platoro fault zone. This fault zone and the associated mineralization are younger than the Summitville caldera, and the Platoro veins are therefore only incidentally located within

the resurgent block of the Platoro caldera. Ore deposits are uncommon within resurgent cores of other calderas in the San Juan Mountains; deposits in the Creede district—the closest structural analogy to the Platoro district—lie within the resurgent Bachelor caldera but are primarily related to radial graben faults of the Creede caldera (fig. 1; Steven and Ratté, 1965).

JASPER AREA

The Jasper district, along the east margin of the Summitville caldera about 12 km east of Summitville, is another area of intensely altered rock associated with a granitic stock (fig. 61). It is the only sizable area of intense alteration in the southeastern San Juan Mountains that does not lie along the Pass Creek-Elwood Creek-Platoro fault system. Much of the alteration is within the stock, which is exposed near the level of its roof. Numerous shallow prospects within the stock seem to have disclosed no vein deposits of sufficient size to be minable, although the possibility of disseminated mineralization may not have received much attention during early exploration. Quartz-pyrite veins with ore shoots containing gold and silver are localized along the south margin of the highly altered rocks, according to Patton (1917, p. 105-108), but no modern studies of this area have been published.

CRATER CREEK AREA

Several major faults of the Elwood Creek fault zone that define a complex radial graben extend westward from the Summitville caldera (fig. 61) and converge toward the north end of the Bear Creek stock cluster. Hydrothermally altered rock is apparent at places along these faults, and some rather extensive areas within the faulted zone and around the stocks are pervasively argillized. Numerous dikes of coarsely porphyritic rhyodacite and quartz latite fill subparallel fractures within and near the graben (fig. 47).

Shallow prospect pits are scattered throughout the faulted and discontinuously altered area, and the Crater Creek drainage near the northeast end of the stock cluster has been intermittently explored in recent years (1967-70). This exploration has disclosed several veins, ranging in width from a few centimeters to several meters, that contain significant quantities of sphalerite and silver-bearing galena. The veins thus far discovered seem to be along minor fractures rather than along the major faults of the area, which are mostly poorly exposed and have not yet been explored.

CAT CREEK AREA

An extensive area of rather sporadic weak alteration and local pyritization extends southeastward from the Cat Creek stock, about 5 km east of the Platoro caldera wall (fig. 61). Numerous prospect pits and small adits were noted during the present study, but the altered rock

was not examined closely. No mineral production seems to have been recorded from this area, and the possible mineral potential is unknown.

ECONOMIC SIGNIFICANCE

Near Summitville and Platoro, the major foci of igneous intrusion, hydrothermal alteration, and mineralization seem to be localized along the ring-fracture zone of the Summitville caldera, especially where it is intersected by the northwest-trending Pass Creek-Elwood Creek-Platoro fault system. The Platoro caldera apparently exerted little control either on exposed hypabyssal intrusions or on hydrothermal activity related to the intrusions.

The areas of most widespread and intense alteration between Summitville and the Alamosa River show evidence of repeated intrusion and hydrothermal activity. The composite monzonite to quartz monzonite Alamosa River stock was intruded first, and a large block along its north margin was pervasively altered. Alteration was largely localized around the late porphyritic phase in the northern part of the stock, and anomalous concentrations of metals were introduced locally (Calkin, 1967; Sharp and Gaultieri, 1968). These altered rocks are overlain by unaltered rhyodacite lavas of Park Creek, erupted from the vicinity of Summitville, and are locally cut by coarsely porphyritic rhyodacitic and quartz latitic dikes and plugs. Similar coarsely porphyritic quartz latite of South Mountain, erupted from a vent along the northwest-trending Summitville fault, was altered and mineralized; ores from this center have provided most of the production from the Platoro caldera area.

The whole area from Summitville south across the Alamosa River and east to Jasper thus is a zone of recurrent intrusion, extrusion, and hydrothermal alteration and mineralization controlled by the ring-fracture zone of the Summitville caldera. The environment is similar to that in the intensely altered and mineralized Red Mountain district along the northwest margin of the Silverton caldera in the western San Juan Mountains (fig. 1; Burbank, 1941; Luedke and Burbank, 1968). The ores are also similar; pyrite and enargite are common in both districts, although numerous other ore minerals, including abundant sulfosalts of copper and silver, are present at Red Mountain. The gangues consist of pipelike masses of strongly leached silicified rocks that formed by replacement of preexisting volcanic or shallow intrusive rocks in shallow solfataric environments.

Deeper parts of this type of volcanic association—characterized by repeated hypabyssal intrusion of differentiated monzonitic to quartz monzonitic stocks, widespread and intense hydrothermal alteration, and local anomalous concentrations of gold, silver, copper, and molybdenum—are similar to those in

which porphyry-type disseminated deposits of copper and molybdenum occur throughout western North America. Now-exposed levels at Summitville are shallow and within the volcanic pile (Steven and Ratté, 1960, p. 50-51), whereas most porphyry-type deposits seem to have formed at lower volcanic levels or in the stocks beneath the volcanic pile. Favorable zones for exploration thus still exist at depth.

The monzonitic and quartz monzonitic compositions of the known intrusive bodies in the Summitville-Alamosa River area are more normally associated with predominantly copper-bearing porphyry deposits (Stringham, 1966) than with predominantly molybdenum-bearing deposits, where mineralization seems related to relatively silica-rich rhyolite and granite porphyry (Wallace and others, 1968; Carpenter, 1968). The abundance of copper and the dearth of molybdenum in the known ores at Summitville further suggest this association. Molybdenum and copper, however, both are present in the mineralized area around Alum Creek, south of Summitville (Calkin, 1967, p. 144-147; Sharp and Gaultieri, 1968).

Mineral deposits in the northwest-trending fracture zones range from quartz-pyrite veins with shoots of gold and silver tellurides and associated silver and copper sulfosalts minerals in the Stunner, Gilmore, and Platoro districts to silver-bearing galena-sphalerite veins near Crater Creek. A close analogy exists between the environment of the lead-zinc-silver veins along Crater Creek and that of the major producing base-metal veins in radial faults around the margins of the Creede caldera (Steven and Ratté, 1965) and the Lake City and Silverton calderas (Luedke and Burbank, 1968). The Crater Creek area is appreciably farther from the apparent focus of intrusive and hydrothermal activity between Summitville and the Alamosa River than are the Stunner, Gilmore, and Platoro districts. This general distribution of gold, silver, and copper relatively near the source and of silver, lead, and zinc more distant is reminiscent of the metal zoning around many western mining districts, as previously suggested by Calkin (1967, p. 154). The northwest-trending fracture zones have been poorly explored and seemingly deserve more attention.

PETROLOGIC EVOLUTION

Petrologic studies on rocks of the Platoro caldera complex and related volcanic rocks of the San Juan field are still in progress (1972). Accordingly, petrologic evolution will not be interpreted in any great detail at this time, but a few features of petrogenetic significance are documented so well in the Platoro area that some discussion seems appropriate.

Perhaps the most interesting feature of the Platoro caldera complex is the close spatial, temporal, and

petrogenetic association of andesites with more silicic igneous rocks in a resurgent-caldera ash-flow setting. In general, calderas and related ash flows seem divisible into two broad groups (Smith and Bailey, 1968): the Krakatoan type (resurgence rare), which is associated with large andesitic volcanoes in a eugeosynclinal continental-margin or island-arc environment, and the Glen Coe type (resurgence common), which is associated with more silicic volcanism and intrusive activity in an epicontinental cratonic environment. Contrasts between continental-margin and continental-interior volcanism in the Western United States have also been emphasized recently by Gilluly (1971), who regards Cenozoic volcanic activity along the western continental margin as genetically related to plate-tectonic events but who considers volcanism as far from the continental margin as the San Juan field (about 1,500 km) as fundamentally different and unrelated to motions of tectonic plates.

However, the rocks of the San Juan field, and of the Platoro caldera complex in particular, constitute a predominantly andesitic association in a continental-interior setting, so the numerous resurgent calderas do not fit simply into either Krakatoan or Glen Coe types. Furthermore, the San Juan volcanic field seems to be the inner part of a broad middle Tertiary zone of predominantly andesitic volcanism in the Western United States that can be interpreted as related to a complex subduction boundary between American and Pacific tectonic plates (Lipman and others, 1971, 1972).

The relations at the Platoro caldera complex strongly suggest that the quartz latitic and low-silica rhyolitic ash-flow tuffs are differentiates of andesitic magma. In the San Juan region in general, the caldera structures resulting from ash-flow eruptions are within the more extensive region of vents for the early intermediate-composition rocks (Lipman and others, 1970, fig. 1). The Platoro caldera formed within a cluster of only slightly older andesitic volcanoes of the Conejos Formation (fig. 5); shortly after eruption of the quartz latitic La Jara Canyon Member and caldera collapse, the caldera filled with andesitic lavas that are virtually indistinguishable from the precaldera lavas. Further ash-flow eruptions formed the upper two widespread sheets of Treasure Mountain Tuff and caused collapse of the Summitville caldera, which was subsequently filled by similar andesitic lavas. These andesitic lavas and more silicic tuffs of the Platoro caldera complex define a compositional continuum for all major oxides (fig. 66). Similar compositional sequences are displayed by a few individual differentiated early intermediate centers, such as Summer Coon volcano (Lipman, 1968; Mertzman, 1971).

The continued availability of andesitic magma during later ash-flow eruptions of the San Juan field is indicated by similarly interlayered andesites such as the

Sheep Mountain Andesite, the Huerto Andesite, and the partly andesitic volcanics of Table Mountain (Steven and Lipman, 1973). Regionally, the nonsystematic alternating eruption of andesitic, rhyodacitic, and quartz latitic lavas indicates that this range of magma types was available during the time of caldera formation. Many of the ash-flow sheets, such as those of the Treasure Mountain Tuff, are monotonous quartz latites that are only slightly more silicic than the associated lavas; but other large ash-flow sheets are rhyolites. Compositional zonations from rhyolite upward into quartz latite within individual ash-flow sheets, such as the Carpenter Ridge Tuff (fig. 32), extend over the entire compositional range of all the Oligocene ash-flow sheets (figs. 4, 66) and are interpreted as representing in inverse order the vertical differentiation of the source magma chambers. The most mafic parts of the sheets, compositionally as low as 61 percent SiO_2 (table 6, No. 15), bridge the compositional transition between the lavas and the more silicic tuffs (figs. 4, 66).

In addition, at several calderas, including the Platoro caldera complex, postcollapse intrusions along the ring fractures are granodiorite or monzonite, compositionally similar to the andesitic lavas that preceded and followed the ash-flow eruptions. The caldera structures thus are thought to have formed by collapse resulting from eruption of silicic magmas in cupolas at the tops of larger, more mafic batholiths. The andesitic and related lavas probably represent the composition of the greater parts of these batholiths (mainly diorite, granodiorite, and monzonite), and the ash-flow sheets represent their differentiated granitic tops.

The overall area of the San Juan caldera cluster (fig. 1) also coincides with a large negative gravity anomaly, the dimensions of which are compatible with the subsurface presence of a large shallow batholith (Plouff and Pakiser, 1972). The evolution of the San Juan caldera cluster suggests progressive rise, differentiation, and crystallization of this batholith inward from its margins. The earliest calderas—Platoro, San Juan, Uncompahgre, and Bonanza—are at the edges of the gravity anomaly (fig. 1), and the ages of calderas generally converging toward the center of the cluster near Creede. (The only major exception, Lake City caldera, is about 4 m.y. younger than any of the others, and its tuffs are different in petrology; probably it is best considered as a separate event.) The Platoro caldera complex is just outside the gravity low (Plouff and Pakiser, 1972). This location, in conjunction with the relatively unfractuated petrologic character of the Treasure Mountain Tuff and its associated caldera-filling lavas, suggest that the magmas related to the Platoro caldera complex were derived from the batholith at an early stage in its evolution, when it was still fairly deep, relatively undifferentiated, and somewhat different in shape than in its final

form. The younger ash-flow sheets, which are related to the central San Juan caldera cluster within the core of the gravity anomaly, tend to be more fractionated, as indicated by compositional zonations of the sheets, and the postcaldera lavas are more silicic than at Platoro.

Except for the resurgent uplift after its first collapse, the Platoro caldera complex is strikingly similar to some of the great Pleistocene calderas of the Japanese volcanic chain, such as Aso in Kyūshū (Matumoto, 1943; Williams, 1941). Like the Platoro caldera complex, Aso caldera is a composite collapse structure from which three major ash-flow sheets were erupted (Ono, 1965). The caldera is about 17 by 25 km and has walls somewhat rectangular in plan and strikingly scalloped by slumping; the geometry is closely similar to that of the Platoro caldera complex (fig. 67). Before the ash-flow eruptions, the site of the Aso caldera was among a cluster of large andesitic stratovolcanoes within the central volcanic highland of Kyūshū Island. The related ash-flow tuffs were deposited as a nearly continuous volcanic blanket for about 15 km out in every direction from the caldera rim, and they followed major radial valleys outward from the central highland for as much as 75 km (fig. 67). Although this extent is greater than that recognized for the Treasure Mountain Tuff, a great proportion of distal tuff deposits of the Aso eruptions is confined to the deep valleys. The Aso ash-flow tuffs are distinctly more silicic in bulk composition than the precaldera andesite, and at least two of these sheets are compositionally zoned, from basal phenocryst-poor rhyodacite upward into phenocryst-rich alkali andesite. The composition change, becoming more mafic upward, apparently reflects in inverse order the compositional zonation in the magma chamber, in which more silicic differentiated magma overlay more mafic magma (Lipman, 1967). The composition of the last erupted andesitic tuff is generally similar to that of the precaldera andesitic lavas. As at Platoro caldera, the postcollapse volcanism at Aso (which is still in progress) is andesitic in composition and produced large cones of andesitic lava and scoria on the caldera floor.

Circum-Pacific andesitic arcs, such as Japan, are clearly associated with subduction at the convergence of lithospheric plates, where chains of andesitic volcanoes are aligned above dipping Benioff seismic zones (Dickinson and Hatherton, 1967; Isacks and others, 1968; Hamilton, 1969). Volcanoes of the active arcs, although mostly less alkalic than andesites of the San Juan region, are characterized by systematic variations in chemistry, especially in alkalis, that are transverse to the arc and that correlate with depth to the Benioff seismic zone (Kuno, 1959; Dickinson and Hatherton, 1967; Dickinson, 1970; Jakes and White, 1972). The lower and middle Tertiary volcanic rocks of the Western United States, including those of the San Juan field, also display

transverse variations in alkali content, with alkalis generally increasing toward the continental interior (Merriam and Anderson, 1942; Moore, 1962; Lipman and others, 1971). The compositions of these continental-interior andesites, although generally more alkalic than modern arc andesites, are within the spectrum of circum-Pacific andesites (Lipman and others, 1972, fig. 7). For example, the Oligocene andesites of the San Juan field are compositionally similar to Quaternary andesites of the Chilean Andes (Lipman and others, 1972, fig. 6), where stratovolcanoes of alkali andesite are also associated with voluminous rhyolitic ash-flow tuffs (Zeil and Pichler, 1967; Pichler and Zeil, 1969) in a plate-convergence setting (Hamilton, 1969; James, 1971). These similarities strongly suggest that the middle Cenozoic andesitic rocks of the Western United States, including those of the San Juan field, were also genetically related to a subduction system. The great width of this volcanic belt, extending as much as 1,500 km from the continental margin, can be interpreted in terms of a complex imbricate subduction system (Lipman and others, 1971, 1972).

At about the beginning of Miocene time, the volcanic associations in the San Juan region changed notably. Whereas the Oligocene volcanic rocks are predominantly intermediate-composition lavas and genetically related ash-flow tuffs, the younger rocks are largely a bimodal association of alkali olivine basalt and high-silica alkali rhyolite. Basalt and minor rhyolite were erupted intermittently through the Miocene and Pliocene, and at one time they formed a widespread veneer over most of the older volcanic terrane.

The general petrologic progression of the prolonged postcollapse igneous activity (29-20 m.y.) at the Platoro caldera complex is also toward rock types that are more silicic as age decreases, from voluminous dark andesites (56-59 percent SiO_2) to minor scattered lava domes of porphyritic rhyolite (73-76 percent SiO_2) that are contemporaneous with nearby widespread flows of alkali olivine basalt. The postcollapse igneous activity at Platoro caldera therefore spans the regional transition from predominantly andesitic volcanism to bimodal basalt-rhyolite association.

The contrast between the Oligocene intermediate to low-silica rhyolite magmas and the later basaltic and rhyolitic bimodal magmas implies either different conditions of magma generation or different processes of fractionation for the two magmatic assemblages. This petrologic change coincides approximately in time with nearby development of the Rio Grande depression, a major rift that is the local expression of widespread late Cenozoic crustal extension (Hamilton and Myers, 1966; Scholz and others, 1971). The change from predominantly intermediate to bimodal basalt-rhyolite volcanism, approximately concurrent with initiation of late Tertiary

PLATORO CALDERA COMPLEX, SAN JUAN MOUNTAINS, COLORADO

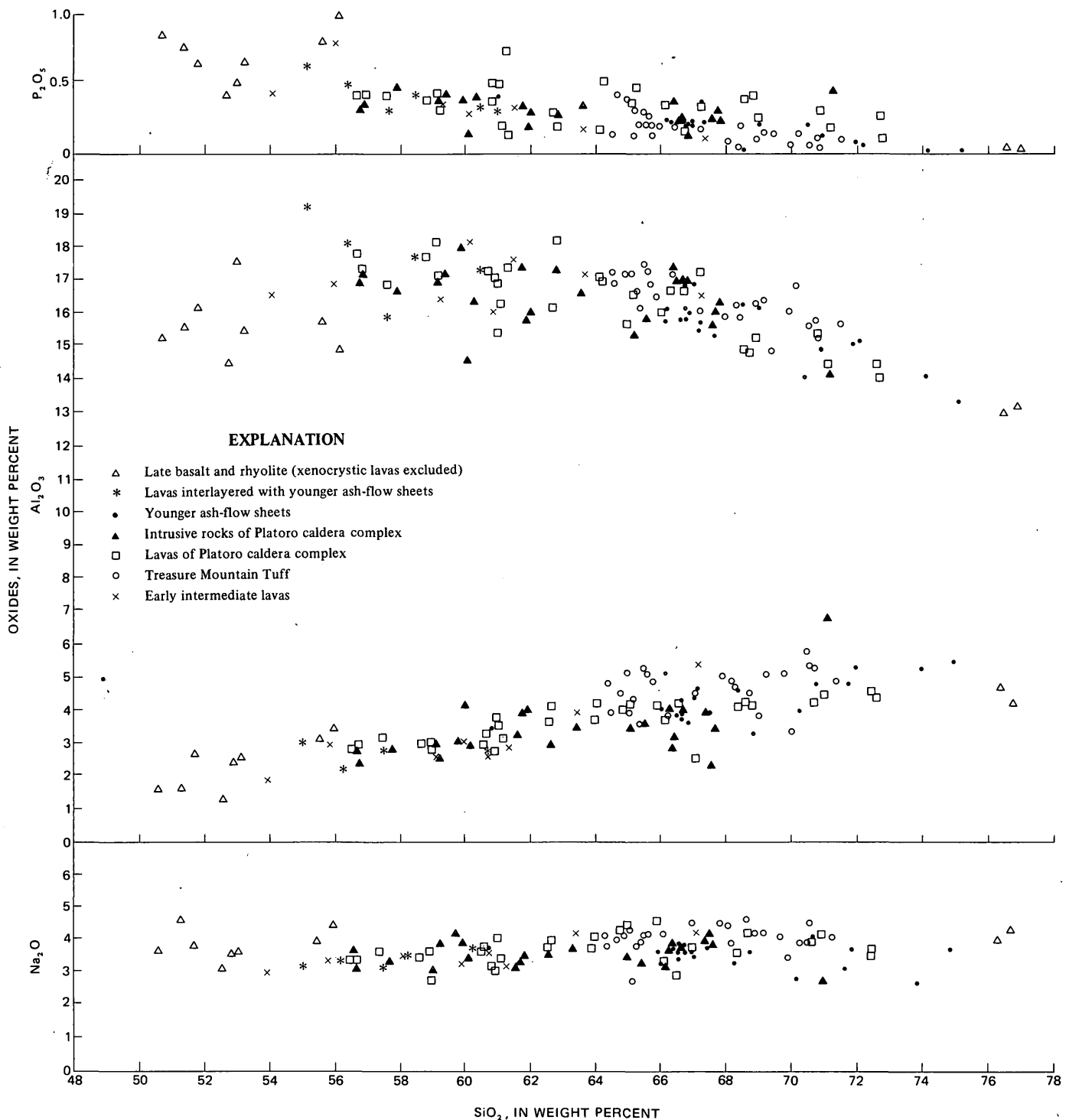


FIGURE 66.— SiO_2 variation diagram for major igneous units of the Platoro caldera complex. All analyses are from tables of this report.

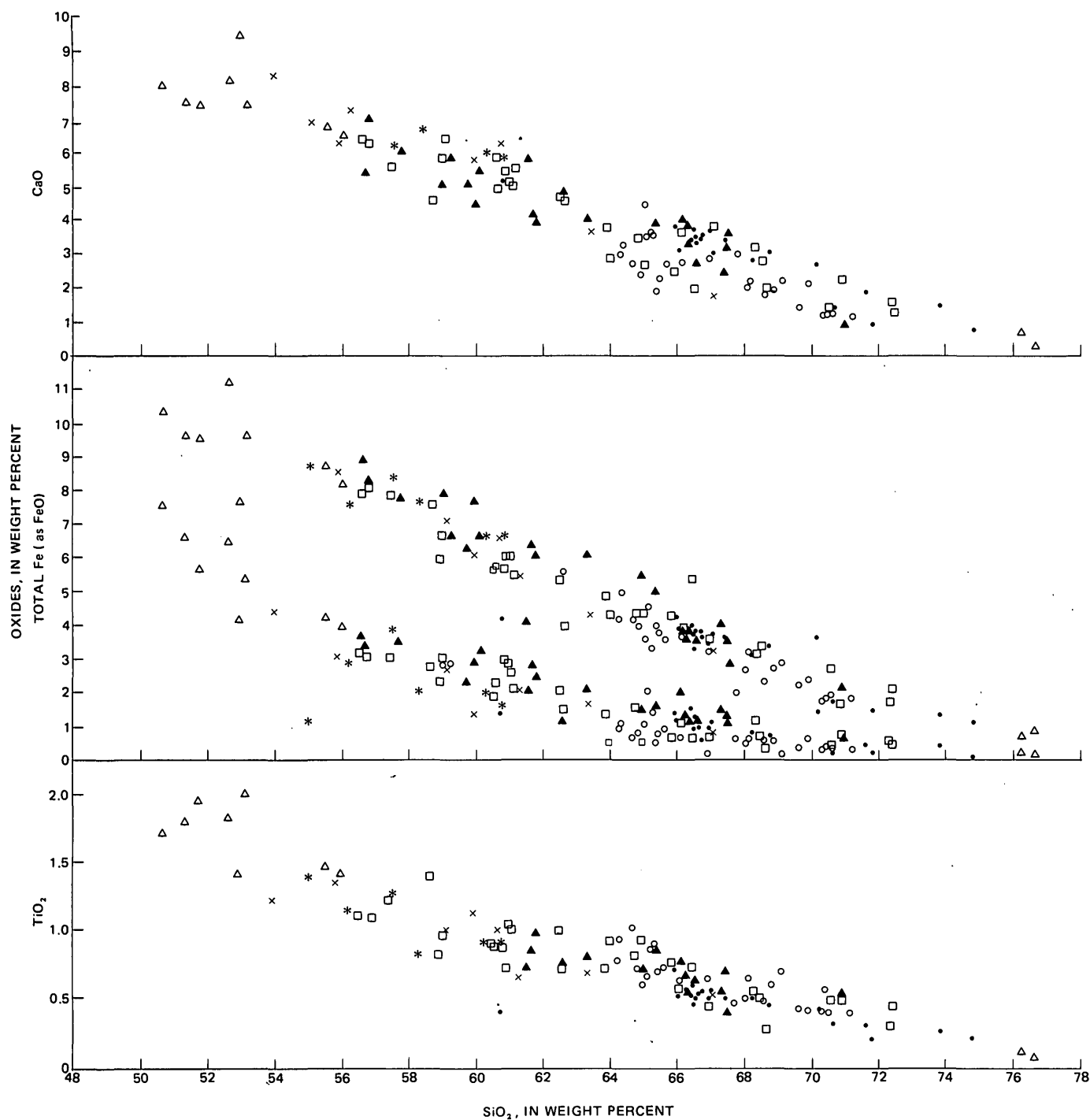


FIGURE 66. — Continued.

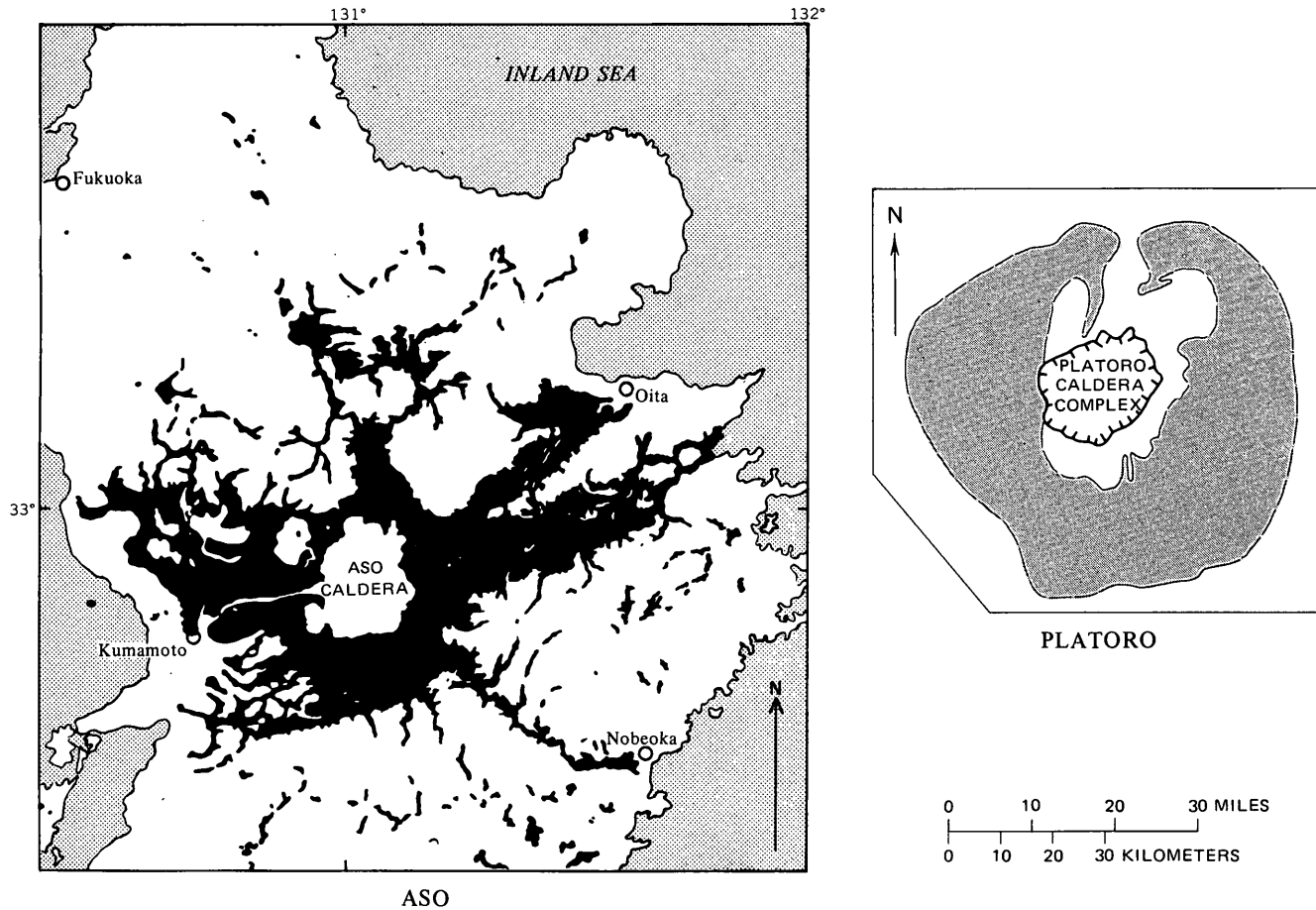


FIGURE 67.—Outlines of Platoro caldera complex in Colorado and Aso caldera in Japan, showing extent of related ash-flow tuffs (shaded). Both maps at same scale. Platoro data are from figure 14 of this report; Aso data are from Matumoto (1943).

crustal extention, seems to be characteristic of Cenozoic volcanism for much of the Western United States (Christiansen and Lipman, 1972). These changes also coincided in time with changes in the geometry of sea-floor spreading recorded in magnetic anomaly patterns in the northeast Pacific (McKenzie and Morgan, 1969; Atwater, 1970), apparently reflecting initial intersection of North America with the East Pacific Rise and destruction of the trench-Benioff zone system.

REFERENCES CITED

- Aoki, Ken-Ichico, 1967, Petrography and petrochemistry of latest Pliocene olivine-tholeiites of Taos area, northern New Mexico, U.S.A.: *Contr. Mineralogy and Petrology*, v. 14, p. 190-203.
- Armstrong, R. L., 1969, K-Ar dating of laccolithic centers of the Colorado Plateau and vicinity: *Geol. Soc. America Bull.*, v. 80, no. 10, p. 2081-2086.
- Atwater, Tanya, 1970, Implications of plate tectonics for the Cenozoic tectonic evolution of western North America: *Geol. Soc. America Bull.*, v. 81, no. 12, p. 3513-3536.
- Barker, Fred, 1958, Precambrian and Tertiary geology of Las Tablas quadrangle, New Mexico: *New Mexico Bur. Mines and Mineral Resources Bull.* 45, 104 p.
- Bastron, Harry, Barnett, P. R., and Murata, K. J., 1960, Method for the quantitative spectrochemical analysis of rocks, minerals, ores, and other materials by a powder d-c arc technique: *U.S. Geol. Survey Bull.* 1084-G, p. 165-182.
- Bhattacharji, Somdev, and Smith, C. H., 1964, Flowage differentiation: *Science*, v. 145, p. 150-153.
- Bingler, E. C., 1968, Geology and mineral resources of Rio Arriba County, New Mexico: *New Mexico Bur. Mines and Mineral Resources Bull.* 91, 158 p.
- Bird, W. H., 1972, Mineral deposits of the southern portion of the Platoro caldera complex, southeast San Juan Mountains, Colorado: *Mountain Geologist*, v. 9, no. 4, p. 379-387.
- Bromfield, C. S., 1967, Geology of the Mount Wilson quadrangle, western San Juan Mountains, Colorado: *U.S. Geol. Survey Bull.* 1227, 100 p.
- Burbank, W. S., 1932, Geology and ore deposits of the Bonanza mining district, Colorado: *U.S. Geol. Survey Prof. Paper* 169, 166 p.
- , 1941, Structural control of ore deposition in the Red Mountains, Sneffels, and Telluride districts of the San Juan Mountains, Colorado: *Colorado Sci. Soc. Proc.*, v. 14, no. 5, p. 141-261.
- Burbank, W. S., and Lovering, T. S., 1933, Relation of stratigraphy, structure, and igneous activity to ore deposition of Colorado and southern Wyoming, in *Ore deposits of the Western States* (Lindgren volume): New York, Am. Inst. Mining Metall. Engineers, p. 272-316.
- Butler, A. P., Jr., 1971, Tertiary volcanic stratigraphy of the eastern Tusas Mountains, southwest of the San Luis Valley, Colorado-New Mexico, in *New Mexico Geol. Soc. Guidebook 22d Field Conf.*, San Luis Basin, Colorado, 1971: p. 289-300.

- Byers, F. M., Jr., Carr, W. J., and Orkild, P. P., 1969, Volcano-tectonic history of southwestern Nevada caldera complex, U.S.A., in International symposium on volcanology—Volcanoes and their roots, Oxford, England, 1969, Volume of Abstracts: Internat. Assoc. Volcanology and Chemistry of the Earth's Interior, p. 84-86.
- Calkin, W. S., 1967, Geology, alteration, and mineralization of the Alum Creek area, San Juan volcanic field, Colorado: Colorado School Mines unpub. Ph. D. thesis, 177 p.
- , 1971, Some petrologic and alteration aspects of the Alum Creek area, San Juan volcanic field, Colorado, in New Mexico Geol. Soc. Guidebook 22d Field Conf., San Luis Basin, Colorado, 1971: p. 235-242.
- Carpenter, R. H., 1968, Geology and ore deposits of the Questa molybdenum mine area, Taos County, New Mexico, in Ridge, J. D., ed., Ore deposits of the United States, 1933-1967 (Graton-Sales Volume), v. 2: Am. Inst. Mining, Metall., and Petroleum Engineers, p. 1328-1350.
- Carr, W. J., and Quinlivan, W. D., 1968, Structure of Timber Mountain resurgent dome, in Eckel, E. B., ed., Nevada Test Site: Geol. Soc. America Mem. 110, p. 99-108.
- Chapin, C. E., 1971, The Rio Grande Rift, Pt. I—Modifications and additions, in New Mexico Geol. Soc. Guidebook 22d Field Conf., San Luis Basin, Colorado, 1971: p. 191-202.
- Christiansen, R. L., and Lipman, P. W., 1966, Emplacement and thermal history of a rhyolite lava flow near Fortymile Canyon, southern Nevada: Geol. Soc. America Bull., v. 77, no. 7, p. 671-684.
- , 1972, Late Cenozoic, pt. 2 of Cenozoic volcanism and plate-tectonic evolution of the Western United States: Royal Soc. London Philos. Trans., v. 271, no. 1213, p. 249-284.
- Christiansen, R. L., Lipman, P. W., Orkild, P. P., and Byers, F. M., Jr., 1965, Structure of the Timber Mountain caldera, southern Nevada, and its relations to basin-range structure, in Geological Survey research 1965: U.S. Geol. Survey Prof. Paper 525-B, p. B43-B48.
- Cohee, G. V., chm., 1961, Tectonic map of the United States, exclusive of Alaska and Hawaii: U.S. Geol. Survey and Am. Assoc. Petroleum Geologists [1962].
- Cross, C. W., and Larsen, E. S., 1935, A brief review of the geology of the San Juan region of southwestern Colorado: U.S. Geol. Survey Bull. 843, 138 p.
- Deer, W. A., Howie, R. A., and Zussman, J., 1963, Framework silicates, v. 4 of Rock-forming minerals: London, Longmans, Green & Co.
- Dickinson, R. G., Leopold, E. B., and Marvin, R. F., 1968, Late Cretaceous uplift and volcanism on the north flank of the San Juan Mountains, Colorado, in Epis, R. C., ed., Cenozoic volcanism in the southern Rocky Mountains: Colorado School Mines Quart., v. 63, no. 3, p. 125-148.
- Dickinson, W. R., 1970, Relations of andesites, granites, and derivative sandstones to arc-trench tectonics: Rev. Geophysics and Space Physics, v. 8, no. 4, p. 813-860.
- Dickinson, W. R., and Hatherton, Trevor, 1967, Andesitic volcanism and seismicity around the Pacific: Science, v. 157, no. 3790, p. 801-803.
- Doe, B. R., Lipman, P. W., Hedge, C. E., and Kurasawa, H., 1969, Primitive and contaminated basalts from the southern Rocky Mountains, U.S.A.: Contr. Mineralogy and Petrology, v. 21, no. 2, p. 142-156.
- Doell, R. R., and Cox, Allan, 1962, Determinations of the magnetic polarity of rock samples in the field, in Short papers in geology, hydrology, and topography: U.S. Geol. Survey Prof. Paper 450-D, p. D105-D108.
- Doney, H. H., 1968, Geology of the Cebolla quadrangle, Rio Arriba County, New Mexico: New Mexico Bur. Mines and Mineral Resources Bull. 92, 114 p.
- Dunn, D. E., 1964, Evolution of the Chama Basin and Archuleta an-
- ticlinorium, eastern Archuleta County, Colorado: Texas Univ. unpub. Ph. D. thesis, 112 p.
- Fisher, R. V., 1966, Mechanism of deposition from pyroclastic flows: Am. Jour. Sci., v. 264, no. 5, p. 350-363.
- Gaca, J. R., and Karig, D. E., 1966, Gravity survey in the San Luis Valley area, Colorado: U.S. Geol. Survey open-file report, 21 p.
- Gilluly, James, 1971, Plate tectonics and magmatic evolution: Geol. Soc. America Bull., v. 82, no. 9, p. 2383-2396.
- Hamilton, Warren, 1969, Mesozoic California and the underflow of Pacific mantle: Geol. Soc. America Bull., v. 80, no. 12, p. 2409-2430.
- Hamilton, Warren, and Myers, W. B., 1966, Cenozoic tectonics of the western United States: Rev. Geophysics., v. 4, no. 4, p. 509-549.
- Harland, W. B., Smith, A. G., and Wilcock, Bruce, eds., 1964, The Phanerozoic time-scale—A symposium dedicated to Professor Arthur Holmes: Geol. Soc. London Quart. Jour., Supp., v. 120s, 458 p.
- Hawkes, L., 1945, The Gardiner River [Yellowstone Park, Wyo.] rhyolite-basalt complex: Geol. Mag., v. 82, no. 4, p. 182-184.
- Isacks, Bryan, Oliver, Jack, and Sykes, L. R., 1968, Seismology and the new global tectonics: Jour. Geophys. Research, v. 73, no. 18, p. 5855-5899.
- Jakes, P., and White, A. R. J., 1972, Major and trace element abundances in volcanic rocks of orogenic areas: Geol. Soc. America Bull., v. 83, no. 1, p. 29-40.
- James, D. E., 1971, Plate tectonic model for the evolution of the central Andes: Geol. Soc. America Bull., v. 82, no. 12, p. 3325-3346.
- Kelley, V. C., 1952, Tectonics of the Rio Grande depression of central New Mexico, in New Mexico Geol. Soc. Guidebook 3d Field Conf., Rio Grande country, central New Mexico: p. 93-103.
- , 1957, General geology and tectonics of the western San Juan Mountains, Colorado, in New Mexico Geol. Soc. Guidebook 8th Field Conf., 1957, p. 154-162.
- King, P. B., compiler, 1969, Tectonic map of North America: U.S. Geol. Survey.
- Knepper, D. H., Jr., and Marrs, R. W., 1971, Geological development of the Bonanza-San Luis Valley-Sangre de Cristo Range area, south-central Colorado, in New Mexico Geol. Soc. Guidebook 22d Field Conf., San Luis Basin, Colorado, 1971: p. 249-264.
- Kuno, Hisashi, 1959, Origin of Cenozoic petrographic provinces of Japan and surrounding areas: Bull. Volcanol., ser. 2, v. 20, p. 37-76.
- Larsen, E. S., Jr., and Cross, C. W., 1956, Geology and petrology of the San Juan region, southwestern Colorado: U.S. Geol. Survey Prof. Paper 258, 303 p.
- Larsen, E. S., Irving, John, Gonyer, F. A., and Larsen, E. S., 3d, 1938, Petrologic results of a study of the minerals from the Tertiary volcanic rocks of the San Juan region, Colorado: Am. Mineralogist, v. 23, no. 7, p. 417-429.
- Leeman, W. P., and Rogers, J. J. W., 1970, Late Cenozoic alkali-olivine basalts of the basin-range province, USA: Contr. Mineralogy and Petrology, v. 25, p. 1-24.
- Lipman, P. W., 1965, Chemical comparison of glassy and crystalline volcanic rocks: U.S. Geol. Survey Bull. 1201-D, 24 p.
- , 1967, Mineral and chemical variations within an ash-flow sheet from Aso caldera, southwestern Japan: Contr. Mineralogy and Petrology, v. 16, p. 300-327.
- , 1968, Geology of the Summer Coon volcanic center, eastern San Juan Mountains, Colorado, in Epis, R. C., ed., Cenozoic volcanism in the southern Rocky Mountains: Colorado School Mines Quart., v. 63, no. 3, p. 211-236.
- , 1969, Alkalic and tholeiitic basaltic volcanism related to the Rio Grande depression, southern Colorado and northern New Mexico: Geol. Soc. America Bull., v. 80, no. 7, p. 1343-1353.
- , 1974, Geologic map of the Platoro caldera area, southeastern San Juan Mountains, southeastern Colorado: U.S. Geol. Survey

- Misc. Geol. Inv. Map I-828 (in press).
- Lipman, P. W., Christiansen, R. L., and O'Connor, J. T., 1966, A compositionally zoned ash-flow sheet in southern Nevada: U.S. Geol. Survey Prof. Paper 524-F, 47 p.
- Lipman, P. W., and Mehnert, H. A., 1969, Structural history of the eastern San Juan Mountains and the San Luis Valley, Colorado [abs.]: Geol. Soc. America Spec. Paper 121, p. 525-526.
- Lipman, P. W., Mutschler, F. E., Bryant, Bruce, and Steven, T. A., 1969, Similarity of Cenozoic igneous activity in the San Juan and Elk Mountains, Colorado, and its regional significance, in Geological Survey research 1969: U.S. Geol. Survey Prof. Paper 650-D, p. D33-D42.
- Lipman, P. W., Prostka, H. J., and Christiansen, R. L., 1971, Evolving subduction zones in the western United States, as interpreted from igneous rocks: Science, v. 174, no. 4011, p. 821-825.
- , 1972, Early and Middle Cenozoic, pt. 1 of Cenozoic volcanism and plate-tectonic evolution of the Western United States: Royal Soc. London Philos. Trans., v. 271, no. 1213, p. 217-248.
- Lipman, P. W., and Steven, T. A., 1970, Reconnaissance geology and economic significance of the Platoro caldera, southeastern San Juan Mountains, Colorado, in Geological Survey research 1970: U.S. Geol. Survey Prof. Paper 700-C, p. C19-C29.
- Lipman, P. W., Steven, T. A., Luedke, R. G., and Burbank, W. S., 1973, Revised volcanic history of the San Juan, Uncompahgre, Silverton, and Lake City calderas in the western San Juan Mountains Colorado: U.S. Geol. Survey Jour. Research, v. 1, no. 6, p. 627-642.
- Lipman, P. W., Steven, T. A., and Mehnert, H. H., 1970, Volcanic history of the San Juan Mountains, Colorado, as indicated by potassium-argon dating: Geol. Soc. America Bull., v. 81, no. 8, p. 2329-2352.
- Luedke, R. G., and Burbank, W. S., 1963, Tertiary volcanic stratigraphy in the western San Juan Mountains, Colorado, in Short papers in geology and hydrology: U.S. Geol. Survey Prof. Paper 475-C, p. C39-C44.
- , 1968, Volcanism and cauldron development in the western San Juan Mountains, Colorado, in Epis, R. C., ed., Cenozoic volcanism in the southern Rocky Mountains: Colorado School Mines Quart., v. 63, no. 3, p. 175-208.
- Macdonald, G. A., and Katsura, T., 1964, Chemical composition of Hawaiian lavas: Jour. Petrology, v. 5, pt. 1, p. 82-133.
- McKenzie, D. P., and Morgan, W. J., 1969, Evolution of triple junctions: Nature, v. 224, no. 5215, p. 125-133.
- Matumoto, Todaiti, 1943, The four gigantic caldera volcanoes of Kyūsyū: Japanese Jour. Geology and Geography, v. 19, 57 p.
- Mayhew, J. D., 1969, Geology of the eastern part of the Bonanza volcanic field, Saguache County, Colorado: Colorado School Mines unpub. M.S. thesis, 94 p.
- Mehnert, H. H., Lipman, P. W., and Steven, T. A., 1973, Age of mineralization at Summitville, Colorado, as indicated by K-Ar dating of alunite: Econ. Geology, v. 68, p. 399-401.
- Merriam, C. W., and Anderson, C. A., 1942, Reconnaissance survey of the Roberts Mountains, Nevada: Geol. Soc. America Bull., v. 53, no. 12, p. 1675-1727.
- Mertzman, S. A., Jr., 1971, The Summer Coon volcano, eastern San Juan Mountains, Colorado, in New Mexico Geol. Soc. Guidebook 22d Field Conf., San Luis Basin, Colorado, 1971: p. 265-272.
- Moore, J. G., 1962, K/Na ratio of Cenozoic igneous rocks of the western United States: Geochim. et Cosmochim. Acta, v. 26, p. 101-130.
- Muehlberger, W. R., 1960, Structure of the central Chama platform, northern Rio Arriba County, New Mexico, in New Mexico Geol. Soc. Guidebook 11th Field Conf., Rio Chama country, 1960: p. 103-109.
- Myers, A. T., Havens, R. G., and Dunton, P. J., 1961, A spectrochemical method for the semiquantitative analysis of rocks, minerals, and ores: U.S. Geol. Survey Bull. 1084-I, p. 207-229.
- Nicholls, J., Carmichael, I. S. E., and Stormer, J. C., Jr., 1971, Silica activity and P_{total} in igneous rocks: Contr. Mineralogy and Petrology, v. 33, no. 1, p. 1-20.
- Nolan, T. B., 1943, The Basin and Range province in Utah, Nevada, and California: U.S. Geol. Survey Prof. Paper 197-D, p. 141-196.
- Olson, J. C., Hedlund, D. C., and Hansen, W. R., 1968, Tertiary volcanic stratigraphy in the Powderhorn-Black Canyon region, Gunnison and Montrose Counties, Colorado: U.S. Geol. Survey Bull. 1251-C, 29 p.
- Ono, Koji, 1965, Geology of the eastern part of Aso caldera, central Kyūshū, southwest Japan: Jour. Geol. Soc. Japan, v. 71, p. 541-553 [in Japanese with English abs.].
- Ozima, Minoru, Kono, M., Kaneoka, I., Kinoshita, H., Kobayashi, Kazuo, Nagata, Tokesi, Larsen, E. E., and Strangeway, D. W., 1967, Paleomagnetism and potassium-argon ages of some volcanic rocks from the Rio Grande gorge, New Mexico: Jour. Geophys. Research, v. 72, no. 10, p. 2615-2622.
- Patton, H. B., 1916, Geology and ore deposits of the Bonanza district, Saguache County, Colo.: Colorado Geol. Survey Bull. 9, 136 p.
- , 1917, Geology and ore deposits of the Platoro-Summitville mining district, Colorado: Colorado Geol. Survey Bull. 13, 122 p. [1918].
- Peck, L. C., 1964, Systematic analysis of silicates: U.S. Geol. Survey Bull. 1170, 89 p.
- Pichler, Hans, and Zeil, Werner, 1969, Die quartäre "Andesit"-Formation in der Hochkordillere Nord-Chiles: Geol. Rundschau, v. 58, no. 3, p. 866-903.
- Plouff, Donald, and Pakiser, L. C., 1972, Gravity study of the San Juan Mountains, Colorado, in Geological Survey research 1972: U.S. Geol. Survey Prof. Paper 800-B, p. B183-B190.
- Ratté, J. C., and Steven, T. A., 1964, Magmatic differentiation in a volcanic sequence related to the Creede caldera, Colorado, in Short papers in geology and hydrology: U.S. Geol. Survey Prof. Paper 475-D, p. D49-D53.
- , 1967, Ash flows and related volcanic rocks associated with the Creede caldera, San Juan Mountains, Colorado: U.S. Geol. Survey Prof. Paper 524-H, 58 p.
- Ross, C. S., and Smith, R. L., 1955, Water and other volatiles in volcanic glasses: Am. Mineralogist, v. 40, nos. 11-12, p. 1071-1089.
- , 1961, Ash-flow tuffs—their origin, geologic relations, and identification: U.S. Geol. Survey Prof. Paper 366, 81 p.
- Scholz, C. H., Barazangi, Muawia, and Sbar, M. L., 1971, Late Cenozoic evolution of the Great Basin, Western United States, as an ensialic interarc basin: Geol. Soc. America Bull., v. 82, no. 11, p. 2979-2990.
- Shapiro, Leonard, 1967, Rapid analysis of rocks and minerals by a single-solution method, in Geological Survey research 1967: U.S. Geol. Survey Prof. Paper 575-B, p. B187-B191.
- Shapiro, Leonard, and Brannock, W. W., 1962, Rapid analysis of silicate, carbonate, and phosphate rocks: U.S. Geol. Survey Bull. 1144-A, 56 p.
- Sharp, W. N., and Gaultier, J. L., 1968, Lead, copper, molybdenum, and zinc geochemical anomalies south of the Summitville district, Rio Grande County, Colorado: U.S. Geol. Survey Circ. 557, 7 p.
- Shoemaker, E. M., 1956, Structural features of the central Colorado Plateau and their relation to uranium deposits, in Page, L. R., Stocking, H. E., and Smith, H. B., compilers, Contributions to the geology of uranium and thorium by the United States Geological Survey and Atomic Energy Commission for the United Nations International Conference on Peaceful Uses of Atomic Energy, Geneva, Switzerland, 1955: U.S. Geol. Survey Prof. Paper 300, p. 155-170.
- Sinclair, W. F., 1963, Geology of the Upper East Fork of the San Juan River area, Mineral and Archuleta Counties, Colorado: Colorado School Mines unpub. M. S. thesis, 133 p.

- Smith, R. L., 1960a, Ash flows—A review: *Geol. Soc. America Bull.*, v. 71, no. 6, p. 795-842.
- _____, 1960b, Zones and zonal variations in welded ash flows: U.S. Geol. Survey Prof. Paper 354-F, p. 149-159.
- Smith, R. L., and Bailey, R. A., 1968, Resurgent cauldrons, in *Studies in volcanology—A memoir in honor of Howel Williams*: *Geol. Soc. America Mem.* 116, p. 613-662.
- Smith, R. L., Bailey, R. A., and Ross, C. S., 1970, Geologic map of the Jemez Mountains, New Mexico: U.S. Geol. Survey Misc. Geol. Inv. Map I-571.
- Steven, T. A., 1967, Geologic map of the Bristol Head quadrangle, Mineral and Hisndale Counties, Colorado: U.S. Geol. Survey Geol. Quad. Map GQ-631.
- _____, 1968, Ore deposits in the central San Juan Mountains, Colorado, in Ridge, J. D., ed., *Ore deposits of the United States, 1933-1967 (Graton-Sales Volume)*, v. 1: Am. Inst. Mining, Metall., and Petroleum Engineers, p. 706-713.
- Steven, T. A., and Epis, R. C., 1968, Oligocene volcanism in south-central Colorado, in Epis, R. C., ed., *Cenozoic volcanism in the southern Rocky Mountains*: Colorado School Mines Quart., v. 63, no. 3, p. 241-258.
- Steven, T. A., and Lipman, P. W., 1968, Central San Juan cauldron complex, Colorado [abs.], in Epis, R. C., ed., *Cenozoic volcanism in the southern Rocky Mountains*: Colorado School Mines Quart., v. 63, no. 3, p. 209; *Geol. Soc. America Spec. Paper* 115, p. 450-451, 1968.
- _____, 1973, Geologic map of the Spar City quadrangle, Mineral County, Colorado: U.S. Geol. Survey Geol. Quad. Map GQ-1052.
- Steven, T. A., Lipman, P. W., Hail, W. J., Jr., Barker, Fred, and Luedke, R. G., 1974, Geologic map of the Durango quadrangle, southwestern Colorado: U.S. Geol. Survey Misc. Geol. Inv. Map I-764.
- Steven, T. A., Lipman, P. W., and Olson, J. C., 1974, Ash-flow stratigraphy and caldera structures in the San Juan volcanic field, southwestern Colorado, in Cohee, G. V., and Wright, W. B., *Changes in stratigraphic nomenclature by the U.S. Geological Survey, 1972*: U.S. Geol. Survey Bull. 1394-A, p. A75-A82.
- Steven, T. A., Luedke, R. G., and Lipman, P. W., 1974, Relation of mineralization to calderas in the San Juan volcanic field, southwestern Colorado: U.S. Geol. Survey Jour. Research, v. 2, no. 4.
- Steven, T. A., Mehnert, H. H., and Obradovich, J. D., 1967, Age of volcanic activity in the San Juan Mountains, Colorado, in *Geological Survey research 1967*: U.S. Geol. Survey Prof. Paper 575-D, p. D47-D55.
- Steven, T. A., and Ratté, J. C., 1960, Geology and ore deposits of the Summitville district, San Juan Mountains, Colorado: U.S. Geol. Survey Prof. Paper 343, 70 p.
- _____, 1964, Revised Tertiary volcanic sequence in the central San Juan Mountains, Colorado, in *Short papers in geology and hydrology*: U.S. Geol. Survey Prof. Paper 475-D, p. D54-D63.
- _____, 1965, Geology and structural control of ore deposition in the Creede district, San Juan Mountains, Colorado: U.S. Geol. Survey Prof. Paper 487, 87 p.
- Steven, T. A., Schmitt, L. J., Jr., Sheridan, M. J., and Williams, F. E., 1969, Mineral resources of the San Juan primitive area, Colorado, with a section on Iron resources in the Irving Formation, by J. E. Gair and Harry Klemic: U.S. Geol. Survey Bull. 1261-F, 187 p.
- Stewart, J. H., 1971, Basin and Range structure; a system of horsts and grabens produced by deep-seated extension: *Geol. Soc. America Bull.*, v. 82, no. 4, p. 1019-1044.
- Stringham, Bronson, 1966, Igneous rock types and host rocks associated with porphyry copper deposits, in Titley, S. R., and Hicks, C. L., eds., *Geology of the porphyry copper deposits, southwestern North America*: Tucson, Ariz., Arizona Univ. Press, p. 35-40.
- Thompson, G. A., 1960, Problem of Late Cenozoic structure of the Basin Ranges: Internat. Geol. Cong., 21st, Copenhagen 1960, Rept., pt. 18, p. 62-68.
- Truesdell, A. H., 1966, Ion-exchange constants of natural glasses by the electrode method: *Am. Mineralogist*, v. 51, nos. 1-2, p. 110-122.
- Van Houten, F. B., 1957, Appraisal of Ridgway and Gunnison "tillites," southwestern Colorado: *Geol. Soc. America Bull.*, v. 68, no. 3, p. 383-388.
- Varnes, D. J., 1963, Geology and ore deposits of the South Silverton mining area, San Juan County, Colorado: U.S. Geol. Survey Prof. Paper 378-A, 56 p.
- Wallace, S. R., Muncaster, N. K., Jonson D. C., Mackenzie, W. B., Bookstrom, A. A., and Surface, V. E., 1968, Multiple intrusion and mineralization at Climax, Colorado, in Ridge, J. D., ed., *Ore deposits of the United States, 1933-1967 (Graton-Sales volume)*, v. 1: Am. Inst. Mining, Metall., and Petroleum Engineers, p. 605-640.
- Wilcox, R. E., 1944, The rhyolite-basalt complex on Gardiner River, Yellowstone Park, Wyoming: *Geol. Soc. America Bull.*, v. 55, no. 9, p. 1047-1079.
- Williams, Howel, 1932, The history and character of volcanic domes: California Univ. Dept. Geol. Sci. Bull., v. 21, p. 51-146.
- _____, 1941, Calderas and their origin: California Univ. Pubs. Geol. Sci. Bull., v. 25, no. 6, p. 239-346.
- Wright, T. L., 1968, An X-ray method for determining the composition and structural state from measurement of 2θ values for three reflections, pt. 2 of X-ray and optical study of alkali feldspar: *Am. Mineralogist*, v. 53, nos. 1-2, p. 88-104.
- Wright, T. L., and Stewart, D. B., 1968, Determination of composition and structural state from refined unit-cell parameters and $2V$, pt. 1 of X-ray and optical study of alkali feldspar: *Am. Mineralogist*, v. 53, nos. 1-2, p. 38-87.
- Zeil, Werner, and Pichler, Hans, 1967, Die känozoische Rhyolith-Formation im mittleren Abschnitt der Anden: *Geol. Rundschau*, v. 57, no. 1, p. 48-81.

INDEX

[Italic page numbers indicate major references]

| A | Page | Analysts—Continued | Page | Calderas—Continued | Page |
|--|----------------------------|---|------------------------|--|-----------------------|
| Adams Fork | 87 | Chloe, Gillison | 11, 20, 42, 60, 80, 94 | Creede | 53, 54, 103, 104, 114 |
| Adams Fork volcano | 12, 87 | Elmore, P. L. D. | 11, 20, 42, 60, 80, 94 | Glen Coe type | 116 |
| Age, andesitic dikes | 87 | Fletcher, J. D. | 11, 20, 42, 60, 80, 94 | island arc environment | 116 |
| Bear Creek stock cluster | 86 | Glenn, John | 11, 20, 42, 60, 80, 94 | Japanese | 117 |
| calderas of San Juan cluster | 116 | Hamilton, J. C. | 20, 42, 94 | Krakatoan type | 116 |
| Carpenter Ridge Tuff | 53 | Harris, J. L. | 60, 80 | La Garita | 47, 104 |
| Cat Creek stock | 84 | Kelsey, James | 11, 20, 42, 60, 80, 94 | Lake City | 93, 97, 116 |
| Conejos Formation | 9 | Neiman, Harriet | 60, 80 | Mount Hope. <i>See</i> Mount Hope caldera. | |
| Cornwall fault | 109 | Neuerburg, F. H. | 42 | northeastern San Juan Mountains | 18 |
| granitic stocks | 78 | Parker, C. L. | 42, 56 | Platoro. <i>See</i> Platoro caldera. | |
| Hinsdale Formation | 92, 96 | Rait, Norma | 11, 42, 60, 80 | relation to earlier volcanoes | 101 |
| Jasper stock | 84 | Smith, H. | 11, 20, 42, 60, 80, 94 | relation to mineralization | 7, 113 |
| La Jara Canyon Member of Treasure | | Smith, V. C. | 42 | relative ages | 116 |
| Treasure Mountain Tuff | 29 | Worthing, H. W. | 80 | resurgence | 101, 107 |
| Los Pinos Formation | 77 | Andesite of Summit Peak | 55, 62, 67, 87 | cause of assymmetry | 107 |
| lower tuff of Treasure | | Animas Formation | 8 | Mount Hope caldera | 49 |
| Mountain Tuff | 23 | Ash-fall tuff | 31 | Platoro caldera | 107 |
| Masonic Park Tuff | 47 | agglutinated | 23, 46, 71 | San Juan caldera cluster | 110 |
| Mount Hope caldera | 46 | Ash-flow lobes | 22, 23, 25 | stage 1 in cycle | 103 |
| Ojito Creek Member of Treasure | | Ash-flow sheets | 7, 14 | stage 2 in cycle | 104 |
| Mountain Tuff | 35 | accumulation concurrent with subsidence | 25 | stage 3 in cycle | 104 |
| ore deposition at Summitville | 113 | compositional zonation | 51, 116 | stage 4 in cycle | 107 |
| quartz latite of South Mountain | 74, 113 | first widespread | 25 | stage 5 in cycle | 107 |
| quartz latitic and rhyolitic dikes | 90 | geometric model | 30 | stage 6 in cycle | 108 |
| Ra Jadero Member of Treasure | | magnetic polarities | 6, 15 | stage 7 in cycle | 108 |
| Mountain Tuff | 40 | most voluminous | 47 | Silverton | 107, 115 |
| regional extensional faulting | 112 | overlying Treasure Mountain Tuff | 41 | Summitville. <i>See</i> Summitville caldera. | |
| rhyodacite of Park Creek | 73 | petrologic features | 15 | Timber Mountain | 107 |
| rhyolite of Cropsy Mountain | 75 | relation between outflow sheets | | Vailes | 104 |
| Rio Grande fault zone | 110 | and intracaldera tuffs | 25, 27, 53 | western San Juan Mountains | 18 |
| San Juan volcanic field | 101 | source magma composition | 116 | California Gulch | 107 |
| Snowshoe Mountain Tuff | 54 | B | | Canyon Diablo stock | 66, 86 |
| Summitville Andesite | 66 | Bachelor Mountain Member of Carpenter | | Carpenter Ridge Tuff | 49, 104 |
| Summitville fault | 112 | Ridge Tuff | 49, 53 | Cat Creek | 16, 67 |
| tuff of Rock Creek | 16 | Banded Peak area | 23, 90 | Cat Creek stock | 67, 82, 84, 87, 114 |
| volcanics of Green Ridge | 69, 70 | Basalt-rhyolite association | 90, 117 | Cat Creek volcano | 47, 67, 77, 82 |
| Wason Park Tuff | 54 | Batholith | 110, 116 | Cataract Creek stock | 86 |
| Alamosa River canyon | 31, 33, 34, 36, 40, 62, 82 | Bear Creek stock | 84, 11 | Chemical composition, alkali content | |
| Alamosa River stock | 35, 78, 109 | Bear Creek stock cluster | 84, 111, 114 | of San Juan andesites | 117 |
| hydrothermal alteration | 78, 114, 115 | Beaver Creek | 49, 77, 96 | Carpenter Ridge Tuff | 51 |
| mineralization | 114, 115 | Beaver Lake Creek | 63, 66, 108 | Conejos Formation | 9 |
| radiating dikes | 78, 86, 87, 89 | Beaver Mountain | 51 | Fish Canyon Tuff | 49 |
| radiometric date | 78 | Beidell Quartz Latite | 8 | Hinsdale basalts | 92 |
| relation to Summitville Andesite | 66 | Bennett Peak | 16, 40, 41, 69, 106 | Huerto Andesite | 55 |
| Alteration | 113 | Bibliography | 120 | La Jara Canyon Member of | |
| Cat Creek stock | 84, 114 | Treasure Mountain Tuff | 28 | Treasure Mountain of | |
| Treasure Mountain Tuff | 84 | magma of San Juan volcanic field | 116 | Treasure Mountain Tuff | 28 |
| quartz latite of South Mountain | 78 | Masonic Park Tuff | 46 | See also Analyses. | |
| <i>See also</i> Hydrothermal alteration; Mineralization. | | Ojito Creek Member of Treasure | | Treasure Mountain Tuff | 35 |
| Alum Creek Porphyry | 114 | Mountain Tuff | 35 | quartz latite of South Mountain | 73 |
| Analyses, ash-flow sheets overlying Treasure | | Brazos Arch | 101 | Ra Jadero Member of Treasure | |
| Mountain Tuff | 42 | Brazos Basalt | 92 | Mountain Tuff | 40 |
| methods | 5 | Burnt Creek | 84 | relation to phenocryst content | 5, 19, 29, 40 |
| postcollapse Platoro caldera | | C | | rhyodacite of Fisher Gulch | 58 |
| lava flows | 60 | Calderas | 7, 101 | rhyolite of Cropsy Mountain | 75 |
| Treasure Mountain Tuff | 20 | Aso | 117 | San Juan volcanic rocks | 6 |
| tuff of Rock Creek | 20 | Bachelor | 49, 104, 110, 114 | Treasure Mountain Tuff | 19, 116 |
| <i>See also</i> Chemical composition. | | central San Juan Mountains | 41 | tuff of Rock Creek | 16 |
| Analysts, Artis, Lowell | 11, 20, 42, 60, 80, 94 | Cochetopa | 107 | volcanics of Green Ridge | 69, 70 |
| Botts, Samuel | 11, 20, 42, 60, 80, 94 | cratonic environment | 116 | <i>See also</i> Analyses. | |

INDEX

| | Page | | Page |
|---|-----------------------|--|-----------------------|
| Conejos Formation—Continued | | Faults—Continued | Page |
| age | 9 | Rio Grande zone | 110 |
| analyses | 9, 11 | Summitville | 71, 111, 112, 113 |
| associated intrusives | 78, 84, 86, 87 | Summitville caldera ring-fracture | |
| chemical composition | 9 | zone | 35, 84, 108, 113, 115 |
| cone breccias | 9, 12 | Fieldwork | 2 |
| definition | 14 | Fish Canyon Tuff | 47, 104 |
| lithology | 9, 12, 13, 62, 65, 67 | Fisher Gulch | 63 |
| radiometric dates | 9 | Fisher Quartz Latite | 70, 73, 74 |
| similar later volcanic activity | 108 | Forest King area | 64 |
| upper lava unit | 9, 13 | Fossils | 66 |
| vent facies | 9, 12, 77 | Gilpin Peak Tuff | 16 |
| volcaniclastic facies | 9, 13, 77 | Goose Creek | 41, 55 |
| volcanoes | 8, 9, 12, 16, 27, 101 | Grabens | 77, 110, 113, 114 |
| Conejos Peak | 12, 33, 64, 66, 86 | Gravity anomaly | 116 |
| Conejos River | 8, 12, 22, 107 | Grayback Mountain | 96 |
| Cornwall fault | 66, 78, 108, 109 | Green Ridge | 47, 49, 69, 70, 77 |
| Cornwall Mountain | 27, 97 | Gunnison River | 47, 49 |
| Cornwall Mountain resurgent block | 65, 103 | H, I, J | |
| cause of resurgence | 87, 107 | Handkerchief Mesa | 71, 97, 98 |
| intracaldera tuff exposure | 27, 107 | Hinsdale Formation | 8, 90 |
| volume of initial collapse | 105 | age | 92, 96 |
| Cornwall Mountain stock | 87 | analyses | 94 |
| Cornwalls Nose | 64, 66, 109 | basaltic lavas | 90, 97 |
| Correlation, andesite of Summit Peak | 67 | chemical composition | 92 |
| Conejos Formation | 8 | cinder cones | 97, 98 |
| Hinsdale basalts | 92 | faulting | 112 |
| Sheep Mountain Andesite | 67 | lithology | 92, 96, 98 |
| volcanics of Green Ridge | 62, 67 | mixed-lava complexes | 97 |
| Crater Creek stock | 84, 114 | radiometric dates | 92, 96 |
| Cretaceous sedimentary rocks | 8 | rhyolitic lavas and tuffs | 93 |
| Cropsy Mountain | 73, 74 | vents | 92 |
| Crustal extension, coincidence | | xenocrysts | 92, 98 |
| with petrologic change | 8, 117 | Horseshoe Mountain | 27 |
| Cumbres Pass | 112 | Huerto Andesite | 55, 65, 67 |
| D, E | | Huerto Formation | 55 |
| Del Norte Peak | 27, 41 | Hydrothermal alteration | 7 |
| Dikes | 7, 78, 86 | Alamosa River stock | 78, 114, 115 |
| Adams Fork volcano | 87 | Bear Creek stock cluster | 85, 111, 114 |
| Alamosa River stock | 78, 86, 87, 89 | Jasper stock | 84, 114 |
| andesitic | 86 | Pass Creek fault zone | 110 |
| Cat Creek stock | 84, 87 | resurgent-caldera cycle | 108 |
| Cataract Creek stock | 86 | <i>See also</i> Alteration; Mineralization. | |
| cutting Alamosa River stock | 114 | Intracaldera tuffs | 104 |
| distribution | 87, 88 | Carpenter Ridge Tuff | 53 |
| Elwood Creek fault zone | 88 | Fish Canyon Tuff | 47 |
| mafic | 87 | geometric model | 30 |
| most spectacular | 88 | indicator of concurrent eruption and collapse | 104 |
| Pass Creek fault zone | 110 | La Jara Canyon Member of Treasure | |
| quartz latitic and rhyolitic | 88 | Mountain Tuff | 27 |
| rhyodacitic | 87 | lithology | 27 |
| rhyolitic | 98 | relation to outflow sheets | 25, 27, 53 |
| upper Alamosa River | 87 | Intrusive rocks | 7, 78 |
| Durango map | 2 | Isopach maps | 3, 110 |
| Elephant Mountain | 96 | Isotopic dates. <i>See</i> Radiometric dates. | |
| Elwood Creek stock | 84 | Jacobs Hill | 69, 70 |
| Elwood Pass | 71 | Jasper stock | 84, 109, 114 |
| Eruption concurrent with caldera collapse | 103 | L | |
| Eruption from differentiated | | La Garita Member of Fish Canyon Tuff | 47 |
| magma chamber | 12, 29, 52, 104 | La Garita Quartz Latite | 47 |
| F, G | | La Jara Canyon | 25 |
| Fault-graben systems | 110 | La Jara Canyon Member of Treasure | |
| Faults, along Beaver Creek | 49 | Mountain Tuff | 25, 46, 58, 103 |
| antithetic | 112, 113 | Laccoliths | 7, 82, 86 |
| California Gulch | 107 | Lake Fork Formation | 8 |
| Cornwall | 66, 78, 108, 109 | Lake sediments | 108 |
| Creede caldera | 114 | Landslides | 65, 106 |
| Elwood Creek zone | 88, 110, 114 | Laramide structural features | 101 |
| influence on mineralization | 113, 115 | Latite of Red Mountain | 92 |
| La Jara Reservoir | 92 | Lava domes | 70, 73, 93 |
| La Jara Reservoir-Cumbres Pass system | 112 | ring | 108 |
| Pass Creek-Elwood Creek-Platoro | | Lava flows, analyses | 11, 56, 60, 94 |
| system | 110, 113, 115 | early intermediate-composition | 6, 8, 13 |
| Pass Creek zone | 110 | late basalts and rhyolites | 90 |
| Platoro caldera ring-fracture zone | 104, 107, 113 | overlying Treasure Mountain Tuff | 54 |
| Platoro zone | 107, 110, 112, 114 | M | |
| regional caldera-related | 110 | Lava Flows—Continued | |
| INDEX | | postcollapse Platoro caldera | 55, 58 |
| | | Lithology, Alamosa River stock | 78 |
| | | andesite of Summit Peak | 67 |
| | | Carpenter Ridge Tuff | 49 |
| | | Conejos Formation | 9, 12, 13, 62, 65, 67 |
| | | Fish Canyon Tuff | 47 |
| | | granitic stocks | 78 |
| | | Hinsdale Formation | 92, 96, 98 |
| | | Huerto Andesite | 55, 65, 67 |
| | | La Jara Canyon Member of Treasure | |
| | | Mountain Tuff | 27, 46, 58 |
| | | lower tuff of Treasure Mountain Tuff | 22 |
| | | Masonic Park Tuff | 45 |
| | | middle tuff of Treasure Mountain Tuff | 32 |
| | | mixed-lava complexes | 98 |
| | | most distinctive ash-flow unit | 47 |
| | | Ojito Creek Member of Treasure | |
| | | Mountain Tuff | 33 |
| | | quartz latite of South Mountain | 71, 73 |
| | | Ra Jadero Member of Treasure | |
| | | Mountain Tuff | 40 |
| | | rhyodacite of Fisher Gulch | 58 |
| | | rhyodacite of Park Creek | 71 |
| | | Sheep Mountain Andesite | 55 |
| | | Snowshoe Mountain Tuff | 54 |
| | | Summitville Andesite | 62, 71, 84 |
| | | tuff of Rock Creek | 16 |
| | | volcanics of Green Ridge | 67, 69, 70 |
| | | Wason Park Tuff | 53 |
| | | Lookout Mountain | 74, 90 |
| | | Los Mogotes shield volcano | 77, 92 |
| | | Los Pinos Formation | 69, 70, 76 |
| | | M | |
| | | Magmas, differentiation | |
| | | before eruption | 12, 29, 52, 104, 116 |
| | | differentiation of rhyodacitic intrusives | 87 |
| | | mixing before eruption | 75, 92, 98, 99 |
| | | Magnetic polarities | 6 |
| | | ash-flow sheets | 6, 15 |
| | | Carpenter Ridge Tuff | 53 |
| | | Fish Canyon Tuff | 49 |
| | | La Jara Canyon Member of Treasure | |
| | | Mountain Tuff | 29 |
| | | lower tuff of Treasure Mountain Tuff | 23 |
| | | Masonic Park Tuff | 47 |
| | | middle tuff of Treasure Mountain Tuff | 32 |
| | | Ojito Creek Member of Treasure | |
| | | Mountain Tuff | 33, 36 |
| | | Ra Jadero Member of Treasure | |
| | | Mountain Tuff | 40 |
| | | Snowshoe Mountain Tuff | 54 |
| | | Summitville Andesite | 67 |
| | | Treasure Mountain Tuff | 19 |
| | | tuff of Rock Creek | 16 |
| | | Wason Park Tuff | 54 |
| | | Mammoth Mountain | 107 |
| | | Mapping | 2 |
| | | Maps, summary | 3 |
| | | Marble Mountain | 65, 66, 109 |
| | | Masonic Park Tuff | 18, 41 |
| | | Mineralization | 7, 113 |
| | | Alamosa River stock | 114, 115 |
| | | Bear Creek stock cluster | 111 |
| | | Jasper stock | 114 |
| | | level of exposure of deposits | 115 |
| | | metal zoning | 115 |
| | | relation to caldera margins | 7, 113 |
| | | Platoro fault zone | 114 |
| | | Summitville caldera margin | 108 |
| | | Summitville ore body | 73, 113 |
| | | <i>See also</i> Alteration; Hydrothermal alteration. | |
| | | Mining districts | 113 |
| | | Mixed-lava complexes | 97 |
| | | Cornwall Mountain | 97 |
| | | evidence for mixing | 98 |
| | | Gardiner River in Yellowstone | |
| | | National Park | 97, 98 |
| | | Handkerchief Mesa | 97 |
| | | North Mountain | 75, 112 |

| Page | | Page | | | | | | | | | | | | | | | | | | | | | |
|--|---------------------|---|-----------------------|---|-------------|---------------------------|------------|---|-------------|---------------------------|------------|---|----------|---------------------------|------------|------------------------------------|----------|---------------------------|--------|---------------------------------|---------|---------------------------|--------|
| Modal compositions | 3 | Platoro caldera—Continued | | | | | | | | | | | | | | | | | | | | | |
| Mount Hope | 47 | relation to Conejos volcanoes | 12, 104 | | | | | | | | | | | | | | | | | | | | |
| Mount Hope caldera | 41, 45, 47 | resurgence | 107 | | | | | | | | | | | | | | | | | | | | |
| age | 46 | ring-fracture zone | 104, 107, 113 | | | | | | | | | | | | | | | | | | | | |
| marginal volcanoes | 55 | similarity to caldera in Japan | 117 | | | | | | | | | | | | | | | | | | | | |
| resurgence | 49 | topography before ash-flow | | | | | | | | | | | | | | | | | | | | | |
| eruption | 9, 27 | eruption | 9, 27 | | | | | | | | | | | | | | | | | | | | |
| and emplacement | 29, 35, 40, 51 | topography during ash-flow | | | | | | | | | | | | | | | | | | | | | |
| eruption | 22, 27, 45 | eruption | 22, 27, 45 | | | | | | | | | | | | | | | | | | | | |
| tumescence | 103 | volume of collapse | 105 | | | | | | | | | | | | | | | | | | | | |
| volume of collapse | 105 | wedging of tuffs at topographic walls | 27, 30 | | | | | | | | | | | | | | | | | | | | |
| Platoro fault zone | 107, 110, 112, 114 | Platoro map | 2 | | | | | | | | | | | | | | | | | | | | |
| Platoro map | 2 | Platoro Reservoir area | 107 | | | | | | | | | | | | | | | | | | | | |
| Plugs | 88, 114 | Plugs | 88, 114 | | | | | | | | | | | | | | | | | | | | |
| Adams Fork | 87 | Ojito Creek | 89 | | | | | | | | | | | | | | | | | | | | |
| Ojito Creek | 89 | Park Creek | 90 | | | | | | | | | | | | | | | | | | | | |
| Park Creek | 90 | Trail Lake | 90 | | | | | | | | | | | | | | | | | | | | |
| Poage Lake | 98 | Pollen | 66 | | | | | | | | | | | | | | | | | | | | |
| Pollution | 115 | Porphyry ore deposits | 115 | | | | | | | | | | | | | | | | | | | | |
| Precambrian rocks | 8 | Preliminary work | 2 | | | | | | | | | | | | | | | | | | | | |
| Previous studies | 2 | Prospect Mountain | 23, 27, 87 | | | | | | | | | | | | | | | | | | | | |
| Prospect Mountain stock | 87 | Pumice fragments, sorting during eruption | | | | | | | | | | | | | | | | | | | | | |
| Pumice fragments, sorting during eruption | | emplacement | 51 | | | | | | | | | | | | | | | | | | | | |
| Pyroclastic cones | 71, 75, 96 | Pyroclastic cones | 71, 75, 96 | | | | | | | | | | | | | | | | | | | | |
| Q, R | | | | | | | | | | | | | | | | | | | | | | | |
| Quartz latite of South Mountain | 73, 112 | Quartz latite of South Mountain | 73, 112 | | | | | | | | | | | | | | | | | | | | |
| age | 74, 113 | associated intrusives | 89, 90 | | | | | | | | | | | | | | | | | | | | |
| ore deposits | 113, 115 | ore deposits | 113, 115 | | | | | | | | | | | | | | | | | | | | |
| Ra Jadero Member of Treasure | | Ra Jadero Member of Treasure | | | | | | | | | | | | | | | | | | | | | |
| Mountain Tuff | 36, 108 | Mountain Tuff | 36, 108 | | | | | | | | | | | | | | | | | | | | |
| Radiometric dates | 6 | Radiometric dates | 6 | | | | | | | | | | | | | | | | | | | | |
| Alamosa River stock | 78 | Alamosa River stock | 78 | | | | | | | | | | | | | | | | | | | | |
| Conejos Formation | 9 | Hinsdale Formation | 92, 96 | | | | | | | | | | | | | | | | | | | | |
| Hinsdale Formation | 92, 96 | igneous rocks at Summitville caldera | 110 | | | | | | | | | | | | | | | | | | | | |
| La Jara Canyon Member of Treasure | | La Jara Canyon Member of Treasure | | | | | | | | | | | | | | | | | | | | | |
| Mountain Tuff | 29 | Mountain Tuff | 29 | | | | | | | | | | | | | | | | | | | | |
| lower tuff of Treasure | | Masonic Park Tuff | 47 | | | | | | | | | | | | | | | | | | | | |
| Mountain Tuff | 23 | mineralization at Summitville | 113 | | | | | | | | | | | | | | | | | | | | |
| Masonic Park Tuff | 45 | quartz latite of | | | | | | | | | | | | | | | | | | | | | |
| Ojito Creek Member of Treasure | | South Mountain | 74, 113 | | | | | | | | | | | | | | | | | | | | |
| Mountain Tuff | 35 | rhyolite of Cropsy Mountain | 75 | | | | | | | | | | | | | | | | | | | | |
| quartz latitic and rhyolitic intrusives | 90 | sanidine porphyry dike | 90 | | | | | | | | | | | | | | | | | | | | |
| Ra Jadero Member of Treasure | | Ranger Creek | 108 | | | | | | | | | | | | | | | | | | | | |
| Mountain Tuff | 40 | Rawley Andesite | 8 | | | | | | | | | | | | | | | | | | | | |
| relation to bulk-rock | | Reconnaissance mapping | 2 | | | | | | | | | | | | | | | | | | | | |
| composition | 5, 19, 29, 40 | Red Mountain | 62, 65, 92, 108 | | | | | | | | | | | | | | | | | | | | |
| rhodocrite of Fisher Gulch | 58 | Regional faulting | 110, 112 | | | | | | | | | | | | | | | | | | | | |
| rhodocrite of Park Creek | 71 | Regional tilting | 67, 77, 112, 113 | | | | | | | | | | | | | | | | | | | | |
| rhyolite of Cropsy Mountain | 74 | Rhyodacite of Fisher Gulch | 56, 107, 108 | | | | | | | | | | | | | | | | | | | | |
| rhyolite of Park Creek | 75 | Rhyodacite of Park Creek | 70, 87, 109 | | | | | | | | | | | | | | | | | | | | |
| Snowshoe Mountain Tuff | 54 | Rhyolite of Cropsy Mountain | 74, 89, 90 | | | | | | | | | | | | | | | | | | | | |
| sorting during eruption | | Rio Grande fault zone | 110 | | | | | | | | | | | | | | | | | | | | |
| and emplacement | 29, 35, 40, 51, 104 | Rio Grande rift depression | 7, 113, 117 | | | | | | | | | | | | | | | | | | | | |
| Summitville Andesite | 62 | Rito Gato | 66, 108 | | | | | | | | | | | | | | | | | | | | |
| Treasure Mountain Tuff | 18 | Rock Creek | 16, 23 | | | | | | | | | | | | | | | | | | | | |
| tuff of Rock Creek | 16 | S | | | | | | | | | | | | | | | | | | | | | |
| volcanics of Green Ridge | 69, 70 | Saddle Mountain | 55 | | | | | | | | | | | | | | | | | | | | |
| Wason Park Tuff | 53 | San Francisco Creek | 12 | | | | | | | | | | | | | | | | | | | | |
| Pinos Creek | 12 | San Jose Formation | 6 | | | | | | | | | | | | | | | | | | | | |
| Plate tectonics | 116, 117 | San Juan Formation | 8 | | | | | | | | | | | | | | | | | | | | |
| Platoro caldera | 103 | San Juan volcanic field | 6, 101 | | | | | | | | | | | | | | | | | | | | |
| ash-flow eruptions | 104 | relation to plate tectonics | 116 | | | | | | | | | | | | | | | | | | | | |
| collapse | 25, 104 | San Luis Valley graben system | 77 | | | | | | | | | | | | | | | | | | | | |
| marginal volcanoes | 49 | Servilleta Formation | 8, 93 | | | | | | | | | | | | | | | | | | | | |
| moat | 107 | Shards, sorting during eruption | | | | | | | | | | | | | | | | | | | | | |
| east side | 33, 66 | and emplacement | 51 | | | | | | | | | | | | | | | | | | | | |
| northeast side | 47, 107 | Sheep Mountain Andesite | 55, 67 | | | | | | | | | | | | | | | | | | | | |
| southeast side | 56, 65, 108 | Sheep Mountain Formation | 55 | | | | | | | | | | | | | | | | | | | | |
| southwest side | 62, 66, 107 | T | | | | | | | | | | | | | | | | | | | | | |
| postcollapse igneous activity | 55 | Table Mountain | 55 | | | | | | | | | | | | | | | | | | | | |
| postresurgence volcanism | 107, 117 | Telluride Conglomerate | 6 | | | | | | | | | | | | | | | | | | | | |
| premonitory eruptions | 23, 104 | Terminology | 3, 5 | | | | | | | | | | | | | | | | | | | | |
| Pino Creek | 12 | Terrace Reservoir | 23, 27 | | | | | | | | | | | | | | | | | | | | |
| Plate tectonics | 116, 117 | Terrace Reservoir laccolith | 82 | | | | | | | | | | | | | | | | | | | | |
| Platoro caldera | 103 | Topography, before ash-flow eruption | | | | | | | | | | | | | | | | | | | | | |
| ash-flow eruptions | 104 | Conejos | 9, 22, 27 | | | | | | | | | | | | | | | | | | | | |
| collapse | 25, 104 | during ash-flow eruption | 22, 27, 45 | | | | | | | | | | | | | | | | | | | | |
| marginal volcanoes | 49 | Platoro caldera walls | 105, 106 | | | | | | | | | | | | | | | | | | | | |
| moat | 107 | pre-Conejos | 9 | | | | | | | | | | | | | | | | | | | | |
| east side | 33, 66 | resurgent calderas | 103 | | | | | | | | | | | | | | | | | | | | |
| northeast side | 47, 107 | Summitville caldera walls | 66, 71, 108, 109 | | | | | | | | | | | | | | | | | | | | |
| southeast side | 56, 65, 108 | See also Paleotopography. | | | | | | | | | | | | | | | | | | | | | |
| southwest side | 62, 66, 107 | Tracy Creek Quartz Latite | 8 | | | | | | | | | | | | | | | | | | | | |
| postcollapse igneous activity | 55 | Treasure Mountain | 16, 23, 29 | | | | | | | | | | | | | | | | | | | | |
| postresurgence volcanism | 107, 117 | U | | | | | | | | | | | | | | | | | | | | | |
| premonitory eruptions | 23, 104 | Sheepshead | 74, 75, 90 | | | | | | | | | | | | | | | | | | | | |
| N | | Sills | 87, 90 | | | | | | | | | | | | | | | | | | | | |
| O | | Silver Mountain | 69, 70 | | | | | | | | | | | | | | | | | | | | |
| Navajo Peak | 9, 23 | Snowball Park | 9, 23 | | | | | | | | | | | | | | | | | | | | |
| Needle Mountains | 47, 49 | Snowshoe Mountain Tuff | 54, 104 | | | | | | | | | | | | | | | | | | | | |
| Needle Mountains uplift | 101 | Sorting of phenocrysts during eruption | | | | | | | | | | | | | | | | | | | | | |
| Nomenclature | 5 | and emplacement | 29, 35, 40, 51 | | | | | | | | | | | | | | | | | | | | |
| North Mountain | 27, 74, 75, 109 | Sources, Carpenter Ridge Tuff | 49 | | | | | | | | | | | | | | | | | | | | |
| Ojito Creek | 33, 89 | Los Pinos Formation | 69 | | | | | | | | | | | | | | | | | | | | |
| Ojito Creek Member of Treasure | | lower tuff of Treasure | | | | | | | | | | | | | | | | | | | | | |
| Mountain Tuff | 33, 108 | Mountain Tuff | 23 | | | | | | | | | | | | | | | | | | | | |
| Ore deposits. See Mineralization. | | Masonic Park Tuff | 41, 45, 46 | | | | | | | | | | | | | | | | | | | | |
| Outcrop distribution | 3 | Ojito Creek Member of Treasure | | | | | | | | | | | | | | | | | | | | | |
| Outflow sheets, relation to intracaldera tuffs | 26, 27, 53 | Mountain Tuff | 33 | | | | | | | | | | | | | | | | | | | | |
| P | | Ra Jadero Member of Treasure | | | | | | | | | | | | | | | | | | | | | |
| Paleotopography, Alamosa River stock area | 78 | Mountain Tuff | 36 | | | | | | | | | | | | | | | | | | | | |
| Cornwall Mountain resurgent block | 66 | Snowshoe Mountain Tuff | 54 | | | | | | | | | | | | | | | | | | | | |
| Mount Hope caldera area | 49 | Summitville Andesite | 66, 82, 84, 86 | | | | | | | | | | | | | | | | | | | | |
| Platoro caldera area | 22, 27, 45, 55 | volcanics of Green Ridge | 67, 82 | | | | | | | | | | | | | | | | | | | | |
| See also Topography. | | Wason Park Tuff | 53 | | | | | | | | | | | | | | | | | | | | |
| Park Creek | 65, 71, 73, 77, 90 | See also Vents. | | | | | | | | | | | | | | | | | | | | | |
| Petrography | 3 | South Mountain | 73, 74, 75 | | | | | | | | | | | | | | | | | | | | |
| Petrologic change, coincidence | | Spring Creek | 84 | | | | | | | | | | | | | | | | | | | | |
| with crustal extension | 8, 117 | Stocks | 7, 78 | | | | | | | | | | | | | | | | | | | | |
| Petrologic evolution | 8, 115 | Alamosa River. See Alamosa River stock. | | | | | | | | | | | | | | | | | | | | | |
| postcollapse activity | 56 | Bear Creek | 84, 111 | | | | | | | | | | | | | | | | | | | | |
| Petrology, ash-flow sheets | 15 | Bear Creek cluster | 84, 111, 114 | | | | | | | | | | | | | | | | | | | | |
| transition to Hinsdale Formation | 76 | Canyon Diablo | 66, 86 | | | | | | | | | | | | | | | | | | | | |
| transition to quartz latite of | | Cat Creek | 67, 82, 84, 87, 114 | | | | | | | | | | | | | | | | | | | | |
| South Mountain | 71 | Cataract Creek | 86 | | | | | | | | | | | | | | | | | | | | |
| Phenocrysts, Carpenter Ridge Tuff | 51 | Cornwall Mountain | 87 | | | | | | | | | | | | | | | | | | | | |
| determination of composition | 5 | Crater Creek | 84, 114 | | | | | | | | | | | | | | | | | | | | |
| Fish Canyon Tuff | 47 | Elwood Creek | 84 | | | | | | | | | | | | | | | | | | | | |
| La Jara Canyon Member of Treasure | | Jasper | 84, 109, 114 | | | | | | | | | | | | | | | | | | | | |
| Mountain Tuff | 28 | Prospect Mountain | 87 | | | | | | | | | | | | | | | | | | | | |
| lower tuff of Treasure | | Stratigraphy, volcanic | 6 | | | | | | | | | | | | | | | | | | | | |
| Mountain Tuff | 23 | Stratovolcanoes. See Volcanoes. | | | | | | | | | | | | | | | | | | | | | |
| Masonic Park Tuff | 45 | Structural evolution | 101 | | | | | | | | | | | | | | | | | | | | |
| Ojito Creek Member of Treasure | | Subduction | 117 | | | | | | | | | | | | | | | | | | | | |
| Mountain Tuff | 35 | Summer Coon volcano | 9, 12, 69, 116 | | | | | | | | | | | | | | | | | | | | |
| quartz latitic and rhyolitic intrusives | 90 | Summit Peak | 67 | | | | | | | | | | | | | | | | | | | | |
| Ra Jadero Member of Treasure | | Summitville Andesite | 58 | | | | | | | | | | | | | | | | | | | | |
| Mountain Tuff | 40 | age | 66 | | | | | | | | | | | | | | | | | | | | |
| relation to bulk-rock | | associated intrusives | 90 | | | | | | | | | | | | | | | | | | | | |
| composition | 5, 19, 29, 40 | lithology | 62, 71, 84 | | | | | | | | | | | | | | | | | | | | |
| rhodocrite of Fisher Gulch | 58 | Platoro caldera moat | 107, 108 | | | | | | | | | | | | | | | | | | | | |
| rhodocrite of Park Creek | 71 | relation to Alamosa River stock | 66 | | | | | | | | | | | | | | | | | | | | |
| rhyolite of Cropsy Mountain | 74 | stratovolcano remnant | 82 | | | | | | | | | | | | | | | | | | | | |
| rhyolite of Park Creek | 75 | Summitville caldera | 109 | | | | | | | | | | | | | | | | | | | | |
| Snowshoe Mountain Tuff | 54 | stratigraphic relations at caldera wall | 109 | | | | | | | | | | | | | | | | | | | | |
| sorting during eruption | | Summitville caldera | 33, 36, 103, 108 | | | | | | | | | | | | | | | | | | | | |
| and emplacement | 29, 35, 40, 51, 104 | collapse | 108 | | | | | | | | | | | | | | | | | | | | |
| Summitville Andesite | 62 | Hinsdale rhyolites | 93 | | | | | | | | | | | | | | | | | | | | |
| Treasure Mountain Tuff | 18 | influence on intrusion | 78 | | | | | | | | | | | | | | | | | | | | |
| tuff of Rock Creek | 16 | lava-dome complexes | 70 | | | | | | | | | | | | | | | | | | | | |
| volcanics of Green Ridge | 69, 70 | margin | 66, 108, 109 | | | | | | | | | | | | | | | | | | | | |
| Wason Park Tuff | 53 | postcollapse volcanism | 109, 117 | | | | | | | | | | | | | | | | | | | | |
| Pinos Creek | 12 | radiating fracture zones | 113 | | | | | | | | | | | | | | | | | | | | |
| Plate tectonics | 116, 117 | ring-fracture zone | 35, 84, 108, 113, 115 | | | | | | | | | | | | | | | | | | | | |
| Platoro caldera | 103 | topographic walls | 66, 71, 108, 109 | | | | | | | | | | | | | | | | | | | | |
| ash-flow eruptions | 104 | Summitville fault | 71, 111, 112, 113 | | | | | | | | | | | | | | | | | | | | |
| collapse | 25, 104 | Sunshine Peak Tuff | 97 | | | | | | | | | | | | | | | | | | | | |
| marginal volcanoes | 49 | Surficial deposits | 101 | | | | | | | | | | | | | | | | | | | | |
| moat | 107 | T | | | | | | | | | | | | | | | | | | | | | |
| east side | 33, 66 | Table Mountain | 55 | | | | | | | | | | | | | | | | | | | | |
| northeast side | 47, 107 | Telluride Conglomerate | 6 | | | | | | | | | | | | | | | | | | | | |
| southeast side | 56, 65, 108 | Terminology | 3, 5 | | | | | | | | | | | | | | | | | | | | |
| southwest side | 62, 66, 107 | Terrace Reservoir | 23, 27 | | | | | | | | | | | | | | | | | | | | |
| postcollapse igneous activity | 55 | Terrace Reservoir laccolith | 82 | | | | | | | | | | | | | | | | | | | | |
| postresurgence volcanism | 107, 117 | Topography, before ash-flow eruption | | | | | | | | | | | | | | | | | | | | | |
| premonitory eruptions | 23, 104 | Conejos | 9, 22, 27 | | | | | | | | | | | | | | | | | | | | |
| Pino Creek | 12 | during ash-flow eruption | 22, 27, 45 | | | | | | | | | | | | | | | | | | | | |
| Plate tectonics | 116, 117 | Platoro caldera walls | 105, 106 | | | | | | | | | | | | | | | | | | | | |
| Platoro caldera | 103 | pre-Conejos | 9 | | | | | | | | | | | | | | | | | | | | |
| ash-flow eruptions | 104 | resurgent calderas | 103 | | | | | | | | | | | | | | | | | | | | |
| collapse | 25, 104 | Summitville caldera walls | 66, 71, 108, 109 | | | | | | | | | | | | | | | | | | | | |
| marginal volcanoes | 49 | See also Paleotopography. | | | | | | | | | | | | | | | | | | | | | |
| moat | 107 | Tracy Creek Quartz Latite | 8 | | | | | | | | | | | | | | | | | | | | |
| east side | 33, 66 | Treasure Mountain | 16, 23, 29 | | | | | | | | | | | | | | | | | | | | |
| northeast side | 47, 107 | N | | southeast side | 56, 65, 108 | O | | southwest side | 62, 66, 107 | P | | postcollapse igneous activity | 55 | Sheepshead | 74, 75, 90 | postresurgence volcanism | 107, 117 | Sills | 87, 90 | premonitory eruptions | 23, 104 | Silver Mountain | 69, 70 |
| N | | | | | | | | | | | | | | | | | | | | | | | |
| southeast side | 56, 65, 108 | O | | southwest side | 62, 66, 107 | P | | postcollapse igneous activity | 55 | Sheepshead | 74, 75, 90 | postresurgence volcanism | 107, 117 | Sills | 87, 90 | premonitory eruptions | 23, 104 | Silver Mountain | 69, 70 | | | | |
| O | | | | | | | | | | | | | | | | | | | | | | | |
| southwest side | 62, 66, 107 | P | | postcollapse igneous activity | 55 | Sheepshead | 74, 75, 90 | postresurgence volcanism | 107, 117 | Sills | 87, 90 | premonitory eruptions | 23, 104 | Silver Mountain | 69, 70 | | | | | | | | |
| P | | | | | | | | | | | | | | | | | | | | | | | |
| postcollapse igneous activity | 55 | Sheepshead | 74, 75, 90 | postresurgence volcanism | 107, 117 | Sills | 87, 90 | premonitory eruptions | 23, 104 | Silver Mountain | 69, 70 | | | | | | | | | | | | |
| Sheepshead | 74, 75, 90 | | | | | | | | | | | | | | | | | | | | | | |
| postresurgence volcanism | 107, 117 | Sills | 87, 90 | premonitory eruptions | 23, 104 | Silver Mountain | 69, 70 | | | | | | | | | | | | | | | | |
| Sills | 87, 90 | | | | | | | | | | | | | | | | | | | | | | |
| premonitory eruptions | 23, 104 | Silver Mountain | 69, 70 | | | | | | | | | | | | | | | | | | | | |
| Silver Mountain | 69, 70 | | | | | | | | | | | | | | | | | | | | | | |

| | Page | | Page | | Page |
|--|-----------------|---|-----------------------|-----------------------------------|----------------|
| Treasure Mountain Rhyolite | 16, 41 | Vents—Continued | | Volume—Continued | |
| Treasure Mountain Tuff | 16 | ryodacite of Park Creek | 71 | Fish Canyon Tuff | 47 |
| alteration | 84 | rhyolite of Cropsy Mountain | 73, 74, 75 | Hinsdale basalts | 8 |
| associated intrusives | 78, 86, 87, 89 | <i>See also</i> Sources. | | La Jara Canyon Member of Treasure | |
| chemical composition | 19, 116 | Volcanic stratigraphy | 6 | Mountain Tuff | 30, 105 |
| compositional zonation | 116 | Volcaniclastic rocks, Conejos Formation | 9, 13, 77 | lavas interlayered with ash-flow | |
| La Jara Canyon Member | 25, 46, 58, 103 | sheets | 7 | sheets | |
| lower tuff | 19 | Summitville Andesite | 65 | lower tuff of Treasure | |
| middle tuff | 30 | Volcanics of Green Ridge | 62, 67, 84, 87 | Mountain Tuff | 22 |
| Ojito Creek Member | 33, 108 | Volcanics of Table Mountain | 55 | main ash-flow sheets of Treasure | |
| Ra Jadero Member | 36, 108 | Volcanoes, Adams Fork | 12, 87 | Mountain Tuff | 29 |
| radiometric date | 29 | Alamosa River stock area | 82 | Ojito Creek Member of Treasure | |
| transition to later flows | 56 | Baughman Creek | 12 | Mountain Tuff | 108 |
| upper tuff | 40 | Cat Creek | 47, 67, 77, 82 | Platoro caldera collapse | 105 |
| Tuff of Rock Creek | 14 | circum-Pacific | 117 | Ra Jadero Member of Treasure | |
| Tuffs. <i>See</i> Ash-flow sheets; Intracaldera tuffs. | | Conejos | 8, 9, 12, 16, 27, 101 | Mountain Tuff | 40, 108 |
| Turkey Creek | 46 | Los Mogotes shield | 77, 92 | Summitville Andesite | 59 |
| Uncompahgre arch | 101 | Mount Hope caldera margin | 55 | tuff of Rock Creek | 16 |
| V | | Platoro caldera area | 55 | | |
| Vent-dome complexes | 69, 93, 96 | Platoro caldera margin | 49 | W, X | |
| Beaver Creek | 96, 97 | relation to caldera sites | 101, 104 | Wason Park Tuff | 53 |
| Vents, Conejos Formation | 9 | Summitville Andesite | 45 | West Elk Breccia | 8 |
| Hinsdale Formation | 92, 96 | Summitville caldera area | 66 | Wightman Fork | 64, 65, 66, 86 |
| mixed-lava complex at North Mountain | 112 | Summitville caldera margin | 110 | Wightman Fork stock | 86 |
| quartz latite of South Mountain | 112 | Volume, ash-flow sheets | 7, 32 | Willow Mountain | 13, 27 |
| | | ash-flow sheets as related to | | Xenocrysts, Hinsdale Formation | 92, 98 |
| | | caldera collapse | 101, 105 | | |
| | | early intermediate-composition | | | |
| | | rocks | 6, 101 | | |